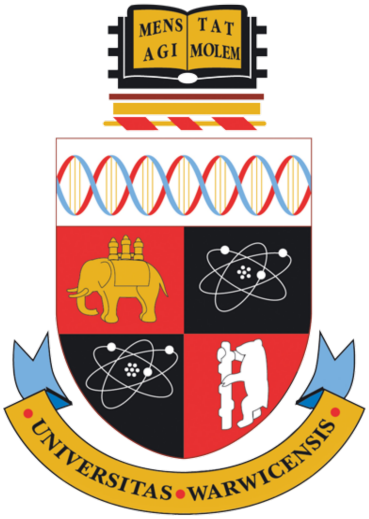

BUOYANT MICROPLASTICS IN THE MARINE ENVIRONMENT

by

Gabriel C. Erni Cassola e Barata

A thesis submitted for the degree of Doctor of Philosophy

University of Warwick, School of Life Sciences

June 2019

Table of Contents

LIST OF ILLUSTRATIONS AND TABLES

ACKNOWLEDGEMENTS

Early 2015, I was undecided about what to do next and on an evening spontaneously checked findaphd.com. I stumbled upon this project called “Plastic Oceans – Can bacteria clean up our mess?”, which had an application deadline on the next day. A rushed application and a few weeks later I had gotten the position and was set to move to the UK. And what an incredibly lucky find this turned out to be!

I am deeply grateful to my mentor Joseph Christie-Oleza, who in a very short time frame decided to hire a non-microbiologist for a microbiology project, which ended up not really being a microbiology project. The granted freedom to just simply work on whatever I was most interested in was truly appreciated. More importantly though, he assembled an amazing team to be part of, by hiring my colleagues and friends Robyn Wright and Vinko Zadjelovic, to work under the same project. Academia can be quite a solitary environment, where even though people are part of the same research group, the topics they work on are different enough, that it is actually hard for colleagues to understand problems and suggest good fixes – we had none of that and I would definitely not have gotten as far as I got without Robyn’s and Vinko’s help – oh, and some of those wine evenings were memorable!

The friendly and fun work atmosphere would not have been what it was without Mar Aguilo, Despoina Sousoni, Audam Chhun, Linda Westermann, Alberto Torcello, Eleonora Silvano and Fabrizio Alberti.

I am also deeply grateful to my parents and sister who have done everything to encourage and support me in my interests and ability to pursuit a career in science. My parents taught me to be open minded and simple, which made me a very adaptable person capable of moving anywhere and simply enjoy the new places, cultures, people and opportunities, and I know that I will always be able to count on them.

At the end of this journey, it is astonishing to realize once more how the course of life can change in a moment of sheer luck. Having been on the right spot at the right time got me to a Ph.D. position, which just recently resulted in an invitation to a meeting at the Joint Research Centre of the European Commission. I could not have dreamt this all up.

DECLARATION

This thesis is submitted to the University of Warwick for the degree of Doctor of Philosophy (Ph.D.). It was composed by me and has not been submitted in any previous application for any degree.

The work presented (including generated data and their analyses) was carried out by myself except in the cases outlined below:

- Chapter 2: Vinko Zadjelovic extracted data for meta-analysis in parallel, as required by good practice guides for meta-analyses to assure quality.
- Chapter 3: Field sampling was performed in collaboration with Richard Thompson from the University of Plymouth.
- Chapter 4: Polyethylene materials were prepared by Bethany Middleton from the Warwick Manufacturing Group (heat pressing) and Vinko Zadjelovic (weathering). Robyn J. Wright performed the library preparation for sequencing of the polyethylene samples.

PUBLISHED WORK

Parts of this thesis have been published by the author as follows:

Chapter 2 (APPENDIX 1):

Erni-Cassola, G., Zadjelovic, V., Gibson, M.I., Christie-Oleza, J.A., 2019. Distribution of plastic polymer types in the marine environment; A meta-analysis. Journal of Hazardous Materials 369, 691–698.

Chapter 3 (APPENDIX 2):

Erni-Cassola, G., Gibson, M.I., Thompson, R.C., Christie-Oleza, J., 2017. Lost, but found with Nile red; a novel method to detect and quantify small microplastics (20 μm–1 mm) in environmental samples. Environmental Science and Technology 51, 13641–13648.

Chapter 4 (APPENDIX 3):

Erni-Cassola, G., Wright, R.J., Gibson, M.I., Christie-Oleza, J., 2019. Early colonization of weathered polyethylene by distinct bacteria in marine coastal seawater. Microbial Ecology.

SUMMARY

Despite growing plastic discharge into the environment, researchers have struggled to detect expected increases of marine plastic debris in sea surfaces, especially at sizes <5 mm. These "missing plastics" not only sparked discussions about final sinks for such debris, but also about our lack of adequate methods to find and quantify smaller size fractions (<1 mm), which all could be contributing to the observed gaps in the plastic budget. Deep-sea sediments have been suggested as the final sink for microplastics (generally particles < 5 mm). The meta-analysis I present in this thesis (Chapter 2) highlights that in open oceans, microplastic polymer types segregated in the water column according to their density. Lower density polymers, such as polypropylene and polyethylene, dominated sea surface samples but became less abundant through the water column, whereas denser polymers (i.e. polyesters and acrylics) were enriched with depth. The need for methods better suited to quantify small microplastics in environmental samples has been flagged. Chapter 3 of this thesis details the optimisation and implementation of a protocol that allows high throughput detection and automated quantification of small microplastic particles (20–1000 μm) using the dye Nile red, fluorescence microscopy and image analysis software. The preliminary application of this protocol showed a power-law increase of small microplastics (*i.e.* <1 mm) with decreasing particle size in coastal sea surface water. This finding suggests that part of the "missing" plastic fraction may have been missed due to the inefficiency of traditional methods to quantify the smaller fraction of microplastics. On sea surfaces, plastic debris is rapidly colonized by a diverse community of microorganisms, and speculation arose about microbes using such plastics as a carbon source. In Chapter 4, I show that weathered polyethylene became enriched by distinct genera within the biofilms, but only during early stages of colonization (*i.e.* after 2 days) in coastal marine water. Given the lack of persistent enrichment over time, common non-hydrolysable polymers might not serve as an important source of carbon for mature colonizing communities and these mainly persist by consuming labile photosynthate generated by primary producers. Overall, this thesis shows that buoyant plastics appear to be more prevalent on sea surfaces than earlier research had suggested, and that plastic biodegradation is likely limited to a minor process that occurs within the biofilm, but can be sped up when combined with abiotic weathering.

LIST OF ABBREVIATIONS

ASV	Amplicon Sequence Variant
BLAST	Basic Local Alignment Search Tool
bp	Base Pairs
CI	Carbonyl Index
DMS	Dimethyl Sulphide
DMSP	Dimethyl Sulfoniopropionate
DNA	Deoxyribonucleic Acid
EU	European Union
FTIR	Fourier-Transform Infrared
GFP	Green Fluorescent Protein
H_2O_2	Hydrogen Peroxide
ITS	Internal Transcribed Spacer
KEGG	Kyoto Encyclopedia Of Genes And Genomes
LED	Light-Emitting Diode
MARPOL	International Convention For The Prevention Of Pollution From Ships
MSFD	Marine Strategy Framework Directive
MWL	Milled Wood Lignin
NaCl	Sodium Chloride
NaI	Sodium Iodide
NCBI	National Center For Biotechnology Information
nMDS	Non-Metric Multidimensional Scaling
NSTI	Nearest-Sequenced Taxon Indices
OHCB	Obligate Hydrocarbon Degrading Bacteria
PC	Polycarbonate
PCoA	Principal Coordinate Analysis
PCR	Polymerase Chain Reaction
PCTE	Polycarbonate Track-Etched (Filter Membrane)
PE	Polyethylene
PET	Poly(Ethylene Terephthalate)
PETase	Poly(Ethylene Terephthalate) Hydrolase
PICRUSt2	Phylogenetic Investigation Of Communities By Reconstruction Of Observed States And Abundances

POP	Persistent Organic Pollutants
PP	Polypropylene
PP&A	Polyesters, Polyamide, And Acrylics
PS	Polystyrene
PUR	Polyurethane
PVC	Polyvinyl Chloride
QA/QC	Quality Assurance And Quality Check
rRNA	Ribosomal Ribonucleic Acid
SE	Standard Error
SRA	Short Read Archive
SSU	Small Subunit
T_g	Glass Transition Temperature
UV	Ultraviolet

CHAPTER 1:

INTRODUCTION

1.1 High volumes of plastic waste becoming problematic

The mass application of plastics for consumer goods starting in the 1960s benefitted society in countless ways, such as reducing weight of packaging, consequently decreasing greenhouse gas emissions by 55%, as beverages were transported in poly(ethylene terephthalate) (PET) instead of glass- or metal containers (Andrady and Neal, 2009). Moreover, well designed food packaging can contribute to reduced food waste and therefore diminish our environmental footprint, especially for food items with high impacts from production relative to the lower impacts of their packaging, such as cheese and meat (Williams et al., 2011, 2012). In Europe, 69.6% of plastic demand is employed for packaging (39.7%), construction (19.8%) and the automotive industry (10.1%; PlasticsEurope, 2018). Although plastics contain ~50% of the carbon that is used to produce them, theoretically turning recycling into an energy saving strategy (Andrady and Neal, 2009), mismanagement of plastic waste is still a widespread problem. Of the estimated 8300 million tons of plastic produced worldwide up until 2015, only 21% have been recycled or incinerated (*i.e.* energy was recovered), leaving 79% to accumulate in landfills and the natural environment (Figure 1) (Geyer et al., 2017). In 2010, approximately 4.8 to 12.7 million tons of plastic entered marine habitats in coastal countries, which was equivalent to 1.7 to 4.6% of total generated waste in coastal areas (Jambeck et al., 2015). Additional plastics from non-coastal areas are transported to the seas *via* rivers. Unsurprisingly, river systems have been found to be highly polluted with plastics as well (Horton et al., 2017; Mani et al., 2015; Wang et al., 2017), and Hurley et al. (2018) reported that flooding events effectively exported plastics, thus "cleaning" river beds from approximately 70% of their load. At a global scale, river derived plastic inputs account for 1.15 to 2.41 million tons per year (Lebreton et al., 2017). These estimates also highlight southeast Asia and China as a plastic pollution hot-spot accounting for 67% of the river emissions, as well as 57.7% of the mismanaged waste (Jambeck et al., 2015; Lebreton et al., 2017). It is nonetheless important to emphasize, that high income countries have primarily exported their waste (accounting for 87% of waste

exports), while China and Hong Kong alone have imported 72.4% of that waste (Brooks et al., 2018). China however, has recently banned plastic waste imports, which will increase pressure to find new solutions in exporting countries (Brooks et al., 2018). Regardless, due to their inertness, littered plastics accumulate so readily and are so persistent, that they can already serve as key markers in sediments for the Anthropocene era (Waters et al., 2016). In light of growing global plastics production (PlasticsEurope, 2018) and still inadequate waste management, the cumulative quantity of plastic waste reaching marine environments has been estimated to reach 150 million tons in 2025 (Jambeck et al., 2015). Growing concerns about impacts of environmental plastic waste have therefore resulted in a call for an international agreement on marine plastic pollution (Borrelle et al., 2017).

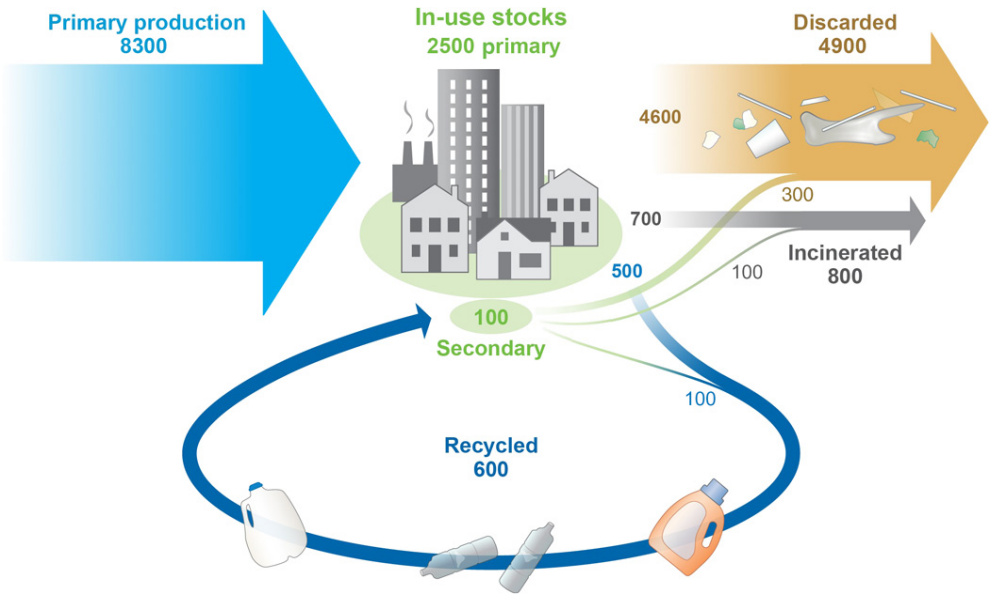

Figure 1. Plastic life cycle. Schematic illustration depicting input and fate of all plastics ever made between 1950 and 2015 in million metric tons. Figure credits: (Geyer et al., 2017).

The present review will provide an overview of environmental impacts derived from plastic pollution, and introduce the reader to the current knowledge of plastic transportation in marine environments. Despite yearly increased plastic production since the 1960s however, several studies have noted that plastic pollution on sea surfaces had not accompanied this trend (Cózar et al., 2014; Eriksen et al., 2014; Thompson et al., 2004), thus suggesting that plastic had gone "missing" (Thompson et al., 2004). The problem of the "missing plastics" will therefore be

addressed in detail and hypotheses that have been proposed to explain this phenomenon will be discussed in the remaining sections.

1.2 Plastic pollution impacting the environment

Despite the recent emphasis, plastic pollution and its potential impacts were noted in the 1970s, when for instance Carpenter and Smith Jr. (1972) reported that brittle pieces of plastic, many in the range of 0.25 to 0.5 cm, were widespread on the surface of the Sargasso Sea. Not only was plastic present in the environment, but it was also being ingested by marine birds (Rothstein, 1973). Marine litter was recognized as a problem, and disposal of persistent waste at sea was banned in 1988 (MARPOL), which interestingly, also coincided with a decline in scientific publications on the topic (Ryan and Moloney, 1993). Yet, monitoring of a remote island between 1984 and 1990 highlighted that debris incidence continued to rise exponentially, and 80% of that litter was plastic (Ryan and Moloney, 1993). That the problem had not been addressed adequately, also emerged from the high percentage of plastics among marine litter, which remained consistent throughout beach surveys in the 1990s (Derraik, 2002). In 2004, Thompson et al. (2004) drew particular attention to the pervasiveness of smaller plastic particles, that were termed "microplastics". Generally, microplastics had been defined as fragments <5 mm in size, but this definition was recently changed to include particles ranging between 1 µm and <1000 µm (Hartmann et al., 2019). Monitoring and reporting of plastic marine debris thus regained its momentum, as demonstrated by the exponentially increasing number of publications since 2004 (Figure 2). Data from contemporary surveys confirmed that plastic waste has reached all corners of the earth, from subalpine lake sediments (Imhof et al., 2013) to the deep sea (Woodall et al., 2014), and from Arctic sea ice (Peeken et al., 2018) to Antarctic waters (Cincinelli et al., 2017), not sparing remote archipelagos, such as Chagos (Readman et al., 2013). In addition to its global presence, plastic also occurs in a wide range of particle sizes, spanning from nano– (1–1000 nm) to macroplastics (1 cm and larger; Hartmann et al., 2019). Plastics have therefore gained the potential to interact with marine biota in all regions and across trophic levels.

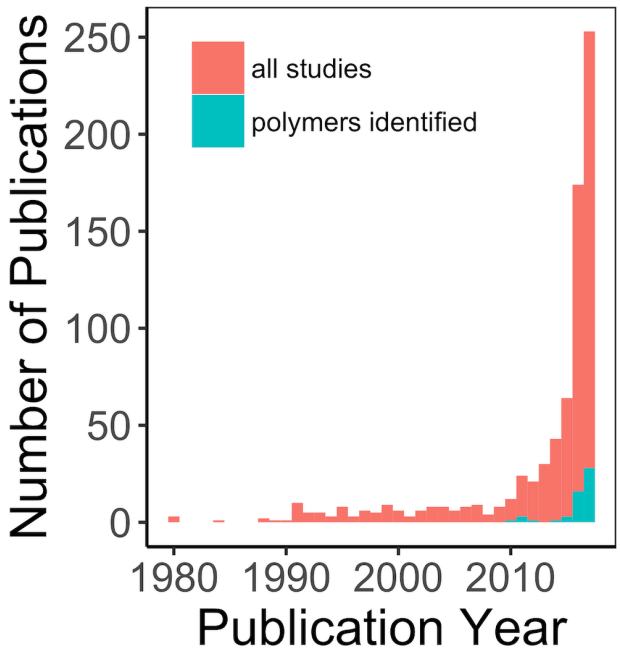

Figure 2. Number of scientific publications on plastic pollution by year. Green indicates studies in which plastic polymers were identified. Literature was searched on Web of Science using the terms "plastic" and "debris" (all studies) and "Raman or FTIR" (polymers identified).

Indeed, 92% of all encounters between marine biota and debris involve plastics (Gall and Thompson, 2015). Depending on the estimates, at least 233–267 species of marine macro fauna, such as turtles and sea birds, are affected by plastic pollution (Kühn et al., 2015; Laist, 1997), and substantial evidence demonstrates that negative impacts at sub- and organismal level can be lethal (Rochman et al., 2016). Beyond problems observed in relation with ingestion, such as gut blockage (Bjorndal et al., 1994) and perforation (Brandão et al., 2011), plastic impacts also involve entanglement in discarded fishing gear, also known as ghost fishing (Carr and Harris, 1997). Even though higher level trophic organisms are described more often to be impacted by plastic pollution (Gall and Thompson, 2015), recent laboratory and field studies have confirmed that plastics can also negatively impact lower trophic organisms, such as copepods, shrimp and corals (Allen et al., 2017; Cole et al., 2013; Devriese et al., 2015; Lamb et al., 2018; Sun et al., 2017). Yet, evidence remains sparse for deleterious effects of plastic pollution at an ecological level (Galloway et al., 2017; Rochman et al., 2016). It is, for instance, difficult to extrapolate results from laboratory studies, because these have typically been performed with plastic concentrations that exceed current reported environmental concentrations by two to

seven orders of magnitude (Lenz et al., 2016), or because common experimental designs lack controls with inert, naturally occurring particles (Ogonowski et al., 2018). While Robards et al. (1995) observed over a time span of 15 years a growing incidence of bird species that ingested plastics, as well as increased numbers of ingested plastics per animal, it is nonetheless worth highlighting that studies have so far found little evidence of plastic accumulation in the digestive organs of fish (Foekema et al., 2013; Hermsen et al., 2017; Rummel et al., 2016) or mussels (Catarino et al., 2018) and, depending on the regions and species studied, ingestion rates may even be negligible (0-0.25%; Hermsen et al., 2017; Liboiron et al., 2018). Given that plastic waste input is predicted to increase in the coming decade, pollution hot-spots could reach concentrations at which impacts at the population level emerge, and preventive measures would require knowing where these hot-spots occur.

Plastic pollution is also further suspected to leach plasticizers and facilitate the transfer of persistent organic pollutants from the environment to biota (Law, 2017; Rochman, 2015). Production of plastic involves the addition of numerous chemical additives, such as phthalate esters, phenolics or mixed metal-salt blends, which modify the properties of the final product, such as translucence, or confer flame- and UV resistance (Hahladakis et al., 2018). For some plastics, such additives can comprise up to 70% of the final product, such as in polyvinyl chloride (PVC) (Hahladakis et al., 2018). As plastics degrade, the additives can leach out into the environment, because they are not covalently bound to the polymer (Haider and Karlsson, 1999; Rani et al., 2015). In addition, plastics display higher affinity for persistent organic pollutants (POPs; Stockholm Convention), such as polycyclic aromatic hydrocarbons, polychlorinated biphenyls, or polybrominated diphenyl ethers, than natural sediments or ambient water do, and can therefore adsorb these at environmentally relevant concentrations, such as evidenced with phenanthrene (Teuten et al., 2007). The affinity for different pollutants varies with polymer type, and in accordance with properties, such as crystallinity, hydrophobicity or diffusivity (Rochman, 2015). Polyethylene (PE) for instance, has been shown to display higher affinity for organic contaminants in comparison with other polymers, perhaps also due to its increased diffusivity (Endo and Koelmans, 2016; Rochman et al., 2013; Teuten et al., 2009), and it has even been used as a passive sampler for POPs (Lohmann, 2012; Ogata et al., 2009). In the environment, PE preproduction pellets

adsorbed between 3.4-35 ng of polychlorinated biphenyls per g of plastic upon exposure to marine water in docking areas (Rochman et al., 2013), but loads as high as 600ng/g have been measured in coastal areas (Ogata et al., 2009) and sampling in the North Pacific subtropical gyre revealed that 84% of the plastics particles contained at least 1 chemical exceeding threshold effect levels (Chen et al., 2018). Indications that plastics could indeed serve as vectors for adsorbed pollutants have for instance been found in fish (Rochman et al., 2013; Wardrop et al., 2016) and birds (Tanaka et al., 2013). Nonetheless, research in birds also shows that the amount of ingested plastic does not necessarily correlate with contamination of tissues with POPs, and that due to chemical fugacity, transfer of pollutants was more likely to occur from bird to plastic, rather than the opposite (Herzke et al., 2016). Moreover, research has also shown that adsorption of contaminants to microplastics may not occur as much as predicted by analytical chemistry, and therefore sedimented plastics did not significantly increase bioavailability of contaminants to fish in a benthic scenario (Sleight et al., 2017). Overall, current data do not support the conclusion that ingestion of small plastics significantly contributes to the exposure of biota to persistent organic pollutants in most current habitats (Galloway et al., 2017; Hartmann et al., 2017; Koelmans et al., 2016). However, given future projections of plastic pollution, increased transfer of pollutants may become a problem in pollution hot-spot areas, especially since data have shown that polychlorinated biphenyl concentrations on environmental plastics are heterogeneous and can vary with plastic polymer type.

1.3 Physical transportation of plastic debris in the environment

To locate plastic pollution hot-spots where encounter rates of biota with plastic debris could be heightened, it is important to understand transportation pathways and deposition sites of marine plastic debris.

At a global scale, marine plastic debris was predicted to be transported to subtropical oceanic gyres through Ekman transport, where it accumulates as the water masses subduct, leaving the buoyant plastics on the surface to form the infamous “garbage patches” (Lebreton et al., 2012; Maximenko et al., 2012; van Sebille et al., 2012). A model simulating 1000 years of advection based on ocean drifter data further illustrated how the residence time of litter in the gyres varied, *i.e.*

plastic “leaked” from some accumulation zones, and ultimately, the North Pacific subtropical gyre stood as the main attractor for plastic debris from southern oceans (van Sebille et al., 2012). According to the latest estimates, the gyre caries debris in the range of 79 thousand tons or 1.8 trillion pieces (Lebreton et al., 2018). Despite the fact that sampling expeditions have repeatedly confirmed these accumulation zones (Beer et al., 2018; Cózar et al., 2014; Enders et al., 2015; Eriksen et al., 2014; Moore et al., 2001), the weight of floating plastics debris was estimated to be up to two orders of magnitude lower than what emission data had led to believe (Cózar et al., 2014; Lebreton et al., 2018). Thus, the decade-old question about where all the debris was going was restated (Thompson et al., 2004), especially due to observed drop-offs in plastic particle abundance for sizes <1 mm (Figure 3) (Cózar et al., 2014; Isobe et al., 2014; Morét-Ferguson et al., 2010).

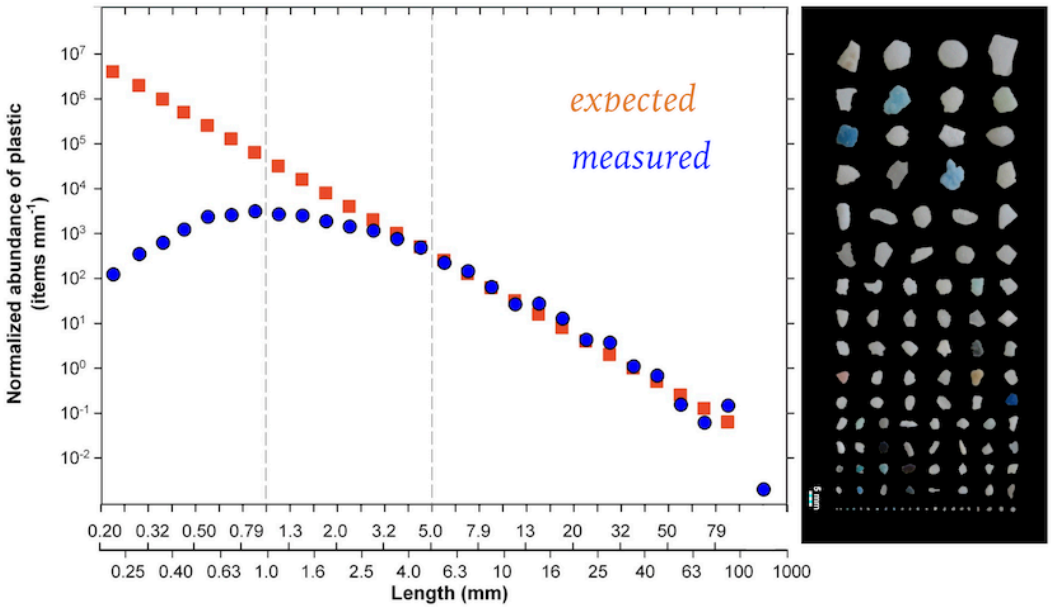

Figure 3. Marine plastic debris abundance on sea surfaces. Note the discrepancy between expected (orange) and detected (blue) plastics with a fragment size <1 mm. Figure re-assembled after (Cózar et al., 2014).

In an attempt to find the missing plastic, ensuing research has therefore focused on exploring overlooked aspects of plastic transportation. For example, by comparing sampling data with model predictions, van Sebille et al. (2015) suggested that 30-70% of the numerically dominant microplastics perhaps still resided outside of the oceanic gyres in the undersampled, low concentration regions. Mixing effects of oceanic surface water also implied that a significant fraction of the plastic debris

could be suspended in oceanic surface layers (Kooi et al., 2016). If wind mixing, even for moderate wind conditions, was accounted for, Kukulka et al. (2012) predicted that estimates of numerical abundance may increase by up to 27 times. Modelling predictions from vertical mixing were indeed found to meet observations from sampling the top 5 m of the water column (Reisser et al., 2015), but numerical and mass concentrations of plastic particles have nonetheless been found to decrease exponentially with depth (Kooi et al., 2016). Recent budgeting efforts have further illustrated how models that describe plastic abundance in sea surface layers are sensitive to variables describing particles sinking away from surface and plastic fragmentation (Koelmans et al., 2017).

Besides sinking and fragmentation, part of the plastics budget missing from sea surfaces could also be deposited on beaches. Simulations and field data have suggested that a combination of stokes drift and plastic buoyancy can selectively trap larger debris in coastal environments (Isobe et al., 2014). Indeed, some of the highest marine plastics concentrations have been reported on beaches (Erni-Cassola et al., 2019), but other hypotheses could equally explain increased plastic prevalence, such as littering or runoff from settlements. Interestingly, a direct comparison of hypotheses, yielded marine onshore transport as the best explanation for plastic deposition on beaches in Tasmania (Willis et al., 2017). Ultimately, proportions of beaching plastics are going to vary significantly in accordance with local factors such as input sources, wind, coastal topography and plastics degradation rates (Critchell and Lambrechts, 2016).

For a better understanding of where the missing plastic is disappearing to, additional aspects which interact with the transportation pathways described above must be considered. For instance, the behaviour of plastics debris in the water column is dependent on the polymer density and shape of a given particle. The buoyancy can further be modified by interactions with organisms that colonize the debris, or ingest particles and defecate them. Missing plastic may also not fully be a consequence of incomplete understanding of its transport processes and interactions, but include methodological problems. It is well established that plastic debris degrades in the environment, generating increasing numbers of smaller particles, and therefore detecting and quantifying them has been recognized as a major difficulty, given commonly employed methods that rely on visual detection (Hidalgo-Ruz et al., 2012). Biases are thus a problem with particle sizes <0.5 mm (Lenz et al., 2015;

Rocha-Santos and Duarte, 2015). These hypotheses shall be outlined in detail in the following sections.

1.4 Properties of plastic polymers varying with their type

The term "plastic" describes a property of materials grouping a great variety of different synthetic polymers. These polymers are categorized as thermoplastics, which can be melt-processed, and thermosets, which cannot (Andrady, 2017). Although not strictly correct, in the context of marine pollution, the term "plastics" is used to refer to many of these synthetic polymers and composites as recently defined (Hartmann et al., 2019). The thermoplastic group, contains commonly used materials, such as PE, polypropylene (PP), polystyrene (PS) and polyesters, while polyurethane and epoxy resins are examples of thermosets.

In the context of aquatic transport, the specific density of these different polymers influences whether the debris is positively or negatively buoyant (Table 1). Another factor that determines buoyancy is polymer crystallinity. As semi-crystalline materials, plastics contain a variable percentage of crystalline (*i.e.* polymer chains organized in parallel bundles) and amorphous (*i.e.* randomly organized) parts (Andrady, 2017). The degree of crystallinity is variable, both within and between polymer types, and can be modified, for instance through temperature; at higher temperatures polymers tend to be more rubbery, *i.e.* less crystalline. The temperature above which a polymer becomes a rubber is referred to as glass transition temperature (T_g), and this is what varies with polymer type (Andrady, 2017). Polymers with higher degrees of crystallinity are denser. Half of the European plastic demand in 2017 consisted of PE and PP (49.1%, PlasticsEurope, 2018), which are positively buoyant in seawater, and are thus predicted to be subjected to sea surface transportation mechanisms as described above. Among different polymer types, PE and PP also have short life cycles and are thus also overrepresented in waste material (Geyer et al., 2017). Most other polymer types however, are denser than seawater (Table 1), and are therefore not expected to accumulate in oceanic gyres, but rather to sink out of the water column, and are projected to be enriched in bottom sediments. Polymer density however, has also been shown to be substantially modified by biota that colonize marine plastic debris, which will be discussed in detail below.

Beyond density effects on plastic particle transportation, it is important to consider the shape as well as the size of the particles themselves. Theoretical exercises and laboratory studies have shown that for the same polymer type, irregular shapes had slower rising or sinking velocities than spheres due to secondary movements in the water column (Waldschläger and Schüttrumpf, 2019); fibres for instance, consistently aligned themselves horizontally. The effect of shape can be so strong that even a particle with higher density but more deviant from the perfect sphere sinks more slowly than a less dense, but more spherical piece (Kowalski et al., 2016). Data from field surveys have so far confirmed these findings. Tests with particles recovered from the sea showed that within the same size class, filamentous plastics rose more slowly than fragments, and the former were therefore more susceptible to removal from sea surface through wind mixing (Kooi et al., 2016). Indeed, when sampling the water column, higher fibre incidence has been found in subsurface and near bottom layers (Bagaev et al., 2017; Zobkov et al., 2019), while fragments exhibited an opposite stratification, and films were found to be intermediate (Zobkov et al., 2019). It is however important to note that particle diameter in combination with density can exert stronger effects than shape (Waldschläger and Schüttrumpf, 2019), and departures from theoretical values in sinking and rising velocities calculated for perfect spheres were lower for smaller particles (< 1mm). Such size selective effects are again consistent with field data (Kooi et al., 2016; Reisser et al., 2015; Zobkov et al., 2019), reporting that sea surface water at depths between 0.5 and 5 m contained 20% of the particles between 0.5-1mm, but only 8% of the particles with 2.5-3 mm (Reisser et al., 2015). In accordance, numerical microplastic concentrations decreased more slowly than microplastic mass concentrations (Kooi et al., 2016). Interestingly, it appears that coastal waters have higher incidence in fibres in the sea surface compared with off-shore sampling sites (Bagaev et al., 2017; Zobkov et al., 2019), perhaps indicating that fibres are more likely to sediment. Field studies performed in the North Atlantic subtropical gyre also suggest that most buoyant plastic remains concentrated in the top layers of the oceans (Kooi et al., 2016). Evidence for the disappearance of plastics from the sea surface is therefore mixed and not equally applicable to all polymer types, fragment sizes and shapes, and therefore requires further hypothesis testing.

Table 1. Polymer abbreviations and specific density

Abbreviation	Polymer	Density [g cm^{-3}]
PP	polypropylene	0.85–0.92
PE	polyethylene	0.89–0.98*(LD+HD)
PS	polystyrene	1.04
PP&A		
PEST	polyester	1.10–1.40
PA	polyamide	1.12–1.15
Acrylic (includes PMMA)		1.18
OTHER		
EPR	poly(ethylene-co-propylene)	0.86–0.88
PUR	polyurethane	1.20–1.26
PVC	poly(vinyl chloride)	1.38–1.41
IR	polyisoprene	0.91
PEVA	poly(ethylene-vinyl acetate)	0.92–0.95
PDMS	polydimethylsiloxane	0.97
ABS	acrylonitrile butadiene styrene	1.04–1.08
PCL	polycaprolactone	1.15
PAN	polyacrylonitrile	1.18
PVA	poly(vinyl acetate)	1.19
PVOH	poly(vinyl alcohol)	1.19
PC	polycarbonate	1.20–1.22
NBR	nitrile rubber	1.3
PTFE	polytetrafluoroethylene	2.10–2.30
PSS	poly(styrenesulfonate)	
VCE	poly(vinyl chloride-ethylene)	
PAS	poly(acrylate/styrene)	
rubber		
other		

Notes: PE includes HD- and LD-PE; PS includes foamed and non-foamed forms.

1.5 Plastics becoming too small to be seen

Over time in marine environments, plastics embrittle and progressively fragment into small particles, referred to as micro- (1 to <1000 μm) and nanoplastics (1 to < 1000 nm; Hartmann et al., 2019), and it has been noted that current methods may underestimate plastic pollution due to difficulties in detecting and quantifying small microplastics (< 500 μm; Hidalgo-Ruz et al., 2012; Lenz et al., 2015; Rocha-Santos and Duarte, 2015). This deterioration process can be induced by light and/or temperature, and occurs primarily through oxidation. Oxidation provides free radicals that cleave the polymer chain, such as the carbon-carbon backbone in PE and PP, or the ester bonds in PET (Gewert et al., 2015). The onset of polymer degradation can be monitored through Fourier-transform infrared (FTIR) spectroscopy exploiting the formation of new functional groups, such as carbonyl or hydroxyl groups in carbon-hydrogen polymers like PE and PP (Andrady et al., 1993; Luongo, 1960), or new alkyne- and alkane bonds in PET (Ioakeimidis et al., 2016). The progress of surface oxidation is then measured as ratios of the increasing absorbance of these added groups in comparison with the constant absorbance in areas unaffected by the weathering. Measures of surface oxidation are good indicators for the initial degradation process, but more advanced material deterioration is then commonly measured via material properties, such as elasticity. Finally, highly weathered polymers become brittle and break. The breakup process is not yet thoroughly understood, but in principle oxidative degradation primarily takes place in amorphous parts of the polymer, due to better oxygen diffusion, compared with crystalline areas and ultimately fragmentation occurs, for instance through mechanical action, or as surface ablation of the weathered outer layer after repeated swell and dry cycles (Figure 4) (Andrady, 2017).

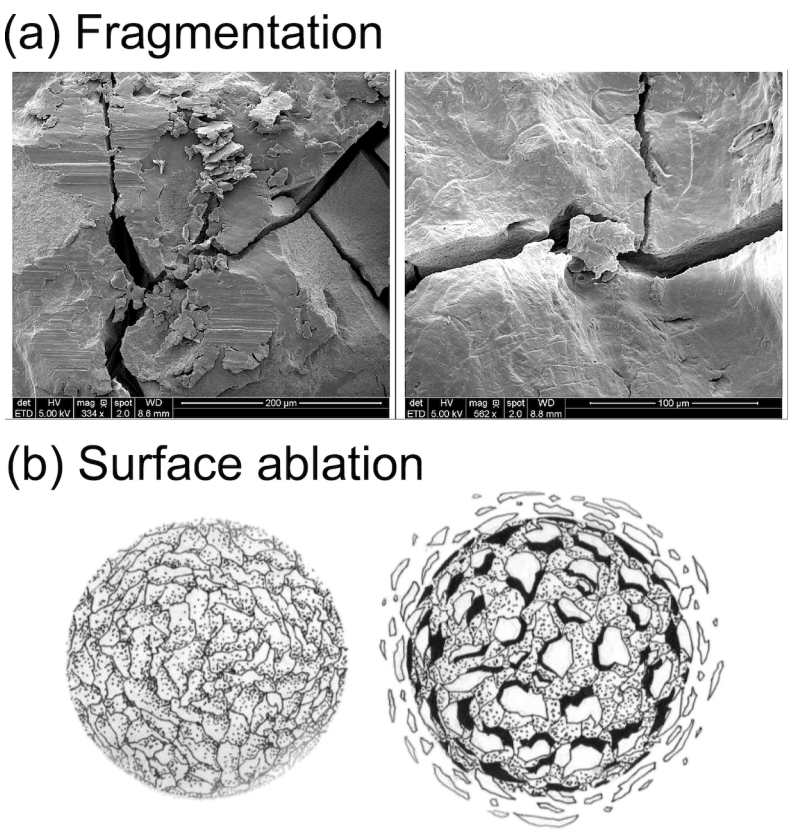

Figure 4. Plastic fragmentation as consequence of weathering. (a) SEM images of polyethylene particles collected in the North Atlantic subtropical gyre; credits (ter Halle et al., 2017). (b) Schematic depiction of fragmentation through surface ablation; credits (Andrady, 2017).

Even though chemically the degradation is similar in seawater and on land, the rate at which it occurs differs starkly, and is significantly accelerated on land (Andrady, 2011; Pegram and Andrady, 1989). For example, after 12 months in the sea, a PE film had lost 12% in ultimate extension, while the air exposed film had lost 95% in six months (Pegram and Andrady, 1989). Through additives, polymers can be made so resistant, that after one year of exposure to the environment, no degradation in the tensile properties of a PE net was noticed (Pegram and Andrady, 1989). One reason that degradation occurs more rapidly on land, is that solar irradiation can cause a "heat build-up" in the plastic particle, an effect that is reduced in water due to temperature buffering and lower UV penetration (Gregory and Andrady, 2003). In water, interestingly the plastic fragment shape also influences its decay. For instance, films floated with one side up and were thus found to be highly weathered on one side compared with the reverse, while more cubic shapes "rolled"

in water, consequently acquiring more homogeneous weathering, which implied that the latter fragment more quickly (ter Halle et al., 2016). Fragmentation rates can further be influenced by the polymer type. Contrary to other materials, foamed polystyrene deteriorated more rapidly in water than on land because the brittle layer on the polymer surface, which protected underlying PS layers, was removed more frequently in water (Andrady and Pegram, 1991). If however, UV-irradiation was combined with mechanical abrasion using sand, foamed PS produced more fragments after 12 months than PP (~1×10^4 compared with ~0.6×10^4 particles/pellet, respectively), and both fragmented significantly more than PE (~0.2×10^2 particles/pellet) (Song et al., 2017). It is further worth noting that 97% of the generated fragments were <300 μm (Song et al., 2017), again illustrating the difficulty of visually finding and quantifying microplastics in environmental samples.

1.6 Colonization of plastic debris and its consequences

Like other surfaces in marine environments, marine plastic debris is biofouled and it has consequently been hypothesized that the added density from the colonizing organisms could account for the removal of some of the missing buoyant plastic from sea surfaces. Exposure studies in coastal environments using floating films and pieces of PE demonstrated that it took between two and eight weeks to lose buoyancy, and smaller items sank earlier (Fazey and Ryan, 2016; Lobelle and Cunliffe, 2011). The organisms that colonize the plastic debris can range from macro organisms, such as barnacles, bryozoans, hydroids or multicellular algae, to microbial communities composed of diverse bacteria, single-celled algae and fungi (De Tender et al., 2017; McCormick et al., 2014; Reisser et al., 2014; Zettler et al., 2013). From these fouling communities, calcified organisms, such as barnacles or bryozoans, were determined as the primary inducers of sinking (Fazey and Ryan, 2016). Yet, there are considerable uncertainties about the ultimate effect of bioencrustation on the final fate of plastics. For instance, the extent of biofouling in coastal settings is likely to differ from nutrient poor, off-shore sites or with latitude. Comparisons between communities of macro organisms from plastic debris and *Sargassum* washed ashore from the Sargasso sea during storm events showed that not only did plastic carry 10% of the species present on *Sargassum*, but also that the

plastic communities were dominated by a single bryozoan species (Winston, 1982), indicating that only a subset of the biofouling communities may colonize plastic; these colonizers appear to be primarily filter feeding organisms, which is typical on inert surfaces (Thiel and Gutow, 2005). Research on the biofouling of marine debris has also established that towards higher latitudes, macro colonizers become rare (Thiel and Gutow, 2005), which would indicate that plastic removal through increased density by fouling biota might not be a generally applicable hypothesis. Moreover, the fouling community can also increase buoyancy (Winston et al., 1997), or be removed after submergence, for instance through predation or lack of light, which leads the plastic debris to re-emerge (Ye and Andrady, 1991).

As detailed above, particle size is again a key aspect that needs considering. While calcified macro organisms can colonize and drive sinking of larger particles, smaller pieces (ex. <1 mm) are less likely to be colonized by such organisms (Fazey and Ryan, 2016), and the fouling community will be more limited to microorganisms. Although selected from planktonic communities, substrate colonizing bacterial assemblies in aquatic environments have been found to differ distinctly from planktonic assemblies (Dang & Lovell 2016), which has equally been observed for microplastics (De Tender et al., 2015; Zettler et al., 2013). The colonization can be divided into different stages, with observable shifts in abundance of community members and as biofilms mature (Datta et al., 2016; De Tender et al., 2017; Lee et al., 2008), communities gradually converge over time as they are conditioned by environmental variables. Mature biofilms on inert surfaces may be similar, even if the initially colonized substrates that differed, such as in their wettability (Huggett et al., 2009). Even though cells with silica shells and thus higher density than seawater, such as diatoms, colonize plastics (Reisser et al., 2014; Zettler et al., 2013), it is not clear whether the added density of natural biofilms formed on microplastics is sufficient to cause sedimentation of single pieces. Modelling exercises suggested that, depending on particle size, microplastics may oscillate in the water column with most particles <0.1 mm perhaps never resurfacing, but neither sedimenting (Kooi et al., 2017). The simulations also indicated that differences between oceanic regions should be expected as it took 100 days until a particle lost its buoyancy in the North Pacific, but the same never happened in the North Atlantic (Kooi et al., 2017). Simulations also illustrated that biofouling amplified shape effects, such as described above, because films and fibres offer more area for

colonization relative to their volume as opposed to spheres, and hence accumulate more biofilm (Chubarenko et al., 2016). However, as outlined by Filella (2015), it could prove productive to consider heterocoagulation of microplastic with other particles, as is common in aquatic environments with colloids. Biofilms are known to be sticky through interactions between exopolysaccharides in the extracellular matrices (Sutherland, 2001), and recent experiments with roller tanks and natural seawater showed that microplastics aggregate and are quickly integrated into biofilms, intermixed with particulate organic carbon (Geyer et al., 2017; Michels et al., 2018; Porter et al., 2018). Even particles less dense than seawater were readily included into such aggregates, although at lower percentages than negatively buoyant microplastics (79% vs. 100%), but regardless of the polymer type, aggregates finally sank (Porter et al., 2018). In the field, downward transport of PP as part of marine snow has also been observed at approximately 2 m depth (Zhao et al., 2017). It is also important to emphasize that most (>97%) organic matter does not reach the deep sea (>1000 m depth) because the carbon is remineralized in the water column (Turner, 2015), which in the context of microplastics in marine snow would suggest that buoyant plastics would either re-emerge or be ingested.

1.7 Plastic ingestion as removal pathway

Removal of floating plastics has also been attributed to animals that cause it to sink *via* defecation, a process that may be aided by biofouling of marine plastic debris. Different factors may drive ingestion. For example, it has been suggested that certain colours are more attractive, such as yellow, blue or green (Carson, 2013; Ryan, 1987; Santos et al., 2016), but also shapes, such as oblong bottles (Carson, 2013). Recent research however, has revealed that plastics, which were exposed to seawater for three weeks, acquired a dimethyl sulphide (DMS) signature (Savoca et al., 2016). DMS is a volatile metabolite from dimethyl sulfoniopropionate (DMSP), with the latter being produced by phytoplankton and metabolized by heterotrophic cells (Curson et al., 2011). Research has shown that concentration gradients of these molecules are exploited by foraging animals to identify potential feeding patches (Debose et al., 2008; Savoca and Nevitt, 2014), and interestingly, the incidence of plastic ingestion was higher in DMS sensitive birds (48%), compared to non-DMS responders (7.5%; Savoca et al., 2016). Moreover, microplastics “flavoured” in

natural seawater have also been shown to induce foraging behaviour in anchovies (Savoca et al., 2017) or increase ingestion rates in copepods (Vroom et al., 2017), demonstrating that abundant marine foragers may be induced to specifically target plastic particles. A curious exception was described by Allen et al. (2017), who demonstrated that a coral (chemoreceptive feeder) consistently preferred pristine plastic pellets over biofouled ones. Moreover, particle aggregation may interact negatively with ingestion, as mussels ingested more plastics when they were biofouled and coagulated (Porter et al., 2018), showing that ingestion by some organisms may be underestimated in single particle feeding experiments. Overall, cue driven, targeted ingestion of plastics by foragers in combination with more general consumption by abundant filter feeders, such as larvaceans (Katija et al., 2017), could explain some of the removal of plastic from sea surfaces. This removal would occur through defecation, thus exporting plastics incorporated into denser aggregations (Cole et al., 2016), or attached to other material, such as the "houses" of the larvaceans (Katija et al., 2017). Further support for this process may be lent by the previously discussed observations of fish with plastics in their guts (*i.e.* confirmed ingestion), but the lack of evidence for accumulation in their digestive organs (*i.e.* defecation) (Hermsen et al., 2017; Liboiron et al., 2016). Beyond the "simple" removal by sinking, "pseudo"-removal may also occur through animal driven fragmentation. For instance, laboratory experiments showed that the highly abundant Antarctic krill could ingest and fragment microplastics down to nanoplastics (Dawson et al., 2018), effectively rendering particles undetectable by current, standard sampling methodologies. Assessing the overall importance of plastic removal by ingestion through sampling biota is however difficult, as such sampling might be biased against animals with high ingestion rates, since those would naturally be removed. High incidences of buoyant microplastics should nonetheless be found in marine sediments.

1.8 Common plastics serving as carbon source for microorganisms

Another proposed mechanism for removal of plastic from sea surfaces is biodegradation, especially given the high fragmentation rates and consequent increase in exposed plastic surface. The biodegradation of common plastic polymers involves overcoming several barriers, such as surface hydrophobicity, insolubility and crystallinity, as well as the high molecular weight of the polymers (Krueger et al., 2015; Restrepo-Flórez et al., 2014).

High molecular weight is a principal attribute of plastics that contributes to their longevity, but it is helpful to distinguish between non-hydrolysable polymers, such as PE or PP that have a carbon-carbon backbone, and hydrolysable polymers, such as PET or polyurethane that have heteroatoms in their backbones. The latter can be cleaved by various extracellular hydrolases, similar to microbial degradation of natural macromolecules, such as cellulose or proteins. Non-hydrolysable polymers on the contrary, are less likely to be biodegraded due to the unfavorability of the reaction of cleaving a carbon-carbon (Krueger et al., 2015). Proposed pathways therefore involve abiotic oxidation steps, the chain scission products of which can then be further metabolized intracellularly *via* the β-oxidation pathway for fatty acids. Low density PE for instance, can have a typical chain length of C_{4000}–$C_{40,000}$, while bacteria specialized in metabolizing such linear aliphatic compounds, *i.e.* n-alkanes, have been found to be capable of metabolizing only $<C_{50}$ n-alkanes (Rojo, 2009). Previous experiments have indeed shown that a reduction of molecular weight via UV-irradiation improved biodegradation rates, even though the overall degradation rate remained low with 1.3-5.7% weight loss after 10 years, measured *via* $^{14}CO_2$ liberation (Albertsson and Karlsson, 1990). Nonetheless, strongly oxidizing extracellular enzymes with low substrate specificity, such as laccases have potential (Theerachat et al., 2019), and a particular copper binding laccase has been shown to reduce the molecular weight of weathered PE by 20% over two weeks (Santo et al., 2013). In aquatic environments however, not only is abiotic weathering slowed down by lower temperatures, but the colonizing organisms may also protect the polymer surface from further UV-irradiation, for instance through microbially derived sunscreens (Gao and Garcia-Pichel, 2011), or shading by macro organisms. As with the laccase however, the widespread ability of marine heterotrophic bacteria

to produce superoxides (Diaz et al., 2013) offers an interesting avenue to investigate the potential of such cells in oxidizing plastic polymers.

In turn, biodegradation of a hydrolysable polymer without prior treatment of the material has recently been well documented. The proteobacterium *Ideonella sakaiensis*, which was isolated from a PET bottle recycling site, was capable of using PET as a carbon source (Yoshida et al., 2016). Yoshida et al. (2016) suggested that hydrolysis of PET into its monomers was achieved through an enzyme that may have newly evolved, and was termed PETase. Follow-up engineering experiments of this secreted enzyme also demonstrated that its function could be improved relative to the wildtype (Austin et al., 2018), demonstrating that there was room for further evolution in the environment.

In a marine setting, much less is known about the availability of genes and thus the potential for biodegradation of plastics. A PETase homolog gene search in terrestrial and marine metagenomes revealed that, although generally very rare, they were on average more common in terrestrial- than marine systems (157 vs. 42 homologs; Danso et al., 2018). Noteworthy was the observation that while in terrestrial systems, Actinobacteria and Proteobacteria were the main holders of these genes, in marine systems it was bacteria belonging to the Bacteroidetes phylum that were the main hosts for PETases (Danso et al., 2018), indicating that searching marine communities by analogy to terrestrial groups or taxa involved in degradation may not necessarily prove fruitful. Among non-hydrolysable polymers, PE has received the most attention (Krueger et al., 2015), and so far, 17 bacterial and 9 fungal genera have been associated with its degradation (Restrepo-Flórez et al., 2014). Nonetheless, of the 24 studies listed by Restrepo-Flórez et al. (2014), only one study was conducted in aquatic marine conditions (Sudhakar et al., 2008), thus highlighting a significant research gap – or dearth of positive results. Speculation on plastic biodegradation in marine systems soared, after two studies documented so far unidentified, round, ~2 μm sized cells embedded in pits on the surface of microplastics obtained from the North Atlantic and Australian waters respectively (Reisser et al., 2014; Zettler et al., 2013). Based on 16S rRNA gene sequencing, Zettler et al. (2013) described a network of presumed hydrocarbon degraders, for instance some of its members being also associated with the Deepwater Horizon oil spill.

As stated above, polymer properties beyond molecular weight also affect biodegradability. For instance, the wild type PETase from *Ideonella sakaiensis* primarily degraded low-crystallinity (1.9%) PET, and even though an effect was demonstrated for more crystalline (>30%) PET, such as used for plastic bottles, degradation was significantly reduced (Yoshida et al., 2016). Similar observations have been made in PE, where amorphous polymer parts were reduced before its crystalline areas (Santo et al., 2013). Interestingly, while weathering reduces the molecular weight of a polymer, making it more accessible for biodegradation, it also increases crystallinity, as pre-existing crystals grow with the short chain segments generated by chain scissions in a process termed "chemi-crystallization" (Rabello and White, 1997), which in turn may reduce degradability. Surface hydrophobicity can also be a hindrance for biodegradation, as the adsorption of proteins to such surfaces is reduced. Research with a fungal cutinase that can hydrolyse PET has shown that adding a class of proteins termed hydrophobins not only reduced surface hydrophobicity of the polymer, but also stimulated enzyme activity (Espino-Rammer et al., 2013). Similarly, fusion of a bacterial cutinase with different hydrophobins increased PET hydrolysis 16-fold (Ribitsch et al., 2015). The importance of such effects in aquatic environments is not clear, given that surfaces are quickly coated with an adsorbome of natural organic molecules, collectively referred to as ecocorona (Galloway et al., 2017), and including the general observation that in water, surfaces of colloidal particles become negatively charged (Filella, 2007).

1.9 Conclusion

Undeniably, plastic waste enters marine environments and as a consequence of mounting plastic production, incidence of marine plastic debris increased in the North Atlantic over the past 60 years (Ostle et al., 2019). From the present review however, considerable uncertainties emerge about the fate of smaller plastic debris, such as microplastics. As discussed by Ostle et al. (2019), increases in large plastic debris could be used as proxy for small debris, and while it is well established that plastics degrade and fragment in the environment, it is also evident that fragmentation rates differ between aquatic and terrestrial conditions and especially debris originating from fishing material may be very resistant. Furthermore, degradation and break-up of plastic debris may in addition be slowed down because

colonizing organisms protect the surfaces from aging effects. Biofouling may also contribute to the removal of plastics from sea surfaces directly through added density and promoting heterocoagulation in marine snow, or increased ingestion rates and sinking as part of faeces. Although still limited, data from sediment traps in the North Atlantic gyre do not support consistent plastic sedimentation, and despite detection of plastics in deep sea sediments, relative abundances of polymer types are not consistent with proportions from inputs. Finally, plastic debris size has also been described to affect particle position in the water column, as well as complicating accurate detection and quantification.

RESEARCH AIMS FOR THE PHD THESIS

The objectives of the present PhD thesis revolved around the investigation of different hypotheses for the missing plastics from sea surfaces and were threefold. Firstly, to address the uncertainty about sinks for buoyant marine plastics debris, given the different factors described above, which act on plastic particles. Secondly, to develop a better methodology to detect and quantify small microplastics, by eliminating the visual bias inherent to most current methods and expand the lower limit of the size range at which plastics can be detected for the purposes of environmental monitoring. This method should then be tested with environmental samples. Thirdly, to investigate the effect of polymer weathering on the community composition of the colonizing microorganisms with the aim of elucidating to what extent a Plastisphere community may possess biodegradation potential. In the following chapters, each aim will be introduced individually.

CHAPTER 2:

DISTRIBUTION OF PLASTIC POLYMER TYPES IN THE MARINE ENVIRONMENT; A META-ANALYSIS.

2.1 Summary

Despite growing plastic discharge into the environment, researchers have struggled to detect expected increases of marine plastic debris in sea surfaces, sparking discussions about "missing plastics" and final sinks, which are hypothesized to be coastal and deep-sea sediments. While it holds true that the highest concentrations of plastic particles are found in these locations (10^3-10^4 particles m^{-3} in sediments vs. 0.1–1 particles m^{-3} in the water column), our meta-analysis also highlights that in open oceans, microplastic polymer types segregated in the water column according to their density. Lower density polymers, such as polypropylene and polyethylene, dominated sea surface samples (25% and 42%, respectively) but decreased in abundance through the water column (3% and 2% in the deep-sea, respectively), whereas only denser polymers (i.e. polyesters and acrylics) were enriched with depth (5% in surface seawater vs. 77% in deep-sea locations). The meta-analysis demonstrates that some of the most abundant and recalcitrant manufactured plastics are more persistent in the sea surface than previously anticipated. We thus show that further research is required to determine what the ultimate fate for low density polymer types is, given that deep sea sediments were most prominently enriched with high density polymer types.

2.2 Introduction

Plastics benefit human society in numerous ways, such as improved consumer health and product durability or reduced CO_2 emissions with lightweight materials (Andrady and Neal, 2009), but in recent years plastic has been identified as a widespread and recalcitrant pollutant in aquatic environments. It was estimated that over 8 million tons of plastic enter the oceans annually (Jambeck et al., 2015), and plastic is now found in all major oceanic gyres (Cózar et al., 2014), polar seas (Lusher et al., 2015) and deep sea sediments (Woodall et al., 2014). In the

environment, plastic is known to deteriorate and fragment (Andrady, 2017, 2011) therefore occurring in a wide range of sizes (Eriksen et al., 2014; Lebreton et al., 2018), for which standardized categories have very recently been proposed: macro- (≥ 1 cm), meso- (1-10 mm) and micro- (1 - 1000 μm) and nanoplastics (1 – 1000 nm; Hartmann et al., 2019), with smaller particles being numerically most prevalent on sea surfaces (Cózar et al., 2014). In the water however, degradation is slowed down by lower temperatures and limited UV penetration (Andrady, 2011), leading plastic debris to persist and accumulate (Andrady, 2015; Krueger et al., 2015).

The global distribution of marine plastic debris and its broad range of particle sizes imply interactions with marine fauna at all trophic levels (Boerger et al., 2010; Carreras-Colom et al., 2018; Gall and Thompson, 2015; Kühn et al., 2015; Lamb et al., 2018; Sun et al., 2017). Thus far, much of the science has focused on the severity of impacts, while the probability of encounter received less attention. A complete understanding of risk however, can only be achieved by evaluating the availability of microplastics to biota (Everaert et al., 2018) and potential release of additives embedded in them (Hahladakis et al., 2018), which requires knowledge about the major sinks for plastic debris in marine ecosystems. Severity of ecological impacts will presumably be higher at plastic sink sites, which can be found through a better understanding of maritime plastic transportation (Worm et al., 2017; Zhang, 2017).

Despite growing plastic production and discharge into the environment, researchers have struggled to detect predicted increases of small microplastic (< 1 mm) in sea surfaces, which has sparked discussion about possible sinks for marine plastic debris in deep sea sediments (Beer et al., 2018; Cózar et al., 2014; Thompson et al., 2004). Various plastic polymer types have higher densities than seawater ($\rho >$ 1.02 g cm^{-3}, Table 1) which should logically lead to sinking, and in fact, plastics are plentifully found in the deep sea (Van Cauwenberghe et al., 2013; Woodall et al., 2014). Even the most abundantly manufactured polymers, *i.e.* polyethylene (PE), polypropylene (PP) and some forms of polystyrene (PS) which are less dense than seawater, can sink when biofouled because of the increased density (Fazey and Ryan, 2016; Ye and Andrady, 1991), or when included in faecal pellets after ingestion and marine snow (Cole et al., 2016; Long et al., 2015; Michels et al., 2018). Some factors in these processes remain uncertain though, such as the extent to which oligotrophic marine systems support biofilms large enough to cause sinking, or the effect of de-

fouling and particle disaggregation, which would ultimately cause lower density plastic debris to resurface (Ye and Andrady, 1991).

In light of uncertainties about the final sink for microplastic in aquatic environments, we conducted a meta-analysis in an attempt to identify patterns in the abundance of common synthetic polymer types in different aquatic zones. Investigating incidence of individual polymer types is now possible, owing to the routine implementation of spectroscopic methods to identify polymer types in environmental surveys (Figure 2). By focusing on polymer type, we demonstrate that relative abundance of specific synthetic polymers differs with sampled aquatic zone.

2.3 Methods

2.3.1 Eligibility criteria and search method

Literature on aquatic plastic debris was systematically reviewed considering only studies that clearly specified the aquatic zones that had been sampled, and in which the polymer type was identified.

Literature was searched using all databases in *Web of Science* and, as in Rochman et al. (2016), the databases of the journals *Environmental Science & Technology* and *Marine Pollution Bulletin* due to their relevance in the field, yielding additional articles not found through *Web of Science*. The following Boolean search terms and modifiers were employed: *plastic* AND debris AND environment* AND (FT$IR or Raman). The search included every available publication until March 2018, but was restricted to accepted, peer-reviewed publications in English with original data (Figure 5).

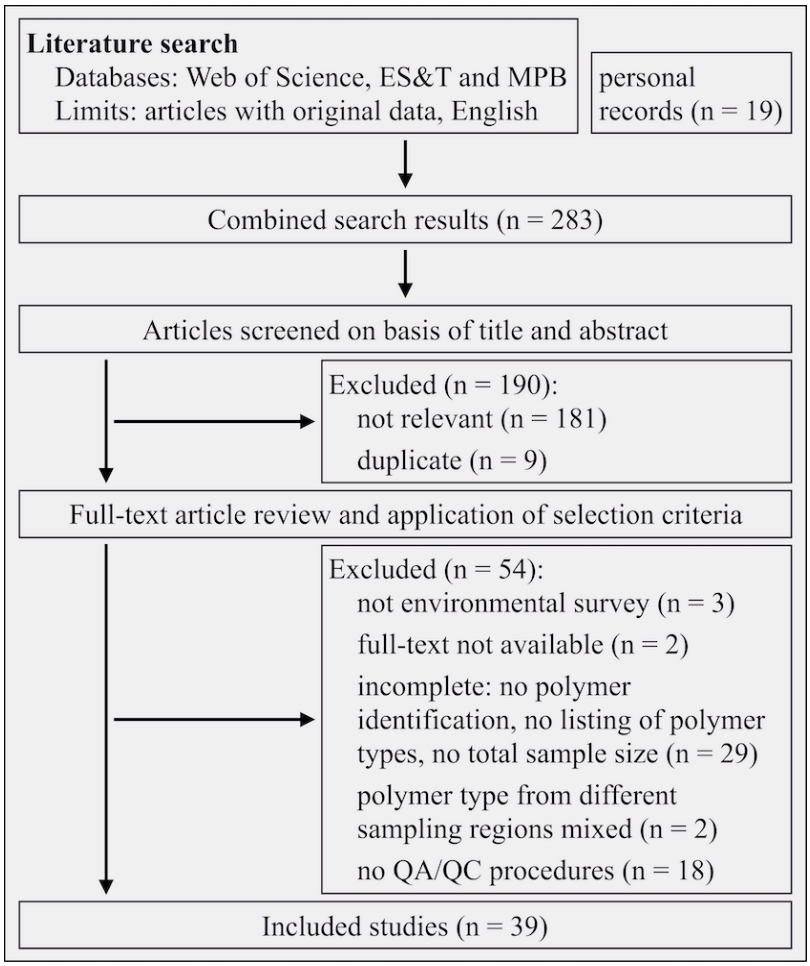

Figure 5. Flow diagram of study selection. ES&T: Environmental Science & Technology; MPB: Marine Pollution Bulletin.

2.3.2 Quality assessment and data extraction

Literature assessment was performed, in accordance with the predefined criteria described above. In a first step, publications were screened for relevance as environmental surveys by their title and abstract. In a second step, the materials and methods section of each publication was checked to assure that synthetic polymer types had been identified, and total sample size of the characterized polymer types was reported. If total sample size was missing, respective corresponding authors were contacted *via* email. Given the importance of controlling for contamination in microplastic research (Hidalgo-Ruz et al., 2012), studies were further checked for quality assurance and quality check (QA/QC) procedures. Studies that failed to describe any type of control measures were no longer considered.

A sheet was developed for systematic data extraction. Data was recorded independently by two authors as follows: sample type (*i.e.* water or sediment), water

type (*i.e.* marine or fresh), sampled zone (*i.e.* intertidal, subtidal, sea surface, water column, deep sea water (> 200 m depth) and deep sea sediment (> 200 m depth)), plastic extraction method (*i.e.* visual or density separation including employed density), maximum considered particle size, total sample size of characterized plastic particles, identified polymer types, and their respective relative abundance. Disagreements between reviewers during data extraction were resolved by consensus. In microplastic studies that did not report maximum particle size, a maximum particle size of 5 mm was assumed if such a definition was found in the introduction. In studies that reported microplastics from the environment as well as from biota, only microplastics from the free environment were considered. Separate entries were recorded for data from the same study if researchers sampled in different zones (*i.e.* depth related). Because the present analysis focused on purely synthetic polymers, where relevant, total sample sizes and polymer proportions were adjusted to account for the exclusion of cellulose-based polymers, such as rayon, cellophane and cellulose acetate, which in some studies were included as artificial polymers. The raw data are included in APPENDIX 4.

Despite the focus on prevalence of polymer types in each sampled zone, we also considered reported plastic concentrations (particles m^{-3}). For studies that did not report particle concentrations by volume, these were calculated using total reported number of particles and total reported sampling volume. Polymer specific concentrations were then obtained based on respective polymer type prevalence. Absolute particle concentrations could be obtained or calculated from 20 studies.

2.3.3 Statistical analysis

The main outcome of interest in meta-regression models was the proportion of individual polymer types. The pooled prevalence of polymer types was calculated with arcsine square root transformed proportion data, because proportions of 0 commonly occurred. Potential bias at the level of polymer type was investigated *via* funnel plots and the significance of eventual biases was tested for using *Trim and Fill* followed by Egger's regression tests. Heterogeneity was assessed using the I^2 statistic *via* random effects models using the Paule-Mandel estimation method, which was previously found to be a better alternative for dichotomous data than other estimators (Veroniki et al., 2016). Mixed effects meta-regression models were then employed for each of the studied polymer types separately, to test if the

moderators sampling zone, debris size (*i.e.* studies reporting microplastic only or general plastic debris) and water type (*i.e.* fresh or saline) affected polymer type prevalence. To find the simplest possible model, explanatory variables were dropped stepwise and likelihood ratio tests were used to assess if the simplified models were significantly different from their previous versions.

To evaluate how methods to extract microplastics from sediments could have biased our results, such as an inflated prevalence of low-density polymers due to lower density extraction protocols, we estimated diversity of polymer types in sediment samples from intertidal and subtidal zones, as well as the effect of different extraction methods (*i.e.* solutions with density $\rho < 1.5$ g cm^{-3} and $\rho \geq 1.5$ g cm^{-3}). For this, Shannon's diversity indices were calculated and, for ease of interpretation, converted to effective numbers of polymer types (Jost, 2006). Standard errors (SE) were obtained *via* bootstrapping with 100 iterations. The threshold for density separation was set at $\rho = 1.5$ g cm^{-3}, because all but one of the polymer types considered here, should theoretically be extracted *via* a solution of $\rho \geq 1.5$ g cm^{-3} (Table 1).

All analyses and plotting were performed in R (version 3.4.3, R Core Team 2017), using the packages *meta* (Schwarzer, 2007), *metaphor* (Viechtbauer, 2010), *vegetarian* (Charney and Record, 2012), and *ggplot2* (Wickham, 2009).

2.4 Results

2.4.1 Summary of included studies

The present meta-analysis draws data from 39 studies. Initially, our literature search identified a total of 283 studies, but 190 were discarded after title and abstract screening, because they were not relevant to the topic (Figure 5). After full-text review of the remaining 93 studies, another 53 were discarded mainly because authors did not report the polymer types and/or total sample size remained incomplete after contacting corresponding authors (n = 29), but also due to absent QA/QC measures (n = 18). Further studies were excluded because they did not contain environmental data (n = 3), full text was not available (n = 2), or authors did not report polymer types from different sampling depths separately (n = 2). Missing total sample size or clarifications on the data were obtained from corresponding

authors in seven of the final 39 studies considered (Bergmann et al., 2017; Castillo et al., 2016; Cózar et al., 2014; Graca et al., 2017; Hendrickson et al., 2018; Readman et al., 2013; Song et al., 2014).

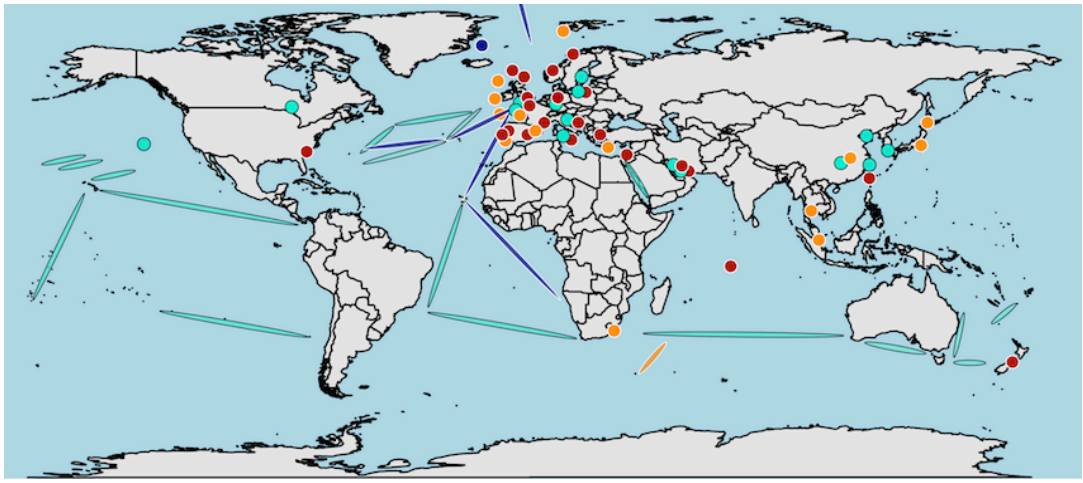

Figure 6. Sampling sites of studies included in the review. Sampling zones are indicated: teal, surface water; dark blue, water column; orange, subtidal and deep sea; red, intertidal.

Polymer type data for different sampling zones stemmed from 17 water surface studies, 4 water column studies, 13 intertidal studies, 6 subtidal studies and three deep sea studies, including double entries for four studies (for references see Figure 8). The subtidal studies were conducted in shallow regions with average sampling depths ranging between 6–59 m (median = 17.25 m), while the deep sea studies sampled at average depths of 2250 m, 2227 m, and 3496 m. Eight studies contained data from fresh water and estuarine sites, while 32 studies had marine data (including one study that sampled in both). In total, data on 24 different polymer types were recorded (Table 1), but due to sparsity of the data, meta-regression models were employed to study those that were most abundant: PE, PP, polystyrene (PS) and the group PP&A (polyesters, PEST; polyamide, PA; and acrylics). The latter were grouped to improve data (higher counts) and facilitate classification (composited); all members are denser than seawater. Despite that rare polymer types were not studied in greater detail, they were not subtracted from total particle counts; estimated relative abundance of PE, PP, PS and PP&A are therefore based on total characterized particle counts from all 24 polymer types.

2.4.2 Prevalence of polymer types in different aquatic zones

Pooled prevalence data confirmed that PE was the most abundant plastic type polluting aquatic environments with a predicted relative abundance of 23% (95% confidence interval 15-32%). The second most abundant polymer was of the group PP&A (20%; 95% confidence interval 11-32%), followed by PP (13%; 95% confidence interval 7-20%) and PS (4%; 95% confidence interval 2-9%). No significant publication bias was revealed by Egger's regression tests for any of the investigated polymer types (Figure 7, PE: Z = –1.59, p = 0.111; PP: Z = 1.08, p = 0.279; PS: Z = –0.48, p = 0.635; PP&A: Z = 1.42, p = 0.156). Nevertheless, we found high heterogeneity (I^2 = 98%) between studies at the level of all polymer types (Figure 8 and APPENDIX 5.1-5.5), indicating that the surveys did not share a common effect size.

Potential sources of heterogeneity were explored with meta-regressions using three categorical moderators, *i.e.* debris size, water type, and sampling zone. The simplest model for all polymer types, except PS, included a single significant moderator (*i.e.* sampling zone; see Table 2 for statistical details), indicating that of the moderators considered here, only "sampling zone" could explain part of the variability in polymer type prevalence observed between studies. PE and PP were relatively more abundant in surface samples (PE: 42% and PP: 25%) compared to water column- (PE: 9%, Z = -2.55, p = 0.011 and PP: 3%, Z = -2.46, p = 0.014), and intertidal samples (PE: 18%, Z = 2.61, p = 0.009 and PP: 5%, Z = 2.66, p = 0.008, Figure 8). While the

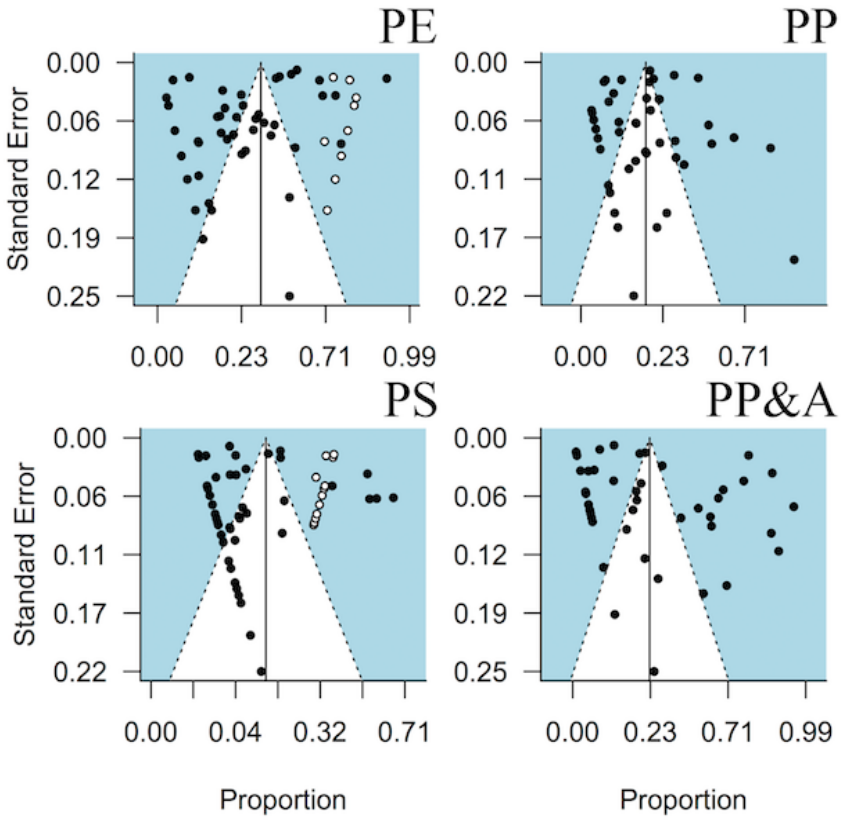

Figure 7. Bias testing for prevalence of different polymer types in aquatic environments. Full circles represent studies and empty circles represent imputed studies. PE, polyethylene; PP, polypropylene; PS, polystyrene; PP&A, polyester, polyamide and acrylics; EPR, ethylene-propylene rubber.

Table 2. Summary of model simplification for meta-regression.

Models	LRT-score, *p*-value							
	PE		PP		PS		PP&A	
~debris type*sampling location	02.6	0.108	0.08	0.783	3.97	0.046	0.00	1.000
~sampling location	03.3	0.069	0.01	0.909	1.66	0.198	0.09	0.755
~1	15.3	**0.004**	11.5	**0.022**	5.74	0.219	17.9	**0.001**

Note: Full starting model included the explanatory variables water type*debris type*sampling zone*; rows in table depict sequentially simplified models (*i.e. *after dropping a variable) for each investigated polymer type (*i.e. *PE, PP, PS, PP&A) with associated likelihood ratio test scores for comparison between preceding and simplified models and corresponding* p-*values. A* p-*value in bold denotes significant model simplifications,* i.e. *the dropped variable should be kept in the model.*

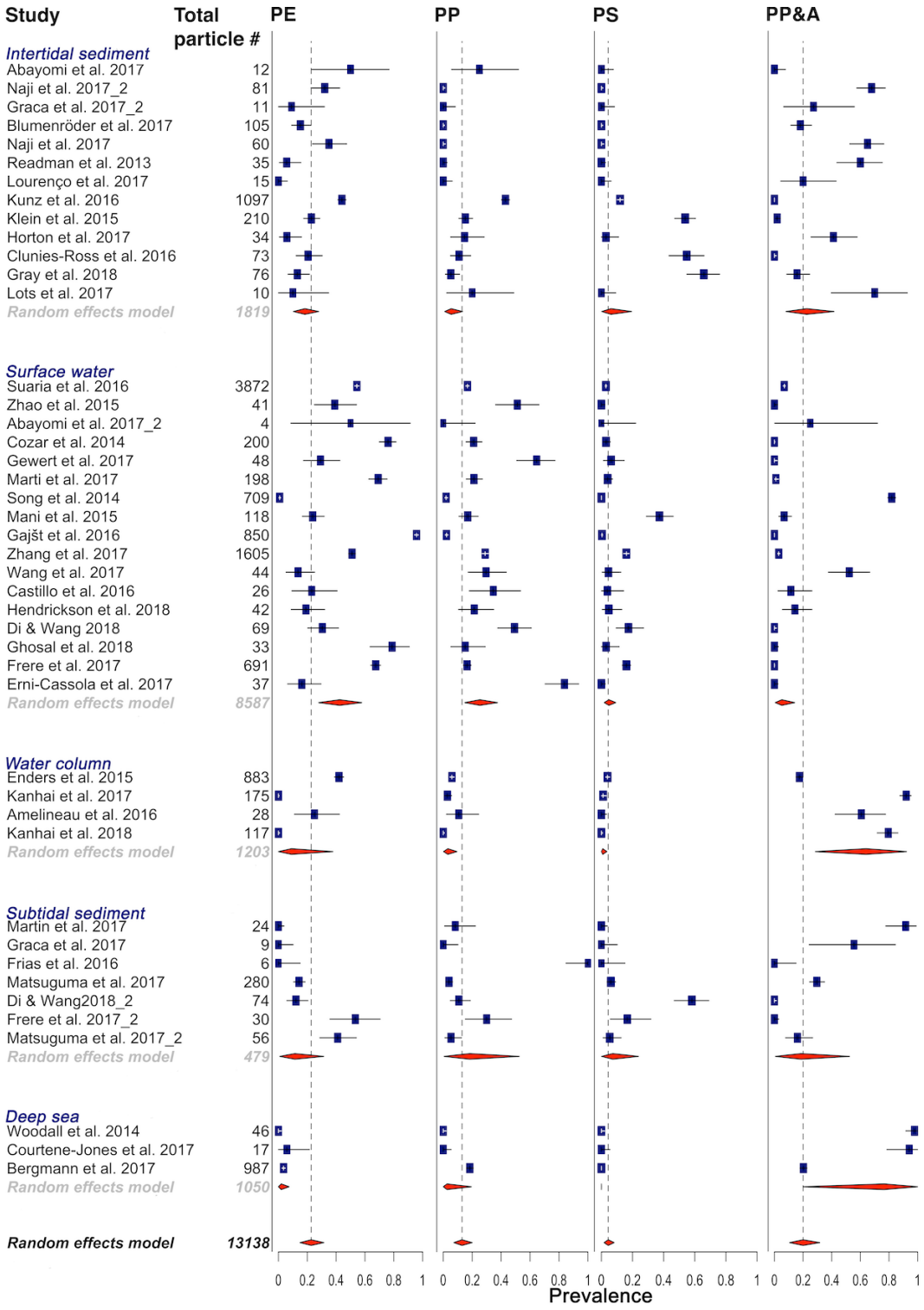

Figure 8. Prevalence forest plots for analysed polymer types. For statistical details, including heterogeneity (I^2), see individual polymer type forest plots in APPENDIX 5.1-5.5. Red diamonds represent subgroup means, while the bottommost indicates the overall mean, also represented via the dotted line. PE: polyethylene; PP: polypropylene; PS: polystyrene; PP&A: polyester, polyamide and acrylic.

abundance of PE was also higher in surface water than subtidal sediments (11%, Z = -2.29, p = 0.022) and the deep sea (2%, Z = -3.15, p = 0.002), differences between PP prevalence in surface water compared to subtidal sediments and deep sea remained statistically insignificant (18%, Z = -1.08, p = 0.279; 3%, Z = -1.87, p = 0.061). In contrast, prevalence of PP&A was highest in deep sea- (77%) and water column samples (64%), and significantly lower in sea surface samples (5%, Z = 3.519, p = 0.0004; Z = 3.344, p = 0.0008 respectively). Despite accounting for sampling zone, heterogeneity remained very high throughout subgroups (I^2 > 87 %, APPENDIX 5.1-5.5) indicating that further important moderators were missing from the models and that subgroups still did not share common effect sizes.

Additional variation can for instance stem from inconsistencies among sampling methodologies. We therefore investigated whether variations in microplastic extraction methods for sediment samples yielded different effective numbers of polymer types between and within intertidal- and subtidal samples (subset of 20 studies with Graca *et al.* (2017) having sampled both intertidal and subtidal sediments). Microplastics were extracted using three different methods: visually in two studies (1 intertidal, 1 subtidal), with lower density solutions in 12 studies ($\rho < 1.5$ g cm^{-3}, 9 intertidal, 2 subtidal), and with higher density solutions in 6 studies ($\rho \geq 1.5$ g cm^{-3}, 3 intertidal, 3 subtidal). Due to only one study employing visual extraction in each sampling zone, these were not further considered. The analysis showed that extractions with higher density solutions (*i.e.* $\rho \geq 1.5$ g cm^{-3}) yielded more diverse samples compared to lower density solutions (Figure 9). This suggests that results from studies employing lower density separation solutions could be biased against higher density polymer types and, therefore, underestimate total plastic loads. Moreover, we acknowledge that further variables can influence results from density extractions, such as shaking- and settling times, which also varied considerably among the considered studies, and remained unaccounted for in this meta-analysis.

Among the sea surface studies, the most common mesh sizes were comparable, ranging between 300–335 µm, with three studies deviating (120 µm, Castillo et al., 2016; 48 µm, Di and Wang, 2018; 200 µm, Suaria et al., 2016). Similarly, Kanhai et al. (2018, 2017) employed 250 µm sieves to sample subsurface water, while Amélineau et al. (2016) analysed the fraction > 500 µm. Narrower mesh sizes were used to filter deep sea water (80 µm, Courtene-Jones et al., 2017), as well

as for recovery of particles from deep sea sediments (Whatman GF/A or 32 µm, Woodall et al., 2014), which unfortunately reduces comparability. Particle concentrations from intertidal samples stemmed from the widest ranges of mesh and sieve sizes: 0.025–1 mm. Despite surface water sampling being rather standardized, *i.e.* most studies performed surface tows and used similar mesh sizes (200 – 300 µm), it is noteworthy, that where PP&A was present, its concentration was similar to the other polymer types (Figure 10). This could be site specific, but may also indicate that PP&A are missed by surface tow sampling. Interestingly, Song et al. (2014) showed that surface microlayer sampling not only yielded ~82 % PP&A (see outlier in Figure 8), but also resulted in the highest particle concentrations when compared to other surface sampling methods and therefore surface microlayer sampling offers an interesting complementary sampling to surface tows.

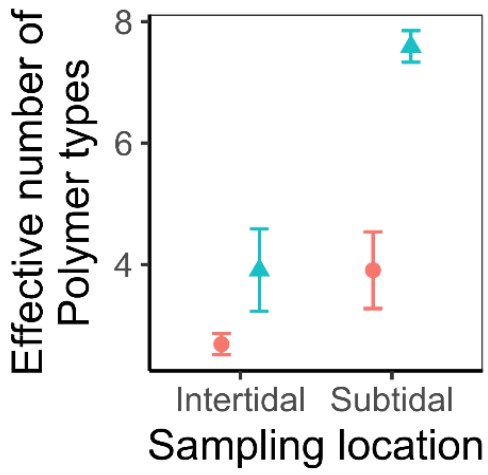

Figure 9. Effective number of polymer types from sediment samples. Number (± SE) is based on Shannon alpha diversity. Red, round: extracted with $\rho < 1.5$ g cm^{-3}, n = 12; turquois triangle: extracted with $\rho \geq 1.5$ g cm^{-3}, n = 6.

2.4.3 Polymer concentrations in different aquatic zones

All common polymer types were most enriched in intertidal sediments (~ 10^3 – 10^4 particles m^{-3}, Figure 10). In surface waters, concentrations were four orders of magnitude lower than in intertidal sediments (~ 0.1 – 1 particle m^{-3}), with three exceptions from China and Korea, which presented similar concentrations to intertidal sediments. The data further indicated that subsurface waters contained plastics in similar concentrations to sea surfaces, although the water column was mainly polluted by PP&A (Figure 11). As previously reported, the concentration of particles detected in deep sea sediments was higher than what was found in intertidal sediments (> 10^4 particles m^{-3}; Woodall et al., 2014) although, interestingly, no PE or PP were reported in that study.

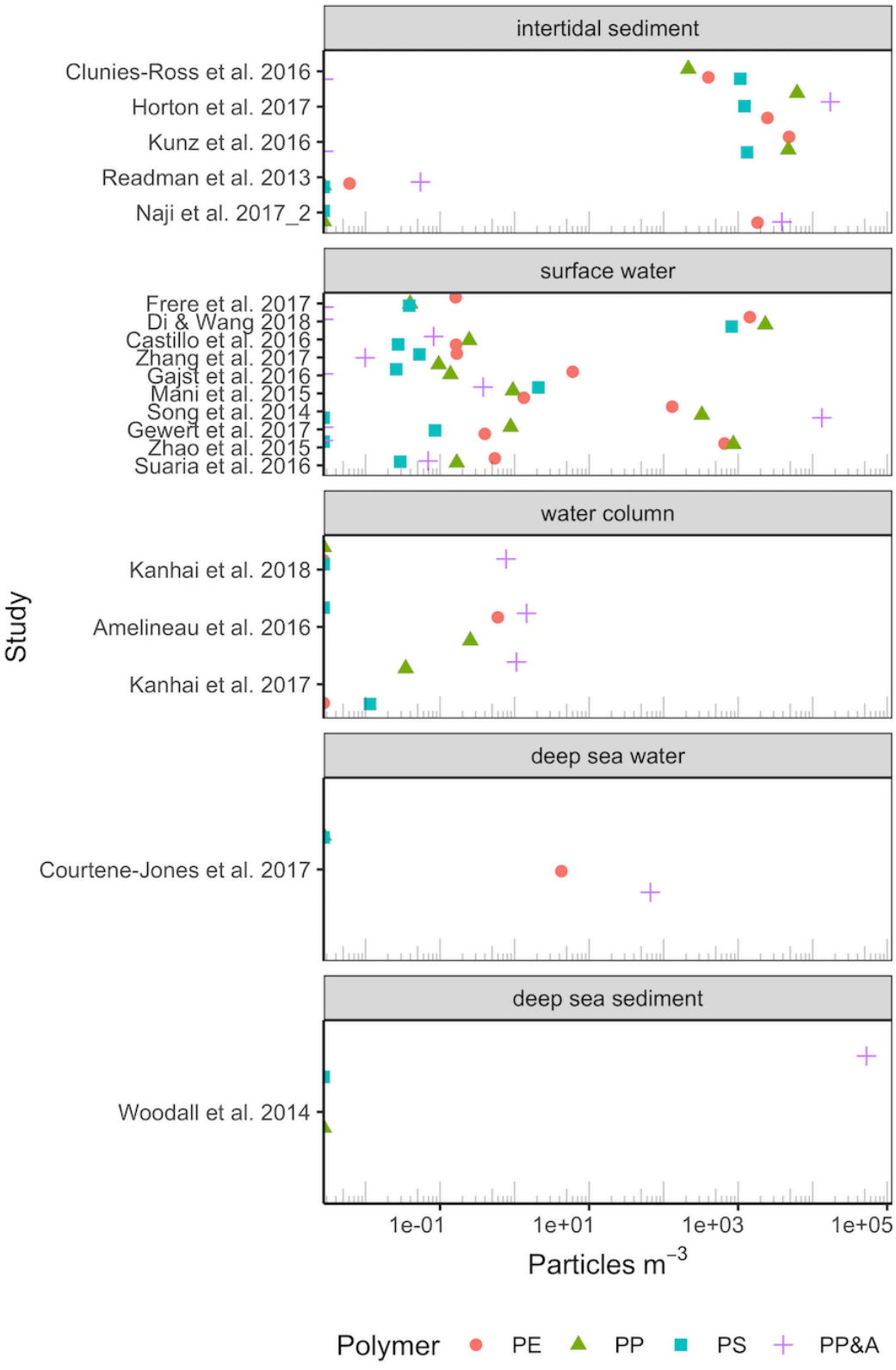

Figure 10. Concentration of different polymer types within the different sampling zones. PE: polyethylene; PP: polypropylene; PS: polystyrene; PP&A: polyester, polyamide and acrylic.

2.5 Discussion

Our meta-analysis confirmed that PE, PP, PS and PP&A were among the most abundant polymer types in aquatic environments. This is not surprising as these materials accounted for 74% of global plastic production in 2015 and are commonly used in short life-cycle products (Geyer et al., 2017; PlasticsEurope, 2018). Here we show that the relative abundance of low-density polymer types (*i.e.* PE and PP) is highest in open sea surfaces, but lower in intertidal- or subtidal samples, and further decreases in subsurface water (Figure 11). In turn, plastics denser than seawater, such as polyester, polyamide and acrylics (PP&A), were relatively more abundant in subsurface water than on sea surfaces. The available data from the deep sea further revealed PP&A as the dominant group of plastics in these environments (77%, Figure 11), as well as chlorinated PE (Bergmann et al., 2017), which is similarly dense and mostly added to PVC ($\rho \sim 1.16$ g cm^{-3}, Akovali, 2012). The relative abundance of different polymers remained similar between shallow intertidal and subtidal sediments, which indicates similar sedimentation rates for the examined polymer types. Data from the open ocean further off-shore however, suggests a segregation between polymers through the water column. The idea that deep sea sediments constitute a final sink for all polymer types, i.e. low- and high density, is thus not well supported, as only high density polymers were highly enriched in deep sea water and sediments.

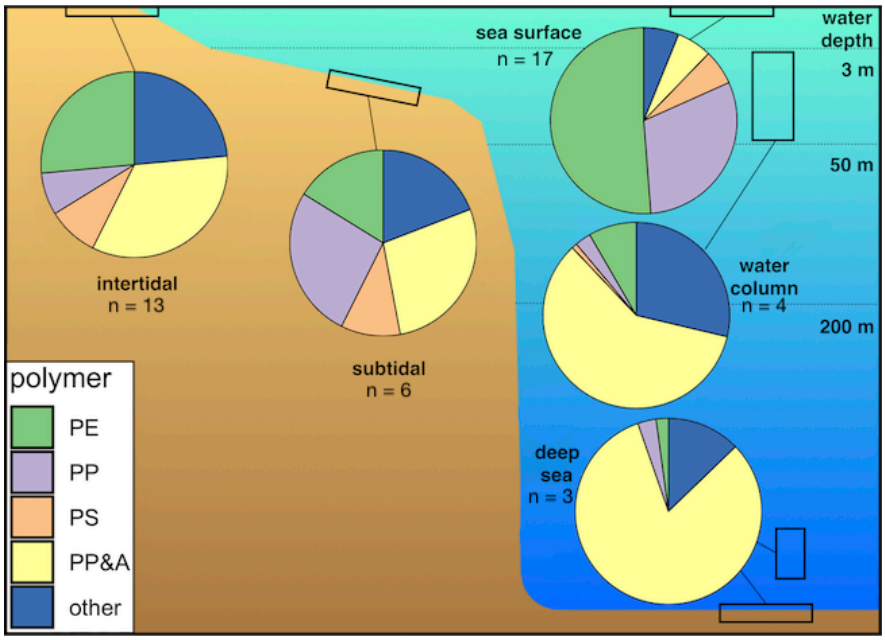

Figure 11. Relative abundance of common polymer types in different sampling zone. Pie charts represent abundance data normalized to model predictions. For details see forest plots in supplementary information (Figs. S2–S5). PE: poly- ethylene; PP: polypropylene; PP&A: polyester, polyamide and acrylic; PS: polystyrene. Number of studies in each zone is indicated (n).

If deep sea sediments were the major sink for microplastics in marine systems, we would expect to find throughout the water column similar proportions of polymer types as observed in coastal zones. Moreover, if sinking was a principal mechanism for removal of all types of sea surface plastics, then relative abundance of polymer types should remain similar between surface water and the water column, as well as the deep sea. Particle concentrations supported the trends observed from our prevalence-based analyses (Figure 11). Given the segregation of different polymer types found here, it is important to reconsider the sink of those plastics "missing" from surface seawater (mainly PE and PP; Cózar et al., 2014). Recent studies have already highlighted that up to 97% of this material might have been overlooked, if sampling methods and analysis did not account for vertical mixing (Brunner et al., 2015; Kooi et al., 2016) or if methods for quantifying the smaller fraction of microplastics (*i.e.* <1 mm) were not implemented (Enders et al., 2015; Erni-Cassola et al., 2017). Simulations predicted that buoyant PE microparticles would persist and oscillate in the water column (Kooi et al., 2017), but the overall relatively low abundance of PE and PP in studies that have sampled the water column (Figure 8 and APPENDIX 5.1-5.5), and the lack of evidence for significant

plastic debris in sediment traps from the North Atlantic gyre (Law et al., 2010), suggest that this issue may be more complex than anticipated. For instance, small buoyant microplastics sink as part of faecal pellets when ingested (Cole et al., 2016) or when incorporated in marine snow (Long et al., 2015; Porter et al., 2018), but it is uncertain for how long microplastics remain in such particulate organic matter, since (I) faecal pellets containing microplastics are more likely to fragment (Cole et al., 2016), (II) zooplankton is known to break up larger aggregates (Moriceau et al., 2018), and (III) organic material is remineralized in marine aphotic zones (Azzaro et al., 2006), altogether perhaps leading buoyant microplastics to reemerge. Deposition of buoyant microplastics may therefore occur more likely in photic-, rather than aphotic sediments, which would stand in agreement with our results (Figure 11). All of these points, coupled to the analysis we present here, do not allow to conclude that buoyant polymer types reliably sink out of the water column, and emphasize that additional sampling of the deep sea water column and sediments, as well as data from sedimentation traps are necessary to provide an answer to this question.

Unexplained heterogeneity between studies remained very high, despite accounting for sampling depth, highlighting that important moderators remained unaccounted for in the analysis. For instance, local prevalence of specific polymer types may vary with the presence of production plants or specific activities that release characteristic types of polymers (*e.g.* the large number of acrylics found in Song et al., 2014; Figures 10, 11), but it is currently not possible to have higher spatial resolution. Moreover, it is evident that differences between sampling methods, such as different surface water sampling techniques or the densities employed to extract plastics from sediments can account for variability in results, as detailed above (section 2.4.2), and we thus concur with Hanvey *et al.*'s (2017) call to harmonize methods of plastic extraction from samples and to standardize the density of the extraction solution.

Occurrence and transportation of microplastics in the oceans is subject to wave-driven turbulent mixing (Brunner et al., 2015), as well as plastic properties, such as particle size and shape (Filella, 2015; Zhang, 2017). For instance, unlike other polymers, relative abundance of PS did not significantly change with the sampled zone. This could be explained by the two distinct forms of PS, *i.e.* "solid" PS ($\rho \sim 1.04$ g cm^{-3}) or expanded PS ($\rho < 0.05$ g cm^{-3}), which behave differently in water. The very low-density form is expected to remain on sea surfaces and intertidal

areas (Figure 10; Chubarenko et al., 2016), whereas the denser form of PS should theoretically sink, thus explaining the occurrence of PS in subtidal samples (7%, Figure 8).

Undoubtedly, concentration and prevalence of plastic polymer types in aquatic environments vary with geographic location, *i.e.* in response to local sources of pollution, such as densely populated coastal regions (Browne et al., 2011) and with distance to coast (Pedrotti et al., 2016), but also within sampling sites (Eo et al., 2018), the shape of the particles (Kooi et al., 2016), and with the sampling methodology used. While all polymer types can be found in any given sampling zone, our meta-analysis reveals a general trend in relative abundance of four common polymer types in different sampling zones and highlights important knowledge gaps as well as reporting issues. Here, we cannot confirm that buoyant polymer types reliably sink out of the water column, and hence, further research is required to determine the ultimate fate of buoyant plastic polymers such as PE and PP, a fundamental requirement to assess the real risk plastic pollution poses to aquatic life.

CHAPTER 3:

LOST, BUT FOUND WITH NILE RED; A NOVEL METHOD TO DETECT AND QUANTIFY SMALL MICROPLASTICS (20 µm–1 mm) IN ENVIRONMENTAL SAMPLES

3.1 Summary

Marine plastic debris is a global environmental problem. Surveys have shown that plastic particles <5 mm in size, known as microplastics, are significantly more abundant in surface seawater and on shorelines than larger plastic particles. Nevertheless, quantification of microplastics in the environment is hampered by a lack of adequate high throughput methods to distinguish and quantify smaller size fractions (<1 mm), and this has probably resulted in an underestimation of actual microplastic concentrations. Here we present a protocol that allows high throughput detection and automated quantification of small microplastic particles (20–1000 µm) using the dye Nile red, fluorescence microscopy and image analysis software. This protocol has proven highly effective in the quantification of small polyethylene, polypropylene, polystyrene and nylon 6 particles, which frequently occur in the water column. Our preliminary results from sea surface tows show a power-law increase of small microplastics (*i.e.* <1 mm) with decreasing particle size. Hence, our data helps to resolve speculation on the '*apparent'* loss of this fraction from surface waters. We consider that this method presents a step change in the ability to detect small microplastics by substituting the subjectivity of human visual sorting with a sensitive and semi-automated procedure.

3.2 Introduction

It has been estimated that mismanagement of plastic waste resulted in up to 12.7 million tonnes of plastic entering the ocean in 2010 alone (Jambeck et al., 2015). In the environment, plastics accumulate due to their recalcitrant nature, contaminating sediments and surface seawaters on a global scale (Barnes et al., 2009; Wright et al., 2013). In aquatic systems, polymer types with lower density than seawater have a higher transportability (*via* rivers (Mani et al., 2015) into marine coastal areas and

oceanic gyres (Cózar et al., 2014)) than higher density polymers, which tend to settle out (Claessens et al., 2011; Pedrotti et al., 2016; Woodall et al., 2014). Lower density plastics, such as polypropylene (PP), polyethylene (PE) and certain forms of polystyrene (PS) are frequently used as packaging materials (PlasticsEurope, 2018) and hence, have a very short service life prior to disposal. These types of plastic are also more commonly found in environmental surveys (Gajšt et al., 2016; Suaria et al., 2016).

Eriksen et al. (2014) estimated that about 5.25 trillion plastic fragments are currently floating on the ocean's surface. Extensive sampling of surface seawater and comparison across all size classes (>200 μm) has shown that plastic particles <5 mm are significantly more abundant than larger particles (Cózar et al., 2015, 2014; Eriksen et al., 2014). These plastic fragments (<5 mm) have been considered as microplastics (Moore, 2008; Thompson et al., 2004). Marine microplastics are composed of two main types: (1) primary microplastics that stem directly from the source, such as microbeads contained in cosmetics, or fibres released during washing of synthetic garments (Browne et al., 2011), and (2) secondary microplastics that are generated through macroplastic fragmentation, a break down process influenced by UV-irradiation, high temperatures and mechanical shear forces (Andrady, 2011; Corcoran et al., 2009). Morét-Ferguson et al. (2010) found that the average size of buoyant plastic particles in the Northern Atlantic and Caribbean had halved in size from an average 10 mm in the 1990s to 5 mm in the 2000s. The decrease in average size of plastic marine debris is of concern because the smaller synthetic polymers are ingested by relatively more organisms at the base of the marine food web (Wright et al., 2013). Recent studies suggest that ingested particles can be transferred between trophic levels (Setälä et al., 2014; Watts et al., 2014) and transport persistent organic pollutants (Teuten et al., 2009). The possible environmental effects of microplastics has led to growing public and media attention as well as policy measures to reduce inputs, such as banning the use of plastic microbeads in personal care products (Rochman et al., 2015). Besides these concerns and abatement measures, monitoring of marine litter is currently required in the EU under the Marine Strategy Framework Directive (MSFD; Hanke et al., 2013) and it is therefore essential to have reliable, reproducible, rapid and inexpensive methods for quantification and monitoring of microplastic contamination in the environment.

Current methodology for quantification of environmental microplastic contamination is hampered by a lack of methods that are both sensitive and allow high throughput quantification. Commonly applied methods separate synthetic microparticles from non-synthetic materials *via* density separation and floatation techniques, before visually sorting the particles and finally confirming their identity with spectroscopy (Hidalgo-Ruz et al., 2012). The data generated can result in an underestimate of small microplastics because of the visual step in the process (Lavers et al., 2016). Alternative, faster and less expensive protocols are of particular importance for routine monitoring of plastic contamination by regulatory bodies and the need for developing new methods has been clearly identified as a policy priority (MSFD; Hanke et al., 2013). Here, we adopt the sampling criteria proposed by the EU technical subgroup on marine litter (Hanke et al., 2013), who recommend two categories: *large* microplastics ranging from 5 mm–1 mm in size (visually recognizable) and *small* microplastics ranging from 1 mm–20 µm for which reliable quantification is still challenging.

In this study, we present the application of a fluorescence-based protocol using Nile red to detect and quantify small microplastics in environmental samples. This method is inexpensive, employs readily available equipment and can be semi-automated for high throughput sample analysis. The method requires a sample purification step, fluorescence microscopy (green fluorescence protein settings) and free image analysis software.

3.3 Materials and Methods

3.3.1 Microplastic staining and quantification protocol validation using commercial synthetic polymers

Nile red had been suggested as a tool to fluorescently label microplastics (Andrady, 2011, 2010), and its use was later demonstrated (Cole, 2016; Shim et al., 2016). The dye is commonly dissolved in acetone (Rumin et al., 2015), but here methanol was chosen because common plastics are resistant to it. The fluorescence of Nile red is influenced by its concentration, which lies optimally between 0.1 and 2 µg mL^{-1} (Rumin et al., 2015), and higher concentrations lead to quenching (Rumin et al., 2015). Accordingly, the working solution for this study was prepared by dissolving

Nile red (technical grade, N3013, Sigma-Aldrich) in methanol to a concentration of 1µg mL^{-1}.

Staining efficacy and automated particle detection was tested on nine different polymer types: PE (powder, ~40–48 µm, Sigma-Aldrich), poly(ethylene terephthalate) (PET, powder, ≤300 µm, GoodFellow), PVC (powder, ~80–148 µm, Sigma-Aldrich), nylon 6 (pellets, ~1 mm, Sigma-Aldrich), PP (pellets, ~7 mm, Sigma-Aldrich), PS (pellets, ~5 mm, Sigma-Aldrich), PC (fragment from panel, ~10 mm), polyurethane (PUR, pellets, ~3 mm, Sigma-Aldrich), and black tire rubber (fragment from bicycle tire, 7×4 mm). Nylon 6 microplastics were prepared by heating the pellets and pulling them apart to produce thin fibres, which then were cut to microparticles (~63–91 µm) under a dissection microscope. PP pellets as well as black rubber were ground in liquid nitrogen with mortar and pestle to obtain small microplastic fragments (PP: ~20–130 µm, black rubber: ~57–171 µm). PS and PC microparticles were obtained by sanding the pellets with a metal file and further cutting the obtained particles with a scalpel under a dissection microscope to the final sizes (PS: ~24–196 µm, PC: ~94–169 µm). PUR pellets were directly cut to size under a dissection microscope (~71–154 µm). Sizes of all microparticles produced in the laboratory were calculated from the square root of particle area, which was measured in ImageJ using brightfield microscope images. Ten particles of each polymer type were placed on separate clean PC track-etched filter membranes (PCTE, 25 mm diameter, 10 µm pore size, Whatman) to evaluate the efficiency of detection of our protocol. PCTE filters are optimal for two reasons: (1) their hydrophilic surface avoids Nile red background fluorescence and (2) translucent properties when exposed to methanol allow brightfield microscopy in addition to fluorescence microscopy. About 2–3 drops of Nile red solution were carefully added to cover each filter. Filters were placed on standard microscope slides, covered with cover slips and fixed with tape to avoid movement of the sample. The samples were then maintained for 10 minutes at 60 °C in the dark.

Microscopic imaging was performed using a light microscope (Nikon Eclipse Ti) equipped with a widefield camera (Andor Zyla sCMOS) and a LED for fluorescence. We tested the fluorescence of the nine different polymers stained with Nile red on PCTE filters in green (excitation/emission 460/525 nm) and red (565/630 nm). Green fluorescence was chosen over red fluorescence because (1) synthetic polymers either fluoresced better in green (Figure 12 a-d) or fluorescence did not

differ significantly (Figure 12 e), (2) natural contaminants fluoresced in red but not in green after hydrogen peroxide (H_2O_2) digestion (Figure 13, discussed below) and (3) background signal from the filter membrane was lower. Three types of whole filter images were obtained for each polymer type: red and green fluorescence, as well as brightfield, all at a magnification of 10×. Exposure time for fluorescence was 30 ms at 30% LED strength.

Automated particle recognition and quantification based on the fluorescent images was performed in ImageJ (v1.50i). A macro was written to perform the following tasks: (1) set the scale, (2) subtract the background using a rolling ball radius of 1500 pixels, (3) convert images to 8bit, (4) adjust black and white thresholds using 29 and 175 as the lower and higher values of pixel brightness, and finally (5) quantify particles based on area (400 – ∞ μm^2). The size detection limit was set to 400 μm^2 to ensure that pores from the filter membrane (diameter = 10 μm) did not interfere in particle measurements.

3.3.2 Validation of the pre-staining digestion protocol

To prevent overestimation of synthetic particles in environmental samples, it is of critical importance that biogenic materials, such as lipids, chitin or wood lignin, which fluoresce when stained with Nile red (Figure 13 a, c), are eliminated or cease to fluoresce when stained. While digestion with nitric acid proved highly efficient at removing biogenic matter, its application is limited due to pH-sensitive polymers, such as PS particles, which melt together, or Nylon fibres, which are lost during the process (Claessens et al., 2013). A chemical alternative is given with H_2O_2 treatments, against which common synthetic polymers are resistant (Claessens et al., 2013; Tagg et al., 2015). Hence, digestion of biogenic material was performed as previously described by Claessens et al. (2013) with slight modifications. Briefly, 20 ml of 30% H_2O_2 was added to 250 mL Erlenmeyer flasks containing the filtered samples on PCTE filters, which were then kept at 60 °C for 1 h followed by a prolonged 7 h step at 100 °C.

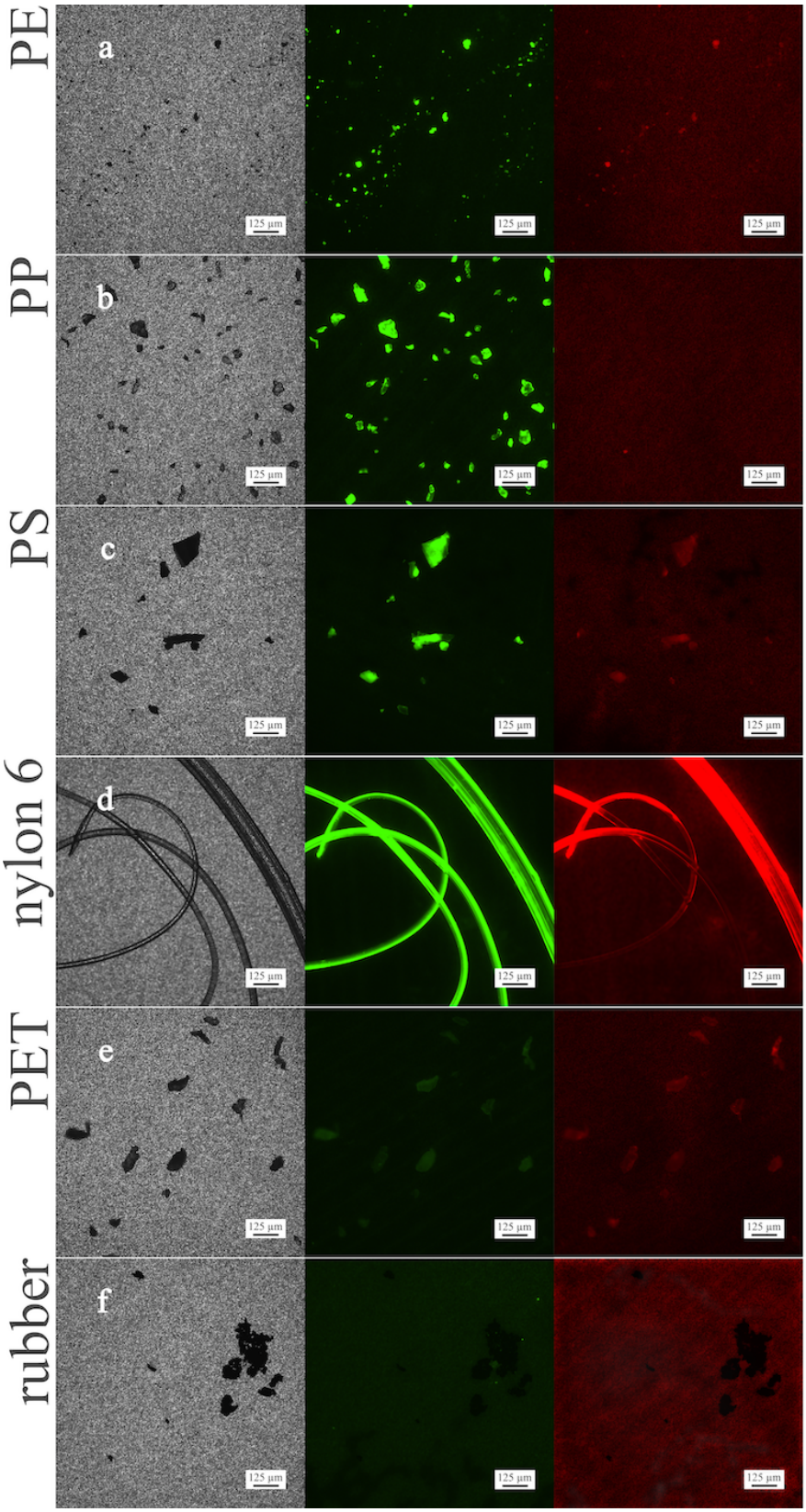

Figure 12. Microscope images of microplastics on PCTE filter membranes stained with Nile red. For each polymer type (a-f) three versions of the same microscope field are shown; from left to right: brightfield images, then fluorescent image at excitation/emission 460/525 nm (green) and fluorescent image at excitation/emission 565/630 nm (red).

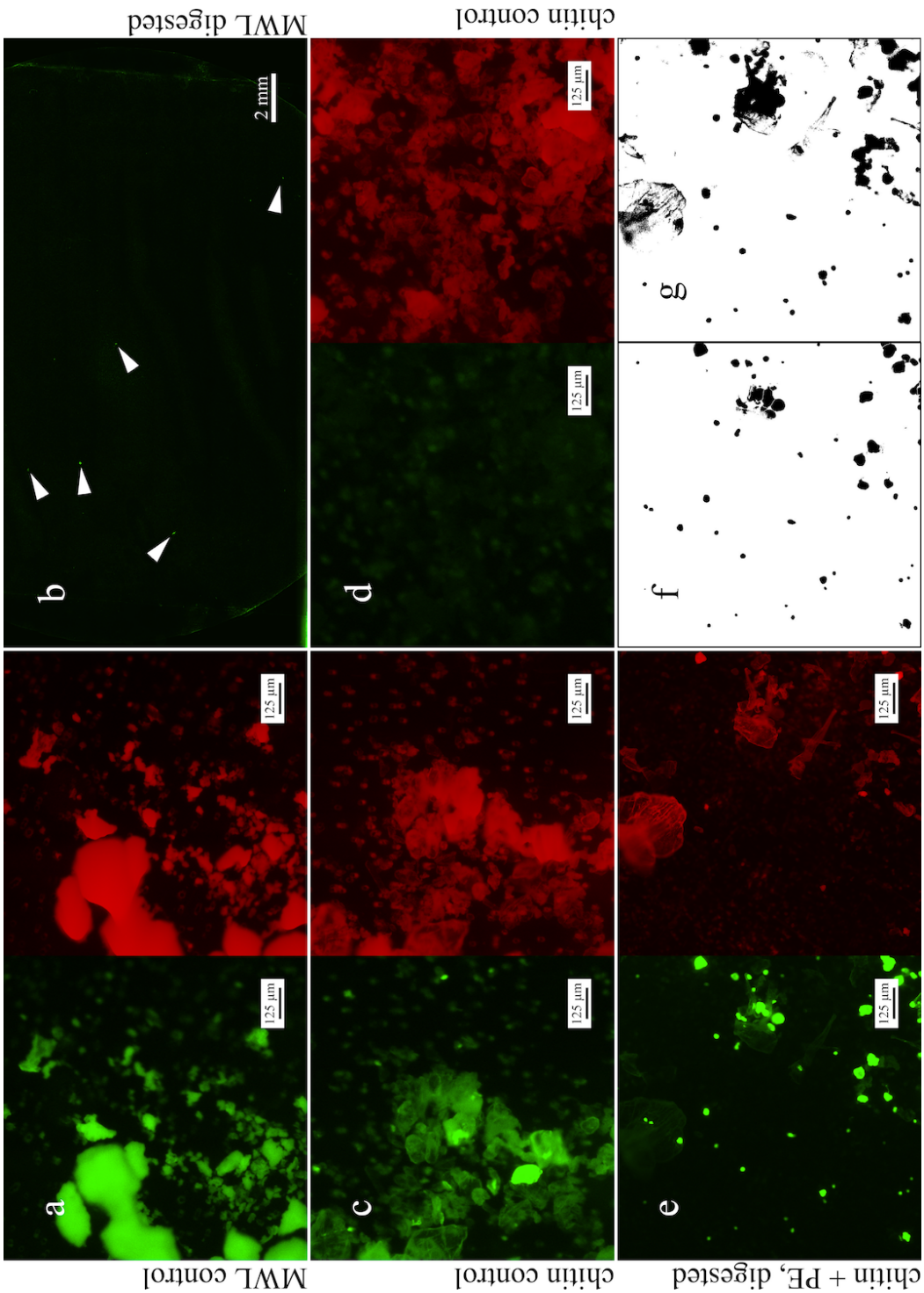

Figure 13. Fluorescent microscope images of natural polymers on PCTE filter membranes stained with Nile red taken at excitation/emission 460/525 nm (green, left panels) and 565/630 nm (red, right panels). Milled wood lignin (MWL) (a, b), chitin (c, d), chitin spiked with PE (e-g). Panels (a) and (c) represent control samples treated with H_2O for 7h at 100 °C. Panels (b), (d) and (e) represent samples that were digested with H_2O_2 for 7h at 100 °C. Part of the whole filter image (b); note fluorescing particles on the filter (denoted with arrowheads) are all microplastics (PE and PP, confirmed *via* Raman spectroscopy) and no MWL was found. Note (d): chitin particles that resisted the H_2O_2 digestion fluoresce in red but not in green. Note (e): PE particles can be distinguished from chitin under green but not red fluorescence. (f & g) binary images generated from the green fluorescent image in (e) using our macro in ImageJ with either the stringent setting (f) or the more sensitive setting (g).

Following the digestion, PCTE filters were thoroughly rinsed with Milli-Q water and then removed. The remaining solution was filtered through a new PCTE filter rinsing all particles from the flask and filtering device with Milli-Q water. The new PCTE filter containing all collected material was stored in Petri dishes until Nile red analysis.

The effect of the H_2O_2 digestion protocol on natural polymers was tested with the two most commonly occurring natural polymers: chitin (powder, Sigma-Aldrich) and wood lignin (below 1 mm in size; kindly provided by Prof. Tim Bugg and prepared according to literature) (Zimmermann et al., 1988).

3.3.3 Validation of the fluorescent-staining protocol with environmental samples

Net tow and beach sand samples were obtained in June 2016 to test our fluorescent-labelling method with environmental samples. Tow samples were collected from within Plymouth Sound, UK. Five consecutive trawls of 15 min were undertaken with a manta net (0.50 m by 0.15 m mouth, 300 µm mesh) at a ship speed of 4 knots. After each tow, the collected material was transferred into a container by rinsing the net and cod end with seawater. In the laboratory, all material was pre-filtered through a 1 mm metallic mesh to eliminate large debris. Retained debris was thoroughly washed with Milli-Q water to extract all small microplastics. Retained debris was visually examined for plastic debris (Figure 14). The flow through containing plastic particles <1 mm was vacuum filtered through PCTE filters (47 mm diameter, 10 µm pore size, Whatman). All filters were placed into a 250 mL flask.

Sediment samples were collected from a beach at Bigbury (UK, 50°16´53N, 3°53´42W) by transferring the top 1 cm layer of five 30 x 30 cm^2 plots with a metallic spoon into 500 mL glass bottles. Microplastics were extracted from sand samples according to the density-separation/floatation protocol described in Nuelle et al. (2014) using NaCl (26% w/v) instead of NaI. The collected supernatant was vacuum filtered through PCTE filters, which were placed in a 250 mL flask. Flasks containing the PCTE filters from net tows and beach sand samples were stored at 60 °C during 24 h for desiccation. The H_2O_2 digestion, staining and imaging was performed as described above.

Figure 14. Microplastic particles from net tow samples retained by the 1 mm metallic mesh. (*): foamed polystyrene spherule.

Micro-Raman spectroscopy was used to verify the identity of the fluorescing and non-fluorescing particles found on the filters in order to ascertain the specificity of Nile red to only stain particles of synthetic origin. In total, 23 fields (23 × 1.8 mm^2) from 6 different filter sections (4 sediment samples, 2 water samples) were imaged as described above. Raman spectra were acquired using an inVia Raman microscope (Renishaw). Raman shifted spectra were recorded using a 442 nm excitation laser in a range of 100 to 3500 waves cm^{-1} and 10 s exposure time accumulating 20 scans. Particles were bleached during 5 min prior to spectrum acquisition as Nile red fluorescence interfered with the Raman signal. The baselines of Raman spectra were corrected in R v3.2.3 (R Core Team, 2018) using the peak detection method from the baseline package (Liland et al., 2015), and then normalized.

To control for procedural contamination, Milli-Q water was processed in equal conditions as described above for environmental samples. To avoid lab contamination, lab coats were worn during all procedures, slides were washed with

acetone, other glassware and filtering devices were thoroughly rinsed with Milli-Q water, pristine plasticware was used (see supplied protocol regarding required precautions during sample handling, such as avoiding low quality pipette tips; Figure 15), and Nile red staining solution was freshly filtered through 0.2 µm filters.

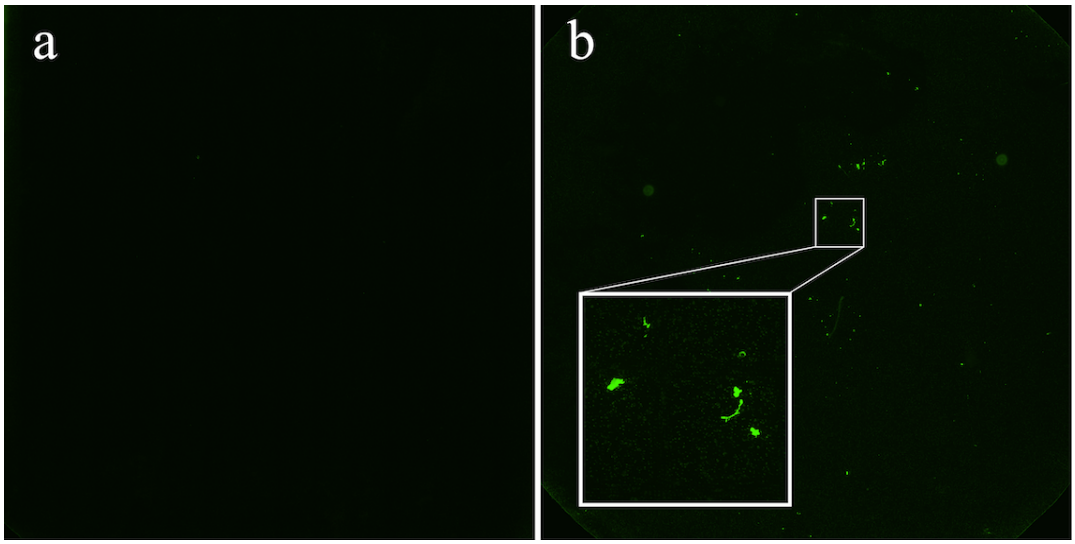

Figure 15. Microscope images of whole PCTE filter membranes (diameter 25 mm) stained with Nile red to assess contamination introduced by low quality pipette tips. Filtered (0.2 µm) Nile red solution applied with syringe and needle (a) or applied with pipette and PP tips (b); note fluorescent microplastic contamination only in panel (b).

3.3.4 Data analysis

Automated quantification of fluorescing particles from tow and blank samples was performed in ImageJ using the macro described above. For each sample type, green fluorescence images (109 total) were randomly taken from 5 different filters. Two power-law models were fitted to the particle size distribution with poweRlaw (Gillespie, 2015) in R. Different x_{min} values were used to estimate the scaling factor: either (1) the smallest particle present in the dataset or (2) an estimate at which the probability distributions of the particle size distribution and the best-fit power-law were most similar above x_{min} (Clauset et al., 2009). The latter discards particles below the estimated x_{min} for which the power-law model is not valid. Testing for other distributions capable of explaining our data was done in accordance with Clauset et al. (2009). Plotting was performed in R using the package ggplot2 (Wickham, 2009).

The detailed protocol and the code for the macro to semi-automatically quantify fluorescent microplastics in ImageJ are provided in APPENDIX 6.

3.4 Results

3.4.1 Validation of the automated Nile red protocol using commercially available plastics

Polymers PE, PP, PS, nylon 6, PC, PET, PVC and PUR fluoresced in green after staining with Nile red (Figure 16) demonstrating the utility of Nile red to detect and quantify small microplastics. Tire rubber did not fluoresce (Figure 12 f). Visual quantification can be performed directly under a microscope, but the implementation of a macro to automate counts allows high throughput counting as well as rapid measurement of the plastic particles. Here, fluorescence based automated detection of microplastics on PCTE membranes was 100 % for 4 polymer types (*i.e.* PE, PP, PS and nylon 6) as all 10 particles of each respective polymer were detected with ImageJ using 29 as the lower threshold for pixel brightness (Figure 16). The other 4 polymers (PUR, PC, PVC and PET) fluoresced weaker and a lower threshold value for pixel brightness (*i.e.* 9) was required to automatically detect all 10 particles (Figure 16).

As fluorescence intensity varied with polymer type and thickness, the original setting for the pixel brightness threshold (*i.e.* 29) in our macro for ImageJ was optimized to capture all particles with strong fluorescence (*i.e.* PE, PP, PS and nylon 6), and to represent particle size accurately, using brightfield images as size references (Figures 16, 17). As stated above, 100% detection of PUR, PC, PET, and PVC was achieved by lowering the threshold value for pixel brightness. However, the adoption of the lower threshold (I) overestimated the size of more strongly fluorescing particles (*i.e.* PE, PP, PS and nylon 6 in Figure 17), (II) counted strongly fluorescent particles in very close proximity as one unique particle, and (III) increased the risk of false positives (*i.e.* chitin in Figure 16; discussed below).

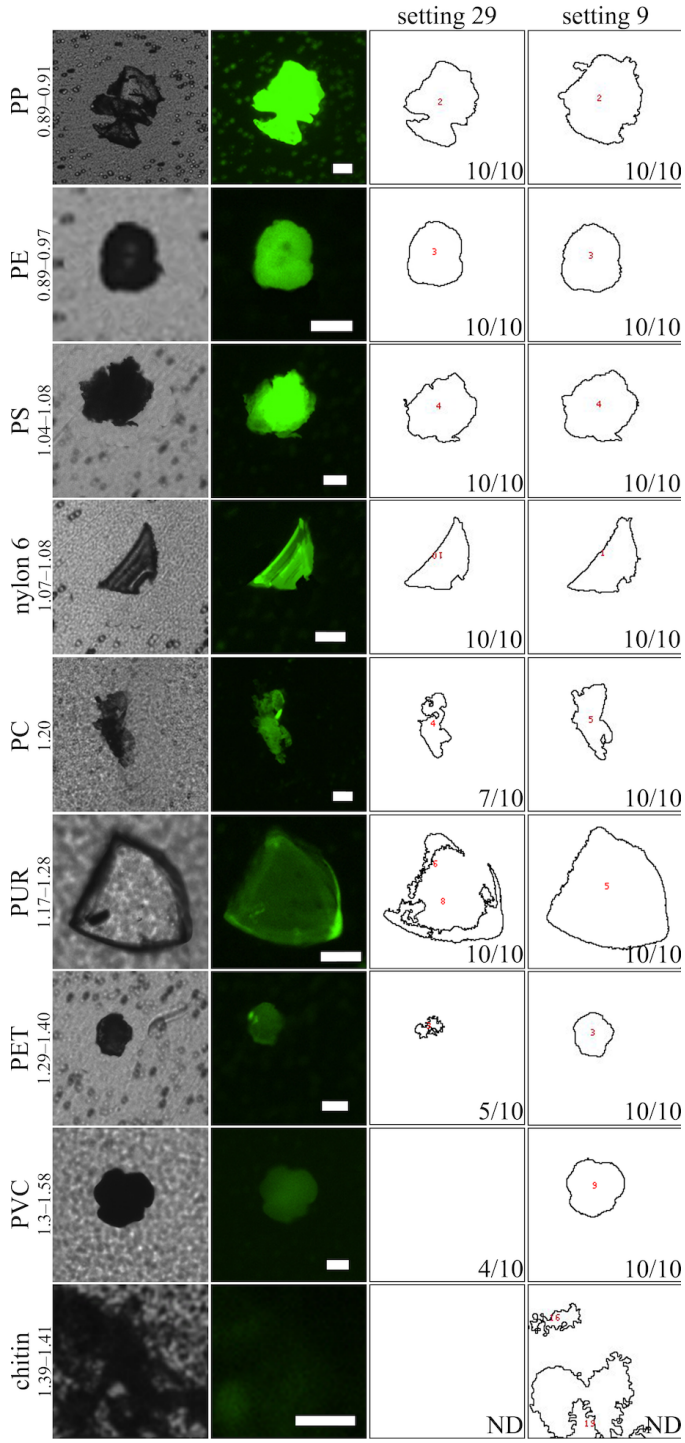

Figure 16. Microscope and ImageJ images of microparticles of different polymer types on PCTE filter membranes stained with Nile red. For each polymer, images show from left to right a particle in bright field, the same particle in green fluorescence (excitation and emission at 460 and 525 nm, respectively), an ImageJ rendition with stringent settings (setting of 29), and an ImageJ rendition with more sensitive settings (setting of 9), respectively. Ratios in ImageJ renditions indicate the number of particles (n = 10) detected with the respective setting and polymer. ND means not determined. Polymers are shown in descending order in accordance with increasing specific density (g cm^{-3}), indicated below the polymer name: PP, polypropylene; PE, polyethylene; PS, polystyrene; PC, polycarbonate; PUR, polyurethane; PET, poly(ethylene terephthalate); PVC, poly- (vinyl carbonate). The scale bar is 50 µm.

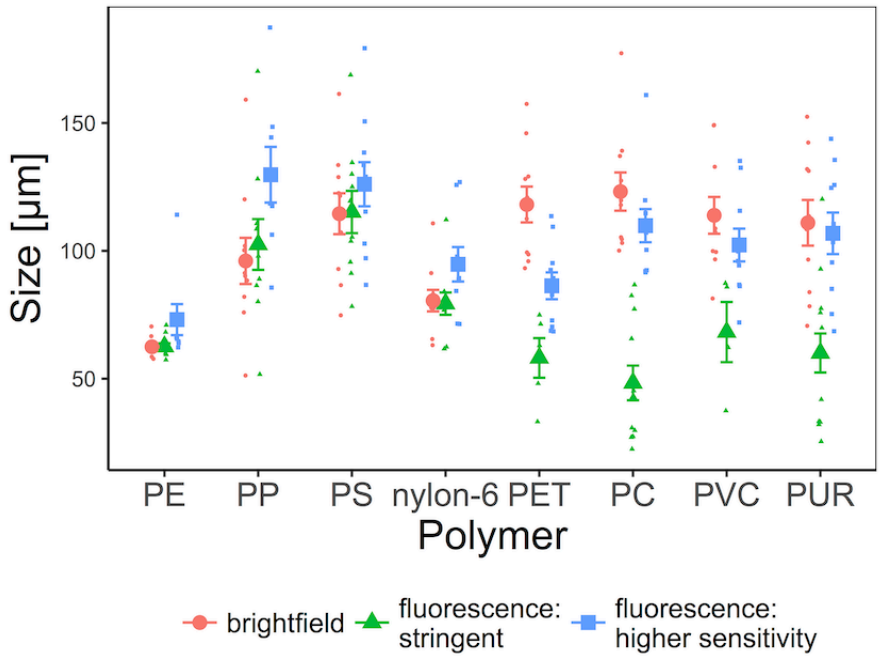

Figure 17. Mean size (± SE) comparison of microplastic particle (n = 10 per polymer type) size measured in ImageJ using either bright-field images or green fluorescence images with our script. Note that stringent represents sizes measured with 29 as the lower threshold for pixel brightness and higher sensitivity corresponds to measurements generated with 9 as the lower threshold for pixel brightness. Size corresponds to the square root of the particle area.

3.4.2 Implementation of the fluorescent-staining protocol to environmental samples

A. Digestion of biogenic material

Wood lignin fluoresces green and red when stained with Nile red (Figure 13 a). However, particles of this natural polymer, which are below 1 mm in size, were completely eliminated after applying a 7-hour H_2O_2 digestion protocol (Figure 13 b). As with wood lignin, chitin also fluoresces in green and red when stained with Nile red (Figure 13 c), but was not completely removed during the 7 hour H_2O_2 treatment. Interestingly, after digestion, chitin showed a strong decrease in green fluorescence intensity (but not red fluorescence; Figure 13 d), possibly due to reduced hydrophobicity in response to oxidation. To test whether chitin would interfere with the detection and quantification of synthetic polymers in the green spectrum, we performed our protocol on a mix of chitin and PE. A stark distinction between PE particles and chitin was observed (Figure 13 e–g) as the weak fluorescence given by

chitin did not interfere when using our highly stringent macro settings (pixel brightness of 29), but chitin is detected to some extent when the settings are brought down (pixel brightness 9). This result highlights two issues that need to be considered when using this protocol: (1) Nile red strongly fluoresces under the GFP settings when staining highly hydrophobic plastics (such as PE, PP, PS) and, hence, green fluorescence should be used to eliminate background and inclusion of natural contaminants; and (2) reducing the sensitivity for the detection of less hydrophobic plastics (e.g. PC, PVC, PUR and PET) can come with a risk of including the detection of particles of natural origin.

B. Detection and quantification of microplastics in environmental samples.

Here we isolated microplastics from environmental samples (*i.e.* beach sediment and sea surface) with saturated NaCl solutions and, hence, expected to extract plastics with densities ≤1.2 g/cm^3 (*e.g.* PE, PP, PS and nylon 6). We applied our Nile red staining protocol to discriminate small microplastic particles from other materials based on fluorescence (Figure 18) as well as to quantify and measure them. The automated ImageJ quantification of microplastics from the sea surface samples using stringent settings resulted in a total of 199 fluorescent particles, ranging between 20 – 338 µm in size (*i.e.* particle size was obtained from the square root of the area measured for each individual particle; Figure 19). Neither of the power-law models describing the data could be dismissed ($p_{x.min = 20.02} = 0.72$ and $p_{x.min = 101.76} = 0.85$). The particle size distribution followed a power-law more closely for particles >101 µm, than if all data were used, *i.e.* the smallest particle size = 20 µm (see Table 3 for statistical details). The calculated scaling factors were 2.13 for $x_{min} = 20.02$ and 4.42 for $x_{min} = 101.76$.

Table 3. Test of power-law behaviour in the sea surface data set and comparison with other potential models.

power-law		log-normal		exponential	
p	LR	*p*	LR	*p*	x_{min} [μm]
0.72	-3.011	**0.002**	-1.378	0.17	20.02
0.85	0.076	0.939	0.718	0.472	101.76

Note: A p-value is given for the power-law model. Likelihood ratios and p-values of their significance are provided for alternative models. A negative value of the likelihood ratio indicates that the alternative model is favoured over the power-law. Statistically significant values are denoted in ***bold****. In both cases the power-law model is supported because it cannot be dismissed with statistical confidence. A log-normal distribution would also be plausible if all data is used, i.e.* x_{min} *= 20.02 μm.*

Only one fluorescent particle was detected in our negative controls (*i.e.* processed Milli-Q water) demonstrating that laboratory contamination was minimal. It is of uttermost importance to include controls in order to assess the contamination acquired during the processing of samples.

For this protocol to be effectively applied to environmental samples we realise it is critical that *only* plastic particles should fluoresce and, hence, be quantified with the semi-automated process. Consequently, we scanned *via* Raman spectroscopy a total of 60 fluorescing and non-fluorescing particles and found that all of the fluorescing particles (n = 37) were of synthetic origin, while all non-fluorescing particles (n = 23) gave *non-plastic* Raman signatures (*e.g.* Figure 18). The environmental samples predominantly contained PP-type polymers (83.8%), although PE was also found (16.2%). The Raman spectra of the PP and PE particles contained slight variations in peak structure (Figure 20), which can occur in commercial polymer materials due to the inclusion of additional compounds and pigments or as a consequence of environmental weathering (Lenz et al., 2015).

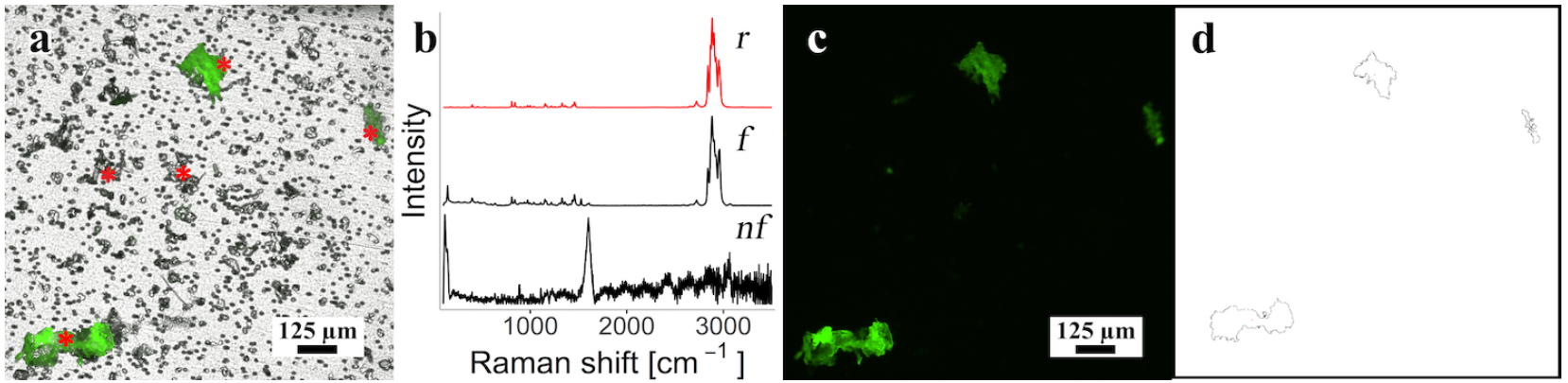

Figure 18. Microscope images of processed sand samples demonstrating selective Nile red fluorescent staining of synthetic polymers with Raman spectra of scanned particles. (a) Composite image of excitation and emission at 460 and 525 nm, respectively, and bright field. Asterisks indicate particles assessed via Raman spectroscopy. (b) Normalized Raman spectra obtained from particles highlighted in panel a: r, PP (Sigma-Aldrich) spectrum; f, typical spectrum of a fluorescent particle in panel a; nf, typical spectrum of a nonfluorescing particle in panel a. (c) Field shown in panel a using green fluorescence only. (d) ImageJ drawing depicting >400 µm2 particles that were quantified via our macro.

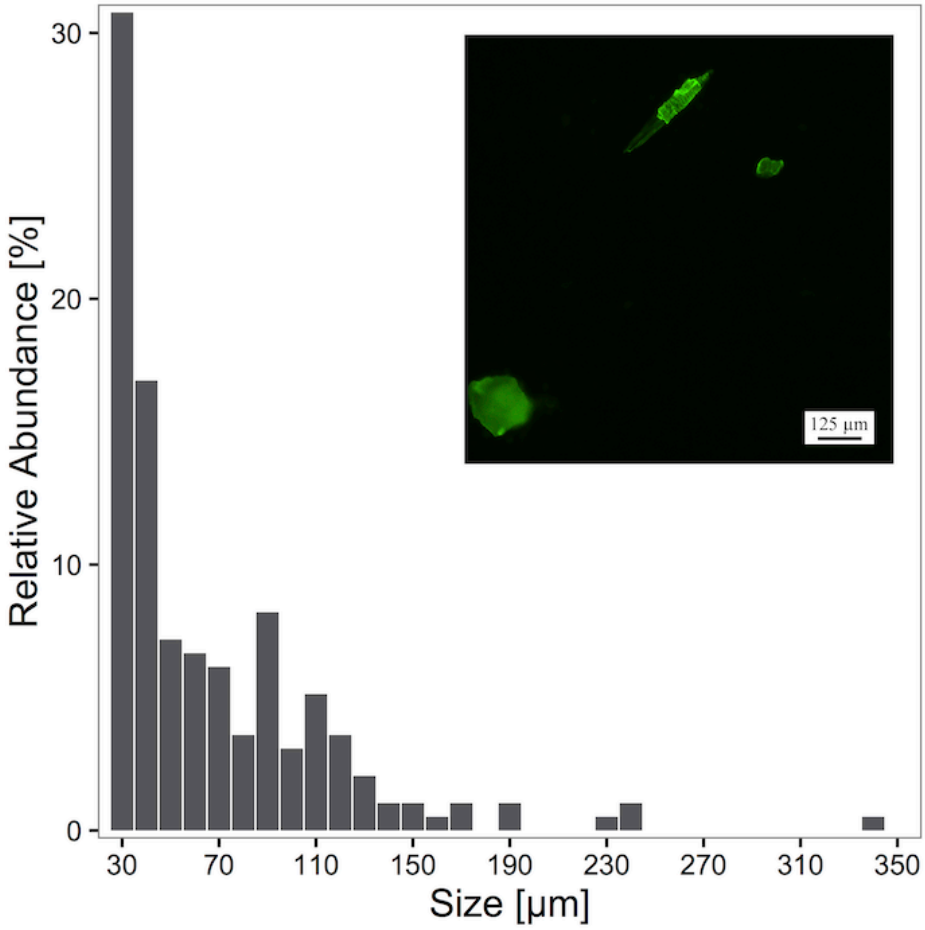

Figure 19. Microplastic particle size distribution. Relative abundance of microplastic particle sizes (n_p = 199) from all sea surface samples analysed via automated counting of fluorescent particles using 109 different microscope fields (one image shown as an example). Size corresponds to the square root of the particle's area.

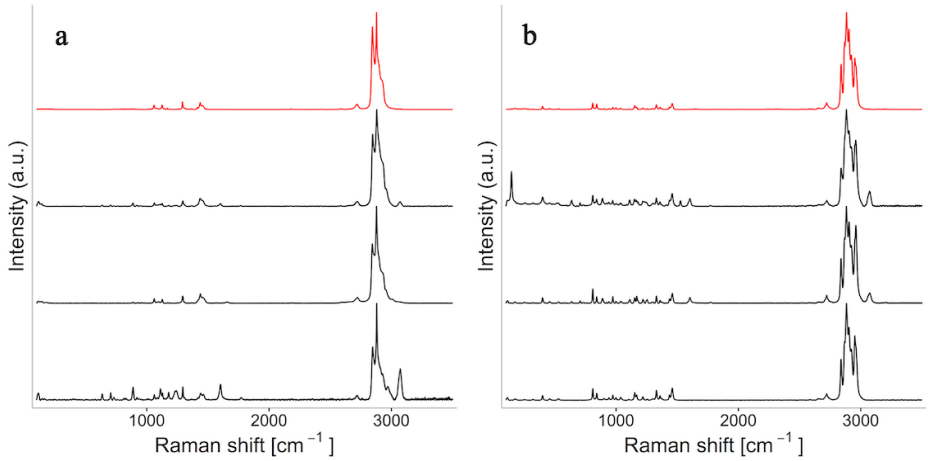

Figure 20. Normalised Raman spectra of PE (a) and PP (b) particles acquired from sand and sea surface samples. Reference spectrum for PE and PP (Sigma-Aldrich) are in red. Note variations in peak structure within samples.

3.5 Discussion

We present a fast, reliable and cost-effective method for detecting, quantifying and determining the size of small PE-, PP-, PS- and nylon 6 type microplastics (20 µm – 1 mm) commonly present in sea surface samples (Ballent et al., 2016; Gajšt et al., 2016; Suaria et al., 2016). This method uses the lipophilic dye Nile red to fluorescently label plastics and requires fluorescence microscopy to capture images at magnification 10× prior to automated, image-based quantification in ImageJ using a macro (both protocol and macro are provided in APPENDIX 6) enabling high throughput image analysis. Specific protocols for collecting and extracting microplastics from the environment were not in the scope of this work.

During the preparation of this manuscript, two studies were published that reasserted our findings (Maes et al., 2017; Shim et al., 2016), demonstrating the effectiveness of Nile red to fluorescently label different types of commercially available synthetic polymers, such as the ones employed here, all of which fluoresce in the green spectrum (black rubber was not used in these previous studies and we show here that it does not fluoresce). Indeed, similarly to us, Shim et al. (2016) concluded that green-yellow fluorescence (excitation/emission 450–490/515–565 nm) provided better particle recognition than red or blue fluorescence. Using a different light and filter set-up, Maes et al. (2017) reported good fluorescence at longer wavelengths ranging from yellow to orange, depending on the polymer type. Such findings agree with previous reports about the behaviour of Nile red, which favours detection of strongly hydrophobic samples at short excitation/emission wavelengths (450–500/≤580 nm) compared to more neutral lipids, which should ideally be visualised at longer excitation wavelengths (*i.e.* red, 515–560/≥590 nm) (Rumin et al., 2015). For example, given that PE and PP are more hydrophobic than PET (Dodbiba et al., 2002), it is expected that the former will fluoresce more intensely at shorter wavelengths (*i.e.* green), while their fluorescence at longer wavelengths remains weak or even absent as we show in Figure 12. We are therefore confident that the Nile red protocol we propose here is effective in detecting strongly hydrophobic plastics such as PE, PP, PS and nylon 6 through the use of GFP settings (green fluorescence), while preventing detection of contaminants, that would fluoresce at longer wavelengths. We acknowledge the protocol's limitations for the less hydrophobic polymers PC, PUR, PET and PVC, which constituted about 25% of

the European plastic demand in 2015 (PlasticsEurope, 2018). These limitations can to some extent be overcome as suggested in the results section by increasing the sensitivity of the method (Figure 16), but this comes at a risk of overestimating the size of strongly fluorescent polymers (Figure 17) as well as incurring the possibility of false positives, such as chitin. It is also worth highlighting that all polymer types that fluoresced weakly in our study when stained with Nile red (PC, PUR, PET, PVC) are denser (≥1.2 g/cm^3) than the polymers that fluoresced more strongly (PE, PP, PS, nylon 6, <1.08 g/cm^3). Hence, the latter can be extracted using a saturated NaCl solution as done in this study, while denser polymers would require a higher density salt solution (*e.g.* NaI).

The successful application of a Nile red protocol to environmental samples relies on the efficient removal of biogenic particles that could be detected as false positives. As we show here, abundant natural polymers such as chitin and wood lignin fluoresced when stained with Nile red (Figure 13 a, c). Shim et al. (2016) remained cautious on applying Nile red to quantify microplastics in environmental samples due to the risk of co-staining undigested biogenic material. We speculate that the problem they encountered resided in the weak digestion treatment they applied on their beach samples (*i.e.* soaking the filters with 35% H_2O_2), which resulted in biogenic debris such as an amphipod carapace and plant parts still being present. In turn, Shim et al. (2016) reported less such contamination for the neuston net samples, which were digested with the more aggressive Fenton reagent (including heating to 75°C). Hence, a harsh digestion protocol such as the one we used here and which was previously suggested by Claessens et al. (2013), is required to prevent co-staining of natural organic polymers and confidently quantify Nile red-stained microplastics in environmental samples. Common plastics such as PE, PP, PS, PET and nylon 6 are resistant to H_2O_2, as demonstrated by Tagg et al. (2015) during a 7-day exposure experiment, where no significant chemical changes were detected *via* FTIR, as opposed to alterations observed elsewhere that were induced by solvents such as acids and bases (e.g. HCl or NaOH) (Cole et al., 2014; Nuelle et al., 2014). In addition to the H_2O_2 digestion, we propose to include a 1 mm mesh-size sieving step prior to the digestion to prevent the inclusion of larger, hard-to-digest natural contaminants, such as amphipods or pieces of wood. If required, enzymatic digestion protocols could be implemented to digest biota-rich environmental samples (Cole et al., 2014; Mani et al., 2015). Indeed, sample purification may further be

optimized by combining digestion procedures with a density separation protocol, such as presented by Maes et al. (2017). Nevertheless, our results show how the 30% H_2O_2 digestion step used here was effective at preventing detection of small natural polymers (below 1 mm in size); wood lignin was completely degraded and chitin was no longer detectable in ImageJ using green fluorescence images (Figure 13). Furthermore, we successfully proved that all of the fluorescing particles from environmental samples assessed with micro-Raman spectroscopy (n = 37) were identified as synthetic plastic materials, whereas no non-fluorescing particles scanned (n = 23) showed a synthetic polymer signature.

Other semi-automatable methods to detect and quantify small microplastics in environmental samples were recently developed (Frère et al., 2016; Löder et al., 2015; Tagg et al., 2015):

Chemical mapping *via* micro-FTIR was shown useful to detect and identify small microplastics directly on filters when combined with FPA detectors (Löder et al., 2015; Tagg et al., 2015); FPA detectors can record several thousand spectra simultaneously and plastics are then identified based on characteristic bands that are shared by synthetic polymers. However, access to such specialised pieces of equipment is not always possible, and the time required to image a whole filter membrane (10.75 h for a 25 mm diameter filter) (Löder et al., 2015) is significantly higher than when using the method in the present study *i.e.* 20 min.

A second semi-automatable approach used to detect small microplastics from environmental samples combined Micro-Raman spectroscopy with particle finding software (Frère et al., 2016). The software provides geographical positions of the particles on a slide, and the particles are then scanned individually *via* a motorised stage. However, Frère et al. (2016) did not apply this technique directly to the sample filter (such as in this study and others (Löder et al., 2015; Tagg et al., 2015)). Instead, particles were visually pre-selected under a dissection microscope and then transferred onto a gold-coated microscope slide. It is therefore not yet clear whether this technique is also applicable to quantify small microplastics without potentially introducing visual bias.

While our Nile red staining method does not provide the chemical identity of the detected plastic particles (as achieved *via* FTIR and Raman), we present it as a sensitive, cost-effective and unbiased way of quantifying and measuring small PE, PP, PS and Nylon 6 particles in environmental sample preparations to acquire large

datasets with high statistical value. Ultimately, a fraction of pinpointed plastic particles should be identified *via* micro-Raman spectroscopy to obtain information on the diversity of polymer types within a sample. Moreover, despite having tested the most common potential natural contaminants, we advocate the use of micro-Raman spectroscopy on subsamples until full reliability of the method presented here has been evaluated.

Micro-Raman spectroscopy of plastic particles detected with Nile red showed that PP microparticles were more prevalent (83.8%) in our environmental samples than PE (16.2%). This is notable as PE is the most commonly produced polymer type (PlasticsEurope, 2015) and literature highlights PE as the most abundant polymer on sea surfaces (Phuong et al., 2016). A recent study, however, found that this is only the case for large microplastics (>1 mm), as the smaller analysed size fraction (0.335 – 1 mm) was dominated by PP (42%) rather than PE (26%) (Frère et al., 2016). Furthermore, the authors reported a lack of PS in size classes below <2 mm (Frère et al., 2016), which resembles our findings. Curiously, PS was present in the fraction retained by the 1 mm sieve (Figure 14) but not found among particles assessed with Raman. Several non-exclusive hypotheses may explain these findings. For instance, fragmentation behaviours may differ with polymer type and shape. Particles have also been observed to adhere to organic matter, such as marine snow, and sink (Long et al., 2015; Zhao et al., 2017). It is unclear, however, why small PE particles would more likely be incorporated into marine snow than PP particles, and further research is required to shed light on this interesting phenomenon.

Plastics in the environment are known to progressively fragment into smaller particles (Barnes et al., 2009). Based on the fragmentation pattern of three dimensional objects, it could be expected that the abundance of microplastic particles increases following a power-law with a factor of 3 as size decreases (Cózar et al., 2014). Contrary to this assumption, Cózar et al. (2014) reported an intriguing loss in abundance of small microplastics after carrying out a global survey of sea surface marine plastic debris. The expected correlation between size and fragment abundance was observed down to a particle size of 2 mm but, surprisingly, the abundance of microplastics sharply decreased for particles below 1 mm in size. This supported speculation regarding the substantial 'missing' fraction of marine plastic debris initiated in 2004 (Thompson et al., 2004), and recently reviewed by Eriksen et al., (2016). We believe that the extremely low incidence of small microplastics

reported by Cózar et al. (2014) may partly be ascribed to the methods employed in identifying and selecting particles, which were based on visual sorting under a dissecting microscope. In fact, in a study whose findings mirrored our own, Enders et al. (2015) showed that small microplastics were indeed present in surface waters with increasing abundance as size decreased, and obtained a scaling factor of 1.96 for the size range of 10 – 110 μm, close to one obtained in this study (*i.e.* scaling factor of 2.13). Further research is nevertheless required, as very little is known about the fragmentation pattern and particle behaviour of different polymer types in the marine environment (Filella, 2015).

Here we suggest the use of a highly sensitive Nile red fluorescent staining method for identifying the smaller size range of lower density microplastics (<1 mm) commonly present in sea surface samples (*i.e.* PE, PP, PS and nylon 6). We acknowledge its limitations, but do not exclude its application, for less hydrophobic polymer types, a separation that coincides with higher polymer densities (>1.2 g/cm^3; Figure 16). Using this time- and cost-effective protocol to quantify and measure small microplastics allowed us to confirm that small microplastics are increasingly abundant with decreasing particle size in sea surface samples (Figure 19). This method therefore addresses the quantification uncertainties and provides an effective tool for rapid quantification of small microplastics by substituting the visual selection and quantification process with an automated process.

CHAPTER 4

EARLY COLONIZATION OF WEATHERED POLYETHYLENE BY DISTINCT BACTERIA IN MARINE COASTAL SEAWATER

4.1 Summary

Plastic debris in aquatic environments is rapidly colonized by a diverse community of microorganisms, often referred to as the "Plastisphere". Given that common plastics are derived from fossil fuels, one would expect that Plastispheres should be enriched with obligate hydrocarbon degrading bacteria (OHCB). So far, however, effects of common polymer types on the composition of the Plastisphere have rarely been observed, and putative biodegrading bacteria are only found as rare taxa within these biofilms. Here we show through 16S rRNA gene sequencing, that the initial enrichment of a prominent OHCB member on weathered and non-weathered polyethylene only occurred at early stages of colonization (i.e. after 2 days of incubation in coastal marine water; 5.8% and 3.7% of relative abundance, respectively, *vs.* 0.6% on glass controls). As biofilms matured, these bacteria decreased in relative abundance on all materials (<0.3% after 9 days). Apart from OHCB, weathered PE significantly enriched for other distinct organisms during early stages of colonization, such as a member of the Roseobacter clade, and *Aestuariibacter* (median 26.9% and 1.8% of the community, respectively), possibly as a consequence of the availability of short oxidized chains generated from weathering. Our results demonstrate that Plastispheres can vary in accordance with the weathering state of the material and that very early colonizing communities are enriched with taxa that are able to degrade hydrocarbons. Given the lack of persistent enrichment and overall community convergence between materials over time however, a common non-hydrolysable polymer might not serve as an important source of carbon for mature Plastispheres in marine environments, once the labile substrates generated from weathering were depleted.

4.2 Introduction

Recent years have seen heightened societal concern about the abundance and impacts of plastic debris in the marine environment (Borrelle et al., 2017; Galloway et al., 2017). Being highly recalcitrant materials, plastics accumulate in the environment polluting sediments and surface seawater around the globe (Browne et al., 2011; Derraik, 2002; Erni-Cassola et al., 2019). Plastic debris greatly varies in size and shape, but smaller particles (ex. <5 mm) numerically dominate (Cózar et al., 2014; Eriksen et al., 2014; Suaria et al., 2016). Once in aquatic systems, these materials are rapidly colonized by a diverse community of macro- and microorganisms, often referred to as the "Plastisphere" (Lobelle and Cunliffe, 2011; McCormick et al., 2014; Reisser et al., 2014; Zettler et al., 2013).

Surface attached assemblies, as opposed to free living cells, benefit from the facilitated access to resources, enhanced interactions and more stable environments that biofilms provide (Dang and Lovell, 2016). Consequently, Plastisphere microbiomes are distinct from planktonic communities (De Tender et al., 2015; Frère et al., 2018; Zettler et al., 2013), and typical genetic traits from biofilms are found, such as those involved in surface attachment (Bryant et al., 2016). Within a core group of bacterial families typically found in the Plastisphere (e.g. Flavobacteriaceae, Hyphomonadaceae and Rhodobacteraceae) (Bryant et al., 2016; De Tender et al., 2017; Zettler et al., 2013), bacterial communities mainly vary with season and geography (Amaral-Zettler et al., 2015; Oberbeckmann et al., 2016, 2014). Subtle colonization differences between polymer types have been shown (Amaral-Zettler et al., 2015; Kirstein et al., 2018) although it remains unclear if these come as a consequence of the material's polymer chemistry or its surface properties (Frère et al., 2018). While the surrounding environment seems to be the main driver in shaping the general Plastisphere community (Amaral-Zettler et al., 2015; De Tender et al., 2015), species-specific variations between different materials draw interest as they may indicate target bacterial strains for biodegradation.

Despite encouraging findings in biodegradation of the polyester poly(ethylene terephthalate) (PET) (Austin et al., 2018; Yoshida et al., 2016), biodegradation of non-hydrolysable polymers, such as polyethylene (PE) or polypropylene (PP), is less likely to be encountered due to the high redox potential required to cleave the carbon-carbon bonds (Krueger et al., 2015). Nonetheless,

similar molecules of lower molecular weight, *i.e.* n-alkanes, are commonly produced in marine environments (Lea-Smith et al., 2015), possibly feeding obligate hydrocarbon degrading bacteria (OHCB) (Yakimov et al., 2007). The latter can metabolize n-alkanes of up to ~50 carbons in length (Rojo, 2009), which are notably shorter than the chains found in low density PE ($C_{4,000}$–$C_{40,000}$) and hence, abiotic weathering and reduction of polymer chain length is thought to be required to facilitate microbial biodegradation on non-hydrolysable plastics (Albertsson et al., 1995; Restrepo-Flórez et al., 2014). Abiotic degradation can occur through photo- and thermal oxidation, adding functional groups to the polymer, such as carbonyl and hydroxyl groups, ultimately inducing chain scissions (Andrady, 2017; Andrady et al., 1993). Laboratory studies employing oxidized PE indeed demonstrated that weathered polymers lead to increased respiration rates (Albertsson and Karlsson, 1990), polymer weight loss (Hadad et al., 2005), or stimulated microbial activity (Romera-Castillo et al., 2018), but pre-weathered polymers were only recently considered in an *in situ* study of microbial plastic colonization (Dussud et al., 2018). Furthermore, pre-weathered polymers may mimic marine plastic debris as it occurs in the environment (ter Halle et al., 2017), and therefore the influence of weathered polymer surfaces on plastic colonization merits closer investigation, especially in light of the discovery of microorganisms potentially involved in polymer biodegradation.

Here we tested the hypothesis that weathering a non-hydrolysable polymer (*i.e.* PE and PP) enhances the colonization of OHCB taxa in the Plastisphere, while the untreated polymer and control material (*i.e.* glass) recruit more similar microbial communities with a lower relative abundance of OHCB. While our hypothesis held true during short incubations in PE (*i.e.* weathered PE enriched a distinct group of microorganisms after two-day incubations), after nine days the differences were no longer discernible between the materials and the relative abundance of these distinct microbes reduced. Our results suggest that more mature biofilms that develop on marine plastic debris mask polymer- or surface-specific microorganisms, hindering the detection of possible polymer biodegraders. Hence, mature biofilms likely consume labile organic matter generated from photosynthesis or from the surrounding environment – more than from the recalcitrant plastic itself.

4.3 Materials and Methods

4.3.1 Plastic weathering and monitoring of surface oxidation.

Polypropylene (PP) sample materials were prepared by cutting commercially available cups into 0.8×2.5 cm strips. The strips were then weathered *via* plasma beam running on compressed air (PlasmaBeam Duo system, Diener Electronic) at two different "intensities" to produce lightly and more heavily weathered plastic surfaces. Each treatment run consisted of a plasma beam scan at 6 mm distance from the PP surface with the beam progressing over the surface at 50 mm/s. This produced a treated band that was ~8 mm wide. For the lightly weathered samples 3 consecutive runs were performed over the same band and on both sides of the PP sheet. To simulate heavier weathering 10 consecutive runs were used. Low density PE strips were obtained by heat pressing low density PE pellets (Sigma-Aldrich) into films (145° C, 10 kN, pressing time 60 s, final thickness: ~0.1 mm). The films were then cut into 0.5×1 cm strips and weathered by thermo-oxidation for 3 months at 80 °C in the dark. Non-weathered PP and PE strips were kept at room temperature.

The carbonyl index (CI) was used as a measure of oxidation for PP and PE as done previously using Fourier-transform infrared spectroscopy (FTIR) (Song et al., 2017; ter Halle et al., 2017). Briefly, the CIs were calculated as the ratios between the carbonyl absorbance peak (1712 cm^{-1}) and a standard reference that remains unaffected by weathering (PP: 973 cm^{-1}; PE: 2030 cm^{-1}) (Luongo, 1960; Satoto et al., 1997). FTIR spectra for PP and PE were obtained in transmission mode by averaging 32 scans in the range of 600 to 4000 waves cm^{-1} with a resolution of 4 cm^{-1} (Spectrum GX, PerkinElmer). For PE, the CIs were measured for both weathered and non-weathered PE strips before *in situ* incubation and post incubation, after DNA had been extracted. Additional controls for the experiment with PE were used; firstly, to assess the effect of the DNA extraction process on the CI of weathered strips (but not exposed *in situ*), and secondly, glass strips (~0.5x1 cm) as additional inert control material, which were generated from microscope coverslips. Prior to experimental exposure, all strips of all materials were stored in absolute ethanol at room temperature.

4.3.2 Experimental set up and sample collection.

In situ incubations in coastal seawater were performed in Mallorca (Spain, 39°29'29.7" N 2°44'09.0" E) on a rocky shore to study the marine microbial colonization of different materials and weathering states (Table 4). This site was chosen due to the oligotrophic conditions, which are more similar to waters further offshore. The first was carried out in April 2017 and involved PP only. The strips (3 lightly oxidized, 3 heavily oxidized, 3 untreated controls) were fixed to a nylon monofilament, and extended between two stones at a depth of ~1.5 m, and samples were recovered after 9 days. The second experiment employed PE and was run in August 2018. Twelve strips per material (n_{total} = 36, weathered and non-weathered PE, as well as glass slides) were fixed to a nylon fishing line and maintained at ~1.5 m depth by attaching each end of the line to a weight or buoy, respectively. Six strips of each material were recovered at each one of the two time points (*i.e.* 2 and 9 days). In both experiments, samples were immediately immersed in 1 mL lysis buffer (Qiagen) and stored at -20 ºC until further analysis. Additionally, the surrounding planktonic community was sampled at day nine in August 2018, by filtering *in situ* 2.5 L of seawater through a 0.2 µm filter membrane (GTTP, Isopore, Millipore). Seawater samples were collected in triplicate and filters were also immediately stored in 1 mL of lysis buffer at -20 ºC.

Table 4. Summary of experimental design for *in situ* colonization studies.

Material	**Sampling time point**	**Sequencing target gene**
Polypropylene (PP) experiment in April 2017		
untreated PP	day 9	16S and 18S rRNA
highly weathered PP	day 9	16S and 18S rRNA
lightly weathered PP	day 9	16S and 18S rRNA
Polyethylene (PE) experiment in August 2018		
weathered PE	days 2 and 9	16S rRNA and ITS
non-weathered PE	days 2 and 9	16S rRNA and ITS
glass	days 2 and 9	16S rRNA and ITS

4.3.3 Primer pair coverage of OHCB.

Given the particular interest to study OHCB among the communities, the universal 16S rRNA gene primer pair employed here (Table 5) was assessed for its coverage of a subset of important taxa of the OHCB group: *Alcanivorax*, *Oleiphilus*, *Oleispira*, *Thalassolituus*, *Cycloclasticus*, *Marinobacter*, *Neptunomonas* and *Thalassospira* (Berry and Gutierrez, 2017). For comparison, the general primers used in recent Plastisphere surveys were also tested for their coverage of OHCB group (De Tender et al., 2017; Oberbeckmann et al., 2018; Zettler et al., 2013), as well as the primer pair suggested by Berry and Gutierrez (Berry and Gutierrez, 2017), due to best coverage for OHCB among general primer sets (Table 5). All primer pairs were assessed with the database SILVA SSU 132 Ref NR. *In silico* testing was performed with TestPrime (Klindworth et al., 2013) v1.0 on the ARB PT server using the most conservative setting ("0 mismatches").

Table 5. Details of primer pairs used in this study for sequencing and testing of OHCB coverage.

Target[1]	Primer name	Sequence	Reference[2]	Example study[3]
18S*	V8F 1510R	ATAACAGGTCTGTGATGCCCT CCTTCYGCAGGTTCACCTAC	(Bradley et al., 2016)	-
16S*	515F-Y 926R	GTGYCAGCMGCCGCGGTAA CCGYCAATTYMTTTRAGTTT	(Parada et al., 2016)	-
ITS2*	fITS7bis ITS4NGSr	GTGAATCATCRAATYTTTG TCCTSCGCTTATTGATATGC	(De Tender et al., 2017)	-
16S	515F 806R	GTGCCAGCMGCCGCGGTAA GGACTACHVGGGTWTCTAAT	-	(Oberbeckmann et al., 2018)
16S	341F 805R	CCTACGGGNGGCWGCAG GACTACHVGGGTATCTAATCC	-	(De Tender et al., 2017)
16S	518F 1046R	CCAGCAGCYGCGGTAAN CGACAGCCATGCANCACCT	-	(Zettler et al., 2013)
16S	341F 785R	CCTACGGGNGGCWGCAG GACTACHVGGGTATCTAATCC	-	(Kirstein et al., 2018)
16S	343F 908R	TACGGRAGGCAGCAG CGTCAATTCMTTTGAGTT	-	(Berry and Gutierrez, 2017)

[1] *Primer pair used in this study is indicated (*)*
[2] *Refences for primer pairs used in PCR for this study*
[3] *16S rRNA gene primer pairs that were tested for OHCB coverage and study in which they were used.*

4.3.4 DNA isolation, amplification and library generation.

DNA from the communities on PP was extracted following indications by Debeljak *et al.* (2017), adopting the procedure to spin columns (see protocol in APPENDIX 7). In short, bead-beating and enzymatic digestion steps (Lysozyme and Proteinase K) were performed prior to continuing extraction using the DNeasy Blood & Tissue kit (Qiagen) in accordance with the manufacturer's instructions. DNA from the biofilms of PE and glass, as well as seawater communities, was extracted using the DNeasy PowerBiofilm kit (Qiagen) according to the manufacturer's instructions, which included a bead-beating step. DNA was quantified using a Qubit® HS DNA kit (Life Technologies Corporation) and samples were diluted to equalise the concentration. PCR amplifications were performed using Q5® Hot Start High-Fidelity 2X Master Mix (New England Biolabs® inc.) and the primer pairs detailed in Table 5, which amplified regions V4-5 of the 16S rRNA gene of bacteria (PP and PE experiments; PCR conditions as in (Parada et al., 2016)), V8-9 of the 18S rRNA gene for eukaryotes (PP experiment only; PCR conditions as in (Bradley et al., 2016)) and the ITS2 for fungi (PE experiment only; PCR conditions as in (De Tender et al., 2017)).

PCR products were purified with Ampliclean magnetic beads (Nimagen, The Netherlands). Index PCR was performed using Illumina Nextera Index Kit v2 adapters. Sample normalization was done with the SequelPrep™ Normalisation Plate Kit (ThermoFisher Scientific) and samples were finally pooled for sequencing. Libraries were pooled and quantified using the NEBNext Library Quant Kit for Illumina (New England Biolabs, UK) and diluted to 4 nM. Negative DNA extraction controls and negative controls for sequencing were processed simultaneously.

4.3.5 Amplicon sequencing and processing.

Libraries were denatured using 0.2N NaOH and sequenced using the MiSeq Illumina system (2 × 300 bp paired-end) with the v3 reagent kit, following the manufacturer's instructions for a 8.5 pM library with 10% phiX as an internal reference for the PP experiment and a 14 pM library with 2% phiX for the PE experiment. Sequence processing was performed in R v3.5.1 (R Core Team, 2018), where amplicon sequence variants (ASVs) (Callahan et al., 2017) were obtained using the DADA2 package (Callahan et al., 2016).

For prokaryote data from PE, 16S forward and reverse primer sequences were trimmed (19 bp and 20 bp respectively), as well as fragment ends, due to dropping quality scores, yielding in final lengths of 276 bp and 200 bp for forward and reverse primers, respectively. Chimeras were removed and taxonomy was assigned using IDTAXA (Murali et al., 2018) implemented in the R package DECIPHER (Wright, 2016) with a classifier trained on the SILVA v132 database (March 2018 release). A maximum likelihood phylogenetic tree was then built using the GTRGAMMA model in RAxML (Stamatakis, 2014). 16S and 18S rRNA data from PP were processed identically, except that phylogenetic trees were built using phangorn in R (GTRGAMMA model; (Schliep, 2011)). For ITS data, primer sequences, including potential reverse complements, were identified and removed using cutadapt v1.18 (Martin, 2011) and a minimum sequence length of 50 bp was enforced. After removal of chimeras, taxonomy was assigned with IDTAXA, using Warcup v2 as the training set (March 2018 release; Deshpande et al., 2016); the phylogenetic tree was built with phangorn as described above. All raw sequence files, including sequencing controls, are available from the National Center for Biotechnology Information's

(NCBI) Short Read Archive (SRA) database (PP: BioProject PRJNA528586; PE: BioProject PRJNA528407).

4.3.6 Data analysis and statistics.

Prior to downstream analysis of all sequencing data sets, unassigned reads at phylum level were removed due to high likelihood of representing artefacts. 16S rRNA gene sequences assigned to Chloroplasts and Mitochondria were removed, as well as phyla with <9 reads across all samples. Data from all samples, including controls, were first inspected *via* principal coordinate analysis (Bray-Curtis distance). Ensuing, samples with <1000 reads (except for the 18S rRNA gene data – discussed below), as well as outliers and controls (*i.e.* extraction- and sequencing blanks), were removed from the data. Sequencing coverage was inspected *via* rarefying curves. To investigate the α-diversity of the communities, indices were calculated for Shannon diversity, inverted Simpson evenness, and Chao1 richness. Differences in Shannon diversity were further assessed for their statistical difference *via* generalized linear modelling using a Gamma link function followed by all pairwise comparisons; the Shannon index was chosen because it is less sensitive to differences between library sizes than other indices (Knight et al., 2018). Then, β-diversity was investigated through non-metric multidimensional scaling (nMDS) using the UniFrac distance metric, both weighted and unweighted (Lozupone et al., 2011). For weighted UniFrac, proportion transformed data were used, while unweighted UniFrac was performed on rarefied data in accordance with Weiss *et al.* (Weiss et al., 2017). Permutation tests (Adonis; Oksanen et al., 2019) were used to statistically explore differences in β-diversity between communities in response to experimental treatments using the UniFrac distance metrics (weighted and unweighted). To find taxa of interest, differential abundance testing was performed *via* the DESeq2 package in R (Love et al., 2014) using raw counts; DESeq2 employs negative binomial generalized linear models, controls for different library sizes and corrects for multiple testing with the Benjamini-Hochberg procedure. The closest cultivated relatives of the taxa of interest were identified through BLAST searches on NCBI against the SSU rRNA gene sequence database. The 16S rRNA gene sequences used in BLAST searches are listed in APPENDIX 8. In addition, metagenomes were predicted for the bacterial communities from PE, based on 16S rRNA sequence

abundances using phylogenetic investigation of communities by reconstruction of observed states and abundances (PICRUSt2; Langille, 2018; Langille et al., 2013); 16S rRNA copy numbers were normalized for. As an indication for the precision of the predictions, nearest-sequenced taxon indices were estimated.

Data analysis, statistics and plotting in R further included the following packages: phyloseq (McMurdie and Holmes, 2013), multcomp (Hothorn et al., 2008), and ggplot2 (Wickham, 2009).

4.4 Results

4.4.1 Weathering of the plastic strips.

FTIR spectra confirmed thermal oxidation of the PE strips that had been kept at 80 ºC for 3 months (CI = 23.5; Figure 21a), comparable to 270 days of UV exposure at 43-45° C (Song et al., 2017), but higher than what has been measured from marine plastic debris, *i.e.* CI < 1 (Brandon et al., 2016; ter Halle et al., 2017). Interestingly, CIs decreased after PE strips had been incubated in seawater (CIs of 15.5 and 19.7 after 2 and 9 days of *in situ* incubations, respectively; Figure 21b). Control strips that only went through the DNA extraction protocol also showed a reduction in their CI (CI = 11.7), whereas surface oxidation remained stable in weathered PE strips that were not processed and remained at room temperature for the duration of the experiment. These results indicated that oxidized polymer chains from the surface of weathered PE strips shed off when the material was in solution as suggested previously (Gewert et al., 2018; Romera-Castillo et al., 2018). In turn, significantly weaker oxidation was observed on the plasma beam treated PP samples, with the heavy weathering treatment resulting in the highest CI (0.087, Figure 21c, d), which was comparable to an oxidation obtained after ~30 days during summer season in India (Rajakumar et al., 2009).

4.4.2 Primer pair coverage of OHCB.

In silico analysis of different 16S rRNA gene primer pairs showed that those used in this study covered 92% of the OHCB present in the reference SILVA database (n = 1867, Table 5). Similar coverage was obtained by other primer pairs (*i.e.* 91%) used in recent Plastisphere surveys (De Tender et al., 2017; Oberbeckmann et al., 2018), and was not far from the coverage obtained with an ideal general primer pair (*i.e.* 93%) suggested by Berry and Gutierrez (Berry and Gutierrez, 2017). In agreement with this last study (Berry and Gutierrez, 2017), we found that the primer pair 518F and 1046R only covered 36% of the OHCB, mainly due to poor coverage of the *Marinobacter* genus (3%, Table 5). Primer pair 515F-Y and 926R was used in the present study because it gave both a good coverage of the OHCB group, as well as the best coverage for marine microbial communities as previously suggested (Parada et al., 2016).

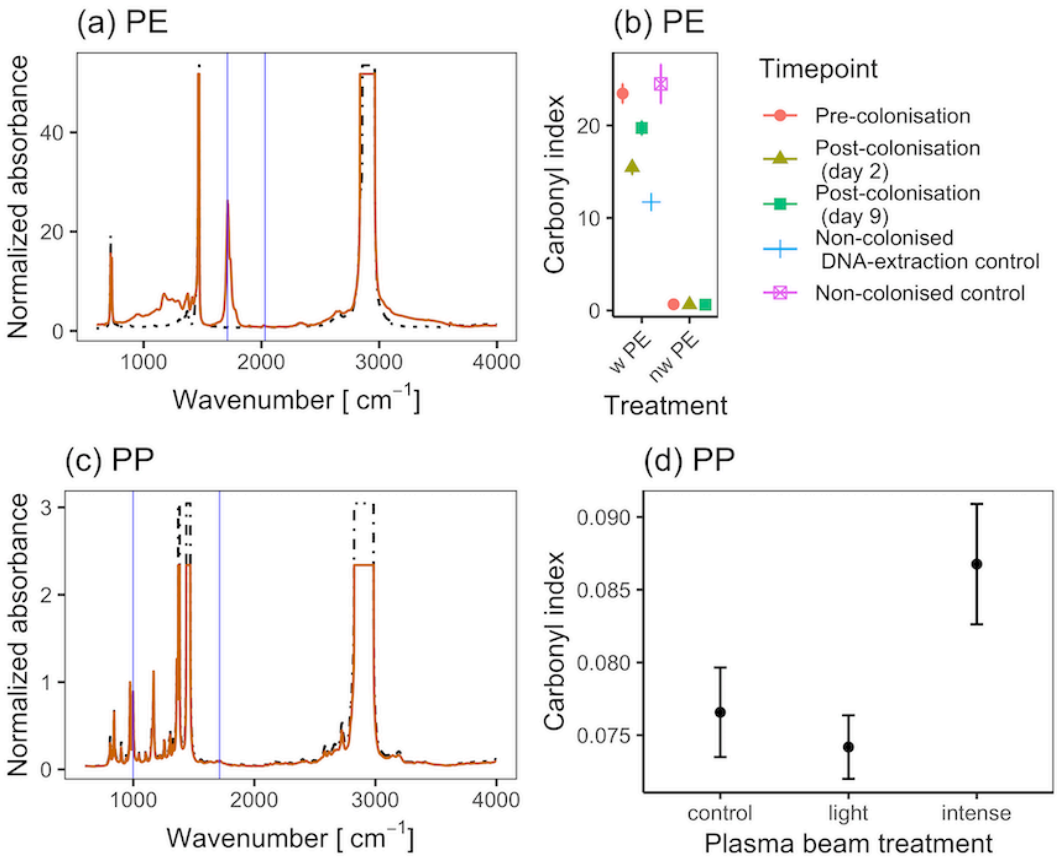

Figure 21. Polyethylene (PE) and polypropylene (PP) weathering. Representative FTIR spectra of weathered (orange line) and non-weathered (dot-dashed black line) PE (a) and PP (c, "intense" treatment only). The peaks used for calculating the carbonyl index (CI) are indicated (blue vertical lines): carbonyl peak at 1712 cm^{-1} and internal reference at 2030 cm^{-1} (PE) and 998 cm^{-1} (PP); (b) CI (± SE, n = 3) obtained from weathered PE (w PE), and non-weathered PE (nw PE) after different experimental exposures; (d) CI (± SE, n = 3) for PP before *in situ* incubations.

Table 6. Coverage of important OHCB genera obtained by different universal 16S rRNA primer pairs.

Primer[1]		HVR[2]	Sequences by genus[3]								Total target sequences	Representative Plastisphere study
Forward	Reverse		*Alcanivorax*	*Oleiphilus*	*Oleispira*	*Thalassolituus*	*Cycloclasticus*	*Marinobacter*	*Neptunomonas*	*Thalassospira*		
343F	908R	V3-5	0.87	0.98	0.96	0.90	0.95	0.94	0.97	0.95	**0.93**	Berry & Gutierrez 2017
515F-Y	926R	V4-5	0.88	0.98	0.93	0.90	0.90	0.93	0.95	0.90	**0.92**	this study
515F	806R	V4	0.88	0.91	0.89	0.95	0.92	0.92	0.92	0.90	**0.91**	Oberbeckmann et al. 2018
341F	785R	V3-4	0.86	0.93	0.89	0.95	0.97	0.92	0.97	0.93	**0.91**	Kirstein et al. 2018
341F	805R	V3-4	0.86	0.93	0.89	0.95	0.97	0.92	0.97	0.94	**0.91**	De Tender et al. 2017
518F	1046R	V4-6	0.76	1.00	0.93	0.85	0.92	0.03	0.95	0.90	**0.36**	Zettler et al. 2013

[1] *For primer sequences and details see Supplementary Table S1.*
[2] *HVR: hyper variable region of 16S rRNA genes.*
[3] *total target sequences: n = 1867; Alcanivorax sequences: n = 397; Oleiphilus sequences: n = 45; Oleispira sequences: n = 27; Thalassolituus sequences: n = 20; Cycloclasticus sequences: n = 59; Marinobacter sequences: n = 1104; Neptunomona sequences: n = 38; Thalassospira sequences: n = 177.*

4.4.3 Analysis of the Plastispheres on PP.

A. Bacterial communities

DNA extraction yields were highest for highly weathered PP (median: 52.4 ng mL^{-1}), intermediate for lightly weathered PP (median45.2 ng mL^{-1}) and lowest for untreated control PP surfaces (median: 30.6 ng mL^{-1}; full data in APPENDIX 9). 16S rRNA gene sequencing data were obtained from biofilms that colonized weathered and non-weathered PP after 9 days of incubation in coastal marine water of the Mediterranean (n = 3 for each material and two technical replicates each). These were inspected together with the 16S rRNA gene data from the blank controls. Plastisphere communities were distinct from the controls, but four were removed nonetheless, as they had <1000 reads (*i.e.* 2× "highly" weathered PP, and 2× non-weathered PP). The mean number of reads for the samples of untreated PP (1410 ± 339 SE) was lower than that obtained from high and low weathering (2558 ± 634 SE and 2906 ± 726 SE, respectively), and therefore coverage of ASV richness was most impacted in the control samples (Figure 22). The dataset contained 1019 taxa in 11 phyla, of which Proteobacteria (n = 698 taxa and 68.5% overall relative abundance) and Bacteroidetes (n = 185 taxa and 18.2% overall relative abundance) were best represented (Figure 23).

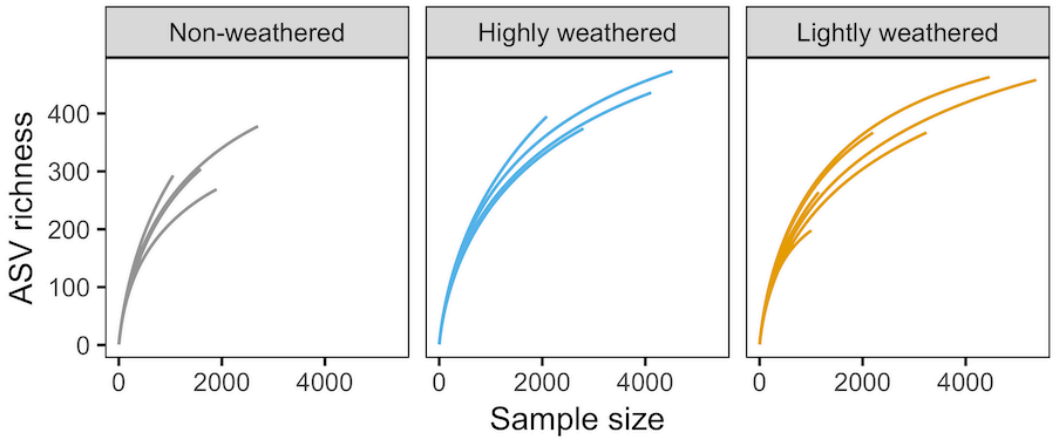

Figure 22. Rarefaction curves for bacterial communities (16S rRNA genes) colonizing weathered polypropylene after 9 days of incubation in coastal Mediterranean seawater.

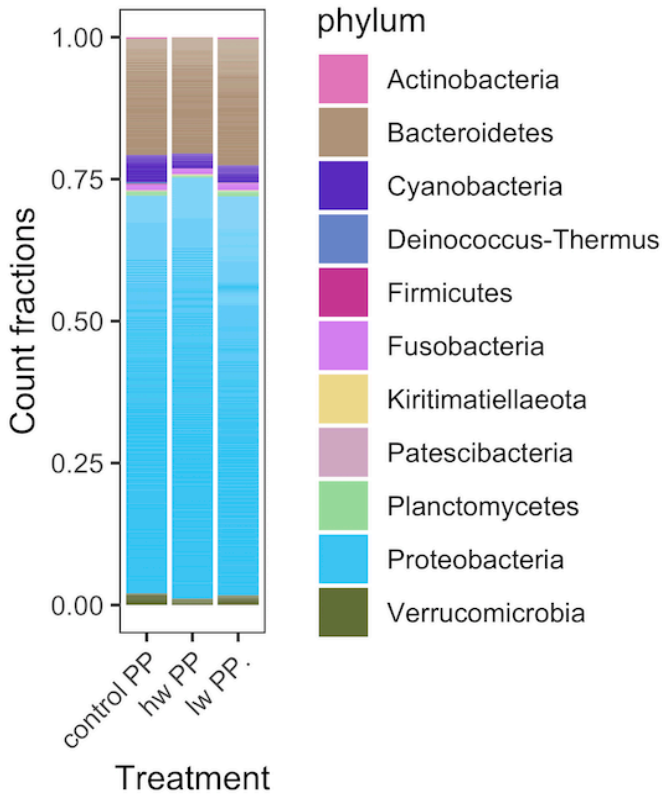

Figure 23. Bar chart showing dominant bacterial phyla (16S rRNA genes) in microbial communities colonizing untreated control PP, heavily weathered polypropylene (hw PP), and lightly weathered PP (lw PP) after 9 days of incubation in coastal Mediterranean seawater.

Overall, bacterial communities from PP lacked differentiation in response to the experimental treatments. Variability in α-diversity was high within treatments (Figure 24), and statistical testing of the Shannon diversity confirmed the overall similarity (Table 7). This pattern persisted throughout β-diversity analyses with neither weighted- nor unweighted UniFracs revealing any distinct patterns (Figure 25, Table 8).

B. Eukaryotic communities

Unfortunately, most eukaryotic community samples (18S rRNA gene) had to be discarded due to very low read numbers (APPENDIX 10), leaving only 1 sample left in each experimental treatment, *i.e.* highly- and lightly weathered. It was therefore not possible explore treatment effects on eukaryotic community composition.

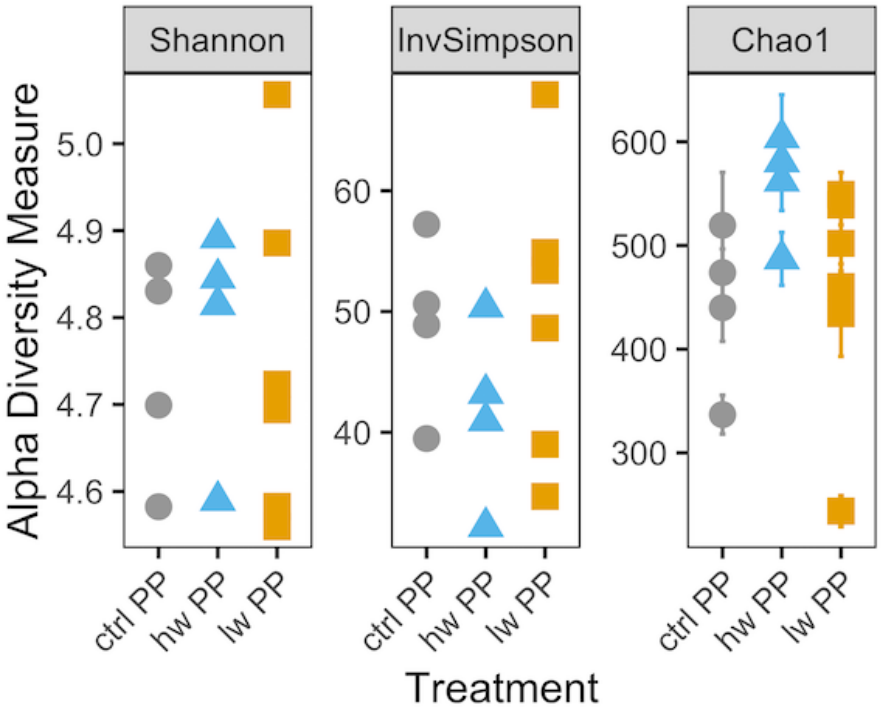

Figure 24. Alpha diversity measures of bacterial communities (16S rRNA gene) on untreated polypropylene (ctrl PP), highly weathered PP (hw PP) and lightly weathered PP (lw PP) after 9 days of incubation in coastal Mediterranean seawater.

Table 7. Contrast summaries of generalized linear model results for Shannon diversity of PP communities.

	16S rRNA gene			
contrast	Estimate	Std. Error	z value	P (>|z|)
hw–ctrl	-0.002	0.005	-0.372	0.926
lw–ctrl	-0.0003	0.005	-0.070	0.997
lw–hw	-0.002	0.005	0.337	0.939

Note: hw: highly weathered, lw: lightly weathered; ctrl: untreated.

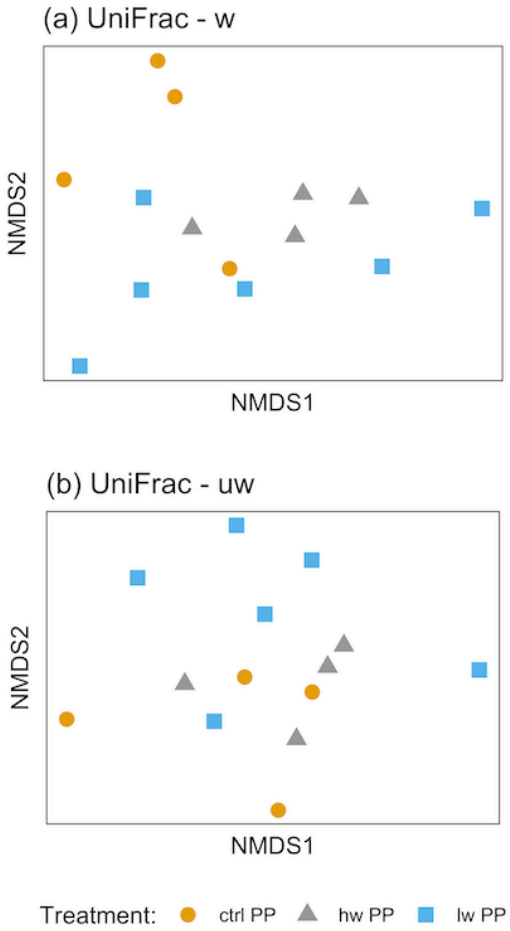

Figure 25. Nonmetric multidimensional scaling (nMDS) plots of bacterial communities (16S rRNA gene) colonizing untreated polypropylene (ctrl PP), highly weathered PP (hw PP) and lightly weathered PP (lw PE) in coastal Mediterranean seawater after 9 days of incubation. Ordinations based on UniFrac distances, both weighted (a) and unweighted (b). (a) k = 2 axes, stress: 0.09; (b) k = 2 axes, stress: 0.19.

Table 8. Statistical summaries of PERMANOVA tests on UniFrac ordinations of 16S rRNA gene data from polypropylene communities.

	16S rRNA gene					
UniFrac: weighted	Df	Sums of Sqs	Mean Sqs	F.Model	R2	Pr(>F)
treatment	2	0.073	0.036	1.453	0.209	0.173
Residuals	11	0.275	0.025		0.791	
UniFrac: unweighted						
treatment	2	0.220	0.110	1.030	0.158	0.356
Residuals	11	1.176	0.107		0.842	

4.4.4 Analysis of the Plastispheres on PE.

A. Bacterial communities

16S rRNA gene sequencing data were obtained from biofilms that colonized weathered and non-weathered PE as well as glass strips after 2 and 9 days of incubation in coastal marine water of the Mediterranean sea (n = 6 for each material and time point). These were inspected together with the 16S rRNA gene data from the planktonic community of the surrounding seawater (n = 3, day 9) and controls: extraction kit blank (n = 2) and negative PCR amplifications (n = 2). DNA extraction yields were higher for day 9 (median ng mL^{-1} for weathered: 200, non-weathered: 232, glass: 57) than day 2 (median ng mL^{-1} for weathered: 40, non-weathered: 20, glass: <10; data in APPENDIX 9). Plastisphere communities were distinct from the planktonic seawater community, as well as controls, except for some samples that were identified as outliers and discarded from downstream analysis, as they had <1000 reads (similar to blanks) or clustered with blank extraction controls (*i.e.* 3× non-weathered PE from day 9, 1× non-weathered PE from day 2, and 1× glass from day 2; Figure 26). The mean number of reads for the samples from day 9 (9,492 ± 1,543 SE) was lower than that obtained from day 2 (25,081 ± 3,066 SE), impacting the coverage of ASV richness (Figure 27). The dataset contained 8259 taxa in 22 phyla, of which Proteobacteria (n = 5409 taxa and 65.5% overall relative abundance) and Bacteroidetes (n = 1284 taxa and 15.6% overall relative abundance) were best represented (Figures 28 and 29).

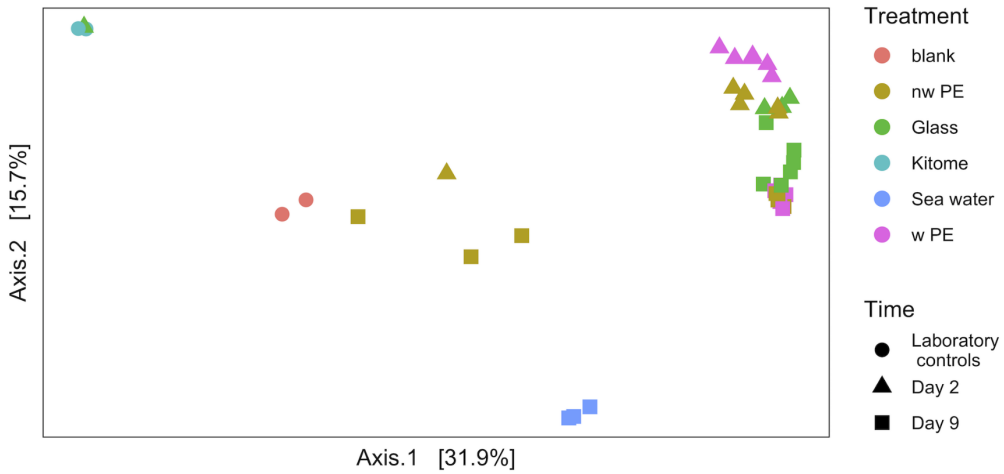

Figure 26. Principal coordinate analysis (PCoA; Bray-Curtis distance) plot of the full 16S rRNA gene sequencing data from communities colonizing weathered polyethylene (w PE), non-weathered PE (nw PE), and glass. Note that controls (Kitome, blank), as well as Sea water samples cluster separately from bulk experimental samples.

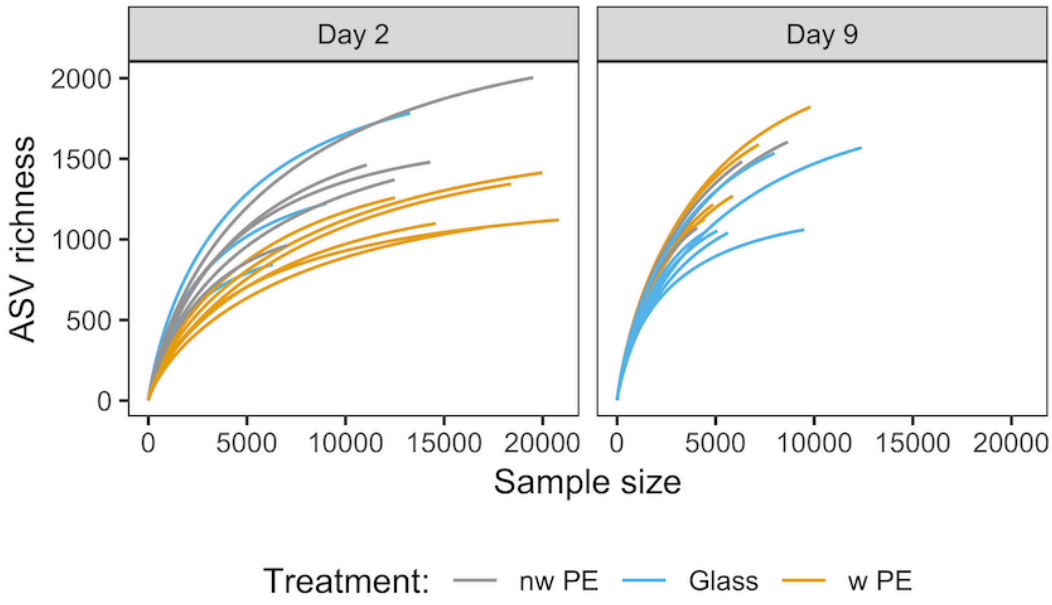

Figure 27. Rarefaction curves for bacterial communities (16S rRNA genes) colonizing weathered polyethylene (w PE), non-weathered PE (nw PE), and glass after 2 and 9 days of incubation in coastal Mediterranean seawater.

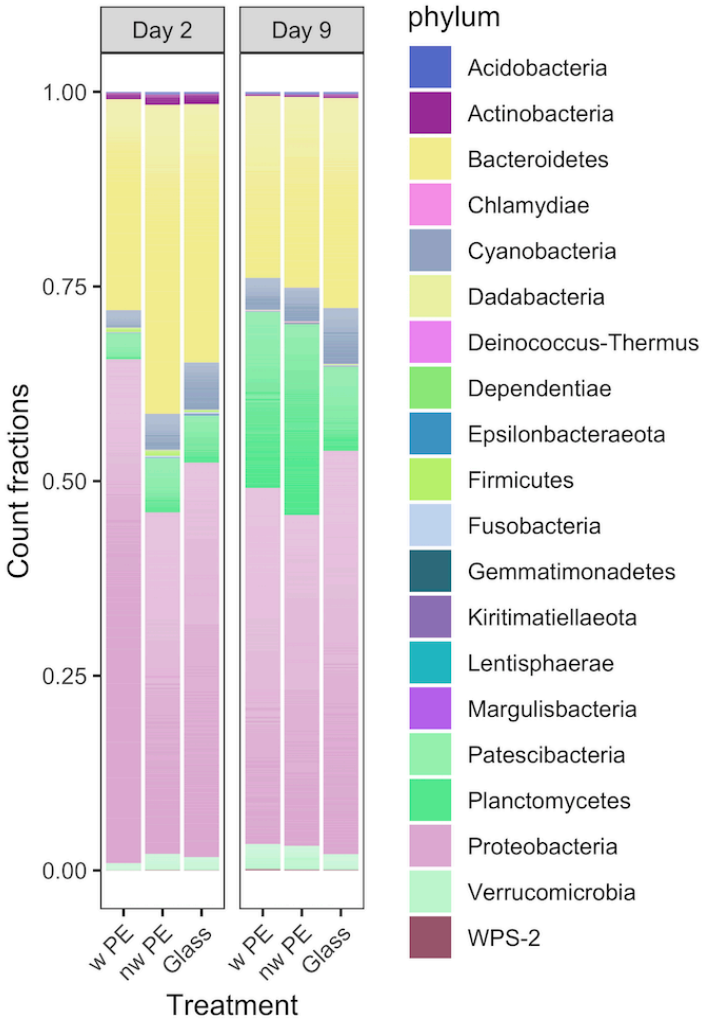

Figure 28. Bar chart showing dominant bacterial phyla (16S rRNA genes) in microbial communities colonizing weathered polyethylene (w PE), non-weathered PE (nw PE), and glass after 2 and 9 days of incubation in coastal Mediterranean seawater.

While the microbial communities differed between the two time points (p = 0.001 for both weighted and unweighted UniFrac; statistical summary is in Table 9), they did not differ as consistently between the three different materials (unweighted UniFrac p = 0.032; weighted UniFrac p = 0.001; Table 9), and stress values suggested that the weighted UniFrac fit the data better on 2 axes (0.069 for weighted- *vs.* 0.151 for unweighted UniFrac: Figure 30). This indicates that all materials were colonized by similar organisms (less support for the measure of presence-absence, *i.e.* unweighted UniFrac; Figure 30a), but their abundance differed between materials which drove differentiation as indicated by the weighted UniFrac analysis (Figure 30b).

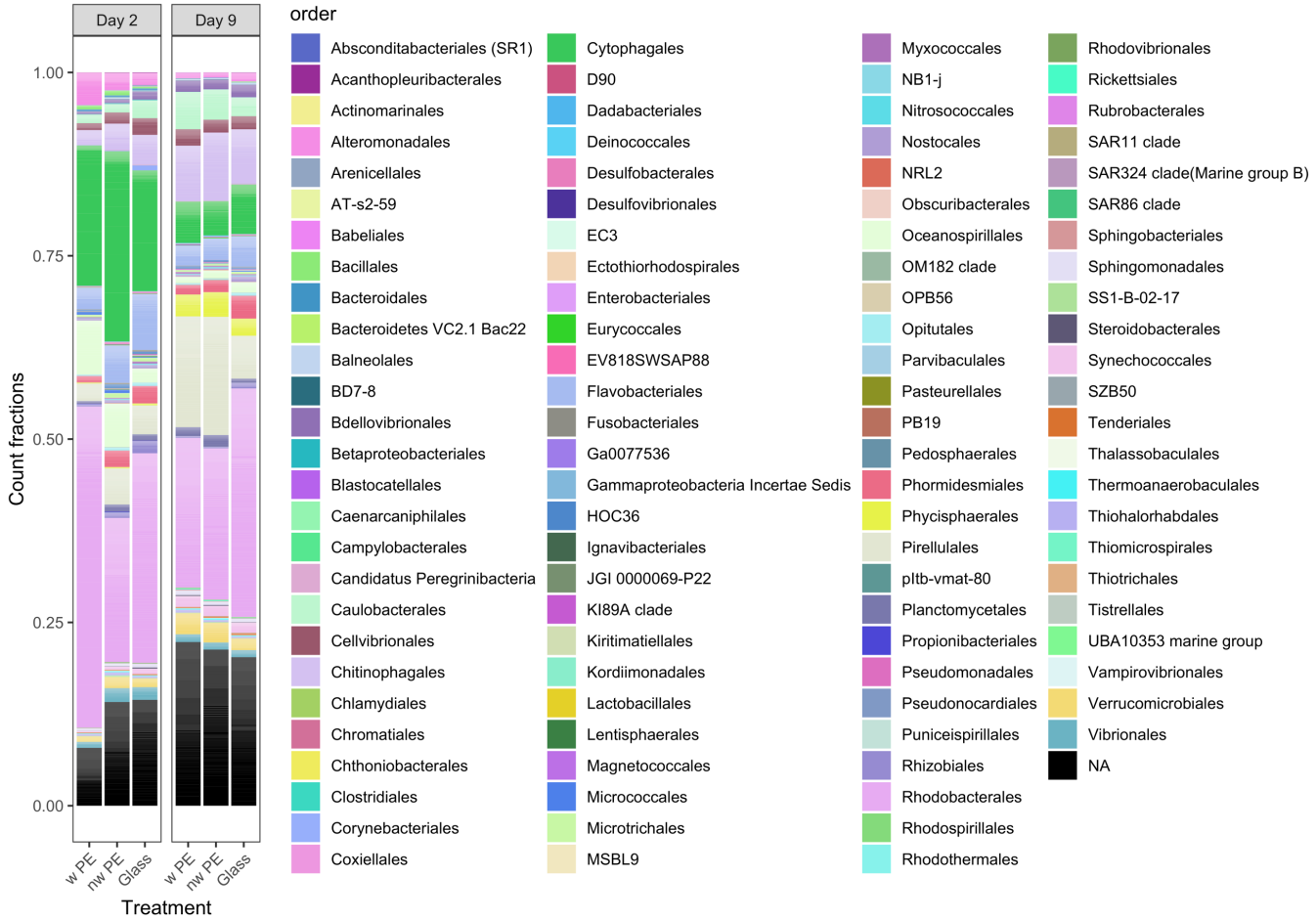

Figure 29. Bar chart showing dominant bacterial orders (16S rRNA gene) in microbial communities colonizing weathered polyethylene (w PE), non-weathered PE (nw PE), and glass after 2 and 9 days of incubation in coastal Mediterranean seawater.

Nonetheless, after longer incubations (*i.e.* 9 days) this difference between materials was lost and all communities converged (Figure 30). The α-diversity measures confirmed this pattern demonstrating that the communities on weathered PE at day 2 were the least diverse (Shannon index in Figure 31; see Table 9 for statistical summary), and also least even (InvSimpson, Figure 31), while ASV richness showed greater overlap with other treatment combinations (Chao1, Figure 31). Shannon diversity remained similar for all other treatment combinations (Figure 31; Table 10).

Table 9. Statistical summary of PERMANOVA tests on UniFrac ordinations of 16S rRNA gene data from polyethylene communities.

UniFrac: weighted	**Df**	**Sums of Sqs**	**Mean Sqs**	**F Model**	**R^2**	**Pr(>F)**
treatment	2	1.737	0.869	5.968	0.148	**0.001**
timepoint	1	5.505	5.505	37.826	0.468	**0.001**
treatment:timepoint	2	1.318	0.659	4.528	0.112	**0.004**
Residuals	22	3.202	0.146		0.272	
UniFrac: unweighted						
treatment	2	0.355	0.177	1.288	0.084	**0.032**
timepoint	1	0.541	0.542	3.936	0.128	**0.001**
treatment:timepoint	2	0.319	0.159	1.159	0.075	0.103
Residuals	22	3.027	0.138		0.714	

Note: significant p-values are denoted in bold.

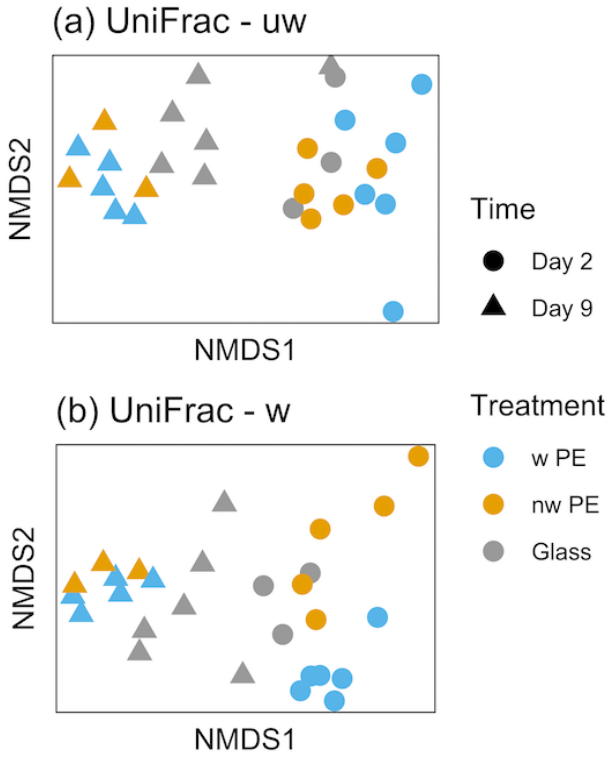

Figure 30. Nonmetric multidimensional scaling (nMDS) plots of bacterial communities (16S rRNA gene) colonizing weathered PE (w PE), non-weathered PE (nw PE) and glass in coastal Mediterranean seawater after 2 and 9 days of incubation. Ordinations based on UniFrac distances, both unweighted (a) and weighted (b). (a) k = 2 axes, stress: 0.151; (b) k = 2 axes, stress: 0.069.

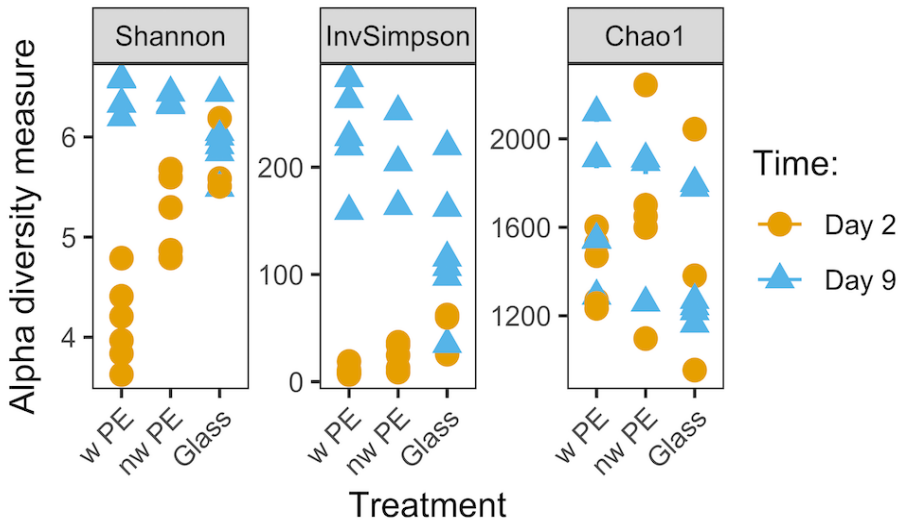

Figure 31. Alpha diversity measures of bacterial communities (16S rRNA gene) on weathered polyethylene (w PE), non-weathered PE (nw PE), and glass after 2 and 9 days of incubation in coastal Mediterranean seawater.

Table 10. Contrast summaries of generalized linear model results for Shannon diversity of bacterial communities (16S rRNA gene) colonizing PE and glass at two different time points.

Compared conditions	Estimate	Std. Error	z value	Pr(>|z|)
glass, day 2 – non-weathered PE, day 2	-0.017	0.009	-1.909	0.393
weathered PE, day 2 – non-weathered PE, day 2	0.051	0.009	5.788	**<0.001**
non-weathered PE, day 9 – non-weathered PE, day 2	-0.033	0.008	-3.976	**<0.001**
glass, day 9 – non-weathered PE, day 2	-0.023	0.007	-3.075	**0.025**
weathered PE, day 9 – non-weathered PE, day 2	-0.034	0.007	-4.623	**<0.001**
weathered PE, day 2 – glass, day 2	0.068	0.009	7.152	**<0.001**
non-weathered PE, day 9 – glass, day 2	-0.017	0.009	-1.803	0.459
glass, day 9 – glass, day 2	0.006	0.008	-0.701	0.982
weathered PE, day 9 – glass, day 2	-0.017	0.008	-2.114	0.276
non-weathered PE, day 9 – weathered PE, day 2	-0.084	0.009	-9.324	**<0.001**
glass, day 9 – weathered PE, day 2	-0.074	0.008	-9.083	**<0.001**
weathered PE, day 9 – weathered PE, day 2	-0.085	0.008	-10.459	**<0.001**
glass, day 9 – non-weathered PE, day 9	0.011	0.008	1.395	0.727
weathered PE, day 9 – non-weathered PE, day 9	0.001	0.008	-0.127	1.000
weathered PE, day 9 –glass, day 9	-0.012	0.007	-1.769	0.482

Note: significant p-values are denoted in bold.

B. Fungal communities

For the fungal communities, inspection of the data from the experimental treatments, together with the controls (*i.e.* extraction kit blank (n = 2) and negative PCR amplifications (n = 2)) was inconclusive, not revealing any distinct clusters (Figure 32). This may partly be due to overall low read numbers across samples, of which eleven were removed due to having <1000 reads (*i.e.* 4× weathered PE from day 9, and 5× non-weathered PE from day 9, 1× non-weathered PE from day 2, and 1× glass day 9). Yields from DNA extractions are as reported for bacterial communities and given in APPENDIX 9. In the remaining samples, plateauing of the ASV accumulation curves showed that sequencing depth was sufficient to capture fungal diversity (Figure 33). After filtering, 231 different taxa emerged belonging to the phyla Ascomycota (n = 88) and Basidiomycota (n = 143). Despite that richness estimates revealed increased fungal α-diversity on day 2 in communities from glass samples compared to the other treatments (Figure 34), generalized linear modelling did not confirm any consistent treatment effects for fungal communities (Table 11). The UniFrac-based analyses, both weighted and unweighted, further corroborated the lack in clear separations among fungal communities in response to experimental treatments (Figure 35, Table 12). Nonetheless, differential abundance testing of day 2 communities revealed the genus *Alternaria* (order: Pleosporales) to be significantly more abundant on PE samples, both weathered and non-weathered, in comparison to glass, but similar between PE treatments (Figure 36). A member of the genus *Piptoporus* (order: Polyporales) however, was significantly more abundant on weathered PE compared to non-weathered PE. In addition, the genus *Peniophora* (order: Russulales) was more abundant on non-weathered PE compared to glass.

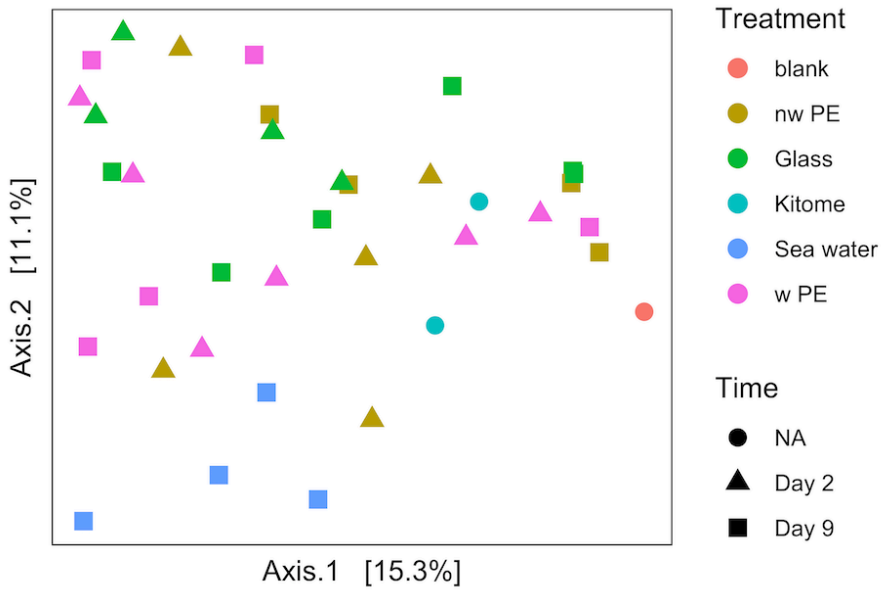

Figure 32. Principal coordinate analysis (PCoA; Bray-Curtis distance) plot of the full ITS sequencing data.

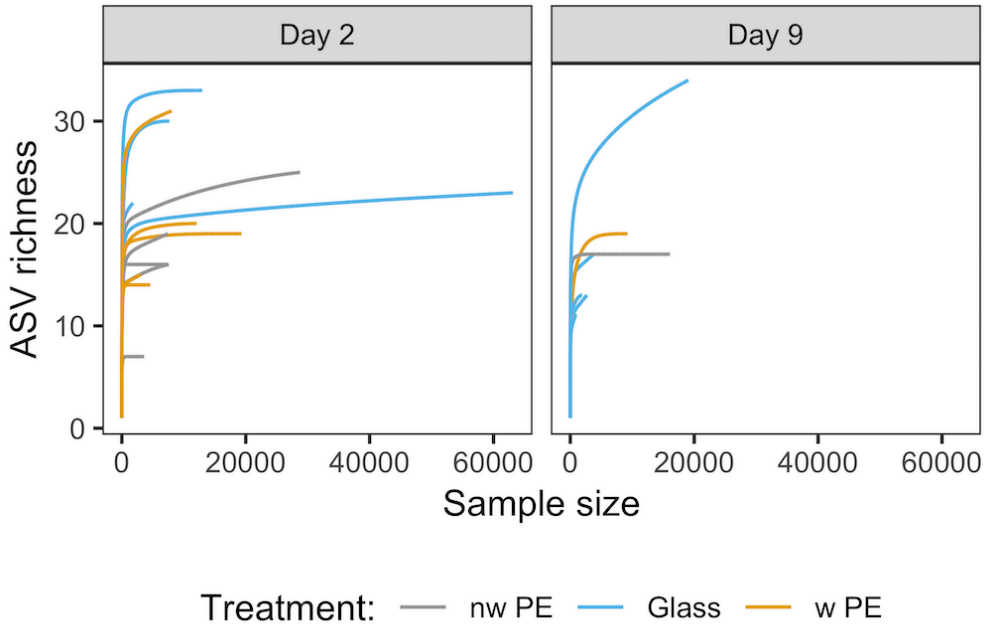

Figure 33. Rarefaction curves for fungal communities (ITS) colonizing weathered polyethylene (w PE), non-weathered PE (nw PE), and glass after 2 and 9 days of incubation in coastal Mediterranean seawater.

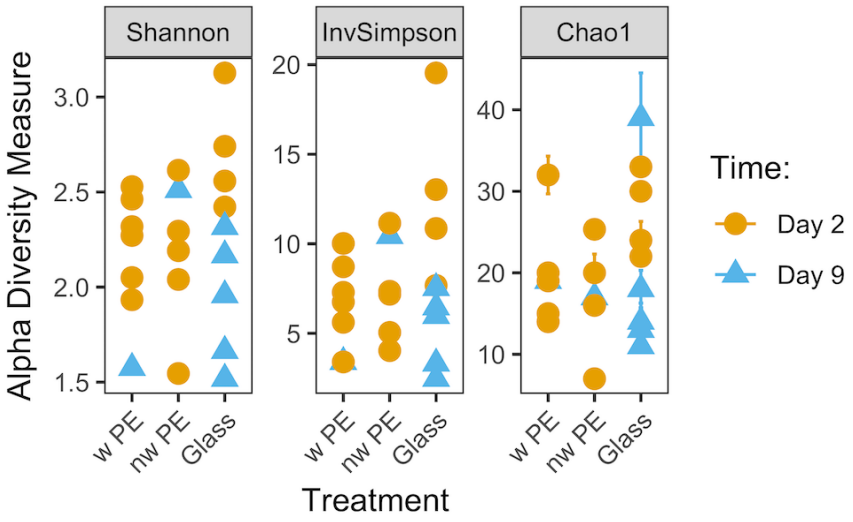

Figure 34. Alpha diversity measures of fungal communities (ITS gene) on weathered polyethylene (w PE), non-weathered PE (nw PE), and glass after 2 and 9 days of incubation in coastal Mediterranean seawater.

Table 11. Contrast summaries of generalized linear model results for Shannon diversity of fungal communities (ITS) colonizing PE and glass at two different time points.

contrast	Estimate	Std. Error	z value	Pr(>|z|)
glass, day 2 – non-weathered, day 2	-0.099	0.041	-2.418	0.135
weathered, day 2 – non-weathered, day 2	-0.026	0.041	-0.629	0.988
non-weathered, day 9 – non-weathered, day 2	-0.069	0.066	-1.052	0.889
glass, day 9 – non-weathered, day 2	0.052	0.046	1.124	0.859
weathered, day 9 – non-weathered, day 2	0.167	0.098	1.699	0.506
weathered, day 2 – glass, day 2	0.074	0.038	1.939	0.352
weathered, day 9 – glass, day 2	0.029	0.065	0.458	0.997
glass, day 9 – glass, day 1	0.151	0.044	3.459	**0.006**
weathered PE, day 9 – glass, day 2	0.266	0.097	2.738	0.059
non-weathered PE, day 9 – weathered PE, day 2	-0.044	0.064	-0.685	0.981
glass, day 9 – weathered PE, day 2	0.077	0.043	1.786	0.448
weathered PE, day 9 – weathered PE, day 2	0.193	0.097	1.984	0.326
glass, day 9 – non-weathered PE, day 9	0.121	0.068	1.789	0.446
weathered PE, day 9 – non-weathered PE, day 9	0.237	0.110	2.147	0.241
weathered PE, day 9 – glass, day 9	0.115	0.099	1.160	0.842

Note: significant p-values are denoted in bold.

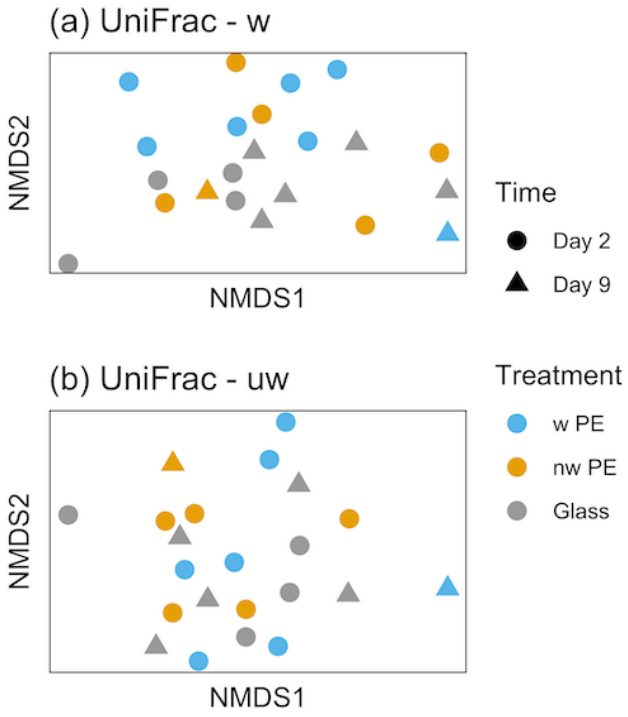

Figure 35. Nonmetric multidimensional scaling (nMDS) plots of fungal communities (ITS) colonizing weathered PE (w PE), non-weathered PE (nw PE) and glass in coastal Mediterranean seawater after 2 and 9 days of incubation. Ordinations based on UniFrac distances, both weighted (a) and unweighted (b). (a) k = 2 axes, stress: 0.11; (b) k = 2 axes, stress: 0.23.

Table 12. Statistical summary of PERMANOVA tests on UniFrac ordinations of ITS data from polyethylene communities.

UniFrac: weighted	**Df**	**Sums of Sqs**	**Mean Sqs**	**F Model**	**R2**	**Pr(>F)**
treatment	2	0.759	0.379	0.789	0.068	0.648
timepoint	1	1.029	1.029	2.143	0.092	0.048
treatment:timepoint	2	1.663	0.832	1.731	0.149	0.087
Residuals	16	7.689	0.481		0.690	
UniFrac: unweighted						
treatment	2	0.387	0.194	1.063	0.095	0.349
timepoint	1	0.277	0.277	1.521	0.068	0.066
treatment:timepoint	2	0.517	0.259	1.421	0.126	0.029
Residuals	16	2.913	0.182		0.712	

Note: significant p-values are denoted in bold.

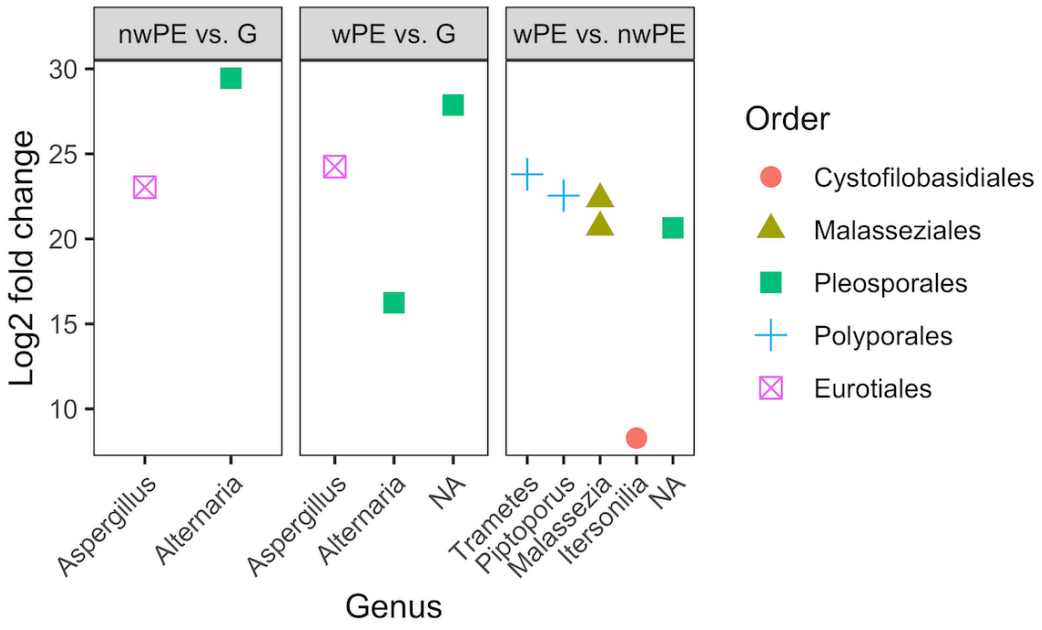

Figure 36. Differentially abundant fungal (ITS) genera from polyethylene (PE; w: weathered; nw: non-weathered) and glass sampled at day 2. NA: features to which genus could not be assigned.

4.4.5 Distinctness of the Plastisphere on weathered PE.

Here we confirm that the low α-diversity displayed by the Plastisphere communities of weathered PE at day 2 (observed in Figures 30b and 31) was due to a small number of abundant species that drove the differentiation of the community. Members of the *Roseobacter*-like genus were most prominently overabundant on weathered PE compared to glass and non-weathered PE (Figure 37a). Interestingly, inspection of the individual *Roseobacter*-like ASVs revealed that overall community difference was mainly driven by ASV3, which represented 27% median of the prokaryotic community on weathered PE at day 2 (DESeq2 normalized counts; Figure 37b). At day 9 though, the median relative abundance of ASV3 on weathered PE had dropped to 0.25% (Figure 37b). A BLAST search of ASV3 returned *Thalassococcus halodurans* (strain UST050418-052, 99.73% 16S rRNA gene sequence identity) as the top hit.

The genera *Oleiphilus* (Order: Oceanospirillales and representative of the OHCB group) and *Aestuariibacter* (Order: Alteromonadales) represented ~5.8% and ~1.8% of the prokaryotic community on weathered PE on day two, respectively (Figure 37c, d). While ASVs of both organisms were overrepresented in communities from weathered PE compared with Glass (Figure 37a), only

Aestuariibacter ASVs remained differentially abundant when comparing weathered PE to non-weathered PE (Figure 37a). The most abundant ASV belonging to *Oleiphilus* (ASV28) showed 94.4% 16S rRNA gene sequence identity with *Oleiphilus messinensis* (strain ME102). The abundant *Aestuariibacter* ASVs, *i.e.* ASV52 and ASV123, displayed 97.3% sequence identity to *Aestuariibacter aggregatus* (strain WH169).

Despite observing enriched taxa on weathered PE in day 2 samples, the artificial metagenomes (PICRUSt2) generated for the bacterial communities did not provide further insight into potentially interesting functional pathways (no differentially abundant KEGGs as per DESeq2), which may partly be explained by low scores of the weighted nearest-sequenced index, indicating low accuracy of the predictions (Figure 38).

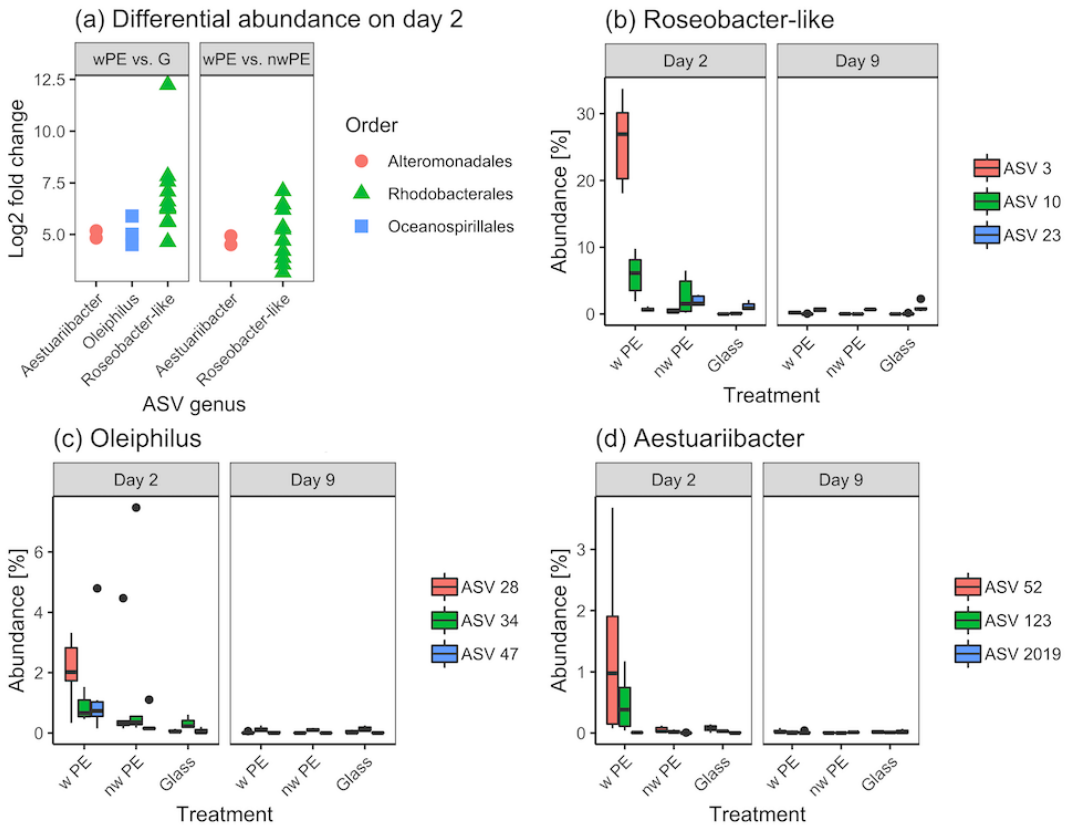

Figure 37. Differentially abundant amplicon sequence variants (ASVs) from polyethylene (PE; w: weathered; nw: non-weathered) and glass. (a) Log2 fold changes for differentially abundant ASVs. (b-d) The three most abundant ASVs within each genus are shown in boxplots displaying median relative abundance using DESeq2 normalized counts.

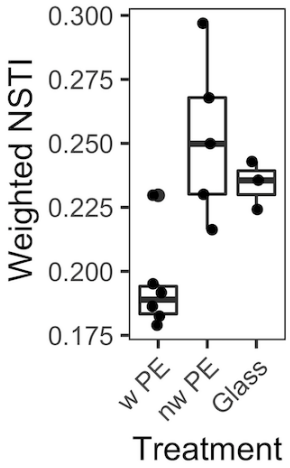

Figure 38. Nearest-sequenced taxon indices (NSTI) for predicted metagenomes based on 16S rRNA gene sequences from day 2 samples. w PE weathered polyethylene; nw PE: non-weathered polyethylene.

4.5 Discussion

We show that weathered PE surfaces selected for a less diverse bacterial community compared with untreated PE or glass only after short-term *in situ* incubations in coastal Mediterranean seawater, mainly due to the enrichment of several distinct bacteria. Identifying bacterial communities on marine plastic debris has been the main focus of a number of recent environmental surveys (Amaral-Zettler et al., 2015; De Tender et al., 2017, 2015; Oberbeckmann et al., 2018, 2016). These studies revealed that geographical and seasonal factors were better predictors of Plastisphere community differentiation than the actual polymer type itself. We believe that the reason for such observations is that these analyses are usually done on mature Plastispheres that have spent weeks, if not months, at sea allowing communities to develop and converge.

Here, for the first time, we analysed the early colonization stages of weathered PE and PP in comparison with non-weathered PE and PP, as well as glass (in the experiment with PE). At a higher taxonomic level, both polymers acquired similar communities, dominated by members of the phyla Bacteroidetes and Proteobacteria, which is typical for plastics in coastal environments (De Tender et al., 2017). At lower taxonomic levels however, communities on PP still exhibited typical compositions among different samples (order level, APPENDIX 11), while on weathered PE differences emerged, especially at genus level at which we observed the enrichment of mainly three organisms: *Roseobacter* clade-, *Oleiphilus*-

and *Aestuariibacter*-like taxa. *T. halodurans* (*Roseobacter* clade-like organism) was particularly abundant only on weathered PE (ASV3; 28% of the prokaryotic community; Figure 37a). Despite that members of the *Rhodobacteraceae*, and especially taxa from the *Roseobacter* clade, are known primary colonisers of surfaces in marine environments (Dang and Lovell, 2000; Elifantz et al., 2013), the specificity of ASV3 for weathered PE was notable. Members of the *Roseobacter* clade are known for their high versatility, and in some cases, their ability to degrade certain hydrocarbon compounds (Buchan et al., 2005; Christie-Oleza et al., 2012; Newton et al., 2010), though further experimentation is required to confirm that this enriched *T. halodurans* strain is able to metabolize subproducts released from the weathered material.

The other two enriched taxa on weathered PE, *i.e. O. messinensis* and *A. aggregatus*, are known hydrocarbon degraders (Golyshin et al., 2002; Wang et al., 2014). *Oleiphilus* is a member of the OHCB group, and is "specialized" in degrading n-alkanes in the C_{11}–C_{20} range (Golyshin et al., 2002; Toshchakov et al., 2017), which would be consistent with the molecules generated by PE weathering (Albertsson et al., 1995; Gewert et al., 2018). While OHCB are generally reported within the rare taxa of the Plastisphere, here we observed a considerable relative abundance of *Oleiphilus* ASV28 during the early colonisation stages of PE (i.e. 5.8 and 3.7% on weathered and non-weathered PE, respectively). Unlike *Oleiphilus*, *Aestuariibacter* ASV52 was preferentially enriched only on weathered PE (1.8% relative abundance and almost 38× more abundant than on non-weathered PE). Both are therefore interesting organisms that deserve further attention in studies of PE biodegradation.

Recalcitrant polymers used to manufacture plastic materials, e.g. PE or PP, are highly inert and difficult to biodegrade (Krueger et al., 2015). Earlier laboratory studies described the release of short-chain compounds from weathered plastics which ultimately enhanced microbial growth (Albertsson et al., 1995, 1987; Gewert et al., 2018; Romera-Castillo et al., 2018). The abiotic reduction in molecular weight of synthetic polymers may be crucial prior to any potential biodegradation (Restrepo-Flórez et al., 2014), as chain scission products such as suberic- or tetradecanedioic acid from photooxidized PE (Gewert et al., 2018) are more amenable for bacterial growth. In light of current marine plastic waste issues, interest in biodegradation of common non-hydrolysable polymers has soared, but the importance of plastic

surface oxidation has only recently been considered for *in situ* colonization studies, confirming tangible treatment effects on plastic colonization (Dussud et al., 2018; Karlsson et al., 2018).

We believe that the higher load of chain scission products from the weathered PE enriched, rather than selected, for the distinct genera given that the weighted-, but not the unweighted, UniFrac-based analyses supported community differentiation, thus indicating that the observed differences were due to relative abundance of community members, instead of the presence-absence of taxa. Crucially, it remains unknown whether such strains merely scavenge released chain scission products (indirect degradation), or if the microorganisms are capable of direct degradation of high molecular weight polymers such as PE or PP, given that the latter requires potent extracellular oxidizing enzymes (Krueger et al., 2015).

Support for chain scission scavenging may be lent by the lack in community differentiation on PP, which correlated with a significantly lower degree in oxidation. The plasma beam treatment, even at "intense", failed to induce carbonyl indices in PP comparable to what was found in the environment (0.085, Figure 21 compared to 0.5-1; ter Halle et al., 2017). Several mutually non-exclusive reasons may explain our results. For instance, obtaining homogeneously oxidized PP surfaces may have been complicated by the melting of the surface which occurred during treatment due to the very high heat (pers. observation). Another reason may be that the PP strips had been prepared from commercial plastics, which typically contain various antioxidants to prolong the service time of the polymers (Hahladakis et al., 2018). The additives in PP may thus have limited the degree of oxidation in comparison with PE, which had been prepared from "pure" polymer pellets. We acknowledge that the weathering treatments are not directly comparable, as they were performed with different methods. The reason for this, was that it was not possible to produce PP films from "pure" pellets (as for PE), because the pressed films were too brittle. Research has nonetheless shown that subproducts from PP can be expected, such as pentane or 2,4-dimethyl-1-heptene (Gewert et al., 2015). Ultimately, the lack in sufficient surface oxidation probably resulted in unobservable treatment effects, as comparably few low molecular weight products were available from PP to OHCB bacteria. As no samples were taken at day 2 however, the lack in community differentiation could also be ascribed to the convergence of the

communities, as observed in PE at day 9. A lack in OHCB members due to insufficient 16S rRNA gene primer coverage can be excluded though (92%, Table 6).

Fungi have so far rarely been considered in Plastisphere studies, despite their role in degrading nonhydrolyzable compounds, such as lignin, through osmotrophy, *i.e.* using secreted enzymes like the oxidizing laccases (Raghukumar, 2017; Richards et al., 2012). Contrary to observations from bacterial communities on PE, fungal communities did not display any community level differences, regardless of substrate or sampling time point. A lack of clear temporal shifts on PE over 44 weeks of exposure had also been noted by De Tender et al. (2017). It is nonetheless interesting to note, that differential abundance testing highlighted a member of the genus *Alternaria* (order: Pleosporales) to be significantly enriched on both PE treatments compared to the glass control (Figure 37). Pleosporales have been observed to form blooms, particularly in correlation with chlorophyll abundance (Taylor and Cunliffe, 2016), and indeed, chlorophyll harbouring cells, such as diatoms, have repeatedly been shown to attach to plastic (Oberbeckmann et al., 2016; Zettler et al., 2013), which in turn may drive the high Pleosporales abundance observed here. Another fungal genus highly abundant on untreated PE in comparison to glass was *Peniophora*, which was found to have high laccase activity (Bonugli-Santos et al., 2010) and could pose an interesting strain for further laboratory study.

Molecular characterization and further confirmation of plastic biodegraders can only be achieved by isolation. This is especially evident through the PICRUSt-based analysis, which did not yield any differentially abundant KEGG orthologs in bacterial (16S rRNA gene) day two communities, probably as a consequence of the low prediction accuracy (*i.e.* NSTI scores >0.15, Figure 39, PICRUSt manual), ultimately highlighting knowledge gaps in our understanding of functional potential of such microbial communities. We show here that isolation efforts of putative biodegrading microorganisms should target very early stages of plastic colonization as more mature biofilms on PE and glass converged, the relative abundance of initially enriched genera decreased, and differences at the community level were no longer evident. Similarly, in an experiment over 45 days, Dussud *et al.* (2018) reported a 1.7–3 fold higher relative abundance of (O)HCB on all tested polymer types in early colonization stages, when compared with seawater communities (Dussud et al., 2018). Moreover, these observations are in accordance with chitin particle colonization experiments, which confirmed that early colonizers were

degraders, while later colonizers were secondary consumers (Datta et al., 2016). Later biofilm stages may thus complicate the identification and isolation of microbial candidates for further study of microbial biodegradation of plastics. Alternatively, the secondary biofilm could be removed to reveal the rare and tightly attached organisms on the surface of plastics, as recently reported (Kirstein et al., 2019).

The present study meets a research gap in the context of biodegradation, highlighting that the isolation of potentially interesting taxa should involve sampling at earlier stages of surface colonization and using pre-oxidized polymers. While recalcitrant plastics do not appear to serve as an important carbon source for mature Plastispheres, early colonizing organisms display potential to metabolize subproducts emerging from plastic weathering. Whether these microbes are able to carry out the first steps of surface oxidation remains an open question.

CHAPTER 5

FINAL CONCLUSIONS AND FUTURE PERSPECTIVES

As outlined in chapter one, monitoring of plastic debris on sea surfaces suggested that a considerable amount of plastic projected to be in the environment was missing, especially in the numerically dominant size range <1 mm. In the present thesis, I set out to tackle some of the hypotheses invoked to explain this mismatch in the plastic debris balance. Chapter two was devoted to the question of whether polymer density correlated with the probability of a given polymer type being found in a specific marine compartment. In chapter three, a microplastic detection method was developed, which avoided the problem of visual bias. The new method was then applied in an attempt to find increasing microplastics with decreasing size. In chapter four, the colonization of artificially weathered plastics in natural seawater was studied, with a particular focus on OHCB. These hypotheses are graphically summarized in Figure 39.

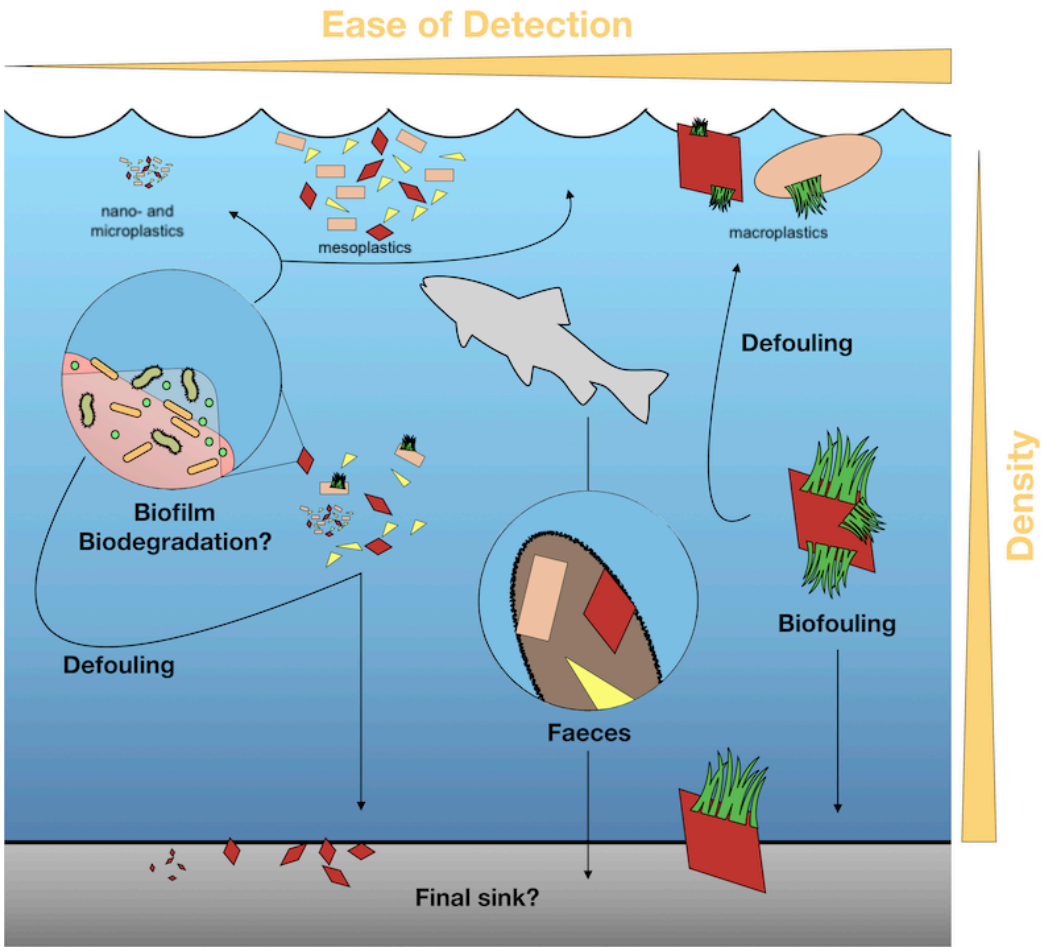

Figure 39. Schematic summary of different hypotheses to explain removal of buoyant plastic debris from sea surfaces.

5.1 Where marine plastic debris is going

Knowing where marine plastic debris accumulates in the environment is of crucial importance for managing this problem and its impacts. At high concentration sites, fauna is more likely to encounter plastic debris, and a recent study has for instance estimated that harmful plastic concentrations may be reached in beaches by 2060 (Everaert et al., 2018). In sea surfaces, such thresholds are far from being realized (> 2100) (Everaert et al., 2018). Higher concentrations of plastics on the seafloor than sea surface however, in combination with the problem of the "missing" plastics, led Woodall et al. (2014) to suggest that deep seas may constitute a major sink for marine plastic debris. This general conclusion was not supported by the meta-analysis, which highlighted deep seas primarily as a sink for higher density microplastics. Sea surfaces in turn carried higher proportions of PE and PP than the global mean.

Besides general trends, the data also pointed towards intricacies that should more attentively be considered in future research. The vast majority of particles considered in the meta-analysis were small fragments (0.3–5 mm), but it has not escaped our notice, that studies during which even smaller filter pore sizes were employed, such as 10–20 µm (Bergmann et al., 2017; Enders et al., 2015), or the surface microlayer was sampled (Song et al., 2014), represented outliers (Figure 8). This effect might be the consequence of the size selective mechanisms outlined in chapter one (section 1.4). Moreover, such observations may also depend on the distance from coast at which sampling occurs. The meta-analysis showed that seafloor sediments in photic zones harboured similar proportions of the most common polymer types compared to beaches. As discussed in section 2.5, this may indicate that in photic zones processes such as biofouling and aggregation, and animal ingestion and defecation may be more effective at removing microplastics from sea surfaces than in aphotic areas further off-shore.

Future studies could focus more closely on studying changes in relative abundance of different plastic polymer types in function of diverse variables. Indications for the significance of the distance to coast have for instance already been reported (Suaria et al., 2016), but more data are needed. Another vital gap in our data stems from the lack of water column sedimentation samples gathered at different depths. The analysis of fine samples had long been a hindrance to progressing the field in this aspect, but more sensitive methods, that eliminated visual biases have been developed (Bergmann et al., 2017; Erni-Cassola et al., 2017; Löder et al., 2015) and will contribute to a more comprehensive understanding of where marine plastic debris is finally deposited.

5.2 Improved detection leading to greater finds

As plastics fragment in the environment, they become increasingly difficult to detect during environmental monitoring efforts, which primarily rely on manual sorting and visual identification steps for quantification. As described in section 3.2, research has shown that these can lead to biases with particles <0.5 µm. In chapter 3, a newly developed method is presented that addresses such issues. Nile red-based methods have already been successfully employed, for instance to study the fragmentation of PE, PP and foamed PS (Song et al., 2017), to detect microplastics in bottled water

(Mason et al., 2018), or to assist in distinction between natural and synthetic fibres ingested by wild mussels (Catarino et al., 2018).

Despite the advantages that Nile red-based methods provide, they require utmost care during sample preparation, due to their sensitivity to contamination with natural materials, that are hydrophobic. While this may not pose a significant hindrance for monitoring tap water or "relatively" clean samples, such as surface sea water (provided digestive pre-treatment nonetheless), sediment samples constitute greater challenges, as they contain higher degrees of organic matter. As described in chapter 3 (section 3.5) alternative methods have been developed, which rely on high throughput FTIR recording the chemical spectra of whole filter sample areas. Based on these spectra, natural materials can then be distinguished from synthetic polymers of interest. These alternative methods have successfully been applied (Bergmann et al., 2017; Peeken et al., 2018), but unfortunately they remain prohibitively expensive.

Given that Nile red offers a more accessible way to detect and count small plastic particles, research looking into improving this method should primarily focus on perfecting sample digestion protocols. Advancements have been made with general purpose digestion protocols (Cole et al., 2014; Löder et al., 2017), but perhaps more sample specific protocols will have to be used.

Irrespectively of what new method was used however, it has been shown here and by other researchers that microplastics are present in the environment at growing abundances with decreasing size (Bergmann et al., 2017; Lenz et al., 2016; Peeken et al., 2018), and that less plastics had gone missing than initially presumed. It remains nonetheless difficult, to estimate whether abundances are higher or lower than predicted, and this may have several causes. For instance, Filella (2015) compellingly argued that assuming a fragmentation behaviour following a power law of 3 may not be correct, and research has already shown that not only do fragmentation rates for a given polymer vary with the environment that it is exposed to, but also that under equal conditions different common polymer types fragment at distinct rates. Such processes need to be better understood, for predictions to be improved. Ultimately, polymer specific variables coupled with waste emission data and environmental transportation pathways, will help future models to better estimate and predict plastic pollution loads in different environmental compartments.

5.3 Microbial colonization of plastic and the communities' potential to its substrate

Recent years have witnessed increased interest in microbial communities that colonize marine plastics debris, especially with regards to the potential for biodegradation. Commonly employed polymer types, in conjunction with their additives, are highly resistant to degradation, and in particular biodegradation. Recent reports have nonetheless shown that microbial species can be capable of degrading such plastics (Santo et al., 2013; Yoshida et al., 2016). *In situ* marine colonization studies however, have often provided mixed results, as community differentiation between polymer types remained small and the consistent presence of putative degraders in communities remained absent. As detailed in the introduction (section 1.8), it has emerged from previous studies, that a preceding abiotic reduction of molecular weight of the polymer could ease access for microbial biodegradation. A key point of improvement upon earlier *in situ* colonization studies was therefore to employ artificially aged plastic substrates.

As reported in chapter 4, we set out to test the hypothesis, that when weathered, aliphatic polymers (*i.e.* PE and PP) become colonized by microbial communities with higher relative abundances of organisms specialized in degrading aliphatic compounds. Our experiments demonstrated that overall effects of weathering on microbial colonization were not pronounced when compared with untreated plastics of glass, and that indicative differences only occurred during early colonization stages. Interestingly, besides a cryptic *Roseobacter*-like organism, that was highly dominant, the two additional bacterial organisms found to be overabundant in those early stages were close relatives of strains known to degrade oil. The quick drop in relative abundance of these distinct taxa may however indicate, that in coastal conditions weathered aliphatic polymers do not serve as an important source of carbon to the communities.

Keystone bacterial species that drive microbiome structures are not necessarily the most abundant though (Banerjee et al., 2018). Given the growing interest in plastic biodegradation and the significant knowledge gap in this field, additional research is urgently needed. An important open question is whether microbes are capable of performing the surface oxidation necessary to reduce molecular weight, or if they merely scavenge the low molecular weight chain

scission products before starving. For a systematic assessment of biodegradation candidate strains must be isolated. Based on the results of the experiments described in chapter 4, we recommended that efforts to isolate candidate strains ought to prioritize short incubation times and employ artificially weathered plastics, as "interesting" strains will be more abundant.

In conclusion, and with regards to biodegradation as a factor contributing to the loss of marine plastic debris, the results presented here do not suggest that specialized communities colonize and persist on weathered aliphatic polymers, and that therefore biodegradation does not constitute a significant removal mechanism in Mediterranean coastal conditions.

REFERENCES

Abayomi, O.A., Range, P., Al-Ghouti, M.A., Obbard, J.P., Almeer, S.H., Ben-Hamadou, R., 2017. Microplastics in coastal environments of the Arabian Gulf. Mar. Pollut. Bull. 124, 181–188.

Akovali, G., 2012. Plastic materials: Chlorinated polyethylene (CPE), chlorinated polyvinylchloride (CPVC), chlorosulfonated polyethylene (CSPE) and polychloroprene rubber (CR), in: Pacheco-Torgal, F., Jalali, S., Fucic, A. (Eds.), Toxicity of Building Materials. Woodhead Publishing Limited, pp. 54–75.

Albertsson, A.-C., Andersson, S.O., Karlsson, S., 1987. The mechanism of biodegradation of polyethylene. Polym. Degrad. Stab. 18, 73–87.

Albertsson, A.-C., Barenstedt, C., Karlsson, S., Lindberg, T., 1995. Degradation product pattern and morphology changes as means to differentiate abiotically and biotically aged degradable polyethylene. Polymer. 36, 3075–3083.

Albertsson, A.C., Karlsson, S., 1990. The influence of biotic and abiotic environments on the degradation of polyethylene. Prog. Polym. Sci. 15, 177–192.

Allen, A.S., Seymour, A.C., Rittschof, D., 2017. Chemoreception drives plastic consumption in a hard coral. Mar. Pollut. Bull. 124, 198–205.

Amaral-Zettler, L.A., Zettler, E.R., Slikas, B., Boyd, G.D., Melvin, D.W., Morrall, C.E., Proskurowski, G., Mincer, T.J., 2015. The biogeography of the Plastisphere: implications for policy. Front. Ecol. Environ. 13, 541–546.

Amélineau, F., Bonnet, D., Heitz, O., Mortreux, V., Harding, A.M.A., Karnovsky, N., Walkusz, W., Fort, J., Grémillet, D., 2016. Microplastic pollution in the Greenland Sea: Background levels and selective contamination of planktivorous diving seabirds. Environ. Pollut. 219, 1131–1139.

Andrady, A.L., 2017. The plastic in microplastics: A review. Mar. Pollut. Bull. 119, 12–22.

Andrady, A.L., 2015. Persistence of Plastic Litter in the Oceans, in: Bergmann, M., Gutow, L., Klages, M. (Eds.), Marine Anthropogenic Litter. Springer, pp. 57–72.

Andrady, A.L., 2011. Microplastics in the marine environment. Mar. Pollut. Bull. 62, 1596–1605.

Andrady, A.L., 2010. Using flow cytometry to detect micro- and nano-scale polymer particles, in: Arthur, C., Baker, J. (Eds.), Proceedings of the Second Research Workshop on Microplastic Debris. NOAA Technical Memorandum NOS-OR&R-39.

Andrady, A.L., Neal, M.A., 2009. Applications and societal benefits of plastics. Phil. Trans. R. Soc. B 364, 1977–1984.

Andrady, A.L., Pegram, J.E., 1991. Weathering of polystyrene foam on exposure in air and in seawater. J. Appl. Polym. Sci. 42, 1589–1596.

Andrady, A.L., Pegram, J.E., Tropsha, Y., 1993. Changes in Carbonyl Index and Average Molecular Weight on Embrittlement of Enhanced-Photodegradable Polyethylenes. J. Environ. Polym. Degrad. 1, 171–179.

Austin, H.P., Allen, M.D., Donohoe, B.S., Rorrer, N.A., Kearns, F.L., Silveira, R.L., Pollard, B.C., Dominick, G., Duman, R., Omari, K. El, Mykhaylyk, V., Wagner, A., Michener, W.E., Amore, A., Skaf, M.S., Crowley, M.F., Thorne, A.W., Johnson, C.W., Woodcock, H.L., McGeehan, J.E., Beckham, G.T., 2018. Characterization and engineering of a plastic-degrading aromatic polyesterase. Proc. Natl. Acad. Sci. 115, E4350–E4357.

Azzaro, M., La Ferla, R., Azzaro, F., 2006. Microbial respiration in the aphotic zone of the Ross Sea (Antarctica). Mar. Chem. 99, 199–209.
Bagaev, A., Mizyuk, A., Khatmullina, L., Isachenko, I., Chubarenko, I., 2017. Anthropogenic fibres in the Baltic Sea water column: Field data, laboratory and numerical testing of their motion. Sci. Total Environ. 599–600, 560–571.
Ballent, A., Corcoran, P.L., Madden, O., Helm, P.A., Longstaffe, F.J., 2016. Sources and sinks of microplastics in Canadian Lake Ontario nearshore, tributary and beach sediments. Mar. Pollut. Bull. 110, 383–395.
Banerjee, S., Schlaeppi, K., van der Heijden, M.G.A., 2018. Keystone taxa as drivers of microbiome structure and functioning. Nat. Rev. Microbiol. 16, 567–576.
Barnes, D.K.A., Galgani, F., Thompson, R.C., Barlaz, M., 2009. Accumulation and fragmentation of plastic debris in global environments. Phil. Trans. R. Soc. B 364, 1985–1998.
Beer, S., Garm, A., Huwer, B., Dierking, J., Nielsen, T.G., 2018. No increase in marine microplastic concentration over the last three decades – A case study from the Baltic Sea. Sci. Total Environ. 621, 1272–1279.
Bergmann, M., Wirzberger, V., Krumpen, T., Lorenz, C., Primpke, S., Tekman, M.B., Gerdts, G., 2017. High quantities of microplastic in Arctic deep-sea sediments from the HAUSGARTEN observatory. Environ. Sci. Technol. 51, 11000–11010.
Berry, D., Gutierrez, T., 2017. Evaluating the detection of hydrocarbon-degrading bacteria in 16S rRNA gene sequencing surveys. Front. Microbiol. 8, 896.
Bjorndal, K.A., Bolten, A.B., Lagueux, C.J., 1994. Ingestion of Marine Debris by Juvenile Sea Turtles in Coastal Florida Habitats. Mar. Pollut. Bull. 28, 154–158.
Blumenröder, J., Sechet, P., Kakkonen, J.E., Hartl, M.G.J., 2017. Microplastic contamination of intertidal sediments of Scapa Flow, Orkney: A first assessment. Mar. Pollut. Bull. 124, 112–120.
Boerger, C.M., Lattin, G.L., Moore, S.L., Moore, C.J., 2010. Plastic ingestion by planktivorous fishes in the North Pacific Central Gyre. Mar. Pollut. Bull. 60, 2275–2278.
Bonugli-Santos, R.C., Durrant, L.R., Sette, L.D., 2010. Laccase activity and putative laccase genes in marine-derived basidiomycetes. Fungal Biol. 114, 863–872.
Borrelle, S.B., Rochman, C.M., Liboiron, M., Bond, A.L., Lusher, A., Bradshaw, H., Provencher, J.F., 2017. Why we need an international agreement on marine plastic pollution. Proc. Natl. Acad. Sci. 114, 9994–9997.
Bradley, I.M., Pinto, A.J., Guest, J.S., 2016. Design and Evaluation of Illumina MiSeq-Compatible, 18S rRNA Gene-Specific Primers for Improved Characterization of Mixed Phototrophic Communities Ian. Appl. Environ. Microbiol. 82, 5878–5891.
Brandão, M.L., Braga, K.M., Luque, J.L., 2011. Marine debris ingestion by Magellanic penguins, Spheniscus magellanicus (Aves: Sphenisciformes), from the Brazilian coastal zone. Mar. Pollut. Bull. 62, 2246–2249.
Brandon, J., Goldstein, M., Ohman, M.D., 2016. Long-term aging and degradation of microplastic particles: Comparing in situ oceanic and experimental weathering patterns. Mar. Pollut. Bull. 110, 299–308.
Brooks, A.L., Wang, S., Jambeck, J.R., 2018. The Chinese import ban and its impact on global plastic waste trade. Sci. Adv. 4, eaat0131.
Browne, M.A., Crump, P., Niven, S.J., Teuten, E., Tonkin, A., Galloway, T., Thompson, R., 2011. Accumulation of microplastic on shorelines woldwide: Sources and sinks. Environ. Sci. Technol. 45, 9175–9179.

Brunner, K., Kukulka, T., Proskurowski, G., Law, K.L., 2015. Passive buoyant tracers in the ocean surface boundary layer: 2. Observations and simulations of microplastic marine debris. J. Geophys. Res. Ocean. 120, 7559–7573.
Bryant, J.A., Clemente, T.M., Viviani, D.A., Fong, A.A., Thomas, K.A., Kemp, P., Karl, D.M., White, A.E., DeLong, E.F., 2016. Diversity and activity of communities inhabiting plastic debris in the North Pacific Gyre. mSystems 1, e00024-16.
Buchan, A., González, J.M., Moran, M.A., 2005. Overview of the Marine Roseobacter Lineage. Appl. Environ. Microbiol. 71, 5665–5677.
Callahan, B.J., McMurdie, P.J., Holmes, S.P., 2017. Exact sequence variants should replace operational taxonomic units in marker-gene data analysis. ISME J. 11, 2639–2643.
Callahan, B.J., Mcmurdie, P.J., Rosen, M.J., Han, A.W., Johnson, A.J.A., Holmes, S.P., 2016. DADA2: High-resolution sample inference from Illumina amplicon data. Nat. Methods 13, 581–583. https://doi.org/10.1038/nmeth.3869
Carpenter, E.J., Smith Jr., K.L., 1972. Plastics on the Sargasso Sea surface. Science. 175, 1240–1241.
Carr, H.A., Harris, J., 1997. Ghost-Fishing Gear: Have Fishing Practices During the Past Few Years Reduced the Impact?, in: Coe, J.M., Rogers, D.B. (Eds.), Marine Debris. Springer, New York, NY, pp. 141–151.
Carreras-Colom, E., Constenla, M., Soler-Membrives, A., Cartes, J.E., Baeza, M., Padrós, F., Carrassón, M., 2018. Spatial occurrence and effects of microplastic ingestion on the deep-water shrimp Aristeus antennatus. Mar. Pollut. Bull. 133, 44–52.
Carson, H.S., 2013. The incidence of plastic ingestion by fishes: From the prey's perspective. Mar. Pollut. Bull. 74, 170–174.
Castillo, A.B., Al-Maslamani, I., Obbard, J.P., 2016. Prevalence of microplastics in the marine waters of Qatar. Mar. Pollut. Bull. 111, 260–267.
Catarino, A.I., Macchia, V., Sanderson, W.G., Thompson, R.C., Henry, T.B., 2018. Low levels of microplastics (MP) in wild mussels indicate that MP ingestion by humans is minimal compared to exposure via household fibres fallout during a meal. Environ. Pollut. 237, 675–684.
Charney, N., Record, S., 2012. vegetarian: Jost Diversity Measures for Community Data. R package version 1.2.
Chen, Q., Reisser, J., Cunsolo, S., Kwadijk, C., Kotterman, M., Proietti, M., Slat, B., Ferrari, F., Schwarz, A., Levivier, A., Yin, D., Hollert, H., Koelmans, A.A., 2018. Pollutants in Plastics within the North Pacific Subtropical Gyre. Environ. Sci. Technol. 52, 446–456.
Christie-Oleza, J.A., Fernandez, B., Nogales, B., Bosch, R., Armengaud, J., 2012. Proteomic insights into the lifestyle of an environmentally relevant marine bacterium. ISME J. 6, 124–135.
Chubarenko, I., Bagaev, A., Zobkov, M., Esiukova, E., 2016. On some physical and dynamical properties of microplastic particles in marine environment. Mar. Pollut. Bull. 108, 105–112.
Cincinelli, A., Scopetani, C., Chelazzi, D., Lombardini, E., Martellini, T., Katsoyiannis, A., Fossi, M.C., Corsolini, S., 2017. Microplastic in the surface waters of the Ross Sea (Antarctica): Occurrence, distribution and characterization by FTIR. Chemosphere 175, 391–400.
Claessens, M., Meester, S. De, Landuyt, L. Van, Clerck, K. De, Janssen, C.R., 2011. Occurrence and distribution of microplastics in marine sediments along the

Belgian coast. Mar. Pollut. Bull. 62, 2199–2204.
Claessens, M., Van Cauwenberghe, L., Vandegehuchte, M.B., Janssen, C.R., 2013. New techniques for the detection of microplastics in sediments and field collected organisms. Mar. Pollut. Bull. 70, 227–233.
Clauset, A., Shalizi, C.R., Newman, M.E.J., 2009. Power-Law distributions in empirical data. Soc. Ind. Appl. Math. 51, 661–703.
Clunies-Ross, P.J., Smith, G.P.S., Gordon, K.C., Gaw, S., 2016. Synthetic shorelines in New Zealand? Quantification and characterisation of microplastic pollution on Canterbury's coastlines. New Zeal. J. Mar. Freshw. Res. 50, 317–325.
Cole, M., 2016. A novel method for preparing microplastic fibers. Sci. Rep. 6, 34519.
Cole, M., Lindeque, P., Fileman, E., Halsband, C., Goodhead, R., Moger, J., Galloway, T.S., 2013. Microplastic ingestion by zooplankton. Environ. Sci. Technol. 47, 6646–6655.
Cole, M., Lindeque, P.K., Fileman, E., Clark, J., Lewis, C., Halsband, C., Galloway, T.S., 2016. Microplastics Alter the Properties and Sinking Rates of Zooplankton Faecal Pellets. Environ. Sci. Technol. 50, 3239–3246.
Cole, M., Webb, H., Lindeque, P.K., Fileman, E.S., Halsband, C., Galloway, T.S., 2014. Isolation of microplastics in biota-rich seawater samples and marine organisms. Sci. Rep. 4, 4528.
Corcoran, P.L., Biesinger, M.C., Grifi, M., 2009. Plastics and beaches: A degrading relationship. Mar. Pollut. Bull. 58, 80–84.
Courtene-Jones, W., Quinn, B., Gary, S.F., Mogg, A.O.M., Narayanaswamy, B.E., 2017. Microplastic pollution identified in deep-sea water and ingested by benthic invertebrates in the Rockall Trough, North Atlantic Ocean. Environ. Pollut. 231, 271–280.
Cózar, A., Echevarría, F., González-Gordillo, J.I., Irigoien, X., Ubeda, B., Hernández-León, S., Palma, A.T., Navarro, S., García-de-Lomas, J., Ruiz, A., Fernández-de-Puelles, M.L., Duarte, C.M., 2014. Plastic debris in the open ocean. Proc. Natl. Acad. Sci. 111, 10239–10244.
Cózar, A., Sanz-Martín, M., Martí, E., González-Gordillo, J.I., Ubeda, B., Gálvez, J.Á., Irigoien, X., Duarte, C.M., 2015. Plastic Accumulation in the Mediterranean Sea. PLoS One 10, e0121762.
Critchell, K., Lambrechts, J., 2016. Modelling accumulation of marine plastics in the coastal zone; what are the dominant physical processes? Estuar. Coast. Shelf Sci. 171, 111–122.
Curson, A.R.J., Todd, J.D., Sullivan, M.J., Johnston, A.W.B., 2011. Catabolism of dimethylsulphoniopropionate: microorganisms, enzymes and genes. Nat. Rev. Microbiol. 9, 849–859.
Dang, H., Lovell, C.R., 2016. Microbial Surface Colonization and Biofilm Development in Marine Environments. Microbiol. Mol. Biol. Rev. 80, 91–138.
Dang, H., Lovell, C.R., 2000. Bacterial primary colonization and early succession on surfaces in marine waters as determined by amplified rRNA gene restriction analysis and sequence analysis of 16S rRNA genes. Appl. Environ. Microbiol. 66, 467–475.
Danso, D., Schmeisser, C., Chow, J., Zimmermann, W., Wei, R., Leggewie, C., Li, X., Hazen, T., Streit, W.R., 2018. New Insights into the Function and Global Distribution of Polyethylene Terephthalate (PET)-Degrading Bacteria and Enzymes in Marine and Terrestrial Metagenomes. Appl. Environ. Microbiol. 84, e02773-17.

Datta, M.S., Sliwerska, E., Gore, J., Polz, M.F., Cordero, O.X., 2016. Microbial interactions lead to rapid micro-scale successions on model marine particles. Nat. Commun. 7, 11965.
Dawson, A.L., Kawaguchi, S., King, C.K., Townsend, K.A., King, R., Huston, W.M., Bengtson Nash, S.M., 2018. Turning microplastics into nanoplastics through digestive fragmentation by Antarctic krill. Nat. Commun. 9, 1001.
De Tender, C., Devriese, L.I., Haegeman, A., Maes, S., Vangeyte, J., Cattrijsse, A., Dawyndt, P., Ruttink, T., 2017. Temporal Dynamics of Bacterial and Fungal Colonization on Plastic Debris in the North Sea. Environ. Sci. Technol. 51, 7350−7360.
De Tender, C.A., Devriese, L.I., Haegeman, A., Maes, S., Ruttink, T., Dawyndt, P., 2015. Bacterial Community Profiling of Plastic Litter in the Belgian Part of the North Sea. Environ. Sci. Technol. 49, 9629–9638.
Debeljak, P., Pinto, M., Proietti, M., Reisser, J., Ferrari, F.F., Abbas, B., Loosdrecht, M.C.M. van, Slat, B., Herndl, G.J., 2017. Extracting DNA from ocean microplastics: a method comparison study. Anal. Methods 47, 7137–7146.
Debose, J.L., Lema, S.C., Nevitt, G.A., 2008. Dimethylsulfoniopropionate as a Foraging Cue for Reef Fishes. Scince 319, 1356.
Derraik, J.G.B., 2002. The pollution of the marine environment by plastic debris: a review. Mar. Pollut. Bull. 44, 842–852.
Deshpande, V., Wang, Q., Greenfield, P., Charleston, M., Porras-Alfaro, A., Kuske, C.R., Cole, J.R., Midgley, D.J., Tran-Dinh, N., 2016. Fungal identification using a Bayesian classifier and the Warcup training set of internal transcribed spacer sequences. Mycologia 108, 1–5.
Devriese, L.I., Meulen, M.D. Van Der, Maes, T., Bekaert, K., Paul-Pont, I., Frère, L., Robbens, J., Vethaak, A.D., 2015. Microplastic contamination in brown shrimp (Crangon crangon, Linnaeus 1758) from coastal waters of the Southern North Sea and Channel area. Mar. Pollut. Bull. 98, 179–187.
Di, M., Wang, J., 2018. Microplastics in surface waters and sediments of the Three Gorges Reservoir, China. Sci. Total Environ. 616–617, 1620–1627.
Diaz, J.M., Hansel, C.M., Voelker, B.M., Mendes, C.M., Andeer, P.F., Zhang, T., 2013. Widespread production of extracellular superoxide by heterotrophic bacteria. Science. 340, 1223–1226.
Dodbiba, G., Haruki, N., Shibayama, A., Miyazaki, T., Fujita, T., 2002. Combination of sink–float separation and flotation technique for purification of shredded PET-bottle from PE or PP flakes. Int. J. Miner. Process. 65, 11–29.
Dussud, C., Hudec, C., George, M., Fabre, P., Higgs, P., Bruzaud, S., Delort, A.M., Eyheraguibel, B., Meistertzheim, A.L., Jacquin, J., Cheng, J., Callac, N., Odobel, C., Rabouille, S., Ghiglione, J.F., 2018. Colonization of non-biodegradable and biodegradable plastics by marine microorganisms. Front. Microbiol. 9, 1571.
Elifantz, H., Horn, G., Ayon, M., Cohen, Y., Minz, D., 2013. Rhodobacteraceae are the key members of the microbial community of the initial biofilm formed in Eastern Mediterranean coastal seawater. FEMS Microbiol. Ecol. 85, 348–57.
Enders, K., Lenz, R., Stedmon, C.A., Nielsen, T.G., 2015. Abundance, size and polymer composition of marine microplastics ≥ 10 μm in the Atlantic Ocean and their modelled vertical distribution. Mar. Pollut. Bull. 100, 70–81.
Endo, S., Koelmans, A.A., 2016. Sorption of Hydrophobic Organic Compounds to Plastics in the Marine Environment: Equilibrium, in: Takada, H., Karapanagioti, H.K. (Eds.), The Handbook of Environmental Chemistry. Springer Berlin

Heidelberg, pp. 41–53.
Eo, S., Hong, S.H., Song, Y.K., Lee, Jongsu, Lee, Jongmyoung, Shim, W.J., 2018. Abundance, composition, and distribution of microplastics larger than 20 μm in sand beaches of South Korea. Environ. Pollut. 238, 894–902.
Eriksen, M., Lebreton, L.C.M., Carson, H.S., Thiel, M., Moore, C.J., Borerro, J.C., Galgani, F., Ryan, P.G., Reisser, J., 2014. Plastic Pollution in the World's Oceans: More than 5 Trillion Plastic Pieces Weighing over 250,000 Tons Afloat at Sea. PLoS One 9, e111913.
Eriksen, M., Thiel, M., Lebreton, L., 2016. Nature of Plastic Marine Pollution in the Subtropical Gyres, in: Takada, H., Karapanagioti, H.K. (Eds.), The Handbook of Environmental Chemistry. Springer Berlin Heidelberg, pp. 1–28.
Erni-Cassola, G., Gibson, M.I., Thompson, R.C., Christie-Oleza, J., 2017. Lost, but found with Nile red; a novel method to detect and quantify small microplastics (20 μm–1 mm) in environmental samples. Environ. Sci. Technol. 51, 13641–13648.
Erni-Cassola, G., Zadjelovic, V., Gibson, M.I., Christie-Oleza, J.A., 2019. Distribution of plastic polymer types in the marine environment; A meta-analysis. J. Hazard. Mater. 369, 691–698.
Espino-Rammer, L., Ribitsch, D., Przylucka, A., Marold, A., Greimel, K.J., Acero, E.H., Guebitz, G.M., Kubicek, C.P., Druzhinina, I.S., 2013. Two novel class ii hydrophobins from Trichoderma spp. Stimulate enzymatic hydrolysis of poly(ethylene terephthalate) when expressed as fusion proteins. Appl. Environ. Microbiol. 79, 4230–4238.
Everaert, G., Van Cauwenberghe, L., De Rijcke, M., Koelmans, A.A., Mees, J., Vandegehuchte, M., Janssen, C.R., 2018. Risk assessment of microplastics in the ocean: Modelling approach and first conclusions. Environ. Pollut. 242, 1930–1938.
Fazey, F.M.C., Ryan, P.G., 2016. Biofouling on buoyant marine plastics: An experimental study into the effect of size on surface longevity. Environ. Pollut. 210, 354–360.
Filella, M., 2015. Questions of size and numbers in environmental research on microplastics: Methodological and conceptual aspects. Environ. Chem. 12, 527–538.
Filella, M., 2007. Colloidal Properties of Submicron Particles in Natural Waters, in: Wilkinson, K.. J.., Lead, J.. R. (Eds.), Environmental Colloids and Particles: Behaviour, Separation and Characterisation. John Wiley & Sons, pp. 17–93.
Foekema, E.M., De Gruijter, C., Mergia, M.T., van Franeker, J.A., Murk, A.J., Koelmans, A.A., 2013. Plastic in north sea fish. Environ. Sci. Technol. 47, 8818–24.
Frère, L., Maignien, L., Chalopin, M., Huvet, A., Rinnert, E., Morrison, H., Kerninon, S., Cassone, A.-L., Lambert, C., Reveillaud, J., Paul-Pont, I., 2018. Microplastic bacterial communities in the Bay of Brest: Influence of polymer type and size. Environ. Pollut. 242, 614–625.
Frère, L., Paul-Pont, I., Moreau, J., Soudant, P., Lambert, C., Huvet, A., Rinnert, E., 2016. A semi-automated Raman micro-spectroscopy method for morphological and chemical characterizations of microplastic litter. Mar. Pollut. Bull. 113, 461–468.
Frère, L., Paul-Pont, I., Rinnert, E., Petton, S., Jaffré, J., Bihannic, I., Soudant, P., Lambert, C., Huvet, A., 2017. Influence of environmental and anthropogenic factors on the composition, concentration and spatial distribution of

microplastics: A case study of the Bay of Brest (Brittany, France). Environ. Pollut. 225, 211–222.
Frias, J.P.G.L., Gago, J., Otero, V., Sobral, P., 2016. Microplastics in coastal sediments from Southern Portuguese shelf waters. Mar. Environ. Res. 114, 24–30.
Gajšt, T., Bizjak, T., Palatinus, A., Liubartseva, S., Kržan, A., 2016. Sea surface microplastics in Slovenian part of the Northern Adriatic. Mar. Pollut. Bull. 113, 392–399.
Gall, S.C., Thompson, R.C., 2015. The impact of debris on marine life. Mar. Pollut. Bull. 92, 170–179.
Galloway, T.S., Cole, M., Lewis, C., 2017. Interactions of microplastic debris throughout the marine ecosystem. Nat. Ecol. Evol. 1, 0116.
Gao, Q., Garcia-Pichel, F., 2011. Microbial ultraviolet sunscreens. Nat. Rev. Microbiol. 9, 791–802.
Gewert, B., Ogonowski, M., Barth, A., MacLeod, M., 2017. Abundance and composition of near surface microplastics and plastic debris in the Stockholm Archipelago, Baltic Sea. Mar. Pollut. Bull. 120, 292–302.
Gewert, B., Plassmann, M., Sandblom, O., MacLeod, M., 2018. Identification of Chain Scission Products Released to Water by Plastic Exposed to Ultraviolet Light. Environ. Sci. Technol. Lett. 5, 272–276.
Gewert, B., Plassmann, M.M., MacLeod, M., 2015. Pathways for degradation of plastic polymers floating in the marine environment. Environ. Sci. Process. Impacts 17, 1513–1521.
Geyer, R., Jambeck, J.R., Law, K.L., 2017. Production, use, and fate of all plastics ever made. Sci. Adv. 3, e1700782.
Ghosal, S., Chen, M., Wagner, J., Wang, Z.M., Wall, S., 2018. Molecular identification of polymers and anthropogenic particles extracted from oceanic water and fish stomach – A Raman micro-spectroscopy study. Environ. Pollut. 233, 1113–1124.
Gillespie, C.S., 2015. Fitting heavy tailed distributions: the poweRlaw package. J. Stat. Softw. 64, 1–16.
Golyshin, P.N., Chernikova, T.N., Abraham, W.-R., Lünsdorf, H., Timmis, K.N., Yakimov, M.M., 2002. Oleiphilaceae fam. nov., to include Oleiphilus messinensis gen. nov., sp. nov., a novel marine bacterium that obligately utilizes hydrocarbons. Int. J. Syst. Evol. Microbiol. 52, 901–911.
Graca, B., Szewc, K., Zakrzewska, D., Dołęga, A., Szczerbowska-Boruchowska, M., 2017. Sources and fate of microplastics in marine and beach sediments of the Southern Baltic Sea—a preliminary study. Environ. Sci. Pollut. Res. 2014, 1–12.
Gray, A.D., Wertz, H., Leads, R.R., Weinstein, J.E., 2018. Microplastic in two South Carolina Estuaries: Occurrence, distribution, and composition. Mar. Pollut. Bull. 128, 223–233.
Gregory, M.R., Andrady, A.L., 2003. Plastics in the marine environment, in: Andrady, A.L. (Ed.), Plastics and the Environment. John Wiley & Sons, Hoboken, pp. 379–401.
Hadad, D., Geresh, S., Sivan, A., 2005. Biodegradation of polyethylene by the thermophilic bacterium Brevibacillus borstelensis. J. Appl. Microbiol. 98, 1093–1100.
Hahladakis, J.N., Velis, C.A., Weber, R., Iacovidou, E., Purnell, P., 2018. An overview of chemical additives present in plastics: Migration, release, fate and

environmental impact during their use, disposal and recycling. J. Hazard. Mater. 344, 179–199.
Haider, N., Karlsson, S., 1999. Migration and release profile of Chimassorb 944 from low-density polyethylene film (LDPE) in simulated landfills. Polym. Degrad. Stab. 64, 321–328.
Hanke, G., Galgani, F., Werner, S., Oosterbaan, L., Nilsson, P., Fleet, D., Kinsey, S., Thompson, R., Palatinus, A., Franeker, J.A. Van, Vlachogianni, T., Scoullos, M., Veiga, J.M., Matiddi, M., Alcarco, L., Maes, T., Korpinen, S., Budziak, A., Leslie, H., Gago, J., Liebezeit, G., 2013. MSFD GES technical subgroup on marine litter. Guidance on monitoring of marine litter in European Seas. Luxembourg.
Hanvey, J.S., Lewis, P.J., Lavers, J.L., Crosbie, N.D., Pozo, K., Clarke, B.O., 2017. A review of analytical techniques for quantifying microplastics in sediments. Anal. Methods 9, 1369–1383.
Hartmann, N., Hüffer, T., Thompson, R.C., Hassellöv, M., Verschoor, A., Daugaard, A.E., Rist, S., Karlsson, T.M., Brennholt, N., Cole, M., Herrling, M.P., Heß, M., Ivleva, N.P., Lusher, A.L., Wagner, M., 2019. Are we speaking the same language? Recommendations for a definition and categorization framework for plastic debris. Environ. Sci. Technol. 53, 1039–1047.
Hartmann, N.B., Rist, S., Bodin, J., Jensen, L.H.S., Schmidt, S.N., Mayer, P., Meibom, A., Baun, A., 2017. Microplastics as vectors for environmental contaminants: Exploring sorption, desorption, and transfer to biota. Integr. Environ. Assess. Manag. 13, 488–493.
Hendrickson, E., Minor, E.C., Schreiner, K., 2018. Microplastic Abundance and Composition in Western Lake Superior As Determined via Microscopy, Pyr-GC/MS, and FTIR. Environ. Sci. Technol. 52, 1787−1796.
Hermsen, E., Pompe, R., Besseling, E., Koelmans, A.A., 2017. Detection of low numbers of microplastics in North Sea fish using strict quality assurance criteria. Mar. Pollut. Bull. 122, 253–258.
Herzke, D., Anker-Nilssen, T., Nøst, T.H., Götsch, A., Christensen-Dalsgaard, S., Langset, M., Fangel, K., Koelmans, A.A., 2016. Negligible Impact of Ingested Microplastics on Tissue Concentrations of Persistent Organic Pollutants in Northern Fulmars off Coastal Norway. Environ. Sci. Technol. 50, 1924–1933.
Hidalgo-Ruz, V., Gutow, L., Thompson, R.C., Thiel, M., 2012. Microplastics in the Marine Environment: A Review of the Methods Used for Identification and Quantification. Environ. Sci. Technol. 46, 3060−3075.
Horton, A.A., Svendsen, C., Williams, R.J., Spurgeon, D.J., Lahive, E., 2017. Large microplastic particles in sediments of tributaries of the River Thames, UK – Abundance, sources and methods for effective quantification. Mar. Pollut. Bull. 114, 218–226.
Hothorn, T., Bretz, F., Westfall, P., 2008. Simultaneous inference in general parametric models. Biometrical J. 50, 346–363.
Huggett, M.J., Nedved, B.T., Hadfield, M.G., 2009. Effects of initial surface wettability on biofilm formation and subsequent settlement of Hydroides elegans. Biofouling 25, 387–399.
Hurley, R., Woodward, J., Rothwell, J.J., 2018. Microplastic contamination of river beds significantly reduced by catchment-wide flooding. Nat. Geosci. 11, 251–257.
Imhof, H.K., Ivleva, N.P., Schmid, J., Niessner, R., Laforsch, C., 2013. Contamination of beach sediments of a subalpine lake with microplastic

particles. Curr. Biol. 23, R867–R868.
Ioakeimidis, C., Fotopoulou, K.N., Karapanagioti, H.K., Geraga, M., Zeri, C., Papathanassiou, E., Galgani, F., Papatheodorou, G., 2016. The degradation potential of PET bottles in the marine environment: An ATR-FTIR based approach. Sci. Rep. 6, 23501.
Isobe, A., Kubo, K., Tamura, Y., Kako, S., Nakashima, E., Fujii, N., 2014. Selective transport of microplastics and mesoplastics by drifting in coastal waters. Mar. Pollut. Bull. 89, 324–330.
Jambeck, J.R., Geyer, R., Wilcox, C., Siegler, T.R., Perryman, M., Andrady, A., Narayan, R., Law, K.L., 2015. Plastic waste inputs from land into ocean. Science. 347, 768–771.
Jost, L., 2006. Entropy and diversity. Oikos 113, 363–375.
Kanhai, L.D.K., Gårdfeldt, K., Lyashevska, O., Hassellöv, M., Thompson, R.C., O'Connor, I., 2018. Microplastics in sub-surface waters of the Arctic Central Basin. Mar. Pollut. Bull. 130, 8–18.
Kanhai, L.D.K., Officer, R., Lyashevska, O., Thompson, R.C., O'Connor, I., 2017. Microplastic abundance, distribution and composition along a latitudinal gradient in the Atlantic Ocean. Mar. Pollut. Bull. 115, 307–314.
Karlsson, T.M., Hassellöv, M., Jakubowicz, I., 2018. Influence of thermooxidative degradation on the in situ fate of polyethylene in temperate coastal waters. Mar. Pollut. Bull. 135, 187–194.
Katija, K., Choy, C.A., Sherlock, R.E., Sherman, A.D., Robison, B.H., 2017. From the surface to the seafloor: How giant larvaceans transport microplastics into the deep sea. Sci. Adv. 3, e1700715.
Kirstein, I.V., Wichels, A., Gullans, E., Krohne, G., Gerdts, G., 2019. The Plastisphere – Uncovering tightly attached plastic "specific" microorganisms. PLoS One 14, e0215859.
Kirstein, I. V., Wichels, A., Krohne, G., Gerdts, G., 2018. Mature biofilm communities on synthetic polymers in seawater - Specific or general? Mar. Environ. Res. 142, 147–154.
Klein, S., Worch, E., Knepper, T.P., 2015. Occurrence and spatial distribution of microplastics in river shore sediments of the Rhine-Main area in Germany. Environ. Sci. Technol. 49, 6070–6076.
Klindworth, A., Pruesse, E., Schweer, T., Peplies, J., Quast, C., Horn, M., Glöckner, F.O., 2013. Evaluation of general 16S ribosomal RNA gene PCR primers for classical and next-generation sequencing-based diversity studies. Nucleic Acids Res. 41.
Knight, R., Vrbanac, A., Taylor, B.C., Aksenov, A., Callewaert, C., Debelius, J., Gonzalez, A., Kosciolek, T., McCall, L.I., McDonald, D., Melnik, A. V., Morton, J.T., Navas, J., Quinn, R.A., Sanders, J.G., Swafford, A.D., Thompson, L.R., Tripathi, A., Xu, Z.Z., Zaneveld, J.R., Zhu, Q., Caporaso, J.G., Dorrestein, P.C., 2018. Best practices for analysing microbiomes. Nat. Rev. Microbiol. 16, 410–422.
Koelmans, A.A., Bakir, A., Burton, G.A., Janssen, C.R., 2016. Microplastic as a Vector for Chemicals in the Aquatic Environment. Critical Review and Model-Supported Re-interpretation of Empirical Studies. Environ. Sci. Technol. 50, 3315−3326.
Koelmans, A.A., Kooi, M., Law, K.L., van Sebille, E., 2017. All is not lost: Deriving a top-down mass budget of plastic at sea. Environ. Res. Lett. 12, 114028.
Kooi, M., Reisser, J., Slat, B., Ferrari, F.F., Schmid, M.S., Cunsolo, S., Brambini, R.,

Noble, K., Sirks, L.-A., Linders, T.E.W., Schoeneich-Argent, R.I., Koelmans, A.A., 2016. The effect of particle properties on the depth profile of buoyant plastics in the ocean. Sci. Rep. 6, 33882.
Kooi, M., Van Nes, E.H., Scheffer, M., Koelmans, A.A., 2017. Ups and downs in the ocean: Effects of biofouling on the vertical transport of microplastics. Environ. Sci. Technol. 51, 7963−7971.
Kowalski, N., Reichardt, A.M., Waniek, J.J., 2016. Sinking rates of microplastics and potential implications of their alteration by physical, biological, and chemical factors. Mar. Pollut. Bull. 109, 310–319.
Krueger, M.C., Harms, H., Schlosser, D., 2015. Prospects for microbiological solutions to environmental pollution with plastics. Appl. Microbiol. Biotechnol. 99, 8857–8874.
Kühn, S., Rebolledo, E.L.B., Franeker, J.A. van, 2015. Deleterious Effects of Litter on Marine Life, in: Bergmann, M., Gutow, L., Klages, M. (Eds.), Marine Anthropogenic Litter. Springer, pp. 75–116.
Kukulka, T., Proskurowski, G., Morét-Ferguson, S., Meyer, D.W., Law, K.L., 2012. The effect of wind mixing on the vertical distribution of buoyant plastic debris. Geophys. Res. Lett. 39, L07601.
Kunz, A., Walther, B.A., Löwemark, L., Lee, Y.C., 2016. Distribution and quantity of microplastic on sandy beaches along the northern coast of Taiwan. Mar. Pollut. Bull. 111, 126–135.
Laist, D.W., 1997. Impacts of Marine Debris: Entanglement ofMarine Life in Marine Debris Including a Comprehensive List of Species with Entanglement and IngestiOn Records, in: Coe, J.M., Rogers, D.B. (Eds.), Marine Debris. Springer, New York, pp. 99–139.
Lamb, J.B., Willis, B.L., Fiorenza, E.A., Couch, C.S., Howard, R., Rader, D.N., True, J.D., Kelly, L.A., Ahmad, A., Jompa, J., Harvell, C.D., 2018. Plastic waste associated with disease on coral reefs. Science. 359, 460–462.
Langille, M.G.I., 2018. Exploring Linkages between Taxonomic and Functional Profiles of the Human Microbiome. mSystems 3, e00163-17.
Langille, M.G.I., Zaneveld, J., Caporaso, J.G., McDonald, D., Knights, D., Reyes, J.A., Clemente, J.C., Burkepile, D.E., Vega Thurber, R.L., Knight, R., Beiko, R.G., Huttenhower, C., 2013. Predictive functional profiling of microbial communities using 16S rRNA marker gene sequences. Nat. Biotechnol. 31, 814–821.
Lavers, J.L., Oppel, S., Bond, A.L., 2016. Factors influencing the detection of beach plastic debris. Mar. Environ. Res. 119, 245–251.
Law, K.L., 2017. Plastics in the Marine Environment. Ann. Rev. Mar. Sci. 9, 10.1-10.25.
Law, K.L., Morét-Ferguson, S., Maximenko, N.A., Proskurowski, G., Peacock, E.E., Hafner, J., Reddy, C.M., 2010. Plastic Accumulation in the North Atlantic Subtropical Gyre. Science. 329, 1185–1188.
Lea-Smith, D.J., Biller, S.J., Davey, M.P., Cotton, C.A.R., Perez Sepulveda, B.M., Turchyn, A. V., Scanlan, D.J., Smith, A.G., Chisholm, S.W., Howe, C.J., 2015. Contribution of cyanobacterial alkane production to the ocean hydrocarbon cycle. Proc. Natl. Acad. Sci. 112, 13591–13596.
Lebreton, L., Slat, B., Ferrari, F., Sainte-Rose, B., Aitken, J., Marthouse, R., Hajbane, S., Cunsolo, S., Schwarz, A., Levivier, A., Noble, K., Debeljak, P., Maral, H., Schoeneich-Argent, R., Brambini, R., Reisser, J., 2018. Evidence that the Great Pacific Garbage Patch is rapidly accumulating plastic. Sci. Rep. 8,

4666.
Lebreton, L.C.-M., Greer, S.D., Borrero, J.C., 2012. Numerical modelling of floating debris in the world's oceans. Mar. Pollut. Bull. 64, 653–661.
Lebreton, L.C.M., Zwet, J. Van Der, Damsteeg, J., Slat, B., Andrady, A., Reisser, J., 2017. River plastic emissions to the world's oceans. Nat. Commun. 8, 1–10.
Lee, J.-W., Nam, J.-H., Kim, Y.-H., Lee, K.-H., Lee, D.-H., 2008. Bacterial communities in the initial stage of marine biofilm formation on artificial surfaces. J. Microbiol. 46, 174–182.
Lenz, R., Enders, K., Gissel, T., 2016. Microplastic exposure studies should be environmentally realistic. Proc. Natl. Acad. Sci. 2–3.
Lenz, R., Enders, K., Stedmon, C.A., Mackenzie, D.M.A., Gissel, T., 2015. A critical assessment of visual identification of marine microplastic using Raman spectroscopy for analysis improvement. Mar. Pollut. Bull. 100, 82–91.
Liboiron, F., Ammendolia, J., Saturno, J., Melvin, J., Zahara, A., Richárd, N., Liboiron, M., 2018. A zero percent plastic ingestion rate by silver hake (Merluccius bilinearis) from the south coast of Newfoundland, Canada. Mar. Pollut. Bull. 131, 267–275.
Liboiron, M., Liboiron, F., Wells, E., Richárd, N., Zahara, A., Mather, C., Bradshaw, H., Murichi, J., 2016. Low plastic ingestion rate in Atlantic cod (Gadus morhua) from Newfoundland destined for human consumption collected through citizen science methods. Mar. Pollut. Bull. 113, 428–437.
Liland, K.H., Mevik, B.-H., Canteri, R., 2015. baseline: Baseline Correction of Spectra.
Lobelle, D., Cunliffe, M., 2011. Early microbial biofilm formation on marine plastic debris. Mar. Pollut. Bull. 62, 197–200.
Löder, M.G.J., Imhof, H.K., Ladehoff, M., Löschel, L.A., Lorenz, C., Mintenig, S., Piehl, S., Primpke, S., Schrank, I., Laforsch, C., Gerdts, G., 2017. Enzymatic purification of microplastics in environmental samples. Environ. Sci. Technol. 51, 14283−14292.
Löder, M.G.J., Kuczera, M., Mintenig, S., Lorenz, C., Gerdts, G., 2015. Focal plane array detector-based micro-Fourier-transform infrared imaging for the analysis of microplastics in environmental samples. Environ. Chem. 12, 563–581.
Lohmann, R., 2012. Critical review of low-density polyethylene's partitioning and diffusion coefficients for trace organic contaminants and implications for its use as a passive sampler. Environ. Sci. Technol. 46, 606–618.
Long, M., Moriceau, B., Gallinari, M., Lambert, C., Huvet, A., Raffray, J., Soudant, P., 2015. Interactions between microplastics and phytoplankton aggregates: Impact on their respective fates. Mar. Chem. 175, 39–46.
Lots, F.A.E., Behrens, P., Vijver, M.G., Horton, A.A., Bosker, T., 2017. A large-scale investigation of microplastic contamination: Abundance and characteristics of microplastics in European beach sediment. Mar. Pollut. Bull. 123, 219–226.
Lourenço, P.M., Serra-Gonçalves, C., Ferreira, J.L., Catry, T., Granadeiro, J.P., 2017. Plastic and other microfibers in sediments, macroinvertebrates and shorebirds from three intertidal wetlands of southern Europe and west Africa. Environ. Pollut. 231, 123–133.
Love, M.I., Huber, W., Anders, S., 2014. Moderated estimation of fold change and dispersion for RNA-seq data with DESeq2. Genome Biol. 15, 1–21.
Lozupone, C., Lladser, M.E., Knights, D., Stombaugh, J., Knight, R., 2011. UniFrac: An effective distance metric for microbial community comparison. ISME J. 5,

169–172.
Luongo, J.P., 1960. Infrared Study of Polypropylene. J. Appl. Polym. Sci. 3, 302–309.
Lusher, A.L., Tirelli, V., O'Connor, I., Officer, R., 2015. Microplastics in Arctic polar waters: the first reported values of particles in surface and sub-surface samples. Sci. Rep. 5, 14947.
Maes, T., Jessop, R., Wellner, N., Haupt, K., Mayes, A.G., 2017. A rapid-screening approach to detect and quantify microplastics based on fluorescent tagging with Nile Red. Sci. Rep. 7, 44501.
Mani, T., Hauk, A., Walter, U., Burkhardt-Holm, P., 2015. Microplastics profile along the Rhine River. Sci. Rep. 5, 17988.
Martí, E., Martin, C., Cózar, A., Duarte, C.M., 2017. Low abundance of plastic fragments in the surface waters of the Red Sea. Front. Mar. Sci. 4, 333.
Martin, J., Lusher, A., Thompson, R.C., Morley, A., 2017. The Deposition and Accumulation of Microplastics in Marine Sediments and Bottom Water from the Irish Continental Shelf. Sci. Rep. 7, 10772.
Martin, M., 2011. Cutadapt Removes Adapter Sequences From High-Throughput Sequencing Reads. EMBnet.journal 17, 10–12.
Mason, S.A., Welch, V.G., Neratko, J., 2018. Synthetic Polymer Contamination in Bottled Water. Front. Chem. 6.
Matsuguma, Y., Takada, H., Kumata, H., Kanke, H., Sakurai, S., Suzuki, T., Itoh, M., Okazaki, Y., Boonyatumanond, R., Zakaria, M.P., Weerts, S., Newman, B., 2017. Microplastics in Sediment Cores from Asia and Africa as Indicators of Temporal Trends in Plastic Pollution. Arch. Environ. Contam. Toxicol. 73, 230–239.
Maximenko, N., Hafner, J., Niiler, P., 2012. Pathways of marine debris derived from trajectories of Lagrangian drifters. Mar. Pollut. Bull. 65, 51–62.
McCormick, A., Hoellein, T.J., Mason, S.A., Schluep, J., Kelly, J.J., 2014. Microplastic is an Abundant and Distinct Microbial Habitat in an Urban River. Environ. Sci. Technol. 48, 11863–11871.
McMurdie, P.J., Holmes, S., 2013. Phyloseq: An R Package for Reproducible Interactive Analysis and Graphics of Microbiome Census Data. PLoS One 8, e61217.
Michels, J., Stippkugel, A., Lenz, M., Wirtz, K., Engel, A., 2018. Rapid aggregation of biofilm-covered microplastics with marine biogenic particles. Proc. R. Soc. B 285, 20181203.
Moore, C.J., 2008. Synthetic polymers in the marine environment: A rapidly increasing, long-term threat. Environ. Res. 108, 131–139.
Moore, C.J., Moore, S.L., Leecaster, M.K., Weisberg, S.B., 2001. A comparison of plastic and plankton in the North Pacific Central Gyre. Mar. Pollut. Bull. 42, 1297–1300.
Morét-Ferguson, S., Lavender, K., Proskurowski, G., Murphy, E.K., Peacock, E.E., Reddy, C.M., 2010. The size, mass, and composition of plastic debris in the western North Atlantic Ocean. Mar. Pollut. Bull. 60, 1873–1878.
Moriceau, B., Iversen, M.H., Gallinari, M., Evertsen, A.-J.O., Le Goff, M., Beker, B., Boutorh, J., Corvaisier, R., Coffineau, N., Donval, A., Giering, S.L.C., Koski, M., Lambert, C., Lampitt, R.S., Le Mercier, A., Masson, A., Stibor, H., Stockenreiter, M., De La Rocha, C.L., 2018. Copepods Boost the Production but Reduce the Carbon Export Efficiency by Diatoms. Front. Mar. Sci. 5, Article 82.

Murali, A., Bhargava, A., Wright, E.S., 2018. IDTAXA: a novel approach for accurate taxonomic classification of microbiome sequences. Microbiome 6, 140.
Naji, A., Esmaili, Z., Khan, F.R., 2017a. Plastic debris and microplastics along the beaches of the Strait of Hormuz, Persian Gulf. Mar. Pollut. Bull. 114, 1057–1062.
Naji, A., Esmaili, Z., Mason, S.A., Dick Vethaak, A., 2017b. The occurrence of microplastic contamination in littoral sediments of the Persian Gulf, Iran. Environ. Sci. Pollut. Res. 24, 20459–20468.
Newton, R.J., Griffin, L.E., Bowles, K.M., Meile, C., Gifford, S., Givens, C.E., Howard, E.C., King, E., Oakley, C.A., Reisch, C.R., Rinta-Kanto, J.M., Sharma, S., Sun, S., Varaljay, V., Vila-Costa, M., Westrich, J.R., Moran, M.A., 2010. Genome characteristics of a generalist marine bacterial lineage. ISME J. 4, 784–798.
Nuelle, M.-T., Dekiff, J.H., Remy, D., Fries, E., 2014. A new analytical approach for monitoring microplastics in marine sediments. Environ. Pollut. 184, 161–169.
Oberbeckmann, S., Kreikemeyer, B., Labrenz, M., 2018. Environmental factors support the formation of specific bacterial assemblages on microplastics. Front. Microbiol. 8, 2709.
Oberbeckmann, S., Loeder, M.G.J., Gerdts, G., Mark Osborn, a, 2014. Spatial and seasonal variation in diversity and structure of microbial biofilms on marine plastics in Northern European waters. FEMS Microbiol. Ecol. 49, 478–492.
Oberbeckmann, S., Osborn, A.M., Duhaime, M.B., 2016. Microbes on a Bottle: Substrate, Season and Geography Influence Community Composition of Microbes Colonizing Marine Plastic Debris. PLoS One 11, e0159289.
Ogata, Y., Takada, H., Mizukawa, K., Hirai, H., Iwasa, S., Endo, S., Mato, Y., Saha, M., Okuda, K., Nakashima, A., Murakami, M., Zurcher, N., Booyatumanondo, R., Zakaria, M.P., Dung, L.Q., Gordon, M., Miguez, C., Suzuki, S., Moore, C., Karapanagioti, H.K., Weerts, S., McClurg, T., Burres, E., Smith, W., Velkenburg, M. Van, Lang, J.S., Lang, R.C., Laursen, D., Danner, B., Stewardson, N., Thompson, R.C., 2009. International Pellet Watch: Global monitoring of persistent organic pollutants (POPs) in coastal waters. 1. Initial phase data on PCBs, DDTs, and HCHs. Mar. Pollut. Bull. 58, 1437–1446.
Ogonowski, M., Gerdes, Z., Gorokhova, E., 2018. What we know and what we think we know about microplastic effects – A critical perspective. Curr. Opin. Environ. Sci. Heal. 1, 41–46.
Oksanen, J., Blanchet, F.G., Friendly, M., Kindt, R., Legendre, P., McGlinn, D., Minchin, P.R., O'Hara, R.B., Simpson, G.L., Solymos, P., Henry, M., Stevens, H., Szoecs, E., Wagner, H., 2019. vegan: Community Ecology Package. R package version 2.5-4.
Ostle, C., Thompson, R.C., Broughton, D., Gregory, L., Wootton, M., Johns, D.G., 2019. The rise in ocean plastics evidenced from a 60-year time series. Nat. Commun. 10, 1622.
Parada, A.E., Needham, D.M., Fuhrman, J.A., 2016. Every base matters: Assessing small subunit rRNA primers for marine microbiomes with mock communities, time series and global field samples. Environ. Microbiol. 18, 1403–1414.
Pedrotti, M.L., Petit, S., Elineau, A., Bruzaud, S., Crebassa, J.-C., Dumontet, B., Martí, E., Gorsky, G., Cózar, A., 2016. Changes in the Floating Plastic Pollution of the Mediterranean Sea in Relation to the Distance to Land. PLoS One 11, e0161581.

Peeken, I., Primpke, S., Beyer, B., Gütermann, J., Katlein, C., Krumpen, T., Bergmann, M., Hehemann, L., Gerdts, G., 2018. Arctic sea ice is an important temporal sink and means of transport for microplastic. Nat. Commun. 9.
Pegram, J.E., Andrady, A.L., 1989. Outdoor weathering of selected polymeric materials under marine exposure conditions. Polym. Degrad. Stab. 26, 333–345.
Phuong, N.N., Zalouk-Vergnoux, A., Poirier, L., Kamari, A., Châtel, A., Mouneyrac, C., Lagarde, F., 2016. Is there any consistency between the microplastics found in the field and those used in laboratory experiments? Environ. Pollut. 211, 111–123.
PlasticsEurope, 2018. Plastics – the facts 2018. Brussels. (https://www.plasticseurope.org/en/resources/publications/619-plastics-facts-2018; accessed 09.10.2019)
PlasticsEurope, 2015. Plastics – the facts 2015. Brussels. (https://www.plasticseurope.org/en/resources/publications/93-plastics-facts-2015; accessed 09.10.2019)
Porter, A., Lyons, B.P., Galloway, T.S., Lewis, C.N., 2018. The role of marine snows in microplastic fate and bioavailability. Environ. Sci. Technol. 52, 7111−7119.
R Core Team, 2018. R: A language and environment for statistical computing.
Rabello, M.S., White, J.R., 1997. Crystallization and melting behaviour of photodegraded polypropylene — I. Chemi-crystallization. Polymer. 38, 6379–6387.
Raghukumar, S., 2017. Fungi in coastal and oceanic marine ecosystems: Marine fungi, Fungi in Coastal and Oceanic Marine Ecosystems: Marine Fungi.
Rajakumar, K., Sarasvathy, V., Thamarai Chelvan, A., Chitra, R., Vijayakumar, C.T., 2009. Natural weathering studies of polypropylene. J. Polym. Environ. 17, 191–202.
Rani, M., Shim, W.J., Han, G.M., Jang, M., Al-Odaini, N.A. hme., Song, Y.K., Hong, S.H., 2015. Qualitative Analysis of Additives in Plastic Marine Debris and Its New Products. Arch. Environ. Contam. Toxicol. 69, 352–366.
Readman, J.W., Deluna, F., Ebinghaus, R., Guzman, A., Price, A.R.G., Emily, E., Sheppard, A.L.S., Sleight, V.A., Thompson, R.C., Tonkin, A., Wright, R.J., Sheppard, Charles R C, 2013. Contaminants, Pollution and Potential Anthropogenic Impacts in Chagos/BIOT, in: Sheppard, C.R.C. (Ed.), Coral Reefs of the United Kingdom Overseas Territories. Springer, Dordrecht, pp. 283–298.
Reisser, J., Shaw, J., Hallegraeff, G., Proietti, M., Barnes, D.K.A., Thums, M., Wilcox, C., Hardesty, B.D., Pattiaratchi, C., 2014. Millimeter-Sized Marine Plastics: A New Pelagic Habitat for Microorganisms and Invertebrates. PLoS One 9, e100289.
Reisser, J., Slat, B., Noble, K., Du Plessis, K., Epp, M., Proietti, M., De Sonneville, J., Becker, T., Pattiaratchi, C., 2015. The vertical distribution of buoyant plastics at sea: An observational study in the North Atlantic Gyre. Biogeosciences 12, 1249–1256.
Restrepo-Flórez, J.-M., Bassi, A., Thompson, M.R., 2014. Microbial degradation and deterioration of polyethylene – A review. Int. Biodeterior. Biodegradation 88, 83–90.
Ribitsch, D., Acero, E.H., Przylucka, A., Zitzenbacher, S., Marold, A., Gamerith, C., Tscheließnig, R., Jungbauer, A., Rennhofer, H., Lichtenegger, H., Amenitsch, H., Bonazza, K., Kubicek, C.P., Druzhinina, I.S., Guebitz, G.M., 2015.

Enhanced cutinase-catalyzed hydrolysis of polyethylene terephthalate by covalent fusion to hydrophobins. Appl. Environ. Microbiol. 81, 3586–3592.
Richards, T.A., Jones, M.D.M., Leonard, G., Bass, D., 2012. Marine Fungi: Their Ecology and Molecular Diversity. Ann. Rev. Mar. Sci. 4, 495–522.
Robards, M.D., Piatt, J.F., Wohl, K.D., 1995. Increasing frequency of plastic particles ingested by seabirds in the subarctic North Pacific. Mar. Pollut. Bull. 30, 151–157.
Rocha-Santos, T., Duarte, A.C., 2015. A critical overview of the analytical approaches to the occurrence, the fate and the behavior of microplastics in the environment. Trends Anal. Chem. 65, 47–53.
Rochman, C.M., 2015. The Complex Mixture, Fate and Toxicity of Chemicals Associated with Plastic Debris in the Marine Environment, in: Bergmann, M., Gutow, L., Klages, M. (Eds.), Marine Anthropogenic Litter. Springer, Cham, pp. 117–140.
Rochman, C.M., Browne, M.A., Underwood, A.J., Van Franeker, J.A., Thompson, R.C., Amaral-Zettler, L.A., 2016. The ecological impacts of marine debris: unraveling the demonstrated evidence from what is perceived. Ecology 97, 302–312.
Rochman, C. M., Hoh, E., Hentschel, B.T., Kaye, S., 2013. Long-term field measurement of sorption of organic contaminants to five types of plastic pellets: Implications for plastic marine debris. Environ. Sci. Technol. 47, 1646–1654.
Rochman, Chelsea M, Hoh, E., Kurobe, T., Teh, S.J., 2013. Ingested plastic transfers hazardous chemicals to fish and induces hepatic stress. Sci. Rep. 3, 3263.
Rochman, C.M., Kross, S.M., Armstrong, J.B., Bogan, M.T., Darling, E.S., Green, S.J., Smyth, A.R., Veríssimo, D., 2015. Scientific Evidence Supports a Ban on Microbeads. Environ. Sci. Technol. 49, 10759–10761.
Rojo, F., 2009. Degradation of alkanes by bacteria. Environ. Microbiol. 11, 2477–2490.
Romera-Castillo, C., Pinto, M., Langer, T.M., Álvarez-Salgado, X.A., Herndl, G.J., 2018. Dissolved organic carbon leaching from plastics stimulates microbial activity in the ocean. Nat. Commun. 9, 1430.
Rothstein, S.I., 1973. Plastic particle pollution of the surface of the Atlantic Ocean: evidence from a seabird. Condor 75, 344–365.
Rumin, J., Bonnefond, H., Saint-Jean, B., Rouxel, C., Sciandra, A., Bernard, O., Cadoret, J.-P., Bougaran, G., 2015. The use of fluorescent Nile red and BODIPY for lipid measurement in microalgae. Biotechnol. Biofuels 8, 42.
Rummel, C.D., Löder, M.G.J., Fricke, N.F., Lang, T., Griebeler, E.-M., Janke, M., Gerdts, G., 2016. Plastic ingestion by pelagic and demersal fish from the North Sea and Baltic Sea. Mar. Pollut. Bull. 102, 134–141.
Ryan, P.G., 1987. The incidence and characteristics of plastic particles ingested by seabirds. Mar. Environ. Res. 23, 175–206.
Ryan, P.G., Moloney, C.L., 1993. Marine litter keeps increasing. Nature 361, 23.
Santo, M., Weitsman, R., Sivan, A., 2013. The role of the copper-binding enzyme - laccase - in the biodegradation of polyethylene by the actinomycete Rhodococcus ruber. Int. Biodeterior. Biodegrad. 84, 204–210.
Santos, R.G., Andrades, R., Fardim, L.M., Martins, A.S., 2016. Marine debris ingestion and Thayer's law - The importance of plastic color. Environ. Pollut. 214, 585–588.
Satoto, R., Subowo, W.S., Yusiasih, R., Takane, Y., Watanabe, Y., Hatakeyama, T., 1997. Weathering of high-density polyethylene in different latitudes. Polym.

Degrad. Stab. 56, 275–279.
Savoca, M.S., Nevitt, G.A., 2014. Evidence that dimethyl sulfide facilitates a tritrophic mutualism between marine primary producers and top predators. Proc. Natl. Acad. Sci. 111, 4157–4161.
Savoca, M.S., Tyson, C.W., Mcgill, M., Slager, C.J., 2017. Odours from marine plastic debris induce food search behaviours in a forage fish. Proc. R. Soc. B 284, 20171000.
Savoca, M.S., Wohlfeil, M.E., Ebeler, S.E., Nevitt, G.A., 2016. Marine plastic debris emits a keystone infochemical for olfactory foraging seabirds. Sci. Adv. 2, e1600395.
Schliep, K.P., 2011. phangorn: Phylogenetic analysis in R. Bioinformatics 27, 592–593.
Schwarzer, G., 2007. meta: An R package for meta-analysis. R News 7, 40–45.
Setälä, O., Fleming-Lehtinen, V., Lehtiniemi, M., 2014. Ingestion and transfer of microplastics in the planktonic food web. Environ. Pollut. 185, 77–83.
Shim, W.J., Song, Y.K., Hong, S.H., Jang, M., 2016. Identification and quantification of microplastics using Nile Red staining. Mar. Pollut. Bull. 113, 469–476.
Sleight, V.A., Bakir, A., Thompson, R.C., Henry, T.B., 2017. Assessment of microplastic-sorbed contaminant bioavailability through analysis of biomarker gene expression in larval zebrafish. Mar. Pollut. Bull. 116, 291–297.
Song, Y.K., Hong, S.H., Jang, M., Han, G.M., Jung, S.W., Shim, W.J., 2017. Combined Effects of UV Exposure Duration and Mechanical Abrasion on Microplastic Fragmentation by Polymer Type. Environ. Sci. Technol. 51, 4368–4376.
Song, Y.K., Hong, S.H., Jang, M., Kang, J.H., Kwon, O.Y., Han, G.M., Shim, W.J., 2014. Large accumulation of micro-sized synthetic polymer particles in the sea surface microlayer. Environ. Sci. Technol. 48, 9014–9021.
Stamatakis, A., 2014. RAxML version 8: A tool for phylogenetic analysis and post-analysis of large phylogenies. Bioinformatics 30, 1312–1313.
Suaria, G., Avio, C.G., Mineo, A., Lattin, G.L., Magaldi, M.G., Belmonte, G., Moore, C.J., Regoli, F., Aliani, S., 2016. The Mediterranean Plastic Soup: synthetic polymers in Mediterranean surface waters. Sci. Rep. 6, 37551.
Sudhakar, M., Doble, M., Murthy, P.S., Venkatesan, R., 2008. Marine microbe-mediated biodegradation of low- and high-density polyethylenes. Int. Biodeterior. Biodegrad. 61, 203–213.
Sun, X., Li, Q., Zhu, M., Liang, J., Zheng, S., Zhao, Y., 2017. Ingestion of microplastics by natural zooplankton groups in the northern South China Sea. Mar. Pollut. Bull. 115, 217–224.
Sutherland, I.W., 2001. Biofilm exopolysaccharides: a strong and sticky framework. Microbiology 147, 3–9.
Tagg, A.S., Sapp, M., Harrison, J.P., Ojeda, J.J., 2015. Identification and Quantification of Microplastics in Wastewater Using Focal Plane Array-Based Reflectance Micro-FT-IR Imaging. Anal. Chem. 87, 6032–6040.
Tanaka, K., Takada, H., Yamashita, R., Mizukawa, K., Fukuwaka, M. aki, Watanuki, Y., 2013. Accumulation of plastic-derived chemicals in tissues of seabirds ingesting marine plastics. Mar. Pollut. Bull. 69, 219–222.
Taylor, J.D., Cunliffe, M., 2016. Multi-year assessment of coastal planktonic fungi reveals environmental drivers of diversity and abundance. ISME J. 10, 2118–2128.

ter Halle, A., Ladirat, L., Gendre, X., Goudounèche, D., Pusineri, C., Routaboul, C., Tenailleau, C., Duployer, B., Perez, E., 2016. Understanding the fragmentation pattern of marine plastic debris. Environ. Sci. Technol. 50, 5668−5675.
ter Halle, A., Ladirat, L., Martignac, M., Mingotaud, A.F., Boyron, O., Perez, E., 2017. To what extent are microplastics from the open ocean weathered? Environ. Pollut. 227, 167–174.
Teuten, E.L., Rowland, S.J., Galloway, T.S., Thompson, R.C., 2007. Potential for plastics to transport hydrophobic contaminants. Environ. Sci. Technol. 41, 7759–7764.
Teuten, E.L., Saquing, J.M., Knappe, D.R.U., Barlaz, M.A., Jonsson, S., Björn, A., Rowland, S.J., Thompson, R.C., Galloway, T.S., Yamashita, R., Ochi, D., Watanuki, Y., Moore, C., Viet, P.H., Tana, T.S., Prudente, M., Boonyatumanond, R., Zakaria, M.P., Akkhavong, K., Ogata, Y., Hirai, H., Iwasa, S., Mizukawa, K., Hagino, Y., Imamura, A., Saha, M., Takada, H., 2009. Transport and release of chemicals from plastics to the environment and to wildlife. Philos. Trans. R. Soc. B 364, 2027–2045.
Theerachat, M., Guieysse, D., Morel, S., Remaud-Siméon, M., Chulalaksananukul, W., 2019. Laccases from Marine Organisms and Their Applications in the Biodegradation of Toxic and Environmental Pollutants: a Review. Appl. Biochem. Biotechnol. 187, 583–611.
Thiel, M., Gutow, L., 2005. the Ecology of Rafting in the Marine Environment. II. the Rafting Organisms and Community. Oceanogr. Mar. Biol. An Annu. Rev. 43, 279–418.
Thompson, R.C., Olsen, Y., Mitchell, R.P., Davis, A., Rowland, S.J., John, A.W.G., McGonigle, D., Russell, A.E., 2004. Lost at sea: where is all the plastic? Science. 304, 838.
Toshchakov, S. V., Korzhenkov, A.A., Chernikova, T.N., Ferrer, M., Golyshina, O. V., Yakimov, M.M., Golyshin, P.N., 2017. The genome analysis of Oleiphilus messinensis ME102 (DSM 13489T) reveals backgrounds of its obligate alkane-devouring marine lifestyle. Mar. Genomics 36, 41–47.
Turner, J.T., 2015. Zooplankton fecal pellets, marine snow, phytodetritus and the ocean's biological pump. Prog. Oceanogr. 130, 205–248.
Van Cauwenberghe, L., Vanreusel, A., Mees, J., Janssen, C.R., 2013. Microplastic pollution in deep-sea sediments. Environ. Pollut. 182, 495–499.
van Sebille, E., England, M.H., Froyland, G., 2012. Origin, dynamics and evolution of ocean garbage patches from observed surface drifters. Environ. Res. Lett. 7, 044040.
van Sebille, E., Wilcox, C., Lebreton, L., Maximenko, N., Hardesty, B.D., Franeker, J.A. Van, Eriksen, M., Siegel, D., Galgani, F., Law, K.L., 2015. A global inventory of small floating plastic debris. Environ. Res. Lett. 10, 124006.
Veroniki, A.A., Jackson, D., Viechtbauer, W., Bender, R., Bowden, J., Knapp, G., Kuss, O., Higgins, J.P., Langan, D., Salanti, G., 2016. Methods to estimate the between-study variance and its uncertainty in meta-analysis. Res. Synth. Methods 7, 55–79.
Viechtbauer, W., 2010. Conducting Meta-Analyses in R with the metafor Package. J. Stat. Softw. 36, 1–48.
Vroom, R.J.E., Koelmans, A.A., Besseling, E., Halsband, C., 2017. Aging of microplastics promotes their ingestion by marine zooplankton. Environ. Pollut. 231, 987–996.
Waldschläger, K., Schüttrumpf, H., 2019. Effects of Particle Properties on the

Settling and Rise Velocities of Microplastics in Freshwater under Laboratory Conditions. Environ. Sci. Technol. 53, 1958–1966.
Wang, J., Peng, J., Tan, Z., Gao, Y., Zhan, Z., Chen, Q., Cai, L., 2017. Microplastics in the surface sediments from the Beijiang River littoral zone: Composition, abundance, surface textures and interaction with heavy metals. Chemosphere 171, 248–258.
Wang, W., Ndungu, A.W., Li, Z., Wang, J., 2017. Microplastics pollution in inland freshwaters of China: A case study in urban surface waters of Wuhan, China. Sci. Total Environ. 575, 1369–1374.
Wang, W., Zhong, R., Shan, D., Shao, Z., 2014. Indigenous oil-degrading bacteria in crude oil-contaminated seawater of the Yellow sea, China. Appl. Microbiol. Biotechnol. 98, 7253–7269.
Wardrop, P., Shimeta, J., Nugegoda, D., Morrison, P.D., Miranda, A., Tang, M., Clarke, B.O., 2016. Chemical Pollutants Sorbed to Ingested Microbeads from Personal Care Products Accumulate in Fish. Environ. Sci. Technol. 50, 4037–4044.
Waters, C.N., Zalasiewicz, J., Summerhayes, C., Barnosky, A.D., Poirier, C., Gałuszka, A., Cearreta, A., Edgeworth, M., Ellis, E.C., Ellis, M., Jeandel, C., Leinfelder, R., McNeill, J.R., Richter, D.D.B., Steffen, W., Syvitski, J., Vidas, D., Wagreich, M., Williams, M., Zhisheng, A., Grinevald, J., Odada, E., Oreskes, N., Wolfe, A.P., 2016. The Anthropocene is functionally and stratigraphically distinct from the Holocene. Science. 351, aad2622.
Watts, A.J.R., Lewis, C., Goodhead, R.M., Beckett, S.J., Moger, J., Tyler, C.R., Galloway, T.S., 2014. Uptake and Retention of Microplastics by the Shore Crab Carcinus maenas. Environ. Sci. Technol. 48, 8823–8830.
Weiss, S., Xu, Z.Z., Peddada, S., Amir, A., Bittinger, K., Gonzalez, A., Lozupone, C., Zaneveld, J.R., Vázquez-Baeza, Y., Birmingham, A., Hyde, E.R., Knight, R., 2017. Normalization and microbial differential abundance strategies depend upon data characteristics. Microbiome 5, 27.
Wickham, H., 2009. ggplot2, Applied Spatial Data Analysis with R. Springer.
Williams, G.J., Work, T.M., Aeby, G.S., Knapp, I.S., Davy, S.K., 2011. Gross and microscopic morphology of lesions in Cnidaria from Palmyra Atoll, Central Pacific. J. Invertebr. Pathol. 106, 165–73.
Williams, H., Wikström, F., Otterbring, T., Löfgren, M., Gustafsson, A., 2012. Reasons for household food waste with special attention to packaging. J. Clean. Prod. 24, 141–148.
Willis, K., Denise Hardesty, B., Kriwoken, L., Wilcox, C., 2017. Differentiating littering, urban runoff and marine transport as sources of marine debris in coastal and estuarine environments. Sci. Rep. 7, 44479.
Winston, J.E., 1982. Drift plastic-An expanding niche for a marine invertebrate? Mar. Pollut. Bull. 13, 348–351.
Winston, J.E., Gregory, M.R., Stevens, L.M., 1997. Encrusters, Epibionts, and Other Biota Associated with Pelagic Plastics: A Review of Biogeographical, Environmental, and Conservation Issues, in: Coe, J.M., Rogers, D.B. (Eds.), Marine Debris. Springer, New York, pp. 81–97.
Woodall, L.C., Sanchez-Vidal, A., Canals, M., Paterson, G.L.J., Coppock, R., Sleight, V., Calafat, A., Rogers, A.D., Narayanaswamy, B.E., Thompson, R.C., 2014. The deep sea is a major sink for microplastic debris. R. Soc. Open Sci. 1, 140317.
Worm, B., Lotze, H.K., Jubinville, I., Wilcox, C., Jambeck, J., 2017. Plastic As a

Persistent Marine Pollutant. Annu. Rev. Environ. Resour. 42, 1–26.
Wright, E.S., 2016. Using DECIPHER v2.0 to Analyze Big Biological Sequence Data in R. R J. 8, 352–359.
Wright, S.L., Thompson, R.C., Galloway, T.S., 2013. The physical impacts of microplastics on marine organisms: A review. Environ. Pollut. 178, 483–492.
Yakimov, M.M., Timmis, K.N., Golyshin, P.N., 2007. Obligate oil-degrading marine bacteria. Curr. Opin. Biotechnol. 18, 257–266.
Ye, S., Andrady, A.L., 1991. Fouling of floating plastic debris under Biscayne Bay exposure conditions. Mar. Pollut. Bull. 22, 608–613.
Yoshida, S., Hiraga, K., Takehana, T., Taniguchi, I., Yamaji, H., Maeda, Y., Toyohara, K., Miyamoto, K., Kimura, Y., Oda, K., 2016. A bacterium that degrades and assimilates poly(ethylene terephthalate). Science. 351, 1196–1199.
Zettler, E.R., Mincer, T.J., Amaral-zettler, L.A., 2013. Life in the "Plastisphere": Microbial Communities on Plastic Marine Debris. Environ. Sci. Technol. 47, 7137−7146.
Zhang, H., 2017. Transport of microplastics in coastal seas. Estuar. Coast. Shelf Sci. 199, 74–86.
Zhang, W., Zhang, S., Wang, J., Wang, Y., Mu, J., Wang, P., Lin, X., Ma, D., 2017. Microplastic pollution in the surface waters of the Bohai Sea, China. Environ. Pollut. 231, 541–548.
Zhao, S., Danley, M., Ward, J.E., Mincer, T.J., 2017. An approach for extraction, characterization and quantitation of microplastic in natural marine snow using Raman microscopy. Anal. Methods 9, 1470–1478.
Zhao, S., Zhu, L., Li, D., 2015. Microplastic in three urban estuaries, China. Environ. Pollut. 206, 597–604.
Zimmermann, W., Paterson, A., Broda, P., 1988. Preparation of Milled Straw Lignin from Barley. Methods Enzymol. 161, 191–199.
Zobkov, M.B., Esiukova, E.E., Zyubin, A.Y., Samusev, I.G., 2019. Microplastic content variation in water column: The observations employing a novel sampling tool in stratified Baltic Sea. Mar. Pollut. Bull. 138, 193–205.

APPENDIX 4

sample_type	water	sampling_depth	sampling_region	extraction_density	max_size	polymer_type	count	conf_plastic	source_ID	densities_pcs_m^3	polymer_concentration	conc_dev	polymer_conc_dev
sediment	salt	20.5	subtidal	0	5	ABS	0	24	Martin2017	NA	NA	NA	NA
sediment	salt	20.5	subtidal	0	5	EPR	0	24	Martin2017	NA	NA	NA	NA
sediment	salt	20.5	subtidal	0	5	IR	0	24	Martin2017	NA	NA	NA	NA
sediment	salt	20.5	subtidal	0	5	NBR	0	24	Martin2017	NA	NA	NA	NA
sediment	salt	20.5	subtidal	0	5	PAN	0	24	Martin2017	NA	NA	NA	NA
sediment	salt	20.5	subtidal	0	5	PC	0	24	Martin2017	NA	NA	NA	NA
sediment	salt	20.5	subtidal	0	5	PCL	0	24	Martin2017	NA	NA	NA	NA
sediment	salt	20.5	subtidal	0	5	PDMS	0	24	Martin2017	NA	NA	NA	NA
sediment	salt	20.5	subtidal	0	5	PE	0	24	Martin2017	NA	NA	NA	NA
sediment	salt	20.5	subtidal	0	5	PEVA	0	24	Martin2017	NA	NA	NA	NA
sediment	salt	20.5	subtidal	0	5	PP	2	24	Martin2017	NA	NA	NA	NA
sediment	salt	20.5	subtidal	0	5	PP&A	22	24	Martin2017	NA	NA	NA	NA
sediment	salt	20.5	subtidal	0	5	PS	0	24	Martin2017	NA	NA	NA	NA
sediment	salt	20.5	subtidal	0	5	PSS	0	24	Martin2017	NA	NA	NA	NA
sediment	salt	20.5	subtidal	0	5	PTFE	0	24	Martin2017	NA	NA	NA	NA
sediment	salt	20.5	subtidal	0	5	PUR	0	24	Martin2017	NA	NA	NA	NA
sediment	salt	20.5	subtidal	0	5	PVA	0	24	Martin2017	NA	NA	NA	NA
sediment	salt	20.5	subtidal	0	5	PVC	0	24	Martin2017	NA	NA	NA	NA
sediment	salt	20.5	subtidal	0	5	PVOH	0	24	Martin2017	NA	NA	NA	NA
sediment	salt	20.5	subtidal	0	5	rubber	0	24	Martin2017	NA	NA	NA	NA
sediment	salt	20.5	subtidal	0	5	VCE	0	24	Martin2017	NA	NA	NA	NA
sediment	salt	20.5	subtidal	0	5	other	0	24	Martin2017	NA	NA	NA	NA
sediment	salt	20.5	subtidal	0	5	PAS	0	24	Martin2017	NA	NA	NA	NA
sediment	salt	2250	deep	1.2	5	ABS	0	46	Woodall2014	53927	0		0
sediment	salt	2250	deep	1.2	5	EPR	0	46	Woodall2014	53927	0		0
sediment	salt	2250	deep	1.2	5	IR	0	46	Woodall2014	53927	0		0

sample_type	water	sampling_depth	sampling_region	extraction_density	max_size	polymer_type	count	conf_plastic	source_ID	densities_pcs_m^3	polymer_concentration	conc_dev	polymer_conc_dev
sediment	salt	2250	deep	1.2	5	NBR	0	46	Woodall2014	53927	0		0
sediment	salt	2250	deep	1.2	5	PAN	0	46	Woodall2014	53927	0		0
sediment	salt	2250	deep	1.2	5	PC	0	46	Woodall2014	53927	0		0
sediment	salt	2250	deep	1.2	5	PCL	0	46	Woodall2014	53927	0		0
sediment	salt	2250	deep	1.2	5	PDMS	0	46	Woodall2014	53927	0		0
sediment	salt	2250	deep	1.2	5	PE	0	46	Woodall2014	53927	0		0
sediment	salt	2250	deep	1.2	5	PEVA	0	46	Woodall2014	53927	0		0
sediment	salt	2250	deep	1.2	5	PP	0	46	Woodall2014	53927	0		0
sediment	salt	2250	deep	1.2	5	PP&A	45	46	Woodall2014	53927	52754.6739		0
sediment	salt	2250	deep	1.2	5	PS	0	46	Woodall2014	53927	0		0
sediment	salt	2250	deep	1.2	5	PSS	0	46	Woodall2014	53927	0		0
sediment	salt	2250	deep	1.2	5	PTFE	0	46	Woodall2014	53927	0		0
sediment	salt	2250	deep	1.2	5	PUR	0	46	Woodall2014	53927	0		0
sediment	salt	2250	deep	1.2	5	PVA	0	46	Woodall2014	53927	0		0
sediment	salt	2250	deep	1.2	5	PVC	0	46	Woodall2014	53927	0		0
sediment	salt	2250	deep	1.2	5	PVOH	0	46	Woodall2014	53927	0		0
sediment	salt	2250	deep	1.2	5	rubber	0	46	Woodall2014	53927	0		0
sediment	salt	2250	deep	1.2	5	VCE	0	46	Woodall2014	53927	0		0
sediment	salt	2250	deep	1.2	5	other	1	46	Woodall2014	53927	1172.3261		0
sediment	salt	2250	deep	1.2	5	PAS	0	46	Woodall2014	53927	0		0
sediment	salt	58.5	subtidal	1.2	5	ABS	0	9	Graca2017	NA	NA	NA	NA
sediment	salt	58.5	subtidal	1.2	5	EPR	1	9	Graca2017	NA	NA	NA	NA
sediment	salt	58.5	subtidal	1.2	5	IR	0	9	Graca2017	NA	NA	NA	NA
sediment	salt	58.5	subtidal	1.2	5	NBR	0	9	Graca2017	NA	NA	NA	NA
sediment	salt	58.5	subtidal	1.2	5	PAN	1	9	Graca2017	NA	NA	NA	NA
sediment	salt	58.5	subtidal	1.2	5	PC	0	9	Graca2017	NA	NA	NA	NA
sediment	salt	58.5	subtidal	1.2	5	PCL	0	9	Graca2017	NA	NA	NA	NA
sedim	sa	58.5	subtidal	1.2	5	PDMS	0	9	Graca20	NA	NA	NA	NA

sample_type	water	sampling_depth	sampling_region	extraction_density	max_size	polymer_type	count	conf_plastic	source_ID	densities_pcs_m^3	polymer_concentration	conc_dev	polymer_conc_dev
ent	lt								17				
sediment	salt	58.5	subtidal	1.2	5	PE	0	9	Graca2017	NA	NA	NA	NA
sediment	salt	58.5	subtidal	1.2	5	PEVA	0	9	Graca2017	NA	NA	NA	NA
sediment	salt	58.5	subtidal	1.2	5	PP	0	9	Graca2017	NA	NA	NA	NA
sediment	salt	58.5	subtidal	1.2	5	PP&A	5	9	Graca2017	NA	NA	NA	NA
sediment	salt	58.5	subtidal	1.2	5	PS	0	9	Graca2017	NA	NA	NA	NA
sediment	salt	58.5	subtidal	1.2	5	PSS	0	9	Graca2017	NA	NA	NA	NA
sediment	salt	58.5	subtidal	1.2	5	PTFE	0	9	Graca2017	NA	NA	NA	NA
sediment	salt	58.5	subtidal	1.2	5	PUR	0	9	Graca2017	NA	NA	NA	NA
sediment	salt	58.5	subtidal	1.2	5	PVA	2	9	Graca2017	NA	NA	NA	NA
sediment	salt	58.5	subtidal	1.2	5	PVC	0	9	Graca2017	NA	NA	NA	NA
sediment	salt	58.5	subtidal	1.2	5	PVOH	0	9	Graca2017	NA	NA	NA	NA
sediment	salt	58.5	subtidal	1.2	5	rubber	0	9	Graca2017	NA	NA	NA	NA
sediment	salt	58.5	subtidal	1.2	5	VCE	0	9	Graca2017	NA	NA	NA	NA
sediment	salt	58.5	subtidal	1.2	5	other	0	9	Graca2017	NA	NA	NA	NA
sediment	salt	58.5	subtidal	1.2	5	PAS	0	9	Graca2017	NA	NA	NA	NA
sediment	salt	0	intertidal	1.2	5	ABS	0	11	Graca2017_2	NA	NA	NA	NA
sediment	salt	0	intertidal	1.2	5	EPR	2	11	Graca2017_2	NA	NA	NA	NA
sediment	salt	0	intertidal	1.2	5	IR	0	11	Graca2017_2	NA	NA	NA	NA
sediment	salt	0	intertidal	1.2	5	NBR	0	11	Graca2017_2	NA	NA	NA	NA
sediment	salt	0	intertidal	1.2	5	PAN	1	11	Graca2017_2	NA	NA	NA	NA
sediment	salt	0	intertidal	1.2	5	PC	0	11	Graca2017_2	NA	NA	NA	NA
sediment	salt	0	intertidal	1.2	5	PCL	0	11	Graca2017_2	NA	NA	NA	NA
sediment	salt	0	intertidal	1.2	5	PDMS	0	11	Graca2017_2	NA	NA	NA	NA
sediment	salt	0	intertidal	1.2	5	PE	1	11	Graca2017_2	NA	NA	NA	NA
sediment	salt	0	intertidal	1.2	5	PEVA	1	11	Graca2017_2	NA	NA	NA	NA
sediment	salt	0	intertidal	1.2	5	PP	0	11	Graca2017_2	NA	NA	NA	NA
sediment	salt	0	intertidal	1.2	5	PP&A	3	11	Graca2017_2	NA	NA	NA	NA

sample_type	water	sampling_depth	sampling_region	extraction_density	max_size	polymer_type	count	conf_plastic	source_ID	densities_pcs_m^3	polymer_concentration	conc_dev	polymer_conc_dev
sediment	salt	0	intertidal	1.2	5	PS	0	11	Graca2017_2	NA	NA	NA	NA
sediment	salt	0	intertidal	1.2	5	PSS	0	11	Graca2017_2	NA	NA	NA	NA
sediment	salt	0	intertidal	1.2	5	PTFE	0	11	Graca2017_2	NA	NA	NA	NA
sediment	salt	0	intertidal	1.2	5	PUR	0	11	Graca2017_2	NA	NA	NA	NA
sediment	salt	0	intertidal	1.2	5	PVA	0	11	Graca2017_2	NA	NA	NA	NA
sediment	salt	0	intertidal	1.2	5	PVC	1	11	Graca2017_2	NA	NA	NA	NA
sediment	salt	0	intertidal	1.2	5	PVOH	0	11	Graca2017_2	NA	NA	NA	NA
sediment	salt	0	intertidal	1.2	5	rubber	0	11	Graca2017_2	NA	NA	NA	NA
sediment	salt	0	intertidal	1.2	5	VCE	1	11	Graca2017_2	NA	NA	NA	NA
sediment	salt	0	intertidal	1.2	5	other	0	11	Graca2017_2	NA	NA	NA	NA
sediment	salt	0	intertidal	1.2	5	PAS	0	11	Graca2017_2	NA	NA	NA	NA
water	salt	0.01	surface		5	ABS	0	709	Song2014	16272	0	13457	0
water	salt	0.01	surface		5	EPR	0	709	Song2014	16272	0	13457	0
water	salt	0.01	surface		5	IR	0	709	Song2014	16272	0	13457	0
water	salt	0.01	surface		5	NBR	0	709	Song2014	16272	0	13457	0
water	salt	0.01	surface		5	PAN	0	709	Song2014	16272	0	13457	0
water	salt	0.01	surface		5	PC	0	709	Song2014	16272	0	13457	0
water	salt	0.01	surface		5	PCL	0	709	Song2014	16272	0	13457	0
water	salt	0.01	surface		5	PDMS	0	709	Song2014	16272	0	13457	0
water	salt	0.01	surface		5	PE	6	709	Song2014	16272	130.176	13457	107.656
water	salt	0.01	surface		5	PEVA	0	709	Song2014	16272	0	13457	0
water	salt	0.01	surface		5	PP	14	709	Song2014	16272	325.44	13457	269.14
water	salt	0.01	surface		5	PP&A	581	709	Song2014	16272	13326.768	13457	11021.283
water	salt	0.01	surface		5	PS	0	709	Song2014	16272	0	13457	0
water	salt	0.01	surface		5	PSS	0	709	Song2014	16272	0	13457	0
water	salt	0.01	surface		5	PTFE	0	709	Song2014	16272	0	13457	0
water	salt	0.01	surface		5	PUR	0	709	Song2014	16272	0	13457	0
water	sa	0.01	surface		5	PVA	0	709	Song201	16272	0	134	0

sample_type	water	sampling_depth	sampling_region	extraction_density	max_size	polymer_type	count	conf_plastic	source_ID	densities_pcs_m^3	polymer_concentration	conc_dev	polymer_conc_dev
	lt								4			57	
water	salt	0.01	surface		5	PVC	0	709	Song2014	16272	0	13457	0
water	salt	0.01	surface		5	PVOH	0	709	Song2014	16272	0	13457	0
water	salt	0.01	surface		5	rubber	4	709	Song2014	16272	97.632	13457	80.742
water	salt	0.01	surface		5	VCE	0	709	Song2014	16272	0	13457	0
water	salt	0.01	surface		5	other	26	709	Song2014	16272	602.064	13457	497.909
water	salt	0.01	surface		5	PAS	78	709	Song2014	16272	1789.92	13457	1480.27
water	fresh	0.01	surface	1.2	5	ABS	0	118	Mani2015	5.6	0	NA	NA
water	fresh	0.01	surface	1.2	5	EPR	0	118	Mani2015	5.6	0	NA	NA
water	fresh	0.01	surface	1.2	5	IR	0	118	Mani2015	5.6	0	NA	NA
water	fresh	0.01	surface	1.2	5	NBR	0	118	Mani2015	5.6	0	NA	NA
water	fresh	0.01	surface	1.2	5	PAN	0	118	Mani2015	5.6	0	NA	NA
water	fresh	0.01	surface	1.2	5	PC	0	118	Mani2015	5.6	0	NA	NA
water	fresh	0.01	surface	1.2	5	PCL	0	118	Mani2015	5.6	0	NA	NA
water	fresh	0.01	surface	1.2	5	PDMS	0	118	Mani2015	5.6	0	NA	NA
water	fresh	0.01	surface	1.2	5	PE	28	118	Mani2015	5.6	1.3289	NA	NA
water	fresh	0.01	surface	1.2	5	PEVA	0	118	Mani2015	5.6	0	NA	NA
water	fresh	0.01	surface	1.2	5	PP	20	118	Mani2015	5.6	0.9492	NA	NA
water	fresh	0.01	surface	1.2	5	PP&A	8	118	Mani2015	5.6	0.3791	NA	NA
water	fresh	0.01	surface	1.2	5	PS	44	118	Mani2015	5.6	2.0882	NA	NA
water	fresh	0.01	surface	1.2	5	PSS	0	118	Mani2015	5.6	0	NA	NA
water	fresh	0.01	surface	1.2	5	PTFE	0	118	Mani2015	5.6	0	NA	NA
water	fresh	0.01	surface	1.2	5	PUR	0	118	Mani2015	5.6	0	NA	NA
water	fresh	0.01	surface	1.2	5	PVA	0	118	Mani2015	5.6	0	NA	NA
water	fresh	0.01	surface	1.2	5	PVC	2	118	Mani2015	5.6	0.0946	NA	NA
water	fresh	0.01	surface	1.2	5	PVOH	0	118	Mani2015	5.6	0	NA	NA
water	fresh	0.01	surface	1.2	5	rubber	0	118	Mani2015	5.6	0	NA	NA
water	fresh	0.01	surface	1.2	5	VCE	0	118	Mani2015	5.6	0	NA	NA

sample_type	water	sampling_depth	sampling_region	extraction_density	max_size	polymer_type	count	conf_plastic	source_ID	densities_pcs_m^3	polymer_concentration	conc_dev	polymer_conc_dev
water	fresh	0.01	surface	1.2	5	other	16	118	Mani2015	5.6	0.7594	NA	NA
water	fresh	0.01	surface	1.2	5	PAS	0	118	Mani2015	5.6	0	NA	NA
water	salt	0.01	surface		5	ABS	2	850	Gajst2016	6.29	0.017	2.68	0.0072
water	salt	0.01	surface		5	EPR	0	850	Gajst2016	6.29	0	2.68	0
water	salt	0.01	surface		5	IR	0	850	Gajst2016	6.29	0	2.68	0
water	salt	0.01	surface		5	NBR	0	850	Gajst2016	6.29	0	2.68	0
water	salt	0.01	surface		5	PAN	0	850	Gajst2016	6.29	0	2.68	0
water	salt	0.01	surface		5	PC	0	850	Gajst2016	6.29	0	2.68	0
water	salt	0.01	surface		5	PCL	0	850	Gajst2016	6.29	0	2.68	0
water	salt	0.01	surface		5	PDMS	0	850	Gajst2016	6.29	0	2.68	0
water	salt	0.01	surface		5	PE	814	850	Gajst2016	6.29	6.0227	2.68	2.5661
water	salt	0.01	surface		5	PEVA	0	850	Gajst2016	6.29	0	2.68	0
water	salt	0.01	surface		5	PP	19	850	Gajst2016	6.29	0.1378	2.68	0.0587
water	salt	0.01	surface		5	PP&A	0	850	Gajst2016	6.29	0	2.68	0
water	salt	0.01	surface		5	PS	3	850	Gajst2016	6.29	0.0258	2.68	0.011
water	salt	0.01	surface		5	PSS	0	850	Gajst2016	6.29	0	2.68	0
water	salt	0.01	surface		5	PTFE	0	850	Gajst2016	6.29	0	2.68	0
water	salt	0.01	surface		5	PUR	0	850	Gajst2016	6.29	0	2.68	0
water	salt	0.01	surface		5	PVA	0	850	Gajst2016	6.29	0	2.68	0
water	salt	0.01	surface		5	PVC	2	850	Gajst2016	6.29	0.017	2.68	0.0072
water	salt	0.01	surface		5	PVOH	0	850	Gajst2016	6.29	0	2.68	0
water	salt	0.01	surface		5	rubber	0	850	Gajst2016	6.29	0	2.68	0
water	salt	0.01	surface		5	VCE	0	850	Gajst2016	6.29	0	2.68	0
water	salt	0.01	surface		5	other	9	850	Gajst2016	6.29	0.0692	2.68	0.0295
water	salt	0.01	surface		5	PAS	0	850	Gajst2016	6.29	0	2.68	0
water	salt	2227	deep		5	ABS	0	17	Courtene2017	70.8	0	NA	NA
water	salt	2227	deep		5	EPR	0	17	Courtene2017	70.8	0	NA	NA
water	sa	2227	deep		5	IR	0	17	Courtene	70.8	0	NA	NA

sample_type	water	sampling_depth	sampling_region	extraction_density	max_size	polymer_type	count	conf_plastic	source_ID	densities_pcs_m^3	polymer_concentration	conc_dev	polymer_conc_dev
	lt								2017				
water	salt	2227	deep		5	NBR	0	17	Courtene 2017	70.8	0	NA	NA
water	salt	2227	deep		5	PAN	0	17	Courtene 2017	70.8	0	NA	NA
water	salt	2227	deep		5	PC	0	17	Courtene 2017	70.8	0	NA	NA
water	salt	2227	deep		5	PCL	0	17	Courtene 2017	70.8	0	NA	NA
water	salt	2227	deep		5	PDMS	0	17	Courtene 2017	70.8	0	NA	NA
water	salt	2227	deep		5	PE	1	17	Courtene 2017	70.8	4.248	NA	NA
water	salt	2227	deep		5	PEVA	0	17	Courtene 2017	70.8	0	NA	NA
water	salt	2227	deep		5	PP	0	17	Courtene 2017	70.8	0	NA	NA
water	salt	2227	deep		5	PP&A	16	17	Courtene 2017	70.8	66.552	NA	NA
water	salt	2227	deep		5	PS	0	17	Courtene 2017	70.8	0	NA	NA
water	salt	2227	deep		5	PSS	0	17	Courtene 2017	70.8	0	NA	NA
water	salt	2227	deep		5	PTFE	0	17	Courtene 2017	70.8	0	NA	NA
water	salt	2227	deep		5	PUR	0	17	Courtene 2017	70.8	0	NA	NA
water	salt	2227	deep		5	PVA	0	17	Courtene 2017	70.8	0	NA	NA
water	salt	2227	deep		5	PVC	0	17	Courtene 2017	70.8	0	NA	NA
water	salt	2227	deep		5	PVOH	0	17	Courtene 2017	70.8	0	NA	NA
water	salt	2227	deep		5	rubber	0	17	Courtene 2017	70.8	0	NA	NA
water	salt	2227	deep		5	VCE	0	17	Courtene 2017	70.8	0	NA	NA
water	salt	2227	deep		5	other	0	17	Courtene 2017	70.8	0	NA	NA
water	salt	2227	deep		5	PAS	0	17	Courtene 2017	70.8	0	NA	NA
water	salt	3	column	surfactant	2.5	ABS	0	883	Enders2015	NA	NA	NA	NA
water	salt	3	column	surfactant	2.5	EPR	0	883	Enders2015	NA	NA	NA	NA
water	salt	3	column	surfactant	2.5	IR	0	883	Enders2015	NA	NA	NA	NA
water	salt	3	column	surfactant	2.5	NBR	0	883	Enders2015	NA	NA	NA	NA
water	salt	3	column	surfactant	2.5	PAN	0	883	Enders2015	NA	NA	NA	NA
water	salt	3	column	surfactant	2.5	PC	0	883	Enders2015	NA	NA	NA	NA
water	salt	3	column	surfactant	2.5	PCL	0	883	Enders2015	NA	NA	NA	NA

sample_type	water	sampling_depth	sampling_region	extraction_density	max_size	polymer_type	count	conf_plastic	source_ID	densities_pcs_m^3	polymer_concentration	conc_dev	polymer_conc_dev
water	salt	3	column	surfactant	2.5	PDMS	0	883	Enders2015	NA	NA	NA	NA
water	salt	3	column	surfactant	2.5	PE	371	883	Enders2015	NA	NA	NA	NA
water	salt	3	column	surfactant	2.5	PEVA	0	883	Enders2015	NA	NA	NA	NA
water	salt	3	column	surfactant	2.5	PP	53	883	Enders2015	NA	NA	NA	NA
water	salt	3	column	surfactant	2.5	PP&A	154	883	Enders2015	NA	NA	NA	NA
water	salt	3	column	surfactant	2.5	PS	35	883	Enders2015	NA	NA	NA	NA
water	salt	3	column	surfactant	2.5	PSS	0	883	Enders2015	NA	NA	NA	NA
water	salt	3	column	surfactant	2.5	PTFE	0	883	Enders2015	NA	NA	NA	NA
water	salt	3	column	surfactant	2.5	PUR	26	883	Enders2015	NA	NA	NA	NA
water	salt	3	column	surfactant	2.5	PVA	0	883	Enders2015	NA	NA	NA	NA
water	salt	3	column	surfactant	2.5	PVC	16	883	Enders2015	NA	NA	NA	NA
water	salt	3	column	surfactant	2.5	PVOH	0	883	Enders2015	NA	NA	NA	NA
water	salt	3	column	surfactant	2.5	rubber	0	883	Enders2015	NA	NA	NA	NA
water	salt	3	column	surfactant	2.5	VCE	0	883	Enders2015	NA	NA	NA	NA
water	salt	3	column	surfactant	2.5	other	232	883	Enders2015	NA	NA	NA	NA
water	salt	3	column	surfactant	2.5	PAS	0	883	Enders2015	NA	NA	NA	NA
water	salt	10	column		2	ABS	0	175	Kanhai2017	1.15	0	1.45	0
water	salt	10	column		2	EPR	0	175	Kanhai2017	1.15	0	1.45	0
water	salt	10	column		2	IR	0	175	Kanhai2017	1.15	0	1.45	0
water	salt	10	column		2	NBR	0	175	Kanhai2017	1.15	0	1.45	0
water	salt	10	column		2	PAN	0	175	Kanhai2017	1.15	0	1.45	0
water	salt	10	column		2	PC	0	175	Kanhai2017	1.15	0	1.45	0
water	salt	10	column		2	PCL	0	175	Kanhai2017	1.15	0	1.45	0
water	salt	10	column		2	PDMS	0	175	Kanhai2017	1.15	0	1.45	0
water	salt	10	column		2	PE	0	175	Kanhai2017	1.15	0	1.45	0
water	salt	10	column		2	PEVA	0	175	Kanhai2017	1.15	0	1.45	0
water	salt	10	column		2	PP	5	175	Kanhai2017	1.15	0.0345	1.45	0.0435
water	sa	10	column		2	PP&A	16	175	Kanhai20	1.15	1.058	1.45	1.334

sample_type	water	sampling_depth	sampling_region	extraction_density	max_size	polymer_type	count	conf_plastic	source_ID	densities_pcs_m^3	polymer_concentration	conc_dev	polymer_conc_dev
	lt						1		17				
water	salt	10	column		2	PS	2	175	Kanhai2017	1.15	0.0115	1.45	0.0145
water	salt	10	column		2	PSS	0	175	Kanhai2017	1.15	0	1.45	0
water	salt	10	column		2	PTFE	0	175	Kanhai2017	1.15	0	1.45	0
water	salt	10	column		2	PUR	2	175	Kanhai2017	1.15	0.0115	1.45	0.0145
water	salt	10	column		2	PVA	0	175	Kanhai2017	1.15	0	1.45	0
water	salt	10	column		2	PVC	4	175	Kanhai2017	1.15	0.023	1.45	0.029
water	salt	10	column		2	PVOH	0	175	Kanhai2017	1.15	0	1.45	0
water	salt	10	column		2	rubber	0	175	Kanhai2017	1.15	0	1.45	0
water	salt	10	column		2	VCE	0	175	Kanhai2017	1.15	0	1.45	0
water	salt	10	column		2	other	133	175	Kanhai2017	1.15	0.874	1.45	1.102
water	salt	10	column		2	PAS	0	175	Kanhai2017	1.15	0	1.45	0
water	salt	0.01	surface	visual	20	ABS	0	3872	Suaria2016	1	0	1.84	0
water	salt	0.01	surface	visual	20	EPR	0	3872	Suaria2016	1	0	1.84	0
water	salt	0.01	surface	visual	20	IR	0	3872	Suaria2016	1	0	1.84	0
water	salt	0.01	surface	visual	20	NBR	0	3872	Suaria2016	1	0	1.84	0
water	salt	0.01	surface	visual	20	PAN	0	3872	Suaria2016	1	0	1.84	0
water	salt	0.01	surface	visual	20	PC	0	3872	Suaria2016	1	0	1.84	0
water	salt	0.01	surface	visual	20	PCL	0	3872	Suaria2016	1	0	1.84	0
water	salt	0.01	surface	visual	20	PDMS	0	3872	Suaria2016	1	0	1.84	0
water	salt	0.01	surface	visual	20	PE	2106	3872	Suaria2016	1	0.5439	1.84	1.0008
water	salt	0.01	surface	visual	20	PEVA	0	3872	Suaria2016	1	0	1.84	0
water	salt	0.01	surface	visual	20	PP	648	3872	Suaria2016	1	0.1674	1.84	0.3079
water	salt	0.01	surface	visual	20	PP&A	267	3872	Suaria2016	1	0.069	1.84	0.1269
water	salt	0.01	surface	visual	20	PS	113	3872	Suaria2016	1	0.0292	1.84	0.0537
water	salt	0.01	surface	visual	20	PSS	0	3872	Suaria2016	1	0	1.84	0
water	salt	0.01	surface	visual	20	PTFE	0	3872	Suaria2016	1	0	1.84	0
water	salt	0.01	surface	visual	20	PUR	0	3872	Suaria2016	1	0	1.84	0

sample_type	water	sampling_depth	sampling_region	extraction_density	max_size	polymer_type	count	conf_plastic	source_ID	densities_pcs_m^3	polymer_concentration	conc_dev	polymer_conc_dev
water	salt	0.01	surface	visual	20	PVA	49	3872	Suaria2016	1	0.0127	1.84	0.0233
water	salt	0.01	surface	visual	20	PVC	105	3872	Suaria2016	1	0.0271	1.84	0.0499
water	salt	0.01	surface	visual	20	PVOH	0	3872	Suaria2016	1	0	1.84	0
water	salt	0.01	surface	visual	20	rubber	0	3872	Suaria2016	1	0	1.84	0
water	salt	0.01	surface	visual	20	VCE	0	3872	Suaria2016	1	0	1.84	0
water	salt	0.01	surface	visual	20	other	584	3872	Suaria2016	1	0.1508	1.84	0.2775
water	salt	0.01	surface	visual	20	PAS	0	3872	Suaria2016	1	0	1.84	0
water	salt	25	column	visual	5	ABS	0	28	Amelineau2016	2.38	0	1.11	0
water	salt	25	column	visual	5	EPR	0	28	Amelineau2016	2.38	0	1.11	0
water	salt	25	column	visual	5	IR	0	28	Amelineau2016	2.38	0	1.11	0
water	salt	25	column	visual	5	NBR	0	28	Amelineau2016	2.38	0	1.11	0
water	salt	25	column	visual	5	PAN	0	28	Amelineau2016	2.38	0	1.11	0
water	salt	25	column	visual	5	PC	0	28	Amelineau2016	2.38	0	1.11	0
water	salt	25	column	visual	5	PCL	0	28	Amelineau2016	2.38	0	1.11	0
water	salt	25	column	visual	5	PDMS	0	28	Amelineau2016	2.38	0	1.11	0
water	salt	25	column	visual	5	PE	7	28	Amelineau2016	2.38	0.595	1.11	0.2775
water	salt	25	column	visual	5	PEVA	0	28	Amelineau2016	2.38	0	1.11	0
water	salt	25	column	visual	5	PP	3	28	Amelineau2016	2.38	0.255	1.11	0.1189
water	salt	25	column	visual	5	PP&A	17	28	Amelineau2016	2.38	1.445	1.11	0.6739
water	salt	25	column	visual	5	PS	0	28	Amelineau2016	2.38	0	1.11	0
water	salt	25	column	visual	5	PSS	0	28	Amelineau2016	2.38	0	1.11	0
water	salt	25	column	visual	5	PTFE	0	28	Amelineau2016	2.38	0	1.11	0
water	salt	25	column	visual	5	PUR	0	28	Amelineau2016	2.38	0	1.11	0
water	salt	25	column	visual	5	PVA	0	28	Amelineau2016	2.38	0	1.11	0
water	salt	25	column	visual	5	PVC	1	28	Amelineau2016	2.38	0.085	1.11	0.0396
water	salt	25	column	visual	5	PVOH	0	28	Amelineau2016	2.38	0	1.11	0
water	salt	25	column	visual	5	rubber	0	28	Amelineau2016	2.38	0	1.11	0
water	sa	25	column	visual	5	VCE	0	28	Amelinea	2.38	0	1.11	0

sample_type	water	sampling_depth	sampling_region	extraction_density	max_size	polymer_type	count	conf_plastic	source_ID	densities_pcs_m^3	polymer_concentration	conc_dev	polymer_conc_dev
	lt								u2016				
water	salt	25	column	visual	5	other	0	28	Amelinea u2016	2.38	0	1.11	0
water	salt	25	column	visual	5	PAS	0	28	Amelinea u2016	2.38	0	1.11	0
sediment	salt	0	intertidal	1.2	5	ABS	0	105	Blumenröder2017	NA	NA	NA	NA
sediment	salt	0	intertidal	1.2	5	EPR	0	105	Blumenröder2017	NA	NA	NA	NA
sediment	salt	0	intertidal	1.2	5	IR	0	105	Blumenröder2017	NA	NA	NA	NA
sediment	salt	0	intertidal	1.2	5	NBR	0	105	Blumenröder2017	NA	NA	NA	NA
sediment	salt	0	intertidal	1.2	5	PAN	3	105	Blumenröder2017	NA	NA	NA	NA
sediment	salt	0	intertidal	1.2	5	PC	0	105	Blumenröder2017	NA	NA	NA	NA
sediment	salt	0	intertidal	1.2	5	PCL	0	105	Blumenröder2017	NA	NA	NA	NA
sediment	salt	0	intertidal	1.2	5	PDMS	3	105	Blumenröder2017	NA	NA	NA	NA
sediment	salt	0	intertidal	1.2	5	PE	16	105	Blumenröder2017	NA	NA	NA	NA
sediment	salt	0	intertidal	1.2	5	PEVA	0	105	Blumenröder2017	NA	NA	NA	NA
sediment	salt	0	intertidal	1.2	5	PP	0	105	Blumenröder2017	NA	NA	NA	NA
sediment	salt	0	intertidal	1.2	5	PP&A	19	105	Blumenröder2017	NA	NA	NA	NA
sediment	salt	0	intertidal	1.2	5	PS	0	105	Blumenröder2017	NA	NA	NA	NA
sediment	salt	0	intertidal	1.2	5	PSS	0	105	Blumenröder2017	NA	NA	NA	NA
sediment	salt	0	intertidal	1.2	5	PTFE	47	105	Blumenröder2017	NA	NA	NA	NA
sediment	salt	0	intertidal	1.2	5	PUR	0	105	Blumenröder2017	NA	NA	NA	NA
sediment	salt	0	intertidal	1.2	5	PVA	0	105	Blumenröder2017	NA	NA	NA	NA
sediment	salt	0	intertidal	1.2	5	PVC	0	105	Blumenröder2017	NA	NA	NA	NA
sediment	salt	0	intertidal	1.2	5	PVOH	0	105	Blumenröder2017	NA	NA	NA	NA
sediment	salt	0	intertidal	1.2	5	rubber	0	105	Blumenröder2017	NA	NA	NA	NA
sediment	salt	0	intertidal	1.2	5	VCE	0	105	Blumenröder2017	NA	NA	NA	NA
sediment	salt	0	intertidal	1.2	5	other	16	105	Blumenröder2017	NA	NA	NA	NA
sediment	salt	0	intertidal	1.2	5	PAS	0	105	Blumenröder2017	NA	NA	NA	NA
sediment	salt	17.25	subtidal	1.1	5	ABS	0	6	Frias2016		0		0
sediment	salt	17.25	subtidal	1.1	5	EPR	0	6	Frias2016		0		0

sample_type	water	sampling_depth	sampling_region	extraction_density	max_size	polymer_type	count	conf_plastic	source_ID	densities_pcs_m^3	polymer_concentration	conc_dev	polymer_conc_dev
sediment	salt	17.25	subtidal	1.1	5	IR	0	6	Frias2016		0		0
sediment	salt	17.25	subtidal	1.1	5	NBR	0	6	Frias2016		0		0
sediment	salt	17.25	subtidal	1.1	5	PAN	0	6	Frias2016		0		0
sediment	salt	17.25	subtidal	1.1	5	PC	0	6	Frias2016		0		0
sediment	salt	17.25	subtidal	1.1	5	PCL	0	6	Frias2016		0		0
sediment	salt	17.25	subtidal	1.1	5	PDMS	0	6	Frias2016		0		0
sediment	salt	17.25	subtidal	1.1	5	PE	0	6	Frias2016		0		0
sediment	salt	17.25	subtidal	1.1	5	PEVA	0	6	Frias2016		0		0
sediment	salt	17.25	subtidal	1.1	5	PP	6	6	Frias2016		0		0
sediment	salt	17.25	subtidal	1.1	5	PP&A	0	6	Frias2016		0		0
sediment	salt	17.25	subtidal	1.1	5	PS	0	6	Frias2016		0		0
sediment	salt	17.25	subtidal	1.1	5	PSS	0	6	Frias2016		0		0
sediment	salt	17.25	subtidal	1.1	5	PTFE	0	6	Frias2016		0		0
sediment	salt	17.25	subtidal	1.1	5	PUR	0	6	Frias2016		0		0
sediment	salt	17.25	subtidal	1.1	5	PVA	0	6	Frias2016		0		0
sediment	salt	17.25	subtidal	1.1	5	PVC	0	6	Frias2016		0		0
sediment	salt	17.25	subtidal	1.1	5	PVOH	0	6	Frias2016		0		0
sediment	salt	17.25	subtidal	1.1	5	rubber	0	6	Frias2016		0		0
sediment	salt	17.25	subtidal	1.1	5	VCE	0	6	Frias2016		0		0
sediment	salt	17.25	subtidal	1.1	5	other	0	6	Frias2016		0		0
sediment	salt	17.25	subtidal	1.1	5	PAS	0	6	Frias2016		0		0
water	salt	0.01	surface	digestion	5	ABS	0	1605	Zhang2017	0.33	0	0.34	0
water	salt	0.01	surface	digestion	5	EPR	0	1605	Zhang2017	0.33	0	0.34	0
water	salt	0.01	surface	digestion	5	IR	0	1605	Zhang2017	0.33	0	0.34	0
water	salt	0.01	surface	digestion	5	NBR	0	1605	Zhang2017	0.33	0	0.34	0
water	salt	0.01	surface	digestion	5	PAN	0	1605	Zhang2017	0.33	0	0.34	0
water	salt	0.01	surface	digestion	5	PC	0	1605	Zhang2017	0.33	0	0.34	0
water	sa	0.01	surface	digestio	5	PCL	0	1605	Zhang20	0.33	0	0.34	0

sample_type	water	sampling_depth	sampling_region	extraction_density	max_size	polymer_type	count	conf_plastic	source_ID	densities_pcs_m^3	polymer_concentration	conc_dev	polymer_conc_dev
	lt			n					17				
water	salt	0.01	surface	digestion	5	PDMS	0	1605	Zhang2017	0.33	0	0.34	0
water	salt	0.01	surface	digestion	5	PE	819	1605	Zhang2017	0.33	0.1683	0.34	0.1734
water	salt	0.01	surface	digestion	5	PEVA	0	1605	Zhang2017	0.33	0	0.34	0
water	salt	0.01	surface	digestion	5	PP	465	1605	Zhang2017	0.33	0.0957	0.34	0.0986
water	salt	0.01	surface	digestion	5	PP&A	48	1605	Zhang2017	0.33	0.0099	0.34	0.0102
water	salt	0.01	surface	digestion	5	PS	257	1605	Zhang2017	0.33	0.0528	0.34	0.0544
water	salt	0.01	surface	digestion	5	PSS	0	1605	Zhang2017	0.33	0	0.34	0
water	salt	0.01	surface	digestion	5	PTFE	0	1605	Zhang2017	0.33	0	0.34	0
water	salt	0.01	surface	digestion	5	PUR	0	1605	Zhang2017	0.33	0	0.34	0
water	salt	0.01	surface	digestion	5	PVA	0	1605	Zhang2017	0.33	0	0.34	0
water	salt	0.01	surface	digestion	5	PVC	0	1605	Zhang2017	0.33	0	0.34	0
water	salt	0.01	surface	digestion	5	PVOH	0	1605	Zhang2017	0.33	0	0.34	0
water	salt	0.01	surface	digestion	5	rubber	0	1605	Zhang2017	0.33	0	0.34	0
water	salt	0.01	surface	digestion	5	VCE	0	1605	Zhang2017	0.33	0	0.34	0
water	salt	0.01	surface	digestion	5	other	16	1605	Zhang2017	0.33	0.0033	0.34	0.0034
water	salt	0.01	surface	digestion	5	PAS	0	1605	Zhang2017	0.33	0	0.34	0
water	fresh	0.3	surface	sieve	10.6	ABS	0	41	Zhao2015	1681.666	0	NA	NA
water	fresh	0.3	surface	sieve	10.6	EPR	0	41	Zhao2015	1681.666	0	NA	NA
water	fresh	0.3	surface	sieve	10.6	IR	0	41	Zhao2015	1681.666	0	NA	NA
water	fresh	0.3	surface	sieve	10.6	NBR	0	41	Zhao2015	1681.666	0	NA	NA
water	fresh	0.3	surface	sieve	10.6	PAN	0	41	Zhao2015	1681.666	0	NA	NA
water	fresh	0.3	surface	sieve	10.6	PC	0	41	Zhao2015	1681.666	0	NA	NA
water	fresh	0.3	surface	sieve	10.6	PCL	0	41	Zhao2015	1681.666	0	NA	NA
water	fresh	0.3	surface	sieve	10.6	PDMS	0	41	Zhao2015	1681.666	0	NA	NA
water	fresh	0.3	surface	sieve	10.6	PE	16	41	Zhao2015	1681.666	656.1861	NA	NA
water	fresh	0.3	surface	sieve	10.6	PEVA	0	41	Zhao2015	1681.666	0	NA	NA
water	fresh	0.3	surface	sieve	10.6	PP	21	41	Zhao2015	1681.666	861.3493	NA	NA

sample_type	water	sampling_depth	sampling_region	extraction_density	max_size	polymer_type	count	conf_plastic	source_ID	densities_pcs_m^3	polymer_concentration	conc_dev	polymer_conc_dev
water	fresh	0.3	surface	sieve	10.6	PP&A	0	41	Zhao2015	1681.666	0	NA	NA
water	fresh	0.3	surface	sieve	10.6	PS	0	41	Zhao2015	1681.666	0	NA	NA
water	fresh	0.3	surface	sieve	10.6	PSS	0	41	Zhao2015	1681.666	0	NA	NA
water	fresh	0.3	surface	sieve	10.6	PTFE	3	41	Zhao2015	1681.666	123.098	NA	NA
water	fresh	0.3	surface	sieve	10.6	PUR	0	41	Zhao2015	1681.666	0	NA	NA
water	fresh	0.3	surface	sieve	10.6	PVA	0	41	Zhao2015	1681.666	0	NA	NA
water	fresh	0.3	surface	sieve	10.6	PVC	1	41	Zhao2015	1681.666	41.0327	NA	NA
water	fresh	0.3	surface	sieve	10.6	PVOH	0	41	Zhao2015	1681.666	0	NA	NA
water	fresh	0.3	surface	sieve	10.6	rubber	0	41	Zhao2015	1681.666	0	NA	NA
water	fresh	0.3	surface	sieve	10.6	VCE	0	41	Zhao2015	1681.666	0	NA	NA
water	fresh	0.3	surface	sieve	10.6	other	0	41	Zhao2015	1681.666	0	NA	NA
water	fresh	0.3	surface	sieve	10.6	PAS	0	41	Zhao2015	1681.666	0	NA	NA
sediment	salt	0	intertidal	1.2	9999	ABS	0	12	Abayomi2017	NA	NA	NA	NA
sediment	salt	0	intertidal	1.2	9999	EPR	3	12	Abayomi2017	NA	NA	NA	NA
sediment	salt	0	intertidal	1.2	9999	IR	0	12	Abayomi2017	NA	NA	NA	NA
sediment	salt	0	intertidal	1.2	9999	NBR	0	12	Abayomi2017	NA	NA	NA	NA
sediment	salt	0	intertidal	1.2	9999	PAN	0	12	Abayomi2017	NA	NA	NA	NA
sediment	salt	0	intertidal	1.2	9999	PC	0	12	Abayomi2017	NA	NA	NA	NA
sediment	salt	0	intertidal	1.2	9999	PCL	0	12	Abayomi2017	NA	NA	NA	NA
sediment	salt	0	intertidal	1.2	9999	PDMS	0	12	Abayomi2017	NA	NA	NA	NA
sediment	salt	0	intertidal	1.2	9999	PE	6	12	Abayomi2017	NA	NA	NA	NA
sediment	salt	0	intertidal	1.2	9999	PEVA	0	12	Abayomi2017	NA	NA	NA	NA
sediment	salt	0	intertidal	1.2	9999	PP	3	12	Abayomi2017	NA	NA	NA	NA
sediment	salt	0	intertidal	1.2	9999	PP&A	0	12	Abayomi2017	NA	NA	NA	NA
sediment	salt	0	intertidal	1.2	9999	PS	0	12	Abayomi2017	NA	NA	NA	NA
sediment	salt	0	intertidal	1.2	9999	PSS	0	12	Abayomi2017	NA	NA	NA	NA
sediment	salt	0	intertidal	1.2	9999	PTFE	0	12	Abayomi2017	NA	NA	NA	NA
sedim	sa	0	intertida	1.2	999	PUR	0	12	Abayomi	NA	NA	NA	NA

sample_type	water	sampling_depth	sampling_region	extraction_density	max_size	polymer_type	count	conf_plastic	source_ID	densities_pcs_m^3	polymer_concentration	conc_dev	polymer_conc_dev
ent	lt		l		9				2017				
sediment	salt	0	intertidal	1.2	9999	PVA	0	12	Abayomi 2017	NA	NA	NA	NA
sediment	salt	0	intertidal	1.2	9999	PVC	0	12	Abayomi 2017	NA	NA	NA	NA
sediment	salt	0	intertidal	1.2	9999	PVOH	0	12	Abayomi 2017	NA	NA	NA	NA
sediment	salt	0	intertidal	1.2	9999	rubber	0	12	Abayomi 2017	NA	NA	NA	NA
sediment	salt	0	intertidal	1.2	9999	VCE	0	12	Abayomi 2017	NA	NA	NA	NA
sediment	salt	0	intertidal	1.2	9999	other	0	12	Abayomi 2017	NA	NA	NA	NA
sediment	salt	0	intertidal	1.2	9999	PAS	0	12	Abayomi 2017	NA	NA	NA	NA
water	salt	0.01	surface	visual	9999	ABS	0	4	Abayomi 2017_2	NA	NA	NA	NA
water	salt	0.01	surface	visual	9999	EPR	1	4	Abayomi 2017_2	NA	NA	NA	NA
water	salt	0.01	surface	visual	9999	IR	0	4	Abayomi 2017_2	NA	NA	NA	NA
water	salt	0.01	surface	visual	9999	NBR	0	4	Abayomi 2017_2	NA	NA	NA	NA
water	salt	0.01	surface	visual	9999	PAN	0	4	Abayomi 2017_2	NA	NA	NA	NA
water	salt	0.01	surface	visual	9999	PC	0	4	Abayomi 2017_2	NA	NA	NA	NA
water	salt	0.01	surface	visual	9999	PCL	0	4	Abayomi 2017_2	NA	NA	NA	NA
water	salt	0.01	surface	visual	9999	PDMS	0	4	Abayomi 2017_2	NA	NA	NA	NA
water	salt	0.01	surface	visual	9999	PE	2	4	Abayomi 2017_2	NA	NA	NA	NA
water	salt	0.01	surface	visual	9999	PEVA	0	4	Abayomi 2017_2	NA	NA	NA	NA
water	salt	0.01	surface	visual	9999	PP	0	4	Abayomi 2017_2	NA	NA	NA	NA
water	salt	0.01	surface	visual	9999	PP&A	1	4	Abayomi 2017_2	NA	NA	NA	NA
water	salt	0.01	surface	visual	9999	PS	0	4	Abayomi 2017_2	NA	NA	NA	NA
water	salt	0.01	surface	visual	9999	PSS	0	4	Abayomi 2017_2	NA	NA	NA	NA
water	salt	0.01	surface	visual	9999	PTFE	0	4	Abayomi 2017_2	NA	NA	NA	NA
water	salt	0.01	surface	visual	9999	PUR	0	4	Abayomi 2017_2	NA	NA	NA	NA
water	salt	0.01	surface	visual	9999	PVA	0	4	Abayomi 2017_2	NA	NA	NA	NA
water	salt	0.01	surface	visual	9999	PVC	0	4	Abayomi 2017_2	NA	NA	NA	NA
water	salt	0.01	surface	visual	9999	PVOH	0	4	Abayomi 2017_2	NA	NA	NA	NA
water	salt	0.01	surface	visual	9999	rubber	0	4	Abayomi 2017_2	NA	NA	NA	NA

sample_type	water	sampling_depth	sampling_region	extraction_density	max_size	polymer_type	count	conf_plastic	source_ID	densities_pcs_m^3	polymer_concentration	conc_dev	polymer_conc_dev
water	salt	0.01	surface	visual	9999	VCE	0	4	Abayomi 2017_2	NA	NA	NA	NA
water	salt	0.01	surface	visual	9999	other	0	4	Abayomi 2017_2	NA	NA	NA	NA
water	salt	0.01	surface	visual	9999	PAS	0	4	Abayomi 2017_2	NA	NA	NA	NA
water	salt	0.25	surface	1.03	100	ABS	0	200	Cozar2014	NA	NA	NA	NA
water	salt	0.25	surface	1.03	100	EPR	0	200	Cozar2014	NA	NA	NA	NA
water	salt	0.25	surface	1.03	100	IR	0	200	Cozar2014	NA	NA	NA	NA
water	salt	0.25	surface	1.03	100	NBR	0	200	Cozar2014	NA	NA	NA	NA
water	salt	0.25	surface	1.03	100	PAN	0	200	Cozar2014	NA	NA	NA	NA
water	salt	0.25	surface	1.03	100	PC	0	200	Cozar2014	NA	NA	NA	NA
water	salt	0.25	surface	1.03	100	PCL	0	200	Cozar2014	NA	NA	NA	NA
water	salt	0.25	surface	1.03	100	PDMS	0	200	Cozar2014	NA	NA	NA	NA
water	salt	0.25	surface	1.03	100	PE	152	200	Cozar2014	NA	NA	NA	NA
water	salt	0.25	surface	1.03	100	PEVA	0	200	Cozar2014	NA	NA	NA	NA
water	salt	0.25	surface	1.03	100	PP	42	200	Cozar2014	NA	NA	NA	NA
water	salt	0.25	surface	1.03	100	PP&A	0	200	Cozar2014	NA	NA	NA	NA
water	salt	0.25	surface	1.03	100	PS	6	200	Cozar2014	NA	NA	NA	NA
water	salt	0.25	surface	1.03	100	PSS	0	200	Cozar2014	NA	NA	NA	NA
water	salt	0.25	surface	1.03	100	PTFE	0	200	Cozar2014	NA	NA	NA	NA
water	salt	0.25	surface	1.03	100	PUR	0	200	Cozar2014	NA	NA	NA	NA
water	salt	0.25	surface	1.03	100	PVA	0	200	Cozar2014	NA	NA	NA	NA
water	salt	0.25	surface	1.03	100	PVC	0	200	Cozar2014	NA	NA	NA	NA
water	salt	0.25	surface	1.03	100	PVOH	0	200	Cozar2014	NA	NA	NA	NA
water	salt	0.25	surface	1.03	100	rubber	0	200	Cozar2014	NA	NA	NA	NA
water	salt	0.25	surface	1.03	100	VCE	0	200	Cozar2014	NA	NA	NA	NA
water	salt	0.25	surface	1.03	100	other	0	200	Cozar2014	NA	NA	NA	NA
water	salt	0.25	surface	1.03	100	PAS	0	200	Cozar2014	NA	NA	NA	NA
sediment	salt	0	intertidal	1.8	5	ABS	0	60	Naji2017	NA	NA	NA	NA
sedim	sa	0	intertida	1.8	5	EPR	0	60	Naji2017	NA	NA	NA	NA

sample_type	water	sampling_depth	sampling_region	extraction_density	max_size	polymer_type	count	conf_plastic	source_ID	densities_pcs_m^3	polymer_concentration	conc_dev	polymer_conc_dev
ent	lt		l										
sediment	salt	0	intertidal	1.8	5	IR	0	60	Naji2017	NA	NA	NA	NA
sediment	salt	0	intertidal	1.8	5	NBR	0	60	Naji2017	NA	NA	NA	NA
sediment	salt	0	intertidal	1.8	5	PAN	0	60	Naji2017	NA	NA	NA	NA
sediment	salt	0	intertidal	1.8	5	PC	0	60	Naji2017	NA	NA	NA	NA
sediment	salt	0	intertidal	1.8	5	PCL	0	60	Naji2017	NA	NA	NA	NA
sediment	salt	0	intertidal	1.8	5	PDMS	0	60	Naji2017	NA	NA	NA	NA
sediment	salt	0	intertidal	1.8	5	PE	21	60	Naji2017	NA	NA	NA	NA
sediment	salt	0	intertidal	1.8	5	PEVA	0	60	Naji2017	NA	NA	NA	NA
sediment	salt	0	intertidal	1.8	5	PP	0	60	Naji2017	NA	NA	NA	NA
sediment	salt	0	intertidal	1.8	5	PP&A	39	60	Naji2017	NA	NA	NA	NA
sediment	salt	0	intertidal	1.8	5	PS	0	60	Naji2017	NA	NA	NA	NA
sediment	salt	0	intertidal	1.8	5	PSS	0	60	Naji2017	NA	NA	NA	NA
sediment	salt	0	intertidal	1.8	5	PTFE	0	60	Naji2017	NA	NA	NA	NA
sediment	salt	0	intertidal	1.8	5	PUR	0	60	Naji2017	NA	NA	NA	NA
sediment	salt	0	intertidal	1.8	5	PVA	0	60	Naji2017	NA	NA	NA	NA
sediment	salt	0	intertidal	1.8	5	PVC	0	60	Naji2017	NA	NA	NA	NA
sediment	salt	0	intertidal	1.8	5	PVOH	0	60	Naji2017	NA	NA	NA	NA
sediment	salt	0	intertidal	1.8	5	rubber	0	60	Naji2017	NA	NA	NA	NA
sediment	salt	0	intertidal	1.8	5	VCE	0	60	Naji2017	NA	NA	NA	NA
sediment	salt	0	intertidal	1.8	5	other	0	60	Naji2017	NA	NA	NA	NA
sediment	salt	0	intertidal	1.8	5	PAS	0	60	Naji2017	NA	NA	NA	NA
sediment	salt	0	intertidal	1.2	4	ABS	0	35	Readman2013	0.091	0	0.0548	0
sediment	salt	0	intertidal	1.2	4	EPR	1	35	Readman2013	0.091	0.002	0.0548	0.0012
sediment	salt	0	intertidal	1.2	4	IR	0	35	Readman2013	0.091	0	0.0548	0
sediment	salt	0	intertidal	1.2	4	NBR	0	35	Readman2013	0.091	0	0.0548	0
sediment	salt	0	intertidal	1.2	4	PAN	0	35	Readman2013	0.091	0	0.0548	0
sediment	salt	0	intertidal	1.2	4	PC	0	35	Readman2013	0.091	0	0.0548	0

sample_type	water	sampling_depth	sampling_region	extraction_density	max_size	polymer_type	count	conf_plastic	source_ID	densities_pcs_m^3	polymer_concentration	conc_dev	polymer_conc_dev
sediment	salt	0	intertidal	1.2	4	PCL	0	35	Readman2013	0.091	0	0.0548	0
sediment	salt	0	intertidal	1.2	4	PDMS	0	35	Readman2013	0.091	0	0.0548	0
sediment	salt	0	intertidal	1.2	4	PE	2	35	Readman2013	0.091	0.0061	0.0548	0.0037
sediment	salt	0	intertidal	1.2	4	PEVA	0	35	Readman2013	0.091	0	0.0548	0
sediment	salt	0	intertidal	1.2	4	PP	0	35	Readman2013	0.091	0	0.0548	0
sediment	salt	0	intertidal	1.2	4	PP&A	21	35	Readman2013	0.091	0.0546	0.0548	0.0329
sediment	salt	0	intertidal	1.2	4	PS	0	35	Readman2013	0.091	0	0.0548	0
sediment	salt	0	intertidal	1.2	4	PSS	0	35	Readman2013	0.091	0	0.0548	0
sediment	salt	0	intertidal	1.2	4	PTFE	0	35	Readman2013	0.091	0	0.0548	0
sediment	salt	0	intertidal	1.2	4	PUR	0	35	Readman2013	0.091	0	0.0548	0
sediment	salt	0	intertidal	1.2	4	PVA	0	35	Readman2013	0.091	0	0.0548	0
sediment	salt	0	intertidal	1.2	4	PVC	1	35	Readman2013	0.091	0.002	0.0548	0.0012
sediment	salt	0	intertidal	1.2	4	PVOH	0	35	Readman2013	0.091	0	0.0548	0
sediment	salt	0	intertidal	1.2	4	rubber	0	35	Readman2013	0.091	0	0.0548	0
sediment	salt	0	intertidal	1.2	4	VCE	0	35	Readman2013	0.091	0	0.0548	0
sediment	salt	0	intertidal	1.2	4	other	10	35	Readman2013	0.091	0.0263	0.0548	0.0158
sediment	salt	0	intertidal	1.2	4	PAS	0	35	Readman2013	0.091	0	0.0548	0
water	fresh	0.01	surface	filter	5	ABS	0	44	WangW2017	NA	NA	NA	NA
water	fresh	0.01	surface	filter	5	EPR	0	44	WangW2017	NA	NA	NA	NA
water	fresh	0.01	surface	filter	5	IR	0	44	WangW2017	NA	NA	NA	NA
water	fresh	0.01	surface	filter	5	NBR	0	44	WangW2017	NA	NA	NA	NA
water	fresh	0.01	surface	filter	5	PAN	0	44	WangW2017	NA	NA	NA	NA
water	fresh	0.01	surface	filter	5	PC	0	44	WangW2017	NA	NA	NA	NA
water	fresh	0.01	surface	filter	5	PCL	0	44	WangW2017	NA	NA	NA	NA
water	fresh	0.01	surface	filter	5	PDMS	0	44	WangW2017	NA	NA	NA	NA
water	fresh	0.01	surface	filter	5	PE	6	44	WangW2017	NA	NA	NA	NA
water	fresh	0.01	surface	filter	5	PEVA	0	44	WangW2017	NA	NA	NA	NA
water	fre	0.01	surface	filter	5	PP	13	44	WangW2	NA	NA	NA	NA

sample_type	water	sampling_depth	sampling_region	extraction_density	max_size	polymer_type	count	conf_plastic	source_ID	densities_pcs_m^3	polymer_concentration	conc_dev	polymer_conc_dev
	sh								017				
water	fresh	0.01	surface	filter	5	PP&A	23	44	WangW2017	NA	NA	NA	NA
water	fresh	0.01	surface	filter	5	PS	2	44	WangW2017	NA	NA	NA	NA
water	fresh	0.01	surface	filter	5	PSS	0	44	WangW2017	NA	NA	NA	NA
water	fresh	0.01	surface	filter	5	PTFE	0	44	WangW2017	NA	NA	NA	NA
water	fresh	0.01	surface	filter	5	PUR	0	44	WangW2017	NA	NA	NA	NA
water	fresh	0.01	surface	filter	5	PVA	0	44	WangW2017	NA	NA	NA	NA
water	fresh	0.01	surface	filter	5	PVC	0	44	WangW2017	NA	NA	NA	NA
water	fresh	0.01	surface	filter	5	PVOH	0	44	WangW2017	NA	NA	NA	NA
water	fresh	0.01	surface	filter	5	rubber	0	44	WangW2017	NA	NA	NA	NA
water	fresh	0.01	surface	filter	5	VCE	0	44	WangW2017	NA	NA	NA	NA
water	fresh	0.01	surface	filter	5	other	0	44	WangW2017	NA	NA	NA	NA
water	fresh	0.01	surface	filter	5	PAS	0	44	WangW2017	NA	NA	NA	NA
sediment	salt	0	intertidal	0	5	ABS	0	15	Lourenco2017	NA	NA	NA	NA
sediment	salt	0	intertidal	0	5	EPR	0	15	Lourenco2017	NA	NA	NA	NA
sediment	salt	0	intertidal	0	5	IR	0	15	Lourenco2017	NA	NA	NA	NA
sediment	salt	0	intertidal	0	5	NBR	0	15	Lourenco2017	NA	NA	NA	NA
sediment	salt	0	intertidal	0	5	PAN	10	15	Lourenco2017	NA	NA	NA	NA
sediment	salt	0	intertidal	0	5	PC	0	15	Lourenco2017	NA	NA	NA	NA
sediment	salt	0	intertidal	0	5	PCL	0	15	Lourenco2017	NA	NA	NA	NA
sediment	salt	0	intertidal	0	5	PDMS	0	15	Lourenco2017	NA	NA	NA	NA
sediment	salt	0	intertidal	0	5	PE	0	15	Lourenco2017	NA	NA	NA	NA
sediment	salt	0	intertidal	0	5	PEVA	0	15	Lourenco2017	NA	NA	NA	NA
sediment	salt	0	intertidal	0	5	PP	0	15	Lourenco2017	NA	NA	NA	NA
sediment	salt	0	intertidal	0	5	PP&A	3	15	Lourenco2017	NA	NA	NA	NA
sediment	salt	0	intertidal	0	5	PS	0	15	Lourenco2017	NA	NA	NA	NA
sediment	salt	0	intertidal	0	5	PSS	0	15	Lourenco2017	NA	NA	NA	NA
sediment	salt	0	intertidal	0	5	PTFE	0	15	Lourenco2017	NA	NA	NA	NA

sample_type	water	sampling_depth	sampling_region	extraction_density	max_size	polymer_type	count	conf_plastic	source_ID	densities_pcs_m^3	polymer_concentration	conc_dev	polymer_conc_dev
sediment	salt	0	intertidal	0	5	PUR	0	15	Lourenco 2017	NA	NA	NA	NA
sediment	salt	0	intertidal	0	5	PVA	0	15	Lourenco 2017	NA	NA	NA	NA
sediment	salt	0	intertidal	0	5	PVC	0	15	Lourenco 2017	NA	NA	NA	NA
sediment	salt	0	intertidal	0	5	PVOH	0	15	Lourenco 2017	NA	NA	NA	NA
sediment	salt	0	intertidal	0	5	rubber	0	15	Lourenco 2017	NA	NA	NA	NA
sediment	salt	0	intertidal	0	5	VCE	0	15	Lourenco 2017	NA	NA	NA	NA
sediment	salt	0	intertidal	0	5	other	2	15	Lourenco 2017	NA	NA	NA	NA
sediment	salt	0	intertidal	0	5	PAS	0	15	Lourenco 2017	NA	NA	NA	NA
sediment	salt	0	intertidal	1.2	5	ABS	11	1097	Kunz2016	10970	109.7	NA	NA
sediment	salt	0	intertidal	1.2	5	EPR	0	1097	Kunz2016	10970	0	NA	NA
sediment	salt	0	intertidal	1.2	5	IR	0	1097	Kunz2016	10970	0	NA	NA
sediment	salt	0	intertidal	1.2	5	NBR	0	1097	Kunz2016	10970	0	NA	NA
sediment	salt	0	intertidal	1.2	5	PAN	0	1097	Kunz2016	10970	0	NA	NA
sediment	salt	0	intertidal	1.2	5	PC	0	1097	Kunz2016	10970	0	NA	NA
sediment	salt	0	intertidal	1.2	5	PCL	0	1097	Kunz2016	10970	0	NA	NA
sediment	salt	0	intertidal	1.2	5	PDMS	0	1097	Kunz2016	10970	0	NA	NA
sediment	salt	0	intertidal	1.2	5	PE	483	1097	Kunz2016	10970	4826.8	NA	NA
sediment	salt	0	intertidal	1.2	5	PEVA	0	1097	Kunz2016	10970	0	NA	NA
sediment	salt	0	intertidal	1.2	5	PP	472	1097	Kunz2016	10970	4717.1	NA	NA
sediment	salt	0	intertidal	1.2	5	PP&A	0	1097	Kunz2016	10970	0	NA	NA
sediment	salt	0	intertidal	1.2	5	PS	132	1097	Kunz2016	10970	1316.4	NA	NA
sediment	salt	0	intertidal	1.2	5	PSS	0	1097	Kunz2016	10970	0	NA	NA
sediment	salt	0	intertidal	1.2	5	PTFE	0	1097	Kunz2016	10970	0	NA	NA
sediment	salt	0	intertidal	1.2	5	PUR	0	1097	Kunz2016	10970	0	NA	NA
sediment	salt	0	intertidal	1.2	5	PVA	0	1097	Kunz2016	10970	0	NA	NA
sediment	salt	0	intertidal	1.2	5	PVC	0	1097	Kunz2016	10970	0	NA	NA
sediment	salt	0	intertidal	1.2	5	PVOH	0	1097	Kunz2016	10970	0	NA	NA
sedim	sa	0	intertida	1.2	5	rubber	0	1097	Kunz201	10970	0	NA	NA

sample_type	water	sampling_depth	sampling_region	extraction_density	max_size	polymer_type	count	conf_plastic	source_ID	densities_pcs_m^3	polymer_concentration	conc_dev	polymer_conc_dev
ent	lt		l						6				
sediment	salt	0	intertidal	1.2	5	VCE	0	1097	Kunz2016	10970	0	NA	NA
sediment	salt	0	intertidal	1.2	5	other	0	1097	Kunz2016	10970	0	NA	NA
sediment	salt	0	intertidal	1.2	5	PAS	0	1097	Kunz2016	10970	0	NA	NA
sediment	fresh	0	intertidal	1.2	5	ABS	0	210	Klein2015	NA	NA	NA	NA
sediment	fresh	0	intertidal	1.2	5	EPR	0	210	Klein2015	NA	NA	NA	NA
sediment	fresh	0	intertidal	1.2	5	IR	0	210	Klein2015	NA	NA	NA	NA
sediment	fresh	0	intertidal	1.2	5	NBR	0	210	Klein2015	NA	NA	NA	NA
sediment	fresh	0	intertidal	1.2	5	PAN	0	210	Klein2015	NA	NA	NA	NA
sediment	fresh	0	intertidal	1.2	5	PC	0	210	Klein2015	NA	NA	NA	NA
sediment	fresh	0	intertidal	1.2	5	PCL	0	210	Klein2015	NA	NA	NA	NA
sediment	fresh	0	intertidal	1.2	5	PDMS	0	210	Klein2015	NA	NA	NA	NA
sediment	fresh	0	intertidal	1.2	5	PE	48	210	Klein2015	NA	NA	NA	NA
sediment	fresh	0	intertidal	1.2	5	PEVA	0	210	Klein2015	NA	NA	NA	NA
sediment	fresh	0	intertidal	1.2	5	PP	32	210	Klein2015	NA	NA	NA	NA
sediment	fresh	0	intertidal	1.2	5	PP&A	4	210	Klein2015	NA	NA	NA	NA
sediment	fresh	0	intertidal	1.2	5	PS	113	210	Klein2015	NA	NA	NA	NA
sediment	fresh	0	intertidal	1.2	5	PSS	0	210	Klein2015	NA	NA	NA	NA
sediment	fresh	0	intertidal	1.2	5	PTFE	0	210	Klein2015	NA	NA	NA	NA
sediment	fresh	0	intertidal	1.2	5	PUR	0	210	Klein2015	NA	NA	NA	NA
sediment	fresh	0	intertidal	1.2	5	PVA	0	210	Klein2015	NA	NA	NA	NA
sediment	fresh	0	intertidal	1.2	5	PVC	0	210	Klein2015	NA	NA	NA	NA
sediment	fresh	0	intertidal	1.2	5	PVOH	0	210	Klein2015	NA	NA	NA	NA
sediment	fresh	0	intertidal	1.2	5	rubber	0	210	Klein2015	NA	NA	NA	NA
sediment	fresh	0	intertidal	1.2	5	VCE	0	210	Klein2015	NA	NA	NA	NA
sediment	fresh	0	intertidal	1.2	5	other	13	210	Klein2015	NA	NA	NA	NA
sediment	fresh	0	intertidal	1.2	5	PAS	0	210	Klein2015	NA	NA	NA	NA
sediment	fresh	0	intertidal	1.75	4	ABS	0	34	Horton2017	42000	0	NA	NA

sample_type	water	sampling_depth	sampling_region	extraction_density	max_size	polymer_type	count	conf_plastic	source_ID	densities_pcs_m^3	polymer_concentration	conc_dev	polymer_conc_dev
sediment	fresh	0	intertidal	1.75	4	EPR	0	34	Horton2017	42000	0	NA	NA
sediment	fresh	0	intertidal	1.75	4	IR	0	34	Horton2017	42000	0	NA	NA
sediment	fresh	0	intertidal	1.75	4	NBR	0	34	Horton2017	42000	0	NA	NA
sediment	fresh	0	intertidal	1.75	4	PAN	0	34	Horton2017	42000	0	NA	NA
sediment	fresh	0	intertidal	1.75	4	PC	0	34	Horton2017	42000	0	NA	NA
sediment	fresh	0	intertidal	1.75	4	PCL	0	34	Horton2017	42000	0	NA	NA
sediment	fresh	0	intertidal	1.75	4	PDMS	0	34	Horton2017	42000	0	NA	NA
sediment	fresh	0	intertidal	1.75	4	PE	2	34	Horton2017	42000	2469.6	NA	NA
sediment	fresh	0	intertidal	1.75	4	PEVA	0	34	Horton2017	42000	0	NA	NA
sediment	fresh	0	intertidal	1.75	4	PP	5	34	Horton2017	42000	6178.2	NA	NA
sediment	fresh	0	intertidal	1.75	4	PP&A	14	34	Horton2017	42000	17295.6	NA	NA
sediment	fresh	0	intertidal	1.75	4	PS	1	34	Horton2017	42000	1218	NA	NA
sediment	fresh	0	intertidal	1.75	4	PSS	0	34	Horton2017	42000	0	NA	NA
sediment	fresh	0	intertidal	1.75	4	PTFE	0	34	Horton2017	42000	0	NA	NA
sediment	fresh	0	intertidal	1.75	4	PUR	0	34	Horton2017	42000	0	NA	NA
sediment	fresh	0	intertidal	1.75	4	PVA	0	34	Horton2017	42000	0	NA	NA
sediment	fresh	0	intertidal	1.75	4	PVC	1	34	Horton2017	42000	1218	NA	NA
sediment	fresh	0	intertidal	1.75	4	PVOH	0	34	Horton2017	42000	0	NA	NA
sediment	fresh	0	intertidal	1.75	4	rubber	0	34	Horton2017	42000	0	NA	NA
sediment	fresh	0	intertidal	1.75	4	VCE	0	34	Horton2017	42000	0	NA	NA
sediment	fresh	0	intertidal	1.75	4	other	11	34	Horton2017	42000	13587	NA	NA
sediment	fresh	0	intertidal	1.75	4	PAS	0	34	Horton2017	42000	0	NA	NA
water	salt	0.01	surface		5	ABS	2	26	Castillo2016	0.71	0.0546	NA	NA
water	salt	0.01	surface		5	EPR	0	26	Castillo2016	0.71	0	NA	NA
water	salt	0.01	surface		5	IR	0	26	Castillo2016	0.71	0	NA	NA
water	salt	0.01	surface		5	NBR	0	26	Castillo2016	0.71	0	NA	NA
water	salt	0.01	surface		5	PAN	0	26	Castillo2016	0.71	0	NA	NA
water	sa	0.01	surface		5	PC	0	26	Castillo2	0.71	0	NA	NA

sample_type	water	sampling_depth	sampling_region	extraction_density	max_size	polymer_type	count	conf_plastic	source_ID	densities_pcs_m^3	polymer_concentration	conc_dev	polymer_conc_dev
	lt								016				
water	salt	0.01	surface		5	PCL	0	26	Castillo2016	0.71	0	NA	NA
water	salt	0.01	surface		5	PDMS	0	26	Castillo2016	0.71	0	NA	NA
water	salt	0.01	surface		5	PE	6	26	Castillo2016	0.71	0.1638	NA	NA
water	salt	0.01	surface		5	PEVA	0	26	Castillo2016	0.71	0	NA	NA
water	salt	0.01	surface		5	PP	9	26	Castillo2016	0.71	0.2458	NA	NA
water	salt	0.01	surface		5	PP&A	3	26	Castillo2016	0.71	0.0819	NA	NA
water	salt	0.01	surface		5	PS	1	26	Castillo2016	0.71	0.0273	NA	NA
water	salt	0.01	surface		5	PSS	0	26	Castillo2016	0.71	0	NA	NA
water	salt	0.01	surface		5	PTFE	0	26	Castillo2016	0.71	0	NA	NA
water	salt	0.01	surface		5	PUR	0	26	Castillo2016	0.71	0	NA	NA
water	salt	0.01	surface		5	PVA	0	26	Castillo2016	0.71	0	NA	NA
water	salt	0.01	surface		5	PVC	0	26	Castillo2016	0.71	0	NA	NA
water	salt	0.01	surface		5	PVOH	0	26	Castillo2016	0.71	0	NA	NA
water	salt	0.01	surface		5	rubber	0	26	Castillo2016	0.71	0	NA	NA
water	salt	0.01	surface		5	VCE	0	26	Castillo2016	0.71	0	NA	NA
water	salt	0.01	surface		5	other	5	26	Castillo2016	0.71	0.1365	NA	NA
water	salt	0.01	surface		5	PAS	0	26	Castillo2016	0.71	0	NA	NA
sediment	fresh	4	subtidal	1.6	5	ABS	0	280	Matsugu ma2017	NA	NA	NA	NA
sediment	fresh	4	subtidal	1.6	5	EPR	44	280	Matsugu ma2017	NA	NA	NA	NA
sediment	fresh	4	subtidal	1.6	5	IR	0	280	Matsugu ma2017	NA	NA	NA	NA
sediment	fresh	4	subtidal	1.6	5	NBR	0	280	Matsugu ma2017	NA	NA	NA	NA
sediment	fresh	4	subtidal	1.6	5	PAN	0	280	Matsugu ma2017	NA	NA	NA	NA
sediment	fresh	4	subtidal	1.6	5	PC	0	280	Matsugu ma2017	NA	NA	NA	NA
sediment	fresh	4	subtidal	1.6	5	PCL	23	280	Matsugu ma2017	NA	NA	NA	NA
sediment	fresh	4	subtidal	1.6	5	PDMS	0	280	Matsugu ma2017	NA	NA	NA	NA
sediment	fresh	4	subtidal	1.6	5	PE	40	280	Matsugu ma2017	NA	NA	NA	NA
sediment	fresh	4	subtidal	1.6	5	PEVA	14	280	Matsugu ma2017	NA	NA	NA	NA

sample_type	water	sampling_depth	sampling_region	extraction_density	max_size	polymer_type	count	conf_plastic	source_ID	densities_pcs_m^3	polymer_concentration	conc_dev	polymer_conc_dev
sediment	fresh	4	subtidal	1.6	5	PP	11	280	Matsugu ma2017	NA	NA	NA	NA
sediment	fresh	4	subtidal	1.6	5	PP&A	83	280	Matsugu ma2017	NA	NA	NA	NA
sediment	fresh	4	subtidal	1.6	5	PS	17	280	Matsugu ma2017	NA	NA	NA	NA
sediment	fresh	4	subtidal	1.6	5	PSS	0	280	Matsugu ma2017	NA	NA	NA	NA
sediment	fresh	4	subtidal	1.6	5	PTFE	0	280	Matsugu ma2017	NA	NA	NA	NA
sediment	fresh	4	subtidal	1.6	5	PUR	0	280	Matsugu ma2017	NA	NA	NA	NA
sediment	fresh	4	subtidal	1.6	5	PVA	0	280	Matsugu ma2017	NA	NA	NA	NA
sediment	fresh	4	subtidal	1.6	5	PVC	6	280	Matsugu ma2017	NA	NA	NA	NA
sediment	fresh	4	subtidal	1.6	5	PVOH	0	280	Matsugu ma2017	NA	NA	NA	NA
sediment	fresh	4	subtidal	1.6	5	rubber	0	280	Matsugu ma2017	NA	NA	NA	NA
sediment	fresh	4	subtidal	1.6	5	VCE	0	280	Matsugu ma2017	NA	NA	NA	NA
sediment	fresh	4	subtidal	1.6	5	other	42	280	Matsugu ma2017	NA	NA	NA	NA
sediment	fresh	4	subtidal	1.6	5	PAS	0	280	Matsugu ma2017	NA	NA	NA	NA
sediment	salt	0	intertidal	1.8	50	ABS	0	81	Naji2017_2	5686.666	0	NA	NA
sediment	salt	0	intertidal	1.8	50	EPR	0	81	Naji2017_2	5686.666	0	NA	NA
sediment	salt	0	intertidal	1.8	50	IR	0	81	Naji2017_2	5686.666	0	NA	NA
sediment	salt	0	intertidal	1.8	50	NBR	0	81	Naji2017_2	5686.666	0	NA	NA
sediment	salt	0	intertidal	1.8	50	PAN	0	81	Naji2017_2	5686.666	0	NA	NA
sediment	salt	0	intertidal	1.8	50	PC	0	81	Naji2017_2	5686.666	0	NA	NA
sediment	salt	0	intertidal	1.8	50	PCL	0	81	Naji2017_2	5686.666	0	NA	NA
sediment	salt	0	intertidal	1.8	50	PDMS	0	81	Naji2017_2	5686.666	0	NA	NA
sediment	salt	0	intertidal	1.8	50	PE	26	81	Naji2017_2	5686.666	1825.4198	NA	NA
sediment	salt	0	intertidal	1.8	50	PEVA	0	81	Naji2017_2	5686.666	0	NA	NA
sediment	salt	0	intertidal	1.8	50	PP	0	81	Naji2017_2	5686.666	0	NA	NA
sediment	salt	0	intertidal	1.8	50	PP&A	55	81	Naji2017_2	5686.666	3861.2462	NA	NA
sediment	salt	0	intertidal	1.8	50	PS	0	81	Naji2017_2	5686.666	0	NA	NA
sediment	salt	0	intertidal	1.8	50	PSS	0	81	Naji2017_2	5686.666	0	NA	NA
sedim	sa	0	intertida	1.8	50	PTFE	0	81	Naji2017	5686.666	0	NA	NA

sample_type	water	sampling_depth	sampling_region	extraction_density	max_size	polymer_type	count	conf_plastic	source_ID	densities_pcs_m^3	polymer_concentration	conc_dev	polymer_conc_dev
ent	lt		l						_2				
sediment	salt	0	intertidal	1.8	50	PUR	0	81	Naji2017_2	5686.666	0	NA	NA
sediment	salt	0	intertidal	1.8	50	PVA	0	81	Naji2017_2	5686.666	0	NA	NA
sediment	salt	0	intertidal	1.8	50	PVC	0	81	Naji2017_2	5686.666	0	NA	NA
sediment	salt	0	intertidal	1.8	50	PVOH	0	81	Naji2017_2	5686.666	0	NA	NA
sediment	salt	0	intertidal	1.8	50	rubber	0	81	Naji2017_2	5686.666	0	NA	NA
sediment	salt	0	intertidal	1.8	50	VCE	0	81	Naji2017_2	5686.666	0	NA	NA
sediment	salt	0	intertidal	1.8	50	other	0	81	Naji2017_2	5686.666	0	NA	NA
sediment	salt	0	intertidal	1.8	50	PAS	0	81	Naji2017_2	5686.666	0	NA	NA
sediment	salt	0	intertidal	1.2	5	ABS	0	73	CluniesRoss2016	1946.667	0	NA	NA
sediment	salt	0	intertidal	1.2	5	EPR	0	73	CluniesRoss2016	1946.667	0	NA	NA
sediment	salt	0	intertidal	1.2	5	IR	0	73	CluniesRoss2016	1946.667	0	NA	NA
sediment	salt	0	intertidal	1.2	5	NBR	0	73	CluniesRoss2016	1946.667	0	NA	NA
sediment	salt	0	intertidal	1.2	5	PAN	0	73	CluniesRoss2016	1946.667	0	NA	NA
sediment	salt	0	intertidal	1.2	5	PC	0	73	CluniesRoss2016	1946.667	0	NA	NA
sediment	salt	0	intertidal	1.2	5	PCL	0	73	CluniesRoss2016	1946.667	0	NA	NA
sediment	salt	0	intertidal	1.2	5	PDMS	0	73	CluniesRoss2016	1946.667	0	NA	NA
sediment	salt	0	intertidal	1.2	5	PE	15	73	CluniesRoss2016	1946.667	399.0667	NA	NA
sediment	salt	0	intertidal	1.2	5	PEVA	0	73	CluniesRoss2016	1946.667	0	NA	NA
sediment	salt	0	intertidal	1.2	5	PP	8	73	CluniesRoss2016	1946.667	214.1333	NA	NA
sediment	salt	0	intertidal	1.2	5	PP&A	0	73	CluniesRoss2016	1946.667	0	NA	NA
sediment	salt	0	intertidal	1.2	5	PS	40	73	CluniesRoss2016	1946.667	1066.7733	NA	NA
sediment	salt	0	intertidal	1.2	5	PSS	0	73	CluniesRoss2016	1946.667	0	NA	NA
sediment	salt	0	intertidal	1.2	5	PTFE	0	73	CluniesRoss2016	1946.667	0	NA	NA
sediment	salt	0	intertidal	1.2	5	PUR	0	73	CluniesRoss2016	1946.667	0	NA	NA
sediment	salt	0	intertidal	1.2	5	PVA	0	73	CluniesRoss2016	1946.667	0	NA	NA
sediment	salt	0	intertidal	1.2	5	PVC	0	73	CluniesRoss2016	1946.667	0	NA	NA
sediment	salt	0	intertidal	1.2	5	PVOH	0	73	CluniesRoss2016	1946.667	0	NA	NA

sample_type	water	sampling_depth	sampling_region	extraction_density	max_size	polymer_type	count	conf_plastic	source_ID	densities_pcs_m^3	polymer_concentration	conc_dev	polymer_conc_dev
sediment	salt	0	intertidal	1.2	5	rubber	0	73	CluniesRoss2016	1946.667	0	NA	NA
sediment	salt	0	intertidal	1.2	5	VCE	0	73	CluniesRoss2016	1946.667	0	NA	NA
sediment	salt	0	intertidal	1.2	5	other	10	73	CluniesRoss2016	1946.667	266.6933	NA	NA
sediment	salt	0	intertidal	1.2	5	PAS	0	73	CluniesRoss2016	1946.667	0	NA	NA
water	salt	0.01	surface		27	ABS	0	48	Gewert2017	1.37	0	NA	NA
water	salt	0.01	surface		27	EPR	0	48	Gewert2017	1.37	0	NA	NA
water	salt	0.01	surface		27	IR	0	48	Gewert2017	1.37	0	NA	NA
water	salt	0.01	surface		27	NBR	0	48	Gewert2017	1.37	0	NA	NA
water	salt	0.01	surface		27	PAN	0	48	Gewert2017	1.37	0	NA	NA
water	salt	0.01	surface		27	PC	0	48	Gewert2017	1.37	0	NA	NA
water	salt	0.01	surface		27	PCL	0	48	Gewert2017	1.37	0	NA	NA
water	salt	0.01	surface		27	PDMS	0	48	Gewert2017	1.37	0	NA	NA
water	salt	0.01	surface		27	PE	14	48	Gewert2017	1.37	0.3996	NA	NA
water	salt	0.01	surface		27	PEVA	0	48	Gewert2017	1.37	0	NA	NA
water	salt	0.01	surface		27	PP	31	48	Gewert2017	1.37	0.8848	NA	NA
water	salt	0.01	surface		27	PP&A	0	48	Gewert2017	1.37	0	NA	NA
water	salt	0.01	surface		27	PS	3	48	Gewert2017	1.37	0.0856	NA	NA
water	salt	0.01	surface		27	PSS	0	48	Gewert2017	1.37	0	NA	NA
water	salt	0.01	surface		27	PTFE	0	48	Gewert2017	1.37	0	NA	NA
water	salt	0.01	surface		27	PUR	0	48	Gewert2017	1.37	0	NA	NA
water	salt	0.01	surface		27	PVA	0	48	Gewert2017	1.37	0	NA	NA
water	salt	0.01	surface		27	PVC	0	48	Gewert2017	1.37	0	NA	NA
water	salt	0.01	surface		27	PVOH	0	48	Gewert2017	1.37	0	NA	NA
water	salt	0.01	surface		27	rubber	0	48	Gewert2017	1.37	0	NA	NA
water	salt	0.01	surface		27	VCE	0	48	Gewert2017	1.37	0	NA	NA
water	salt	0.01	surface		27	other	0	48	Gewert2017	1.37	0	NA	NA
water	salt	0.01	surface		27	PAS	0	48	Gewert2017	1.37	0	NA	NA
water	sa	0.01	surface	1.03	30	ABS	0	198	Marti201	NA	NA	NA	NA

sample_type	water	sampling_depth	sampling_region	extraction_density	max_size	polymer_type	count	conf_plastic	source_ID	densities_pcs_m^3	polymer_concentration	conc_dev	polymer_conc_dev
	lt								7				
water	salt	0.01	surface	1.03	30	EPR	0	198	Marti2017	NA	NA	NA	NA
water	salt	0.01	surface	1.03	30	IR	0	198	Marti2017	NA	NA	NA	NA
water	salt	0.01	surface	1.03	30	NBR	0	198	Marti2017	NA	NA	NA	NA
water	salt	0.01	surface	1.03	30	PAN	0	198	Marti2017	NA	NA	NA	NA
water	salt	0.01	surface	1.03	30	PC	0	198	Marti2017	NA	NA	NA	NA
water	salt	0.01	surface	1.03	30	PCL	0	198	Marti2017	NA	NA	NA	NA
water	salt	0.01	surface	1.03	30	PDMS	0	198	Marti2017	NA	NA	NA	NA
water	salt	0.01	surface	1.03	30	PE	137	198	Marti2017	NA	NA	NA	NA
water	salt	0.01	surface	1.03	30	PEVA	0	198	Marti2017	NA	NA	NA	NA
water	salt	0.01	surface	1.03	30	PP	42	198	Marti2017	NA	NA	NA	NA
water	salt	0.01	surface	1.03	30	PP&A	2	198	Marti2017	NA	NA	NA	NA
water	salt	0.01	surface	1.03	30	PS	8	198	Marti2017	NA	NA	NA	NA
water	salt	0.01	surface	1.03	30	PSS	0	198	Marti2017	NA	NA	NA	NA
water	salt	0.01	surface	1.03	30	PTFE	0	198	Marti2017	NA	NA	NA	NA
water	salt	0.01	surface	1.03	30	PUR	2	198	Marti2017	NA	NA	NA	NA
water	salt	0.01	surface	1.03	30	PVA	0	198	Marti2017	NA	NA	NA	NA
water	salt	0.01	surface	1.03	30	PVC	6	198	Marti2017	NA	NA	NA	NA
water	salt	0.01	surface	1.03	30	PVOH	0	198	Marti2017	NA	NA	NA	NA
water	salt	0.01	surface	1.03	30	rubber	0	198	Marti2017	NA	NA	NA	NA
water	salt	0.01	surface	1.03	30	VCE	0	198	Marti2017	NA	NA	NA	NA
water	salt	0.01	surface	1.03	30	other	2	198	Marti2017	NA	NA	NA	NA
water	salt	0.01	surface	1.03	30	PAS	0	198	Marti2017	NA	NA	NA	NA
sediment	salt	0	intertidal	1.16	5	ABS	0	76	Gray2018	NA	NA	NA	NA
sediment	salt	0	intertidal	1.16	5	EPR	0	76	Gray2018	NA	NA	NA	NA
sediment	salt	0	intertidal	1.16	5	IR	0	76	Gray2018	NA	NA	NA	NA
sediment	salt	0	intertidal	1.16	5	NBR	0	76	Gray2018	NA	NA	NA	NA
sediment	salt	0	intertidal	1.16	5	PAN	0	76	Gray2018	NA	NA	NA	NA

sample_type	water	sampling_depth	sampling_region	extraction_density	max_size	polymer_type	count	conf_plastic	source_ID	densities_pcs_m^3	polymer_concentration	conc_dev	polymer_conc_dev
sediment	salt	0	intertidal	1.16	5	PC	0	76	Gray2018	NA	NA	NA	NA
sediment	salt	0	intertidal	1.16	5	PCL	0	76	Gray2018	NA	NA	NA	NA
sediment	salt	0	intertidal	1.16	5	PDMS	0	76	Gray2018	NA	NA	NA	NA
sediment	salt	0	intertidal	1.16	5	PE	10	76	Gray2018	NA	NA	NA	NA
sediment	salt	0	intertidal	1.16	5	PEVA	0	76	Gray2018	NA	NA	NA	NA
sediment	salt	0	intertidal	1.16	5	PP	4	76	Gray2018	NA	NA	NA	NA
sediment	salt	0	intertidal	1.16	5	PP&A	12	76	Gray2018	NA	NA	NA	NA
sediment	salt	0	intertidal	1.16	5	PS	50	76	Gray2018	NA	NA	NA	NA
sediment	salt	0	intertidal	1.16	5	PSS	0	76	Gray2018	NA	NA	NA	NA
sediment	salt	0	intertidal	1.16	5	PTFE	0	76	Gray2018	NA	NA	NA	NA
sediment	salt	0	intertidal	1.16	5	PUR	0	76	Gray2018	NA	NA	NA	NA
sediment	salt	0	intertidal	1.16	5	PVA	0	76	Gray2018	NA	NA	NA	NA
sediment	salt	0	intertidal	1.16	5	PVC	0	76	Gray2018	NA	NA	NA	NA
sediment	salt	0	intertidal	1.16	5	PVOH	0	76	Gray2018	NA	NA	NA	NA
sediment	salt	0	intertidal	1.16	5	rubber	0	76	Gray2018	NA	NA	NA	NA
sediment	salt	0	intertidal	1.16	5	VCE	0	76	Gray2018	NA	NA	NA	NA
sediment	salt	0	intertidal	1.16	5	other	0	76	Gray2018	NA	NA	NA	NA
sediment	salt	0	intertidal	1.16	5	PAS	0	76	Gray2018	NA	NA	NA	NA
water	fresh	0.01	surface	visual	5	ABS	0	42	Hendrickson2018	NA	NA	NA	NA
water	fresh	0.01	surface	visual	5	EPR	0	42	Hendrickson2018	NA	NA	NA	NA
water	fresh	0.01	surface	visual	5	IR	0	42	Hendrickson2018	NA	NA	NA	NA
water	fresh	0.01	surface	visual	5	NBR	0	42	Hendrickson2018	NA	NA	NA	NA
water	fresh	0.01	surface	visual	5	PAN	0	42	Hendrickson2018	NA	NA	NA	NA
water	fresh	0.01	surface	visual	5	PC	0	42	Hendrickson2018	NA	NA	NA	NA
water	fresh	0.01	surface	visual	5	PCL	0	42	Hendrickson2018	NA	NA	NA	NA
water	fresh	0.01	surface	visual	5	PDMS	0	42	Hendrickson2018	NA	NA	NA	NA
water	fresh	0.01	surface	visual	5	PE	8	42	Hendrickson2018	NA	NA	NA	NA
water	fre	0.01	surface	visual	5	PEVA	0	42	Hendrick	NA	NA	NA	NA

sample_type	water	sampling_depth	sampling_region	extraction_density	max_size	polymer_type	count	conf_plastic	source_ID	densities_pcs_m^3	polymer_concentration	conc_dev	polymer_conc_dev
	sh								son2018				
water	fresh	0.01	surface	visual	5	PP	9	42	Hendrickson2018	NA	NA	NA	NA
water	fresh	0.01	surface	visual	5	PP&A	6	42	Hendrickson2018	NA	NA	NA	NA
water	fresh	0.01	surface	visual	5	PS	2	42	Hendrickson2018	NA	NA	NA	NA
water	fresh	0.01	surface	visual	5	PSS	0	42	Hendrickson2018	NA	NA	NA	NA
water	fresh	0.01	surface	visual	5	PTFE	0	42	Hendrickson2018	NA	NA	NA	NA
water	fresh	0.01	surface	visual	5	PUR	0	42	Hendrickson2018	NA	NA	NA	NA
water	fresh	0.01	surface	visual	5	PVA	0	42	Hendrickson2018	NA	NA	NA	NA
water	fresh	0.01	surface	visual	5	PVC	11	42	Hendrickson2018	NA	NA	NA	NA
water	fresh	0.01	surface	visual	5	PVOH	0	42	Hendrickson2018	NA	NA	NA	NA
water	fresh	0.01	surface	visual	5	rubber	0	42	Hendrickson2018	NA	NA	NA	NA
water	fresh	0.01	surface	visual	5	VCE	0	42	Hendrickson2018	NA	NA	NA	NA
water	fresh	0.01	surface	visual	5	other	6	42	Hendrickson2018	NA	NA	NA	NA
water	fresh	0.01	surface	visual	5	PAS	0	42	Hendrickson2018	NA	NA	NA	NA
water	salt	8.5	column	visual	5	ABS	0	117	Kanhai2018	0.97	0	1.2	0
water	salt	8.5	column	visual	5	EPR	0	117	Kanhai2018	0.97	0	1.2	0
water	salt	8.5	column	visual	5	IR	0	117	Kanhai2018	0.97	0	1.2	0
water	salt	8.5	column	visual	5	NBR	0	117	Kanhai2018	0.97	0	1.2	0
water	salt	8.5	column	visual	5	PAN	8	117	Kanhai2018	0.97	0.0663	1.2	0.0821
water	salt	8.5	column	visual	5	PC	0	117	Kanhai2018	0.97	0	1.2	0
water	salt	8.5	column	visual	5	PCL	0	117	Kanhai2018	0.97	0	1.2	0
water	salt	8.5	column	visual	5	PDMS	0	117	Kanhai2018	0.97	0	1.2	0
water	salt	8.5	column	visual	5	PE	0	117	Kanhai2018	0.97	0	1.2	0
water	salt	8.5	column	visual	5	PEVA	0	117	Kanhai2018	0.97	0	1.2	0
water	salt	8.5	column	visual	5	PP	0	117	Kanhai2018	0.97	0	1.2	0
water	salt	8.5	column	visual	5	PP&A	93	117	Kanhai2018	0.97	0.771	1.2	0.9538
water	salt	8.5	column	visual	5	PS	0	117	Kanhai2018	0.97	0	1.2	0
water	salt	8.5	column	visual	5	PSS	0	117	Kanhai2018	0.97	0	1.2	0

sample_type	water	sampling_depth	sampling_region	extraction_density	max_size	polymer_type	count	conf_plastic	source_ID	densities_pcs_m^3	polymer_concentration	conc_dev	polymer_conc_dev
water	salt	8.5	column	visual	5	PTFE	0	117	Kanhai2018	0.97	0	1.2	0
water	salt	8.5	column	visual	5	PUR	0	117	Kanhai2018	0.97	0	1.2	0
water	salt	8.5	column	visual	5	PVA	0	117	Kanhai2018	0.97	0	1.2	0
water	salt	8.5	column	visual	5	PVC	5	117	Kanhai2018	0.97	0.0415	1.2	0.0513
water	salt	8.5	column	visual	5	PVOH	0	117	Kanhai2018	0.97	0	1.2	0
water	salt	8.5	column	visual	5	rubber	0	117	Kanhai2018	0.97	0	1.2	0
water	salt	8.5	column	visual	5	VCE	0	117	Kanhai2018	0.97	0	1.2	0
water	salt	8.5	column	visual	5	other	11	117	Kanhai2018	0.97	0.0912	1.2	0.1128
water	salt	8.5	column	visual	5	PAS	0	117	Kanhai2018	0.97	0	1.2	0
water	fresh	1	surface	visual	5	ABS	0	69	Di&Wang2018	4703	0	2816	0
water	fresh	1	surface	visual	5	EPR	0	69	Di&Wang2018	4703	0	2816	0
water	fresh	1	surface	visual	5	IR	0	69	Di&Wang2018	4703	0	2816	0
water	fresh	1	surface	visual	5	NBR	0	69	Di&Wang2018	4703	0	2816	0
water	fresh	1	surface	visual	5	PAN	0	69	Di&Wang2018	4703	0	2816	0
water	fresh	1	surface	visual	5	PC	1	69	Di&Wang2018	4703	68.1594	2816	40.8116
water	fresh	1	surface	visual	5	PCL	0	69	Di&Wang2018	4703	0	2816	0
water	fresh	1	surface	visual	5	PDMS	0	69	Di&Wang2018	4703	0	2816	0
water	fresh	1	surface	visual	5	PE	21	69	Di&Wang2018	4703	1431.3478	2816	857.0435
water	fresh	1	surface	visual	5	PEVA	0	69	Di&Wang2018	4703	0	2816	0
water	fresh	1	surface	visual	5	PP	34	69	Di&Wang2018	4703	2317.4203	2816	1387.5942
water	fresh	1	surface	visual	5	PP&A	0	69	Di&Wang2018	4703	0	2816	0
water	fresh	1	surface	visual	5	PS	12	69	Di&Wang2018	4703	817.913	2816	489.7391
water	fresh	1	surface	visual	5	PSS	0	69	Di&Wang2018	4703	0	2816	0
water	fresh	1	surface	visual	5	PTFE	0	69	Di&Wang2018	4703	0	2816	0
water	fresh	1	surface	visual	5	PUR	0	69	Di&Wang2018	4703	0	2816	0
water	fresh	1	surface	visual	5	PVA	0	69	Di&Wang2018	4703	0	2816	0
water	fresh	1	surface	visual	5	PVC	1	69	Di&Wang2018	4703	68.1594	2816	40.8116
water	fre	1	surface	visual	5	PVOH	0	69	Di&Wang	4703	0	281	0

sample_type	water	sampling_depth	sampling_region	extraction_density	max_size	polymer_type	count	conf_plastic	source_ID	densities_pcs_m^3	polymer_concentration	conc_dev	polymer_conc_dev
	sh								2018			6	
water	fresh	1	surface	visual	5	rubber	0	69	Di&Wang 2018	4703	0	2816	0
water	fresh	1	surface	visual	5	VCE	0	69	Di&Wang 2018	4703	0	2816	0
water	fresh	1	surface	visual	5	other	0	69	Di&Wang 2018	4703	0	2816	0
water	fresh	1	surface	visual	5	PAS	0	69	Di&Wang 2018	4703	0	2816	0
sediment	fresh		subtidal	1.8	5	ABS	0	74	Di&Wang 2018_2	NA	NA	NA	NA
sediment	fresh		subtidal	1.8	5	EPR	0	74	Di&Wang 2018_2	NA	NA	NA	NA
sediment	fresh		subtidal	1.8	5	IR	0	74	Di&Wang 2018_2	NA	NA	NA	NA
sediment	fresh		subtidal	1.8	5	NBR	0	74	Di&Wang 2018_2	NA	NA	NA	NA
sediment	fresh		subtidal	1.8	5	PAN	0	74	Di&Wang 2018_2	NA	NA	NA	NA
sediment	fresh		subtidal	1.8	5	PC	8	74	Di&Wang 2018_2	NA	NA	NA	NA
sediment	fresh		subtidal	1.8	5	PCL	0	74	Di&Wang 2018_2	NA	NA	NA	NA
sediment	fresh		subtidal	1.8	5	PDMS	0	74	Di&Wang 2018_2	NA	NA	NA	NA
sediment	fresh		subtidal	1.8	5	PE	9	74	Di&Wang 2018_2	NA	NA	NA	NA
sediment	fresh		subtidal	1.8	5	PEVA	0	74	Di&Wang 2018_2	NA	NA	NA	NA
sediment	fresh		subtidal	1.8	5	PP	8	74	Di&Wang 2018_2	NA	NA	NA	NA
sediment	fresh		subtidal	1.8	5	PP&A	0	74	Di&Wang 2018_2	NA	NA	NA	NA
sediment	fresh		subtidal	1.8	5	PS	43	74	Di&Wang 2018_2	NA	NA	NA	NA
sediment	fresh		subtidal	1.8	5	PSS	0	74	Di&Wang 2018_2	NA	NA	NA	NA
sediment	fresh		subtidal	1.8	5	PTFE	0	74	Di&Wang 2018_2	NA	NA	NA	NA
sediment	fresh		subtidal	1.8	5	PUR	0	74	Di&Wang 2018_2	NA	NA	NA	NA
sediment	fresh		subtidal	1.8	5	PVA	0	74	Di&Wang 2018_2	NA	NA	NA	NA
sediment	fresh		subtidal	1.8	5	PVC	5	74	Di&Wang 2018_2	NA	NA	NA	NA
sediment	fresh		subtidal	1.8	5	PVOH	0	74	Di&Wang 2018_2	NA	NA	NA	NA
sediment	fresh		subtidal	1.8	5	rubber	0	74	Di&Wang 2018_2	NA	NA	NA	NA
sediment	fresh		subtidal	1.8	5	VCE	0	74	Di&Wang 2018_2	NA	NA	NA	NA
sediment	fresh		subtidal	1.8	5	other	1	74	Di&Wang 2018_2	NA	NA	NA	NA
sediment	fresh		subtidal	1.8	5	PAS	0	74	Di&Wang 2018_2	NA	NA	NA	NA

sample_type	water	sampling_depth	sampling_region	extraction_density	max_size	polymer_type	count	conf_plastic	source_ID	densities_pcs_m^3	polymer_concentration	conc_dev	polymer_conc_dev
sediment	salt	0	intertidal	1.2	5	ABS	0	10	Lots2017	NA	NA	NA	NA
sediment	salt	0	intertidal	1.2	5	EPR	0	10	Lots2017	NA	NA	NA	NA
sediment	salt	0	intertidal	1.2	5	IR	0	10	Lots2017	NA	NA	NA	NA
sediment	salt	0	intertidal	1.2	5	NBR	0	10	Lots2017	NA	NA	NA	NA
sediment	salt	0	intertidal	1.2	5	PAN	0	10	Lots2017	NA	NA	NA	NA
sediment	salt	0	intertidal	1.2	5	PC	0	10	Lots2017	NA	NA	NA	NA
sediment	salt	0	intertidal	1.2	5	PCL	0	10	Lots2017	NA	NA	NA	NA
sediment	salt	0	intertidal	1.2	5	PDMS	0	10	Lots2017	NA	NA	NA	NA
sediment	salt	0	intertidal	1.2	5	PE	1	10	Lots2017	NA	NA	NA	NA
sediment	salt	0	intertidal	1.2	5	PEVA	0	10	Lots2017	NA	NA	NA	NA
sediment	salt	0	intertidal	1.2	5	PP	2	10	Lots2017	NA	NA	NA	NA
sediment	salt	0	intertidal	1.2	5	PP&A	7	10	Lots2017	NA	NA	NA	NA
sediment	salt	0	intertidal	1.2	5	PS	0	10	Lots2017	NA	NA	NA	NA
sediment	salt	0	intertidal	1.2	5	PSS	0	10	Lots2017	NA	NA	NA	NA
sediment	salt	0	intertidal	1.2	5	PTFE	0	10	Lots2017	NA	NA	NA	NA
sediment	salt	0	intertidal	1.2	5	PUR	0	10	Lots2017	NA	NA	NA	NA
sediment	salt	0	intertidal	1.2	5	PVA	0	10	Lots2017	NA	NA	NA	NA
sediment	salt	0	intertidal	1.2	5	PVC	0	10	Lots2017	NA	NA	NA	NA
sediment	salt	0	intertidal	1.2	5	PVOH	0	10	Lots2017	NA	NA	NA	NA
sediment	salt	0	intertidal	1.2	5	rubber	0	10	Lots2017	NA	NA	NA	NA
sediment	salt	0	intertidal	1.2	5	VCE	0	10	Lots2017	NA	NA	NA	NA
sediment	salt	0	intertidal	1.2	5	other	0	10	Lots2017	NA	NA	NA	NA
sediment	salt	0	intertidal	1.2	5	PAS	0	10	Lots2017	NA	NA	NA	NA
water	salt	0.01	surface	visual	5	ABS	0	33	Ghosal2018	NA	NA	NA	NA
water	salt	0.01	surface	visual	5	EPR	1	33	Ghosal2018	NA	NA	NA	NA
water	salt	0.01	surface	visual	5	IR	0	33	Ghosal2018	NA	NA	NA	NA
water	salt	0.01	surface	visual	5	NBR	0	33	Ghosal2018	NA	NA	NA	NA
water	sa	0.01	surface	visual	5	PAN	0	33	Ghosal20	NA	NA	NA	NA

sample_type	water	sampling_depth	sampling_region	extraction_density	max_size	polymer_type	count	conf_plastic	source_ID	densities_pcs_m^3	polymer_concentration	conc_dev	polymer_conc_dev
	lt								18				
water	salt	0.01	surface	visual	5	PC	0	33	Ghosal2018	NA	NA	NA	NA
water	salt	0.01	surface	visual	5	PCL	0	33	Ghosal2018	NA	NA	NA	NA
water	salt	0.01	surface	visual	5	PDMS	0	33	Ghosal2018	NA	NA	NA	NA
water	salt	0.01	surface	visual	5	PE	26	33	Ghosal2018	NA	NA	NA	NA
water	salt	0.01	surface	visual	5	PEVA	0	33	Ghosal2018	NA	NA	NA	NA
water	salt	0.01	surface	visual	5	PP	5	33	Ghosal2018	NA	NA	NA	NA
water	salt	0.01	surface	visual	5	PP&A	0	33	Ghosal2018	NA	NA	NA	NA
water	salt	0.01	surface	visual	5	PS	1	33	Ghosal2018	NA	NA	NA	NA
water	salt	0.01	surface	visual	5	PSS	0	33	Ghosal2018	NA	NA	NA	NA
water	salt	0.01	surface	visual	5	PTFE	0	33	Ghosal2018	NA	NA	NA	NA
water	salt	0.01	surface	visual	5	PUR	0	33	Ghosal2018	NA	NA	NA	NA
water	salt	0.01	surface	visual	5	PVA	0	33	Ghosal2018	NA	NA	NA	NA
water	salt	0.01	surface	visual	5	PVC	0	33	Ghosal2018	NA	NA	NA	NA
water	salt	0.01	surface	visual	5	PVOH	0	33	Ghosal2018	NA	NA	NA	NA
water	salt	0.01	surface	visual	5	rubber	0	33	Ghosal2018	NA	NA	NA	NA
water	salt	0.01	surface	visual	5	VCE	0	33	Ghosal2018	NA	NA	NA	NA
water	salt	0.01	surface	visual	5	other	0	33	Ghosal2018	NA	NA	NA	NA
water	salt	0.01	surface	visual	5	PAS	0	33	Ghosal2018	NA	NA	NA	NA
water	salt	0.01	surface	visual	5	ABS	0	691	Frere2017	0.24	0	0.35	0
water	salt	0.01	surface	visual	5	EPR	0	691	Frere2017	0.24	0	0.35	0
water	salt	0.01	surface	visual	5	IR	0	691	Frere2017	0.24	0	0.35	0
water	salt	0.01	surface	visual	5	NBR	0	691	Frere2017	0.24	0	0.35	0
water	salt	0.01	surface	visual	5	PAN	0	691	Frere2017	0.24	0	0.35	0
water	salt	0.01	surface	visual	5	PC	0	691	Frere2017	0.24	0	0.35	0
water	salt	0.01	surface	visual	5	PCL	0	691	Frere2017	0.24	0	0.35	0
water	salt	0.01	surface	visual	5	PDMS	0	691	Frere2017	0.24	0	0.35	0
water	salt	0.01	surface	visual	5	PE	466	691	Frere2017	0.24	0.1619	0.35	0.236

sample_type	water	sampling_depth	sampling_region	extraction_density	max_size	polymer_type	count	conf_plastic	source_ID	densities_pcs_m^3	polymer_concentration	conc_dev	polymer_conc_dev
water	salt	0.01	surface	visual	5	PEVA	0	691	Frere2017	0.24	0	0.35	0
water	salt	0.01	surface	visual	5	PP	114	691	Frere2017	0.24	0.0396	0.35	0.0577
water	salt	0.01	surface	visual	5	PP&A	0	691	Frere2017	0.24	0	0.35	0
water	salt	0.01	surface	visual	5	PS	111	691	Frere2017	0.24	0.0386	0.35	0.0562
water	salt	0.01	surface	visual	5	PSS	0	691	Frere2017	0.24	0	0.35	0
water	salt	0.01	surface	visual	5	PTFE	0	691	Frere2017	0.24	0	0.35	0
water	salt	0.01	surface	visual	5	PUR	0	691	Frere2017	0.24	0	0.35	0
water	salt	0.01	surface	visual	5	PVA	0	691	Frere2017	0.24	0	0.35	0
water	salt	0.01	surface	visual	5	PVC	0	691	Frere2017	0.24	0	0.35	0
water	salt	0.01	surface	visual	5	PVOH	0	691	Frere2017	0.24	0	0.35	0
water	salt	0.01	surface	visual	5	rubber	0	691	Frere2017	0.24	0	0.35	0
water	salt	0.01	surface	visual	5	VCE	0	691	Frere2017	0.24	0	0.35	0
water	salt	0.01	surface	visual	5	other	0	691	Frere2017	0.24	0	0.35	0
water	salt	0.01	surface	visual	5	PAS	0	691	Frere2017	0.24	0	0.35	0
sediment	salt	12.5	subtidal	1.56	5	ABS	0	30	Frere2017_2	4240.74	0	NA	NA
sediment	salt	12.5	subtidal	1.56	5	EPR	0	30	Frere2017_2	4240.74	0	NA	NA
sediment	salt	12.5	subtidal	1.56	5	IR	0	30	Frere2017_2	4240.74	0	NA	NA
sediment	salt	12.5	subtidal	1.56	5	NBR	0	30	Frere2017_2	4240.74	0	NA	NA
sediment	salt	12.5	subtidal	1.56	5	PAN	0	30	Frere2017_2	4240.74	0	NA	NA
sediment	salt	12.5	subtidal	1.56	5	PC	0	30	Frere2017_2	4240.74	0	NA	NA
sediment	salt	12.5	subtidal	1.56	5	PCL	0	30	Frere2017_2	4240.74	0	NA	NA
sediment	salt	12.5	subtidal	1.56	5	PDMS	0	30	Frere2017_2	4240.74	0	NA	NA
sediment	salt	12.5	subtidal	1.56	5	PE	16	30	Frere2017_2	4240.74	2261.728	NA	NA
sediment	salt	12.5	subtidal	1.56	5	PEVA	0	30	Frere2017_2	4240.74	0	NA	NA
sediment	salt	12.5	subtidal	1.56	5	PP	9	30	Frere2017_2	4240.74	1272.222	NA	NA
sediment	salt	12.5	subtidal	1.56	5	PP&A	0	30	Frere2017_2	4240.74	0	NA	NA
sediment	salt	12.5	subtidal	1.56	5	PS	5	30	Frere2017_2	4240.74	706.79	NA	NA
sedim	sa	12.5	subtidal	1.56	5	PSS	0	30	Frere201	4240.74	0	NA	NA

sample_type	water	sampling_depth	sampling_region	extraction_density	max_size	polymer_type	count	conf_plastic	source_ID	densities_pcs_m^3	polymer_concentration	conc_dev	polymer_conc_dev
ent	lt								7_2				
sediment	salt	12.5	subtidal	1.56	5	PTFE	0	30	Frere2017_2	4240.74	0	NA	NA
sediment	salt	12.5	subtidal	1.56	5	PUR	0	30	Frere2017_2	4240.74	0	NA	NA
sediment	salt	12.5	subtidal	1.56	5	PVA	0	30	Frere2017_2	4240.74	0	NA	NA
sediment	salt	12.5	subtidal	1.56	5	PVC	0	30	Frere2017_2	4240.74	0	NA	NA
sediment	salt	12.5	subtidal	1.56	5	PVOH	0	30	Frere2017_2	4240.74	0	NA	NA
sediment	salt	12.5	subtidal	1.56	5	rubber	0	30	Frere2017_2	4240.74	0	NA	NA
sediment	salt	12.5	subtidal	1.56	5	VCE	0	30	Frere2017_2	4240.74	0	NA	NA
sediment	salt	12.5	subtidal	1.56	5	other	0	30	Frere2017_2	4240.74	0	NA	NA
sediment	salt	12.5	subtidal	1.56	5	PAS	0	30	Frere2017_2	4240.74	0	NA	NA
water	salt	0.01	surface	digestion	1	ABS	0	37	ErniCassola2017	NA	NA	NA	NA
water	salt	0.01	surface	digestion	1	EPR	0	37	ErniCassola2017	NA	NA	NA	NA
water	salt	0.01	surface	digestion	1	IR	0	37	ErniCassola2017	NA	NA	NA	NA
water	salt	0.01	surface	digestion	1	NBR	0	37	ErniCassola2017	NA	NA	NA	NA
water	salt	0.01	surface	digestion	1	PAN	0	37	ErniCassola2017	NA	NA	NA	NA
water	salt	0.01	surface	digestion	1	PC	0	37	ErniCassola2017	NA	NA	NA	NA
water	salt	0.01	surface	digestion	1	PCL	0	37	ErniCassola2017	NA	NA	NA	NA
water	salt	0.01	surface	digestion	1	PDMS	0	37	ErniCassola2017	NA	NA	NA	NA
water	salt	0.01	surface	digestion	1	PE	6	37	ErniCassola2017	NA	NA	NA	NA
water	salt	0.01	surface	digestion	1	PEVA	0	37	ErniCassola2017	NA	NA	NA	NA
water	salt	0.01	surface	digestion	1	PP	31	37	ErniCassola2017	NA	NA	NA	NA
water	salt	0.01	surface	digestion	1	PP&A	0	37	ErniCassola2017	NA	NA	NA	NA
water	salt	0.01	surface	digestion	1	PS	0	37	ErniCassola2017	NA	NA	NA	NA
water	salt	0.01	surface	digestion	1	PSS	0	37	ErniCassola2017	NA	NA	NA	NA
water	salt	0.01	surface	digestion	1	PTFE	0	37	ErniCassola2017	NA	NA	NA	NA
water	salt	0.01	surface	digestion	1	PUR	0	37	ErniCassola2017	NA	NA	NA	NA
water	salt	0.01	surface	digestion	1	PVA	0	37	ErniCassola2017	NA	NA	NA	NA
water	salt	0.01	surface	digestion	1	PVC	0	37	ErniCassola2017	NA	NA	NA	NA

sample_type	water	sampling_depth	sampling_region	extraction_density	max_size	polymer_type	count	conf_plastic	source_ID	densities_pcs_m^3	polymer_concentration	conc_dev	polymer_conc_dev
water	salt	0.01	surface	digestion	1	PVOH	0	37	ErniCassola2017	NA	NA	NA	NA
water	salt	0.01	surface	digestion	1	rubber	0	37	ErniCassola2017	NA	NA	NA	NA
water	salt	0.01	surface	digestion	1	VCE	0	37	ErniCassola2017	NA	NA	NA	NA
water	salt	0.01	surface	digestion	1	other	0	37	ErniCassola2017	NA	NA	NA	NA
water	salt	0.01	surface	digestion	1	PAS	0	37	ErniCassola2017	NA	NA	NA	NA
sediment	salt	12	subtidal	1.6	5	ABS	0	56	Matsugu ma2017_2	NA	NA	NA	NA
sediment	salt	12	subtidal	1.6	5	EPR	11	56	Matsugu ma2017_2	NA	NA	NA	NA
sediment	salt	12	subtidal	1.6	5	IR	0	56	Matsugu ma2017_2	NA	NA	NA	NA
sediment	salt	12	subtidal	1.6	5	NBR	0	56	Matsugu ma2017_2	NA	NA	NA	NA
sediment	salt	12	subtidal	1.6	5	PAN	0	56	Matsugu ma2017_2	NA	NA	NA	NA
sediment	salt	12	subtidal	1.6	5	PC	0	56	Matsugu ma2017_2	NA	NA	NA	NA
sediment	salt	12	subtidal	1.6	5	PCL	2	56	Matsugu ma2017_2	NA	NA	NA	NA
sediment	salt	12	subtidal	1.6	5	PDMS	0	56	Matsugu ma2017_2	NA	NA	NA	NA
sediment	salt	12	subtidal	1.6	5	PE	23	56	Matsugu ma2017_2	NA	NA	NA	NA
sediment	salt	12	subtidal	1.6	5	PEVA	1	56	Matsugu ma2017_2	NA	NA	NA	NA
sediment	salt	12	subtidal	1.6	5	PP	3	56	Matsugu ma2017_2	NA	NA	NA	NA
sediment	salt	12	subtidal	1.6	5	PP&A	9	56	Matsugu ma2017_2	NA	NA	NA	NA
sediment	salt	12	subtidal	1.6	5	PS	3	56	Matsugu ma2017_2	NA	NA	NA	NA
sediment	salt	12	subtidal	1.6	5	PSS	0	56	Matsugu ma2017_2	NA	NA	NA	NA
sediment	salt	12	subtidal	1.6	5	PTFE	0	56	Matsugu ma2017_2	NA	NA	NA	NA
sediment	salt	12	subtidal	1.6	5	PUR	0	56	Matsugu ma2017_2	NA	NA	NA	NA
sedim	sa	12	subtidal	1.6	5	PVA	0	56	Matsugu	NA	NA	NA	NA

sample_type	water	sampling_depth	sampling_region	extraction_density	max_size	polymer_type	count	conf_plastic	source_ID	densities_pcs_m^3	polymer_concentration	conc_dev	polymer_conc_dev
ent	lt								ma2017_2				
sediment	salt	12	subtidal	1.6	5	PVC	0	56	Matsugu ma2017_2	NA	NA	NA	NA
sediment	salt	12	subtidal	1.6	5	PVOH	0	56	Matsugu ma2017_2	NA	NA	NA	NA
sediment	salt	12	subtidal	1.6	5	rubber	0	56	Matsugu ma2017_2	NA	NA	NA	NA
sediment	salt	12	subtidal	1.6	5	VCE	0	56	Matsugu ma2017_2	NA	NA	NA	NA
sediment	salt	12	subtidal	1.6	5	other	4	56	Matsugu ma2017_2	NA	NA	NA	NA
sediment	salt	12	subtidal	1.6	5	PAS	0	56	Matsugu ma2017_2	NA	NA	NA	NA
sediment	salt	3496	deep	1.8	5	ABS	0	987	Bergman n2017	NA	NA	NA	NA
sediment	salt	3496	deep	1.8	5	EPR	0	987	Bergman n2017	NA	NA	NA	NA
sediment	salt	3496	deep	1.8	5	IR	0	987	Bergman n2017	NA	NA	NA	NA
sediment	salt	3496	deep	1.8	5	NBR	101	987	Bergman n2017	NA	NA	NA	NA
sediment	salt	3496	deep	1.8	5	PAN	0	987	Bergman n2017	NA	NA	NA	NA
sediment	salt	3496	deep	1.8	5	PC	13	987	Bergman n2017	NA	NA	NA	NA
sediment	salt	3496	deep	1.8	5	PCL	10	987	Bergman n2017	NA	NA	NA	NA
sediment	salt	3496	deep	1.8	5	PDMS	0	987	Bergman n2017	NA	NA	NA	NA
sediment	salt	3496	deep	1.8	5	PE	35	987	Bergman n2017	NA	NA	NA	NA
sediment	salt	3496	deep	1.8	5	PEVA	0	987	Bergman n2017	NA	NA	NA	NA
sediment	salt	3496	deep	1.8	5	PP	181	987	Bergman n2017	NA	NA	NA	NA
sediment	salt	3496	deep	1.8	5	PP&A	200	987	Bergman n2017	NA	NA	NA	NA
sediment	salt	3496	deep	1.8	5	PS	0	987	Bergman n2017	NA	NA	NA	NA
sediment	salt	3496	deep	1.8	5	PSS	0	987	Bergman n2017	NA	NA	NA	NA
sediment	salt	3496	deep	1.8	5	PTFE	31	987	Bergman n2017	NA	NA	NA	NA
sediment	salt	3496	deep	1.8	5	PUR	11	987	Bergman n2017	NA	NA	NA	NA
sediment	salt	3496	deep	1.8	5	PVA	0	987	Bergman n2017	NA	NA	NA	NA
sediment	salt	3496	deep	1.8	5	PVC	21	987	Bergman n2017	NA	NA	NA	NA
sedim	sa	3496	deep	1.8	5	PVOH	0	987	Bergman	NA	NA	NA	NA

sample_type	water	sampling_depth	sampling_region	extraction_density	max_size	polymer_type	count	conf_plastic	source_ID	densities_pcs_m^3	polymer_concentration	conc_dev	polymer_conc_dev
ent	lt								n2017				
sediment	salt	3496	deep	1.8	5	rubber	0	987	Bergmann2017	NA	NA	NA	NA
sediment	salt	3496	deep	1.8	5	VCE	0	987	Bergmann2017	NA	NA	NA	NA
sediment	salt	3496	deep	1.8	5	other	384	987	Bergmann2017	NA	NA	NA	NA
sediment	salt	3496	deep	1.8	5	PAS	0	987	Bergmann2017	NA	NA	NA	NA

APPENDIX 5

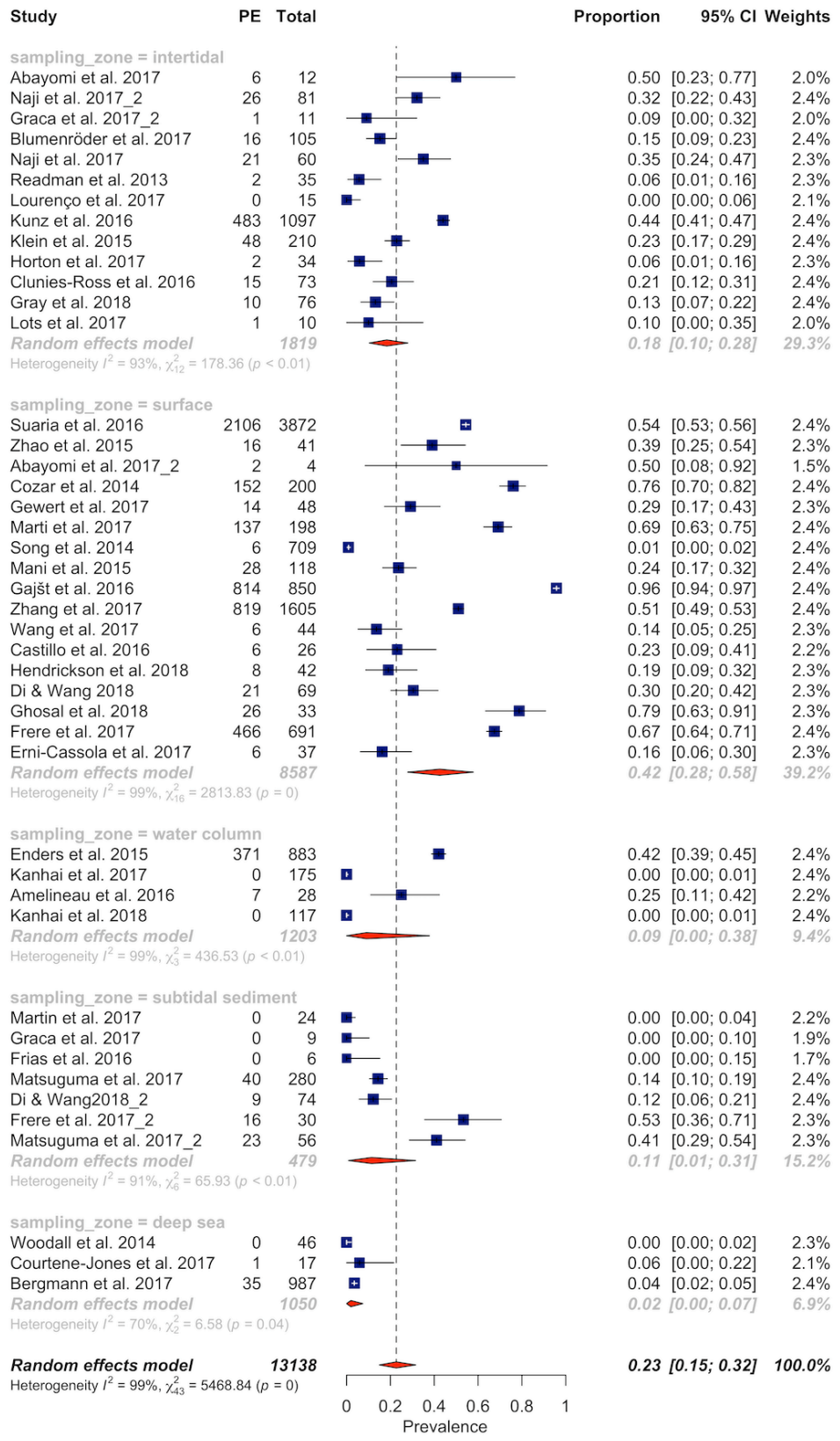

APPENDIX 5.1. Forest plot for PE (polyethylene) subgroup analysis. Red diamonds represent subgroup means, while bottommost indicates overall mean, also represented *via* the dotted line. Total: total particles characterized in each study; PE: number of PE particles in each study.

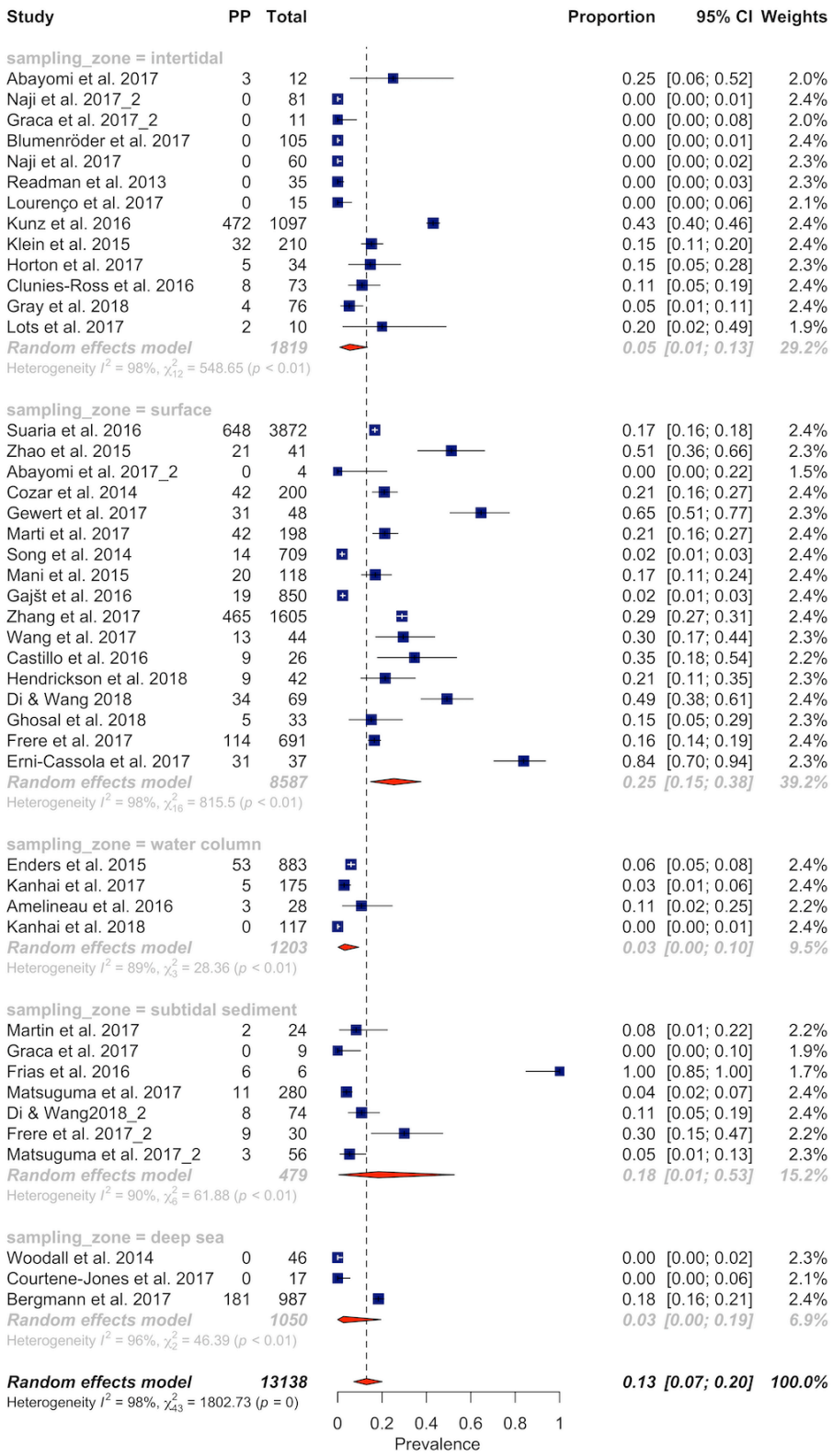

APPENDIX 5.2. Forest plot for PP (polypropylene) subgroup analysis. Red diamonds represent subgroup means, while bottommost indicates overall mean, also represented *via* the dotted line. Total: total particles characterized in each study; PP: number of PP particles in each study.

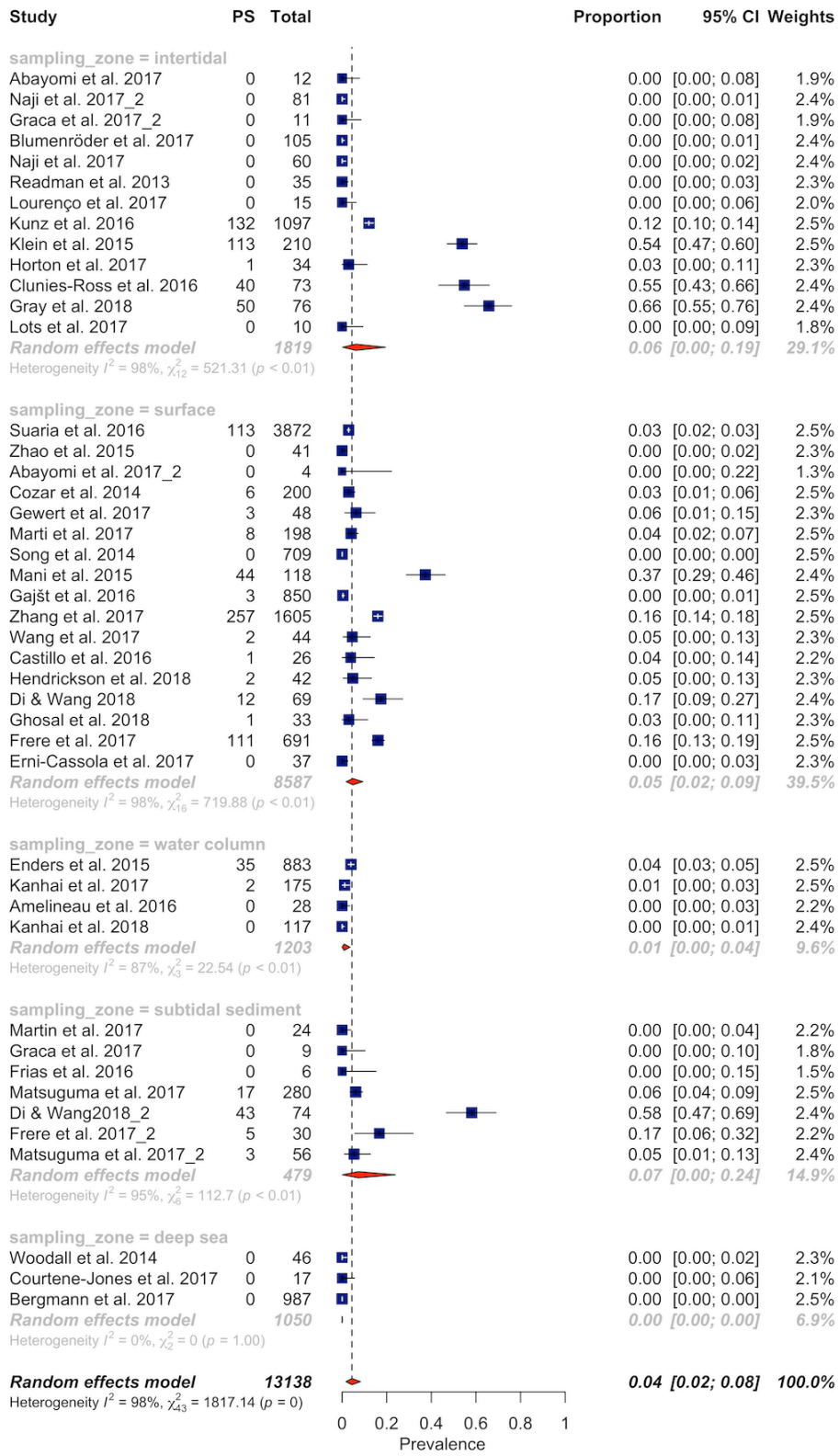

APPENDIX 5.4. Forest plot for PS (polystyrene) subgroup analysis. Red diamonds represent subgroup means, while bottommost indicates overall mean, also represented *via* the dotted line. Total: total particles characterized in each study; PS: number of PS particles in each study.

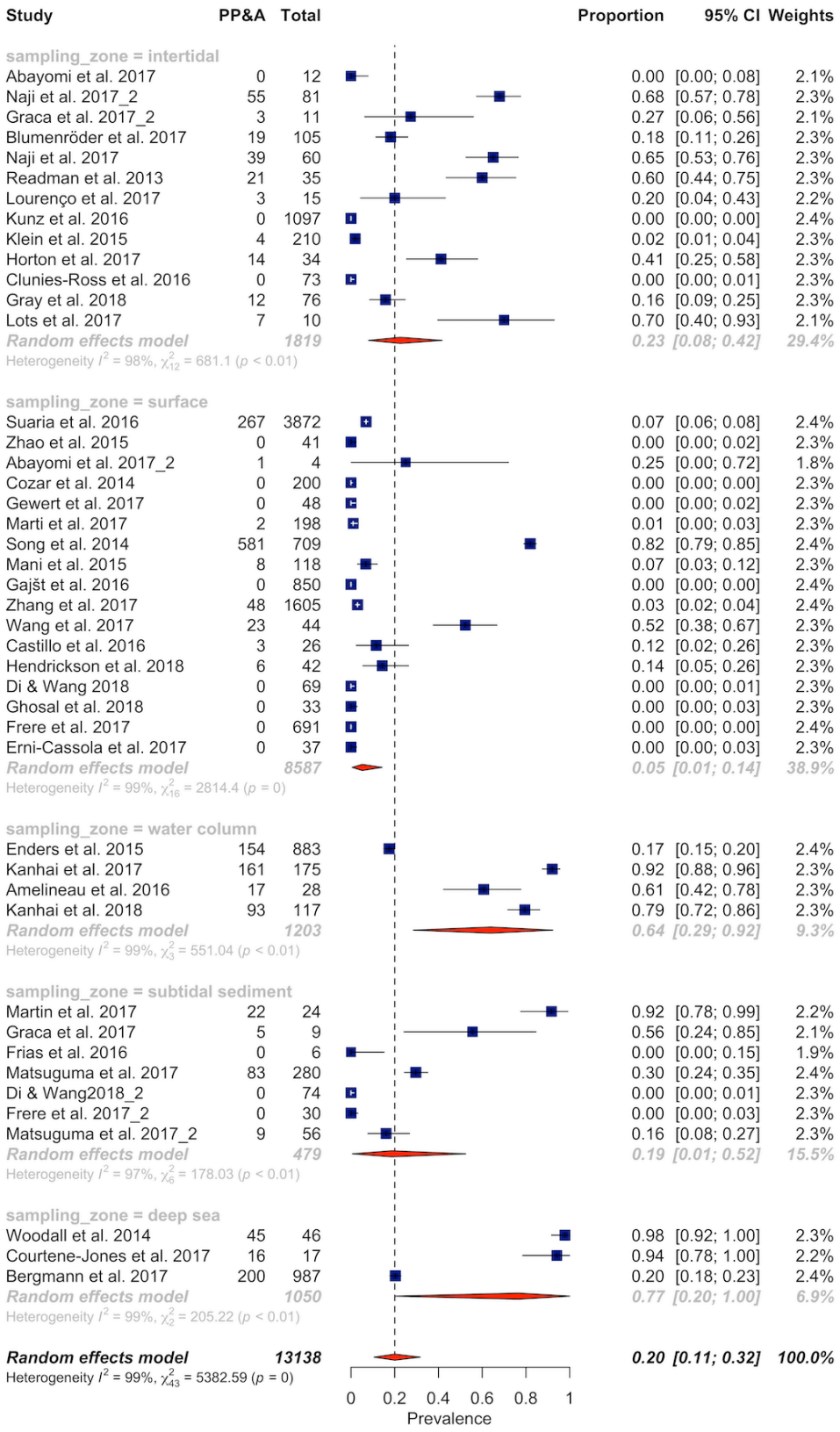

APPENDIX 5.5. Forest plot for PP&A (polyester, polyamide and acrylics) subgroup analysis. Red diamonds represent subgroup means, while bottommost indicates overall mean, also represented *via* the dotted line. Total: total particles characterized in each study; PP&A: number of PP&A particles in each study.

APPENDIX 6

Protocol: Fluorescence-based method to detect small microplastics in environmental samples

This protocol is intended for preparation of environmental samples to detect and quantify small microplastics (20 μm–1 mm) based on fluorescence.

Important points before starting

1. This protocol has not been tested and optimized for large microplastics (1–5 mm). The greater range of sizes obtained by combining large and small microplastics complicates accurate focusing during microscopy and may lead to biased measurement results during automated analysis. As a general guideline, we recommend to separate small from large microplastics by passing the samples through a 1 mm mesh and rinsing thoroughly with Milli-Q water.
2. Pipette tips were found to constitute a significant source of microplastic contamination. It is therefore strongly recommended to filter the dye (0.2 μm) after preparation and to use needle and syringe to apply dye to sample filters.
3. We used filter membranes with a diameter of 47 mm, which were cut into 8 sections in order to fit onto a standard microscopy slide. To avoid cutting of the filter, a 25 mm filter membrane can be used. Generally, it should be avoided to concentrate too much sample on the same filter, as aggregated particles are not counted separately.
4. Before using the ImageJ script (page S10), ascertain that (1) desired input and output directories are indicated and (2) scale settings are correct.

Things to do before starting

1. Prepare the Nile red working solution by dissolving Nile red in methanol to a concentration of 1μg mL^{-1}.
2. If analysing sediment samples, extract microplastics employing a density separation protocol

Procedure

1. Vacuum filter each sample (or flow-trough) onto a polycarbonate track-etched filter membrane (PCTE, hydrophilic, dia. 47 mm, 10 μm).
2. Place the membrane in a clean 250 ml Erlenmeyer flask.
3. Cover flask with clean aluminium foil and store at 60° C for 24 h for desiccation.
4. Add20ml30%H_2O_2andkeepat60°Cduring1h.
5. Increase temperature to 100° C and leave for 7 h.
6. Add 100 mL Milli-Q water to the flask and allow mixture to cool to room temperature.
7. Remove the filter from the flask and thoroughly rinse it into the flask with 100 mL Milli-Q water.
8. Vacuum filter the Erlenmeyer flask content onto a PCTE membrane (PCTE, dia. 47 mm, 10 μm)

9. Transfer filter membrane onto clean microscopy glass slide and store in petri dish >24 h to dry the membrane.
10. Add 2-3 drops of Nile red solution onto the sample membrane on the glass slide.
11. Cover sample with a clean cover slip and fix the cover with sticky tape to the glass slide. This fixes the sample particles and reduces eventual losses.
12. Store slide in darkness during 10 min.
13. Perform fluorescence microscopy using green fluorescence (~ 460 nm excitation and 522 nm emission) and acquire images of randomly selected fields at 10× (or whole filter).
14. Run quantification script (page S4) in ImageJ to generate a .csv file with the measurements for each individual image.

ImageJ script for automated microplastic detection and quantification.
*be sure to set correct scale parameters in "distance= "

```
input = "source directory";
output = "output directory";

setBatchMode(true);
list = getFileList(input);
for (i = 0; i < list.length; i++) action(input, output, list[i]);
setBatchMode(false);

function action(input, output, filename) {
open(input + filename);
run("Set Scale...", "distance=1.5293 known=1 pixel=1 unit=µm global");
run("Subtract Background...", "rolling=1500");
run("8-bit");
setAutoThreshold("Default");
//run("Threshold...");
setThreshold(29, 175);
//setThreshold(29, 175);
setOption("BlackBackground", false);
run("Convert to Mask");
run("Analyze Particles...", "size=400-Infinity display exclude clear include");

saveAs("Results", output + filename + "results.csv"); run("Clear Results");
close();
}
```

APPENDIX 7

Plastisphere DNA extraction (adapted to spin column from (Debeljak et al., 2017))

Prepare buffers

Beads (Biospec zirconia silica beads)
Aliquot: RNase, Proteinase K (10 U/µl)
Dilute Ready Lyse lysozyme to 1000 U/µl
Quiagen Tissue Lyzer

DNA extraction

- Add 1 ml Lysis buffer to 2 ml tube
- Place plastic fragment in tube
- Add 0.25 PCR tube of sterile 0.1 mm zirconium beads to tubes
- Bead-beat for (2x45 + 1x 30 s)
- Add 10 µl Ready Lysozyme (diluted to 1000 U/µl) to each tube and invert 25 times.
- Add 4 µl RNAse A and mix by inverting the tube 25 times
- Incubate at 37 °C for 2 h
- Add 25 µl Proteinase K [blood and tissue kit] to each tube and mix gently.
- Incubate at 56 °C for 18 h.
- Incubate at 80 °C for 5 min
- Cool on ice for 5 min
- Centrifuge at 13000 rpm for 5 min and transfer supernatant into DNeasy Mini spin column and proceed according to step 4 of Animal Tissues Qiagen protocol.

APPENDIX 8

Specific amplicon sequence variants of interest, which were used in BLAST searches:

ASV3:

TACGGAGGGGGTTAGCGTTGTTCGGAATTACTGGGCGTAAAGCGCGCGT
AGGCGGATTGGAAAGTTGGGGGTGAAATCCCGGGGCTCAACCCCGGAAC
TGCCTCCAAAACTATCAGTCTAGAGTTCGAGAGAGGTGAGTGGAATTCCG
AGTGTAGAGGTGAAATTCGTAGATATTCGGAGGAACACCAGTGGCGAAG
GCGGCTCACTGGCTCGATACTGACGCTGAGGTGCGAAAGTGTGGGGAGC
AAACAGGATTAGATACCCTGGTAGTCCACACCGTAAACGATGAATGCCA
GTCGTCAGCAAGCATGCTTGTTGGTGACACACCTAACGGATTAAGCATTC
CGCCTGGGGAGTACGGTCGCAAGATTA

ASV28:

TACGGAGGGTGCAAGCGTTAATCGGAATTACTGGGCGTAAAGCGCGCGT
AGGCGGCTTACTAAGCCAGATGTGAAAGCCCCGGGCTCAACCTGGGAAC
TGCATTTGGAACTGGTTCGCTAGAGTACAGTAGAGGGTGGTGGAATTTCC
AGTGTAGCGGTGAAATGCGTAGAGATTGGAAGGAACATCAGTGGCGAAG
GCGGCCACCTGGACTGATACTGACGCTGAGGTGCGAAAGCGTGGGGAGC
AAACAGGATTAGATACCCTGGTAGTCCACGCCGTAAACGATGTCTACTAG
CCGTTGGGGATCTTGTATCTTTAGTGGCGCAGCTAACGCACTAAGTAGAC
CGCCTGGGGAGTACGGCCGCAAGGTTA

ASV52:

TACGGAGGGTGCGAGCGTTAATCGGAATTACTGGGCGTAAAGCGCACGC
AGGCGGATTGTTAAGCTAGAGGTGAAAGCCCCGCGCTCAACGTGGGAAT
TGCCTTTAGAACTGGCAGTCTAGAGTCTTGGAGAGGGGAGTGGAATTCCA
GGTGTAGCGGTGAAATGCGTAGAGATCTGGAGGAACATCAGTGGCGAAG
GCGACTCCCTGGCCAAAGACTGACGCTCATGTGCGAAAGTGTGGGTAGC
GAACAGGATTAGATACCCTGGTAGTCCACACCGTAAACGCTGTCTACTAG
CTGTTTGTGGTTTTAAACCGTGAGTAGCGAAGCTAACGCGCTAAGTAGAC
CGCCTGGGGAGTACGGCCGCAAGGTTA

APPENDIX 9

APPENDIX 9. Yield of DNA extraction.

PP	
Treatment	**Concentration [ng/mL]**
control	30.4
control	33.2
control	33.2
control	22.0
control	25.6
control	30.8
lightly weathered	40.4
lightly weathered	32.8
lightly weathered	48.4
lightly weathered	42.0
lightly weathered	61.6
lightly weathered	48.8
heavily weathered	73.2
heavily weathered	47.2
heavily weathered	22.0
heavily weathered	36.4
heavily weathered	60.4
heavily weathered	57.6

PE		
Treatment	**Timepoint**	**Concentration [ng/mL]**
glass	day 2	14.2
glass	day 2	<10
glass	day 2	<10
glass	day 2	<10
non-weathered	day 2	29.2
non-weathered	day 2	12.2
non-weathered	day 2	25.2
non-weathered	day 2	14.8
non-weathered	day 2	40.8
non-weathered	day 2	12.6
weathered	day 2	34.4
weathered	day 2	68.2
weathered	day 2	33.6
weathered	day 2	57.8

weathered	day 2	<10
weathered	day 2	45.6
glass	day 9	<10
glass	day 9	70.4
glass	day 9	99.4
glass	day 9	65.6
glass	day 9	37
glass	day 9	48.2
non-weathered	day 9	396
non-weathered	day 9	149.6
non-weathered	day 9	210
non-weathered	day 9	274
non-weathered	day 9	168.6
non-weathered	day 9	254
weathered	day 9	200
weathered	day 9	139
weathered	day 9	250
weathered	day 9	189
weathered	day 9	280
sea water	day 9	5440
sea water	day 9	3460
sea water	day 9	4680
sea water	day 9	5820
KITOME	–	<10
KITOME	–	<10
filter control	–	<10

APPENDIX 10

APPENDIX 10. Detailed information of 18S rRNA gene ASV processing throughout the pipeline.

Treatment[1]	Input	Filtered	DenoisedF	DenoisedR	Merged	Nonchim	Total ASVs
control PP	25536	18965	18905	18952	18856	17611	17350
control PP	53368	47227	47096	47175	46691	43552	42695
control PP	413	174	174	173	172	159	155
control PP	49654	43790	43668	43714	43177	38141	37300
control PP	30958	27089	26789	26941	25418	20454	19796
control PP	51110	44863	44524	44717	42986	30964	30029
lw PP	35893	27	16	26	15	13	13
lw PP	122132	106657	106475	106516	105754	95961	94221
lw PP	30561	120	54	120	53	53	53
lw PP	9929	1	0	1	0	0	0
lw PP	933	0	NA	NA	NA	NA	NA
lw PP	4149	878	866	867	846	332	309
hw PP	53637	43229	43167	43199	43025	39956	39582
hw PP	1051	4	2	1	0	0	0
hw PP	4217	65	61	61	60	44	38
hw PP	1072	3	3	3	3	3	3
hw PP	884	2	2	2	2	0	0
hw PP	3368	0	NA	NA	NA	NA	NA
blank	183971	98	39	98	39	39	39
blank	195689	101	86	101	86	86	86
blank	721	341	335	339	323	161	34
blank	573	40	38	38	38	34	220
blank	1518	307	238	299	234	220	9
blank	284	19	18	18	18	9	51
blank	707	70	51	69	51	51	73366
blank	87460	74058	73860	74035	73617	73366	10
blank	284	13	10	13	10	10	292
blank	994	377	377	377	377	292	96
blank	418	159	155	156	154	96	68
blank	574	111	71	111	71	68	61
blank	535	71	61	70	61	61	119
blank	1768	248	217	248	217	119	43
blank	469	79	72	78	71	43	43
blank	1017	48	43	48	43	43	215
blank	869	253	216	252	215	215	4

APPENDIX 10. Detailed information of 18S rRNA gene ASV processing throughout the pipeline.

Treatment[1]	Input	Filtered	DenoisedF	DenoisedR	Merged	Nonchim	Total ASVs
blank	660	5	4	5	4	4	618
blank	1460	737	693	733	669	618	1235

[1] *control PP: untreated polypropylene; lw PP: lightly weathered PP; hw PP: heavily weathered PP*

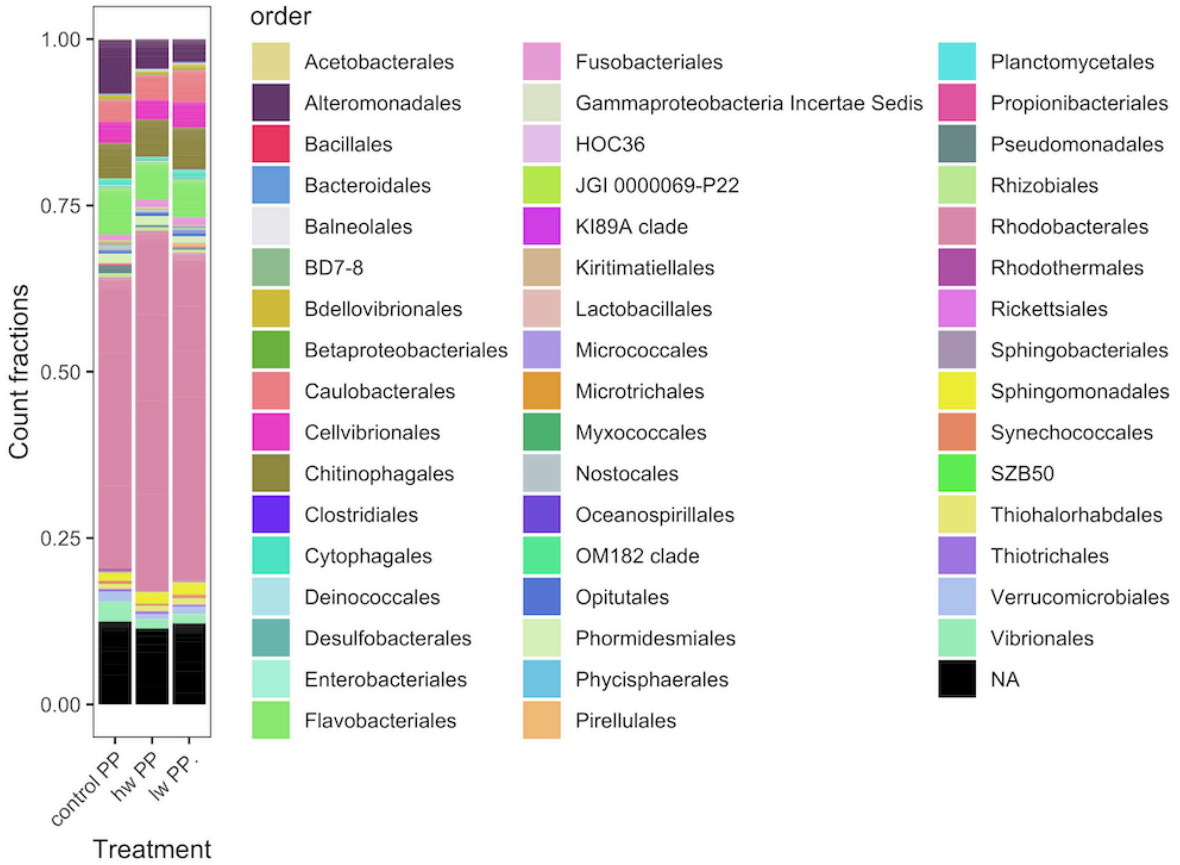

APPENDIX 11. Bar chart showing dominant bacterial orders (16S rRNA gene) in microbial communities colonizing non-weathered polypropylene (control PP), heavily weathered PP (hw PP) and lightly weathered PP (lw PP) after 9 days of incubation in coastal Mediterranean seawater.